Removal of persistent aromatic micropolluants from municipal sewage sludge in anaerobic digesters assisted by microbial electrolysis and conductive materials

Izabel Kronenberg

Izabel KRONENBERG

PhD thesis 2018

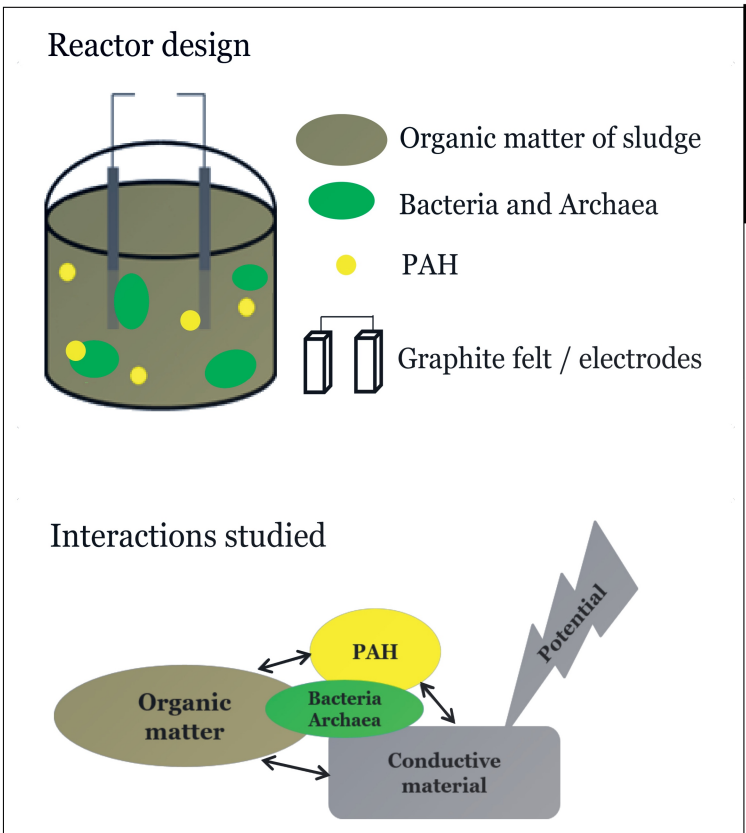

ELIMINATION DES MICROPOLLUANTS AROMATIQUES ET PERSISTANTS DE BOUES DE STATION D'ÉPURATION AU COURS DE LA DIGESTION ANAÉROBIE ASSISTÉE PAR ÉLECTROLYSE MICROBIENNE ET MATÉRIAUX CONDUCTEURS

REMOVAL OF PERSISTENT AROMATIC MICROPOLLUANTS FROM MUNICIPAL SEWAGE SLUDGE IN ANAEROBIC DIGESTERS ASSISTED BY MICROBIAL ELECTROLYSIS AND CONDUCTIVE MATERIALS.

INRA
SCIENCE & IMPACT

Membre fondateur de
agreenium

THÈSE POUR OBTENIR LE GRADE DE DOCTEUR DE MONTPELLIER SUPAGRO

En Génie des Procédés

École doctorale GAIA – Biodiversité, Agriculture, Alimentation, Environnement, Terre, Eau
Portée par l'Université de Montpellier

Laboratoire de Biotechnologie de l'Environnement (LBE, INRA, UR050)

Elimination des micropolluants aromatiques et persistants de boues de station d'épuration au cours de la digestion anaérobie assistée par électrolyse microbienne et matériaux conducteurs

Présentée par Izabel KRONENBERG
Le 29 mars 2018

Sous la direction de Dominique PATUREAU

Devant le jury composé de

Claire ALBASI, Directrice de recherche, CNRS - INP- LGC Toulouse	Rapporteur
Théodore BOUCHEZ, Ingénieur en Chef du corps de Ponts, Eaux et Forêts - IRSTEA Antony	Rapporteur
Catherine GONZALES, Professeur, LGEI - Ecole des Mines d'Ales	Président du jury
Marc CRETIN, Professeur, IEM - UMR5635 Université Montpellier	Examinateur
Nicolas BERNET, Directeur de recherche, LBE - INRA Narbonne	Examinateur
Dominique PATUREAU, Directrice de recherche, LBE - INRA Narbonne	Directeur de thèse
Éric TRABLY, Ingénieur de recherche, LBE - INRA Narbonne	Invité

UNIVERSITÉ DE MONTPELLIER

Montpellier SupAgro

English summary

The elimination of organic micropollutants from the environment has become a public health goal today because of their toxicity and bioaccumulation through the trophic chain. Polycyclic aromatic hydrocarbons (PAHs) and nonylphenol (NP) are found at low concentrations in wastewaters and accumulate by sorption onto sewage sludge due to their hydrophobicity. Anaerobic digestion (AD) plays a central role in reducing the micropollutant load before dissemination to the environment via sludge spreading. The aim of this PhD work is to enhance removal performances by employing two emerging techniques, namely microbial electrolysis and the addition of conductive materials. The results demonstrate that 12 PAHs were improved by 21 to 33 % by both treatments while NP was eliminated to the same extent in all digesters with and without graphite felt (GF). Either the mediatorless electron exchange between the anaerobic syntrophic community and the conductive material or the close contact of syntrophic biota within the biofilm presumably facilitates sludge hydrolysis which, in turn, leads to the enhanced bioavailability of PAHs and their subsequent biodegradation. An enrichment of hydrogenotrophic methanogens was ascertained in GF digesters which was correlated to the observed PAH removals. The addition of carbon plate and platinum eliminated only two low molecular weight PAHs suggesting that conductivity is not a major factor in the dissipation of PAHs. An increase of the specific surface area by the addition of powdered GF indicated a possible cytotoxic effect due to membrane piercing of cells in AD. The use of affordable conductive materials such as GF may present an alternative biodegradation strategy for the removal of PAHs from sludge.

Key words : microbial electrolysis, persistant organic contaminant, anaerobic digestion, endocrine disruptor, conductive material

Résumé français

L’élimination des micropolluants organiques est devenue aujourd’hui un objectif de santé publique car leur toxicité et bioaccumulation au travers de la chaine trophique sont incontestables. Les hydrocarbures aromatiques polycycliques (HAP) et le nonylphénol (NP) présents en faible concentration dans l’eau usée se retrouvent fortement sorbés à la matière organique des boues de station d’épuration. Les procédés de traitement de ces boues, comme la digestion anaérobie (DA) jouent un rôle central car ils constituent une des dernières barrières avant rejet vers l’environnement par épandage. La DA élimine les HAP et le NP mais les performances restent insatisfaisantes. L’objectif de cette thèse est d’améliorer les performances d’élimination des HAP et NP par la DA en utilisant l’électrolyse microbienne et l’ajout de matériaux conducteurs. Les résultats montrent que l’élimination de 12 HAP est accrue par l’ajout de graphite poreux (GF) qui semble (1) faciliter l'échange direct d'électrons avec la communauté syntrophique anaérobie ou (2) offrir une surface d’échange d’électrons et de nutriments suffisante pour la création d’un biofilm sans influence du caractère conducteur du GF. Un enrichissement de méthanogènes hydrogénotrophes a été constaté en présence de GF contribuant à l’amélioration des performances d’hydrolyse de la matière et des contaminants associés. Pour le NP, les performances d‘élimination sont très élevées quelles que soient les conditions appliquées suggérant des mécanismes d’élimination différents. L’addition d’autres matériaux de conductivité variable tels que le charbon plaque et le platine n’éliminait que deux HAP de faible poids moléculaire suggérant que la conductivité du matériau ne constitue pas un facteur majeur dans la dissipation des HAP. Une augmentation de la surface spécifique du GF par pulvérisation a ralenti la production de méthane alors qu’une surface intacte doublée a permis l’installation d’un biofilm favorisant un échange étroit entre les communautés syntrophiques. L'utilisation de matériaux conducteurs économiquement abordables tels que le GF semble être une stratégie alternative pour améliorer l’élimination des HAP des boues.

Mots clés : électrolyse microbienne, contaminant organique persistent, digestion anaérobie, perturbateur endocrinien, matériau conducteur

Publications

Kronenberg, M., Trably, E., Bernet, N., Patureau, D., 2017. Biodegradation of polycyclic aromatic hydrocarbons: Using microbial bioelectrochemical systems to overcome an impasse. Environ. Pollut. 231, 509–523. doi:10.1016/j.envpol.2017.08.048.

Kronenberg, M., Trably, E., Bernet, N., Patureau, D., 2017. Conductive graphite felt enhances polycyclic aromatic hydrocarbon removal during anaerobic digestion of sludge (submitted to the Journal of Hazardous Materials in October 2017).

Conference Poster:

Enhancement of polycyclic aromatic hydrocarbon (PAH) removal during anaerobic digestion of sludge using graphite felt. Kronenberg M., Bernet N., Trably E., Patureau D. 10th Micropol & Ecohazard Conference. 17-20th September 2017, Vienna, Austria.

Pitch talk:

PAH removal during anaerobic digestion of sludge using graphite felt. Kronenberg M., Desmond-Le Quéméner E., Bernet N., Trably E., Patureau D. 15th IWA World Conference on Anaerobic Digestion. 17-20th October 2017, Beijing, China.

Abbreviations

AD: Anaerobic digestion

ALS: Aluminosilicates

BAS: Biochar amended sludge

BES: Bioelectrochemical system

CE: Counter electrode

COD: Chemical oxygen demand

CONT: Anaerobic control digesters

CP: Carbon plate that consists of non-porous graphite

DES: Destroyed

DES1: Destroyed graphite felt surface of 1 m^2

DES2: Destroyed graphite felt surface of 2 m^2

DEET: Direct extracellular electron transfer

DIET: Direct interspecies electron transfer

DNA: Deoxyribonucleic acid

ED: Endocrine disruptor

GF: Graphite felt

HDB: Hydrocarbon degrading bacteria

HT: Heat treated

INT: Intact

INT1: Intact graphite felt surface of 1 m^2

INT2: Intact graphite felt surface of 2 m^2

LMW: Low molecular weight

MEC: Microbial electrolysis cell

MFC: Microbial fuel cell

NP, NPnEO: Nonylphenol, Nonylphenolethoxylates

PAH: Polycyclic aromatic hydrocarbon

PCR: Polymer chain reaction

POP: Persistent organic pollutant

PT: Platinum

rRNA: Ribosomal ribonucleic acid

SHE: Standard hydrogen electrode

SI: Supplementary Information

SMFC: Sediment microbial fuel cell

SRT: Sludge retention time

SSA: Specific surface area

TPPB: Two-phase partitioning reactor

TS: Total solids

VS: Volatile solid

WE: Working electrode

WWTP: Wastewater treatment plant

Résumé français

Table des illustrations

I. Introduction

La présence d'une grande diversité de contaminants organiques provenant des ménages et de l'industrie (détergents, médicaments, produits phytosanitaires) dans les eaux usées et les résidus solides est incontestable. Dans un contexte de mise en conformité avec les exigences européennes de 2015 (DCE 2000/60/EC), l'élimination des micropolluants organiques est devenu aujourd'hui un objectif de santé publique et de protection des milieux récepteurs fragiles (plan micropolluants 2016-2021). Les procédés de traitement des eaux usées urbaines mais aussi des résidus solides associés comme les boues de stations d'épuration jouent un rôle central car ils constituent un point de convergence de ces contaminants avant dissémination vers l'environnement.

Les nonylphenols (NP) et les hydrocarbures aromatiques polycycliques (HAP) constituent deux familles de micropolluants organiques persistants qui contiennent des structures aromatiques qui leur confèrent un caractère réfractaire à la biodégradation. Ils sont fortement toxiques, car reconnus comme perturbateurs endocriniens, et possèdent un fort potentiel carcinogène. Les nonylphénols et leurs précurseurs les nonylphénols polyéthoxylates sont utilisés comme émulsifiants et détergents dans l'industrie ; les HAP proviennent de la combustion incomplète du pétrole ou d'autre matière organique comme le charbon. Ainsi, ils se retrouvent dans les échappements de gaz des véhicules, ou bien sorbés aux particules dans l'air. Après un évènement pluvieux, ils sont alors transférés avec l'eau de ruissellement dans les réseaux d'égout, vers la station d'épuration. Leurs caractères hydrophobe et persistant font qu'ils ne sont pas dégradés par le traitement biologique (par boue activée par exemple) mais simplement transférés vers les solides (les boues). Les teneurs en NP et HAP dans la boue dépendent des teneurs en entrée de la station d'épuration et peuvent varier entre le µg et le mg par kg de matière sèche (Mailler et al., 2014)

Le devenir de ces contaminants au cours du traitement des boues est peu étudié (Mailler et al., 2017). Les deux principaux traitements biologiques mis en œuvre pour stabiliser les boues avant un usage en épandage sur sol agricole sont la méthanisation et le compostage,

les autres traitements physico-chimiques sont le chaulage et le séchage thermique. Selon le concept de valorisation des ressources où l'eau usée devient source d'énergie et de nutriments, la méthanisation joue un rôle central à cause de son pouvoir calorifique qui permet de bruler le méthane pour obtenir de l'énergie. Il est alors nécessaire d'améliorer les performances de dégradation de contaminants organiques types HAP/NP pendant la méthanisation. En digestion anaérobie, les performances d'abattement de ces molécules sont souvent faibles et très variables d'un composé à l'autre ; elles dépendent du temps de séjour hydraulique, de la matière organique, de la température du procédé. Le potentiel microbien de dégradation anaérobie de faibles quantités de micropolluants ne peut s'exprimer qu'après une longue période d'adaptation et est souvent limité par la biodisponibilité de ces composés qui sont fortement associés à la matière organique.

Procédés émergents, la bioélectrochimie microbienne et l'ajout de matériaux conducteurs apparaissent comme une solution innovante pour remédier à la problématique de ces écosystèmes contaminés. Ces procédés ne sont étudiés que depuis une quinzaine d'années au niveau international, essentiellement dans le contexte de la production d'électricité (pile à combustible) et d'hydrogène (électrolyseur microbien) à partir de la matière organique mais aussi dans le but d'améliorer les performances de la méthanisation et de synthétiser des molécules à haute valeur ajoutée. Cependant, les piles à combustible sont aussi utilisées pour la dépollution de sédiments (Li and Yu, 2015), eaux usées (Xu et al., 2015) et sols (Yu et al., 2017) contaminés en métaux lourds et composés organiques comme le phénol (Feng et al., 2015) ou les hydrocarbures de pétrole (Lu et al., 2014) de faibles coûts de traitement. Cependant, malgré le réel potentiel d'amélioration des performances de biodégradation, les mécanismes microbiens qui conditionnent ces performances restent encore peu connus et, de façon surprenante, aucune étude n'a fait état de l'utilisation de bioélectrolyseurs pour éliminer des micropolluants organiques présents dans des systèmes épuratoires réels tels que les boues urbaines. Quant aux matériaux conducteurs, une seule étude montre la capacité d'un composé conducteur, l'oxyde de fer, à aider à la dégradation d'un composé aromatique carboxylé en méthanisation (Zhuang et al., 2015).

II. Objectifs de la thèse

Les objectifs de la thèse sont (i) d'acquérir des connaissances quant aux voies de dissipation de contaminants persistants tels que les HAP et NP en utilisant des bioélectrolyseurs microbiens dans le contexte de la digestion anaérobie de boues, (ii) de voir l'effet des matériaux conducteurs avec des surfaces et conductivités différentes (graphite et platine) afin d'évaluer les capacités épuratoires de ces procédés pour les contaminants et d'en étudier les consortia microbiens associés.

III. Matériels et méthodes

Les diverses expériences ont été réalisées avec des réacteurs anaérobies discontinus dans les conditions suivantes : 35/37°C, 650 tr/min, pH initial 7, durée entre 42 ou 83 jours. Tous les réacteurs ont été ensemencés avec des boues secondaires prélevées sur une station d'épuration municipale. Ces boues ont servi à la fois d'inoculum et de substrat et ont été dopées avec 12 HAP et des NP. Des digesteurs anaérobies sans ajout de matériau et sans électrodes ont servi de témoins. En parallèle, des digesteurs contenant différents matériaux avec des surfaces variées (graphite poreux ou non poreux, platine) ou utilisant le graphite poreux comme électrode (système bioélectrochimique) ont été suivis. Des réacteurs similaires ont été conduits avec la même boue dopée traitée thermiquement dans un autoclave à 120 ° C pendant 20 minutes pour obtenir des réacteurs de contrôle sans communauté microbienne. Les réacteurs bioélectrochimiques ont été réalisés dans des électrolyseurs microbiens à chambre unique sous contrôle potentiométrique (BioLogic Science Instruments, France) avec mesure de la densité de courant (logiciel EC-laboratory v.10.1). Sur l'ensemble de ces digesteurs anaérobies, la production de biogaz ainsi que sa composition ont été suivies. A la fin des expériences, les échantillons de boue ont été centrifugés à 18 600 g pendant 20 minutes et congelés (phases aqueuse et particulaire stockées séparément) ou directement congelés à -20 ° C. Les divers paramètres permettant d'évaluer l'évolution de la matière organique au cours de la digestion ont été quantifiés. Les échantillons totaux et particulaires ont aussi été lyophilisés, broyés et stockés à l'obscurité avant l'extraction des HAP et NP. Les communautés microbiennes des

échantillons "totaux" et des biofilms attachés au graphite poreux ont été caractérisées : leur composition a été déterminée par séquençage et l'abondance relative des espèces présentes par qPCR.

IV. Résultats

Au cours du premier essai, trois conditions ont été comparées : (1) la digestion anaérobie seule (système de référence, réacteur CONT), (2) la digestion en présence d'un matériau conducteur, ici du graphite poreux (réacteur GF_INT2[*]) et (3) la digestion en présence de ce matériau avec l'application d'un courant à +0.8 V (réacteur BES). L'objectif de cet essai était d'évaluer un effet du potentiel électrique appliqué sur la dégradation des micropolluants (HAP et NP). Les trois conditions citées précédemment ont aussi été appliquées sur des réacteurs traités thermiquement afin de quantifier les potentielles pertes abiotiques des contaminants dues à des réactions physico-chimiques (sorption, volatilisation).

Les premiers résultats (Figure 1) ont montré une différence significative d'abattement des matières sèches et organiques ainsi que des contaminants entre les réacteurs avec du graphite poreux [GF_INT2 (vert foncé) et BES (bleu foncé)] et les digesteurs témoins [Cont (rouge foncé)] sans ajout de graphite poreux (21 à 33 % de plus d'abattement pour les contaminants et environ 20 % pour la matière). Toutefois, la présence d'une électrode constituée du même matériau et polarisée à +0.8 V n'a pas permis d'améliorer significativement les performances des réacteurs comparés à la seule présence du matériau. Ceci pourrait être lié à l'application d'un potentiel non adapté pour les microorganismes anaérobies comme mentionné par Schröder et al. (2015) qui suggère que leurs membranes sont endommagées par l'application de potentiel élevé.

[*] matériau GF avec une surface intégrale de 2 m^2

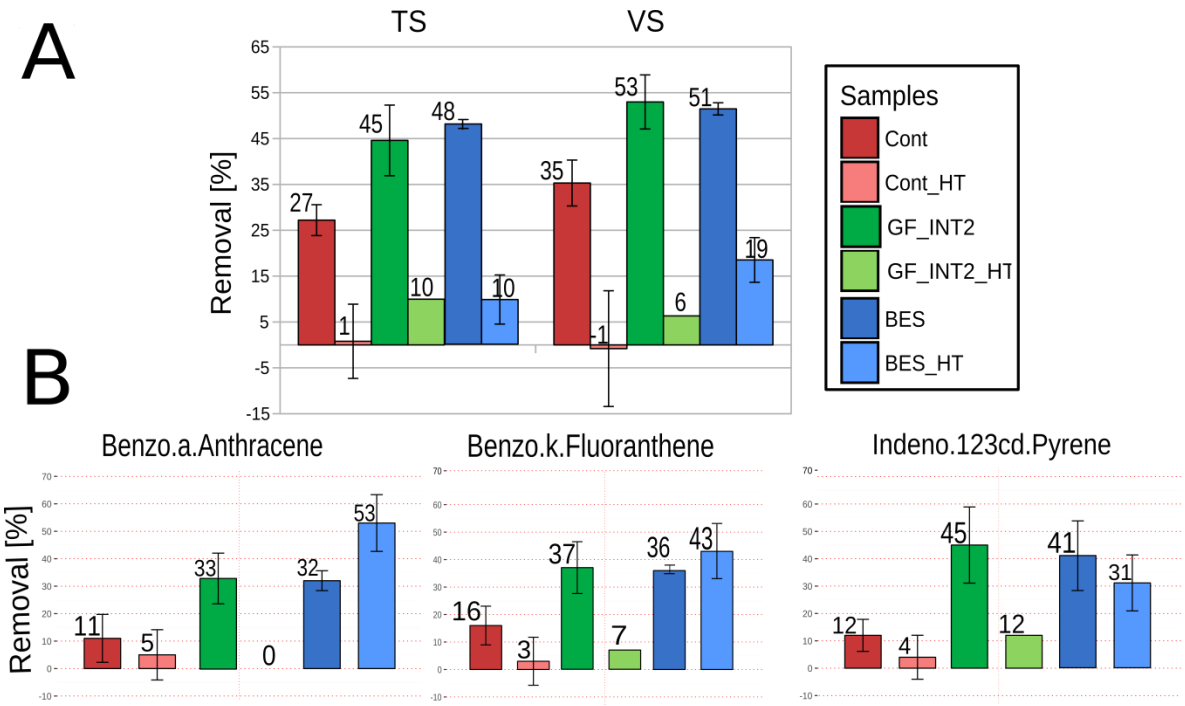

Figure 1: (A) Elimination de matière sèche et volatile lors de la digestion anaérobie des digesteurs témoins traités thermiquement (HT) et non traités. (B) Elimination de trois HAP représentatifs.
Cont : digesteur de contrôle, GF_INT2: digesteur supplémenté de graphite poreux d'une surface spécifique de 2 m^2, BES : digesteur bioélectrochimique avec du graphite poreux de même surface comme électrodes. Les barres d'erreur représentent les écarts-types de quatre ou six valeurs mesurées sur, respectivement les duplicats ou triplicats de réacteurs. (B) Elimination de l'indéno (123cd) pyrène, du benzo(k)fluoranthène et du benzo(a)anthracène au cours de la digestion de boues anaérobies. Les barres d'erreur représentent les écarts-types (STD) de 12 ou 18 valeurs mesurées sur, respectivement les duplicats ou triplicats de réacteurs.

L'observation d'un abattement plus important de la matière et des HAP pour les réacteurs avec du graphite poreux prouve un effet de la présence de ce matériau sur la digestion anaérobie, observation en accord avec ce qui a été récemment montré par (Dang et al., 2016). Nos résultats apportent un élément nouveau puisque simultanément à l'amélioration de la dégradation de la matière organique, des contaminants persistants comme les HAP, intimement associés à cette matière du fait de leur forte hydrophobicité (logK_{ow} élevé), sont aussi substantiellement plus éliminés. Apparemment, l'ajout de graphite poreux aux digesteurs anaérobies a relocalisé les HAP de la phase particulaire vers la phase aqueuse (Figure 2).

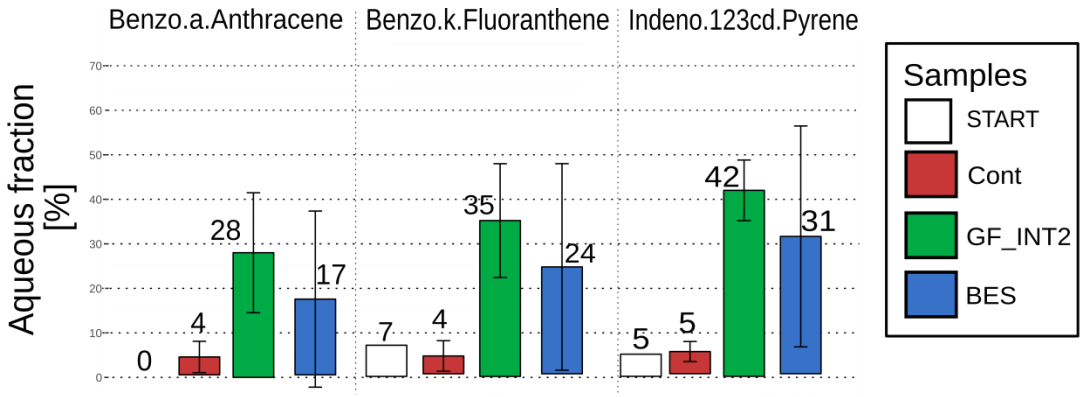

Figure 2:Pourcentage de l'indeno(123cd)Pyrene, du benzo(k)fluoranthene et du benzo(a)anthracene dans la phase aqueuse avant (START) et après la digestion anaérobie des boues (42 jours).
Cont : digesteur de contrôle, GF_INT2: digesteur supplémenté de graphite poreux d'une surface spécifique de 2 m^2, BES : digesteur bioélectrochimique avec du graphite poreux de même surface comme électrodes

Les réacteurs GF ayant une surface spécifique de 2 m^2 présentaient 24, 31 et 37% plus de HAP (BaA, BkF, Ind) dans la phase aqueuse que les digesteurs sans addition de GF. La solubilisation des HAP pourrait être due à une hydrolyse accrue de la matière organique due à la coopération syntrophique entre les acétogènes et les méthanogènes (Dalla Vecchia et al., 2016) qui peuvent utiliser des matériaux conducteurs comme navette d'électrons (Lohner et al., 2014). L'hydrolyse de la matière particulaire aurait ainsi été facilitée par l'échange direct d'électrons entre le matériau conducteur et la communauté syntrophique anaérobie, ce qui a conduit à l'élimination améliorée de la matière sèche et des HAP. Les conducteurs carbonés comme le graphite poreux semblent contourner deux limites à la biodégradation des HAP, le manque d'accepteurs d'électrons terminaux ainsi que la biodisponibilité limitée des HAP.

Les performances d'élimination de NP dépassaient 80% et sont équivalentes entre les différentes conditions (Figure 3).

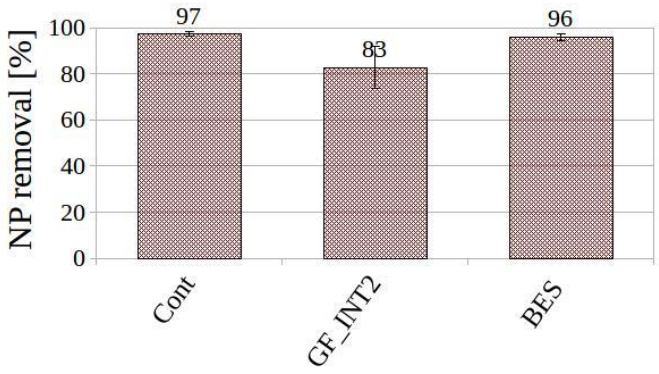

Figure 3: Elimination moyenne de NP en digestion anaérobie sans (Cont) ou avec le graphite poreux intact de 2 m^2 (GF_INT2) et avec un potentiel appliqué (BES).
Les barres d'erreur représentent les écarts-types de 8 ou 12 mesures pour des réacteurs en double ou en triple.

On suppose que cela est dû à la dilution des boues et au fait que les NP sont transférés de la phase particulaire vers la phase aqueuse, ce qui les rend plus biodisponibles. Ici, la biodisponibilité n'est pas un facteur limitant de la dégradation des NP comme le suggéraient des études antérieures (Patureau et al., 2008), ce qui peut expliquer pourquoi l'élimination des NP n'est pas corrélée à l'élimination des MS (27-48%) dans les conditions choisies.

Les réacteurs traités thermiquement Cont_HT et GF_INT2_HT ont montré peu d'élimination des matières sèches et organiques [TS, VS, Figure 1A (rouge et vert clairs)] et des HAP, ce qui indique que les processus abiotiques comme la volatilisation ou la sorption sur le graphite poreux sont des mécanismes mineurs d'élimination des HAP dans ces conditions [Figure 1B (rouge et vert clairs)]. Le réacteur électrochimique traité thermiquement (BES_HT) a montré une élimination des HAP étonnamment élevée (bleu clair, Figure 1B) qui dépassait l'élimination des HAP à 4 et 5 cycles (BaA et BkF) dans les digesteurs non-traités thermiquement. Cette performance élevée pourrait être expliquée par un transfert des HAP vers la phase aqueuse après le traitement thermique et leur dégradation électrochimique pure.

Afin d'évaluer si l'amélioration des performances observées en présence de GF s'accompagne de changements microbiologiques, la composition bactérienne et archéenne des biofilms du GF et des milieux a été déterminée par séquençage. Trois phyla bactériens

(*Firmicutes*, *Bacteriodetes* et *Spirochaetae*) représentaient à eux seuls 64-73% de l'abondance relative des communautés planctoniques et fixées à la surface de GF_INT2 et sur les électrodes de BES en fin de culture après 42 jours (Figure 4A). Des phyla avec des abondances relatives de moins de 2% représentaient 25-37% dans tous les digesteurs anaérobies signifiant une grande diversité bactérienne. Les *Protéobactéries*, en particulier, représentaient moins de 5% de l'abondance relative des communautés planctoniques des boues. Dans les biofilms aux anodes et cathodes du BES, cependant, les abondances relatives de ce phylum augmentait à 10,9 et 6,7% (Figure 4A), suggérant que la présence de bactéries électroactives a été potentiellement favorisée par les électrodes. La communauté

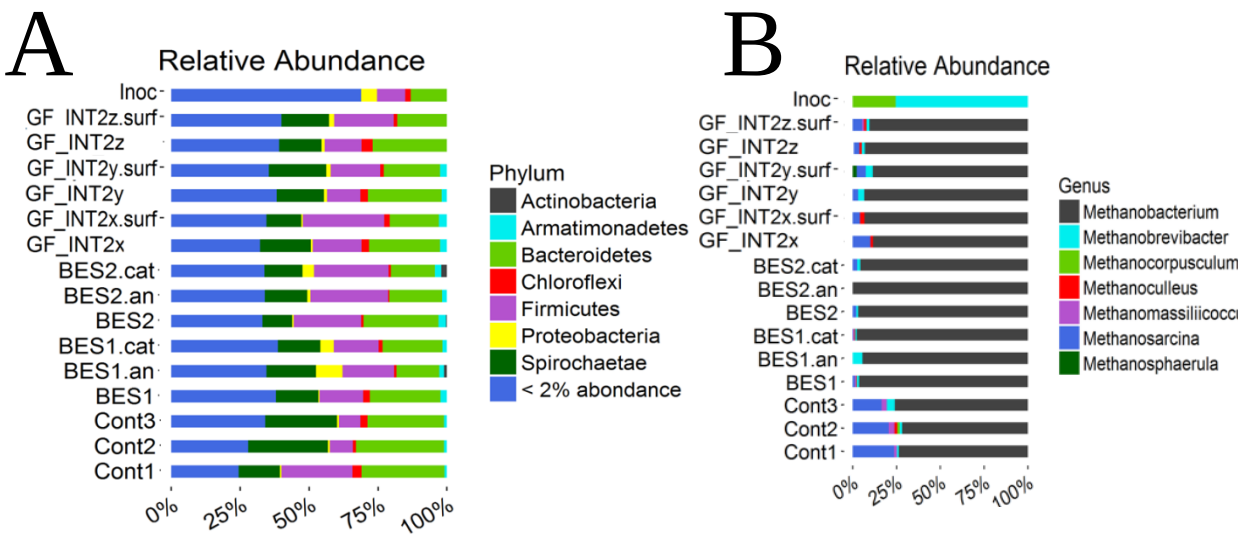

Figure 4: Distribution taxinomique bactérienne (A) et archéenne (B) au niveau du phylum et du genre.
Cont = digesteur anaérobie; GF_INT2 = digesteurs avec graphite poreux; GF.INT2.surf = biofilm à la surface des réacteurs GF_INT2 (surface 2 m2); BES = digesteurs bioélectrochimiques; BES.an/BES.cat= biofilm anodique et cathodique.

des *Archaea* dans les digesteurs contenant du graphite s'est enrichie en genre *Methanobacterium*, qui consomme de l'hydrogène pour produire du méthane (Figure 4B). Cet enrichissement a été observé également sur les systèmes BES (biofilms).

L'ARNr 16S d'*Archaea* était absent de tous les réacteurs traités thermiquement. L'absence d'*Archaea* méthanogène est compatible avec le fait que les réacteurs traités thermiquement n'ont pas produit de méthane. Cependant, le traitement thermique a favorisé la sélection de bactéries sporulantes. Ainsi, les ordres bactériens contenant des bactéries sporulantes (*Clostridiales*, *Bacillales*, *Thermoanaerobacterales*) représentaient jusqu'à 99 et 98% de tous les ARNr 16S bactériens présents dans Cont_HT et BES_HT respectivement (Figure 5A) alors que les abondances absolues ne sont que d'environ 25 et 34% dans les réacteurs non traités thermiquement (Cont 2 et BES2, données non présentées).

En outre, Cont_HT et tous les réacteurs BES_HT ont montré une nette différence dans la

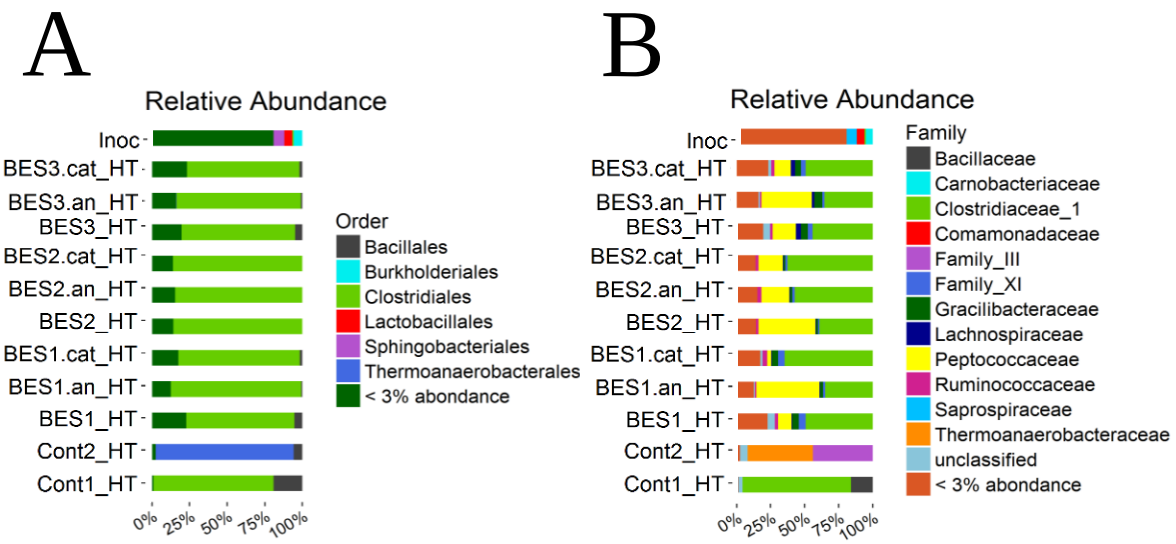

Figure 5: Abondances relatives des séquences de gènes de l'ARNr 16S bactérien.
Réacteurs traités thermiquement (HT) et de l'inoculum, au niveau de l'ordre (A) et au niveau de la famille (B).

composition bactérienne comme observé au niveau de la famille (présence de *Peptococcaceae* seulement dans BES_HT) (Figure 5B).

L'OTU 1 dont la séquence est la plus proche de *Desulfitobacterium* (famille *Peptococcaceae)* représente jusqu'à 42% de l'abondance absolue dans les échantillons BES_HT mais ne se retrouve pas dans Cont_HT ce qui suggère que l'application d'un potentiel a enrichi ce genre bactérien de manière sélective. *Desulfitobacterium* est une bactérie électroactive connue (Chen et al., 2017) et la syntrophie entre *Clostridium* sp. et les

bactéries électroactives a été prouvée dans des co-cultures (Moscoviz et al., 2017), ce qui pourrait expliquer pourquoi les performances de BES_HT au niveau de l'abattement de la matière et des HAP sont parmi les meilleures observées. De plus, les bactéries Gram-positives sporulantes peuvent jouer un rôle important dans la biodégradation anaérobie des hydrocarbures aromatiques non-substitués (Kleemann and Meckenstock, 2011).

En conclusion, il a été mis en évidence que l'ajout du graphite poreux dans des digesteurs microbiens induit un changement de composition de la communauté microbienne ayant eu pour conséquence une activation de la dégradation de la matière et des HAP. Pour le NP, quelles que soient les conditions appliquées, les performances d'élimination sont excellentes mais identiques entres elles suggérant des processus impliqués différents et pour lesquels l'ajout de matériau n'a semblé avoir aucun effet. En effet, l'application d'un potentiel n'améliore en rien les performances de dégradation de la matière ou des HAP.

Cet effet positif du graphite poreux, matériau conducteur, sur la digestion anaérobie et sur les HAP a par la suite été exploré. L'objectif de la deuxième expérience a donc été d'observer l'effet de matériaux de nature et de conductivités différentes sur la dégradation de la matière et l'élimination des HAP. Pour cela, le graphite poreux a été remplacé par d'autres matériaux, le graphite non poreux et le platine, dans les mêmes conditions opératoires que les réacteurs précédents mais sans application d'un potentiel. Cette étude a montré un abattement des HAP de faible poids moléculaire indépendamment de la conductivité du matériau ajouté (graphite ou platine) et l'absence d'abattement pour les HAP de haut poids moléculaire.

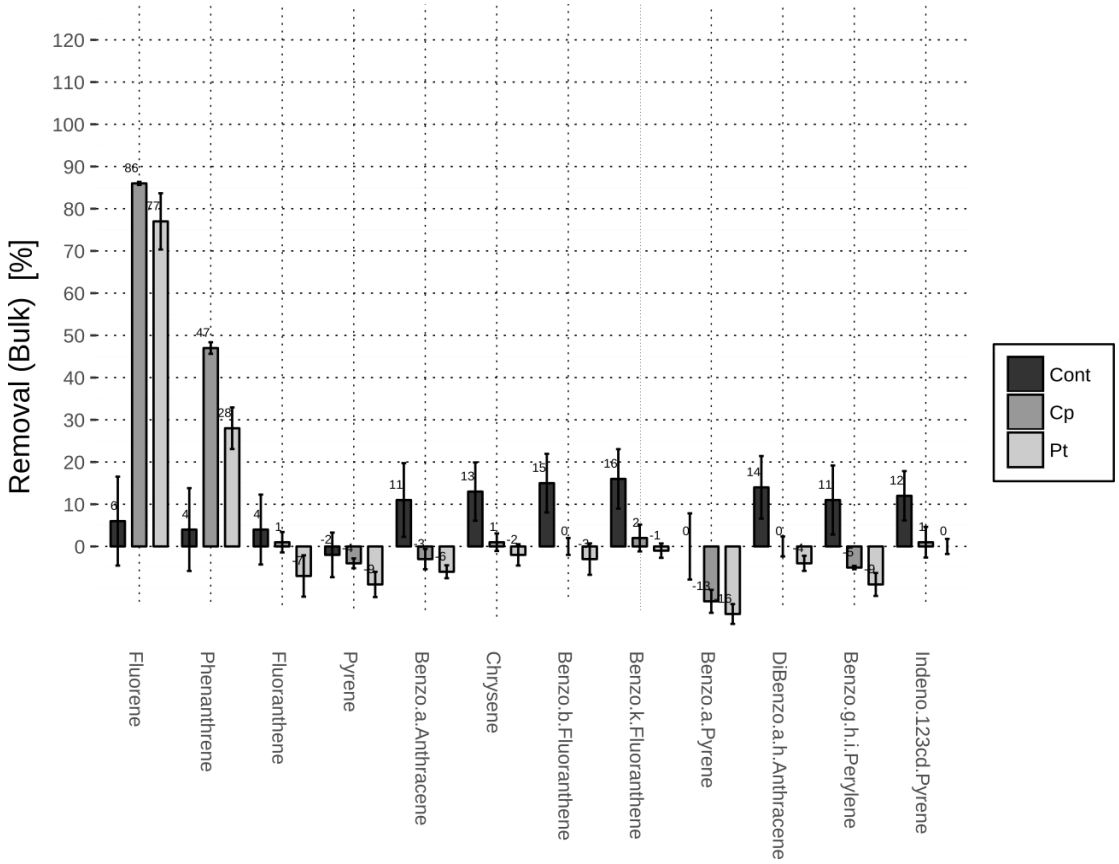

Figure 6: Abattement de 12 HAP dans la boue totale.
Contrôle anaérobie (Cont) et des digesteurs supplémentés avec du graphite non-poreux (Cp) et du platine (Pt). Les erreurs-types représentent 12 valeurs mesurées de réacteurs en triple exemplaire, chacune extraite de la boue deux fois et injectée deux fois en HPLC.

En effet, seuls le fluorène (Flu) et le phénanthrène (Phe) ont présenté des abattements de respectivement 12 à 14 et 7 à 11 fois supérieurs à ceux des digesteurs témoins (Figure 6). Après cette expérience de 42 jours, les réacteurs Pt ont montré une élimination de 77% et 28%, respectivement, de Flu et Phe, alors que Cp dépassait ces abattements atteignant 86% et 47% malgré une conductivité 1000 fois moindre (Bourke et al., 2007; Pauleau and Barna, 1997). Par conséquent, cette étude a montré que la conductivité des matériaux solides ajoutés aux digesteurs anaérobies n'est pas déterminante pour la performance d'élimination de ces 2 HAP dans les boues d'épuration. Aucune différence de production de méthane ou d'élimination de TS/VS entre les réacteurs témoins et les réacteurs avec un conducteur n'a été observée. Néanmoins, il a été observé que les partitions surtout du fluorène et du

phénanthrène (particulaire/aqueux) sont différentes entre la boue initiale (START), la boue des réacteurs témoins et celle des réacteurs Cp et Pt (Figure 7). En effet, ces deux HAP

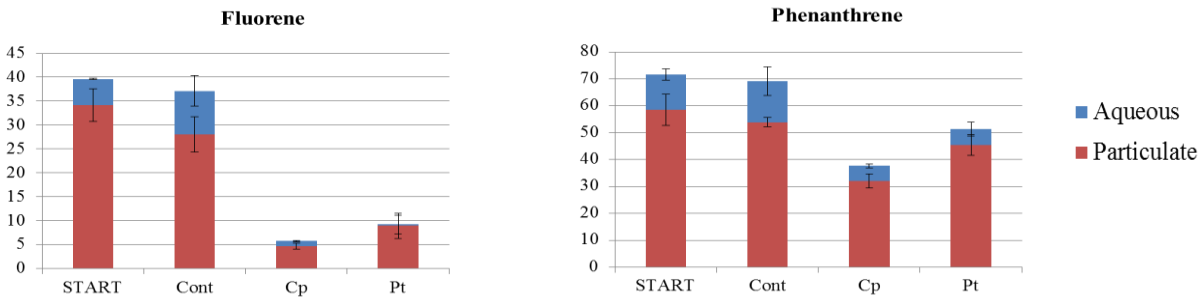

Figure 7: Partition du Fluorène et du Phénanthrène dans les phases particulaires et aqueuses des digesteurs non-traités thermiquement avant et après digestion anaérobie avec l'ajout des différents matériaux conducteurs.
Les erreurs standards correspondent à huit et seize valeurs HPLC (2 injections pour deux extractions des réacteurs en duplicats (Cp) ou triplicats (Cont, Pt) et six valeurs HPLC pour la boue initiale (START) correspondant à trois extractions. (Cp= Plaque de graphite, Pt= platine, Cont= digesteur de contrôle).

étaient moins présents dans la phase aqueuse suggérant un transfert et une élimination facilitée à l'aide des matériaux ajoutés (Barret et al., 2010; Fountoulakis et al., 2006). Dans un deuxième temps, un changement dans la composition de la communauté bactérienne a été observé pour les digesteurs anaérobies utilisant un matériau conducteur avec un enrichissement de 14 à 17% de l'OTU3 présentant une similarité de séquence à 99% avec le genre *Sporosarcina* appartenant à la classe taxonomique *Bacilli*. Les *Bacilli* ont déjà été identifiés dans des systèmes bioélectroactifs et peuvent avoir été enrichis en raison de l'échange d'électrons facilité avec des conducteurs solides établissant une passerelle entre les substrats organiques riches en électrons et les HAP déficients en électrons. De plus, les *Bacilli* ont déjà été identifiés comme bactéries capables de dégrader les hydrocarbures polycycliques. Une augmentation en abondance relative du genre *Methanobacterium* parallèlement avec *Sporosarcina* dans les digesteurs avec matériaux conducteurs suggère de plus une coopération syntrophique possible de ces taxa durant la méthanogénèse hydrogénotrophe. Cette composition bactérienne est différente de celle observée sur les réacteurs précédents avec le graphite poreux (Figure 4) alors que l'enrichissement en méthanogènes hydrogénotrophes est similaire (Figure 8). La première hypothèse formulée est que les espèces enrichies soient également les espèces responsables de l'élimination des 2 HAP en syntrophie ou non. Mais on peut aussi penser que les HAP sont éliminés co-métaboliquement et mieux éliminés grâce à la présence des communautés enrichies qui sont

différentes des réacteurs témoins. Toutefois, il n'est pas exclu qu'en troisième option, les espèces dégradantes soient présentes en faible quantité et donc non identifiées.

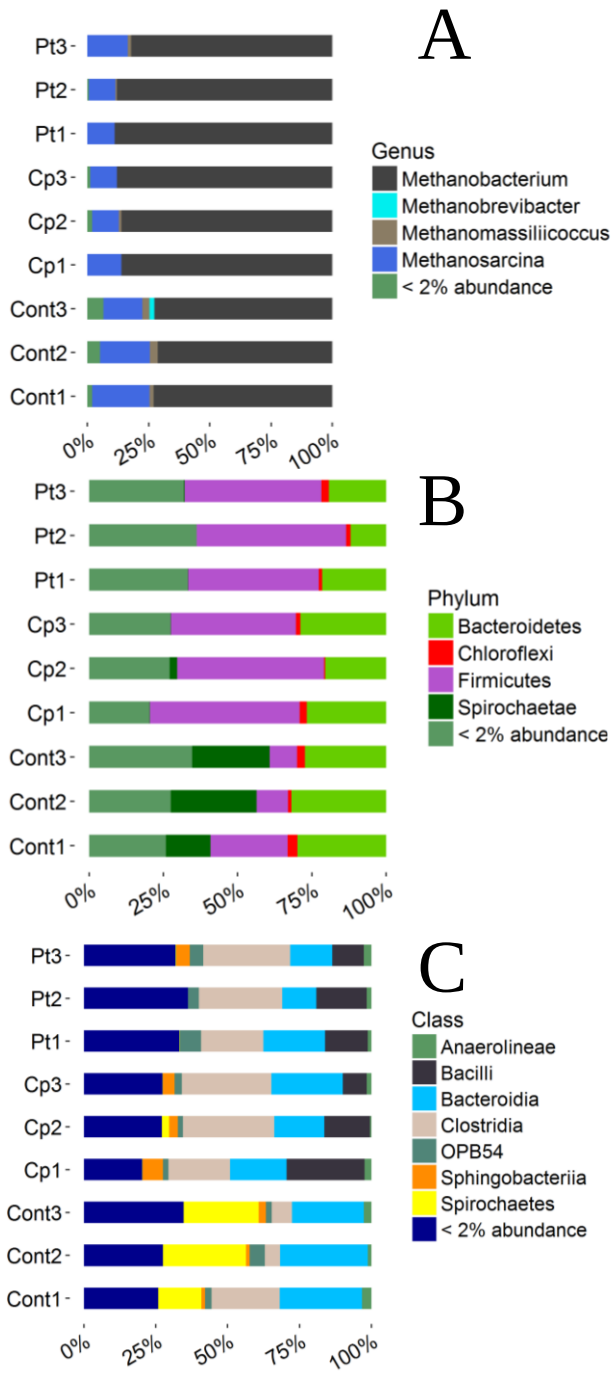

Figure 8: Abondances relatives des séquences de gènes de l'ARNr 16S bactérien.
Composition des communautés des *archées* au niveau du genus (A) et des bactéries au niveau du phylum (B) et de la classe (C).

Le graphite poreux, utilisé lors de la première expérience, avait une surface spécifique plus élevée que celle du graphite non-poreux et du platine de la deuxième expérience et les performances d'abattement étaient meilleures pour des HAP comprenant 4 à 6 cycles. Ces conclusions nous ont alors amené à tester l'effet de la surface spécifique du graphite poreux sur les performances d'élimination des HAP de haut poids moléculaire.

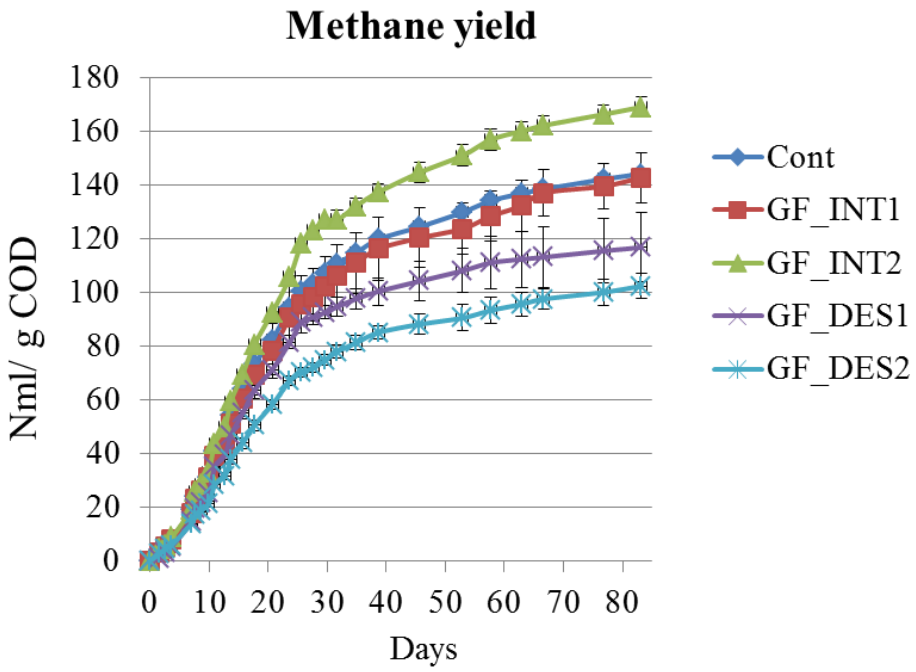

Figure 9: Production de méthane.
Le volume de méthane dans les conditions standards de pression et de température est normalizé par demande chimique en oxygène de la boue initiale.

En tant que résultats, l'analyse statistique des courbes de production de méthane (Figure 9) a montré des différences significatives entre la production de méthane des réacteurs possédant le graphite poreux en poudre (GF_DES1 et GF_DES2), les digesteurs témoins et les digesteurs employant du graphite poreux intact d'une surface spécifique de 2 m^2 (GF_INT2). Ainsi, l'ajout de 2 m^2 de GF intact aux digesteurs anaérobies a entraîné une augmentation significative du rendement en méthane. La plus faible production de méthane des réacteurs contenant du GF pulvérisé (alors même que la surface est augmentée) pourrait être expliquée par la destruction physique des cellules par perforation des membranes. Le

fait que le GF intact d'une surface spécifique de 2 m^2 produise le plus de méthane par rapport aux autres réacteurs pourrait être dû au fait que les espèces électroactives profitent d'un matériau conducteur qui canalise l'échange d'électrons des donneurs vers les accepteurs par analogie avec la coopération syntrophique entre les bactéries fermentaires et les archées. L'hydrogène en tant que molécule navette électronique est alors remplacé par le conducteur solide qui peut permettre un contact étroit et permanent entre ces communautés syntrophiques en offrant une surface adéquate pour la formation de biofilm. Cependant, les résultats du séquençage n'ont pas démontré de différences dans la composition microbienne des réacteurs GF et des témoins sans GF. Par conséquent, il est probable que la production accrue de méthane dans GF_INT2 repose sur la formation d'un biofilm sur la surface de GF sans l'enrichissement spécifique de communautés électroactives. Néanmoins, ce biofilm avec les mêmes abondances microbiennes que dans la boue totale doit avoir permis un échange facilité rendant à la fois les substrats, les métabolites et les communautés dégradantes bactéries et archées plus proches. Un enrichissement de *Methanobacterium* comme dans les expériences précédentes n'a pas été observé.

Les concentrations finales pour 10 HAP étaient les plus faibles lorsque le GF intact de 2 m^2 de surface spécifique était ajouté aux digesteurs, ce qui suggère un effet bénéfique du matériau sur l'élimination de ces composés (Figure 10).

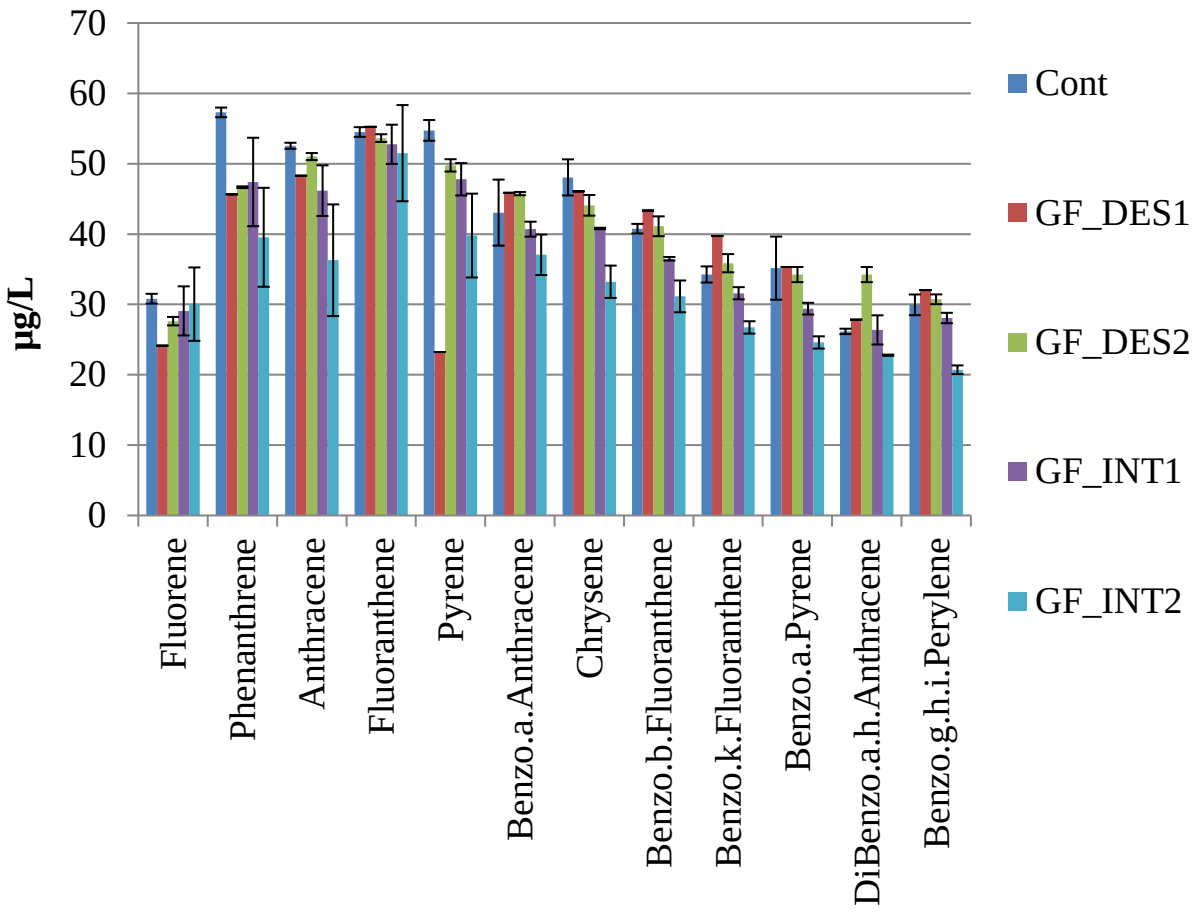

Figure 10: Concentrations finales de 12 HAP après digestion anaérobie dans des digesteurs sans traitement thermique.
Digesteurs de contrôles (Cont) sans matériau et avec du feutre de carbone déstructuré (GF_DES1, GF_DES2) ou intact (GF_INT1, GF_INT2) d'une surface de 1 m^2 et 2 m^2.

Les mécanismes sous-jacents sont cependant difficiles à identifier. Ils pourraient être liés à la formation d'un biofilm spécifique sur la surface de GF_INT2 qui permettrait une meilleure dégradation des HAP (par co-métabolisme par exemple) mais pourraient aussi être dus à l'action conjointe de ce biofilm et de la conductivité de GF. En conclusion, la surface de GF s'est avérée être un paramètre important pour l'élimination de la DCO et des contaminants. Afin de décider si seule la surface influence la production de méthane et l'élimination des HAP en donnant à la communauté microbienne la possibilité de construire des relations étroites ou si ces performances sont dues à l'action conjointe des caractéristiques de surface et de la conductivité de GF, il faudrait réaliser des expériences

supplémentaires. Des expériences de digestion anaérobie de boue pourraient être réalisées avec un polyester non conducteur et un GF conducteur sous la contrainte que les deux matériaux présentent les mêmes caractéristiques de surface en termes de porosité et l'absence de groupes fonctionnels de surface pour une adsorption égale des cellules, des contaminants et autres matières organiques.

Étant donné l'absence de données sur les concentrations initiales de HAP et de NP, il serait intéressant d'analyser les concentrations finales des phases particulaires de tous les digesteurs, comme cela a été fait pour l'addition de Cp et de Pt aux digesteurs anaérobies. Ces phases particulaires n'ont pas encore été extraites, et pourraient aider à comprendre pourquoi l'élimination des 12 HAP a été améliorée dans GF_INT2. On suppose que la partition particulaire/aqueux est différente pour cette condition par rapport à tous les autres digesteurs, comme le montre déjà l'addition de GF, Pt et Cp dans les chapitres précédents (Figure 2 et Figure 7).

De plus, les résultats ont démontré de manière concluante que l'élimination de NP au cours de la digestion anaérobie n'a pas été influencée par l'ajout de GF de différentes surfaces spécifiques avec un taux d'élimination entre 76% et 85% qui sont similaire pour toutes les expériences. L'hypothèse est que la dilution des boues rend ces composés disponibles et que la limitation de la biodégradation observée sur HAP en termes de transfert électronique ne joue pas pour ce type de composé (biomasse et métabolisme impliqués sûrement très différents).

V. Perspectives

Ces systèmes électrochimiques avec des matériaux conducteurs semblent être prometteurs tant pour maximiser l'élimination de contaminants que pour étudier les mécanismes d'élimination. Il faudrait travailler sur des systèmes simplifiés où les divers mécanismes de sorption, dégradation biotique et dégradation abiotique sont dissociés. L'une des conditions potentielles serait de travailler avec des communautés microbiennes traitées thermiquement. En effet, les performances d'élimination les plus élevées ont été observées pour les boues traitées thermiquement en présence de GF et également pour un potentiel

appliqué aux électrodes constituées de GF. Ces boues traitées thermiquement pourraient être centrifugées pour ne travailler qu'avec la phase aqueuse. Une filtration à 0,45 µm permettrait d'éliminer les bactéries. Cette phase aqueuse et filtrée pourrait alors être utilisée à l'intérieur d'une MEC. Le graphite non poreux devrait être utilisé comme électrode pour réduire la possibilité de sorption. Dans cette configuration expérimentale, seuls les HAP qui ont été transférés vers la phase aqueuse par le traitement thermique seraient toujours présents dans le MEC. Cette expérience permettrait ainsi de juger si le prétraitement des boues entraîne une forte élimination des HAP due aux transformations électrochimiques (élimination abiotique) comme déjà confirmé pour l'élimination améliorée des HAP après traitement thermique par oxydation chimique dans le sol (Usman et al., 2016). En cas d'absence d'élimination des HAP, il serait possible de constater un lien de causalité entre la biodégradation des micropolluants et les performances observées préalablement.

L'analyse transcriptomique de l'ARNm pourrait être utilisée pour identifier les protéines qui sont exprimées au cours de la digestion anaérobie en présence et en absence de HAP. Les rares enzymes connues jouant un rôle dans la dégradation des hydrocarbures aromatiques telles que la benzylsuccinate synthase pourrait être spécifiquement ciblée. L'abondance des gènes clés présents lors de la dégradation des HAP doit être quantifiée afin de confirmer l'implication de certains microbes dans la biodégradation anaérobie des HAP. De plus, un marquage isotopique en ^{13}C des HAP pourrait être utilisé pour vérifier si le carbone ^{13}C est assimilé par les microbes. Avec une recherche ciblée de gènes spécifiques par qPCR, cette procédure pourrait aider à confirmer la dégradation anaérobie des HAP par les espèces qui sont enrichies dans des systèmes simplifiés telles que les réacteurs traités thermiquement.

Dans une perspective d'ingénierie des procédés, nous pourrions dans un premier temps nous focaliser sur l'optimisation de la production de méthane par l'ajout de matériaux conducteurs ou par les MEC, par exemple en augmentant les surfaces spécifiques et quantifier ensuite les effets sur l'élimination des contaminants persistants mais aussi émergents (résidus de médicaments, hormones…).

En conclusion, l'utilisation de matériaux conducteurs économiquement abordables tels que le GF intact peut être considérée comme une stratégie d’amélioration de l’élimination des HAP des boues.

Introduction to the manuscript

A wide variety of organic contaminants from individual households, industry and vehicle gas exhausts are transferred through the sewage network into wastewater treatment plants (WWTPs). Both persistent and hydrophobic, polycyclic aromatic hydrocarbons (PAHs) and nonylphenol (NP), are only partly removed during biological treatment which is primarily designed to reduce the level of organic matter in the wastewater. These compounds are strongly sorbed to the particulate phase and, therefore, remain in low concentrations in the sewage sludge instead of being washed out as part of the effluent. The elimination of organic micropollutants has become a public health concern due to their toxicity and bioaccumulation through the trophic chain. Municipal sewage sludge treatments, therefore, plays a central role in reducing the micropollutant load before using the nutrient rich sludge as fertilizer in agriculture and causing diffuse pollution in soil and groundwater. It is, therefore, important to search for sustainable and few energy consuming solutions for the elimination of micropollutants from sludge. Anaerobic digestion is a stable process that not only reduces the amount of sludge matter but also produces methane that can be used for energy production by combustion. The removal performances of PAHs and NP during anaerobic digestion depends amongst others on the characteristics of the substrate, the residence time of the sludge, the hydraulic retention time and the temperature of the process. The use of microbial bioelectrolysis and the addition of conductive materials to anaerobic digesters appear as innovative solutions to address micropollutant contamination of sludge. They use the properties of electroactive bacteria that are bacteria capable of exchanging electrons with a conductive material to accelerate or stabilize the biodegradation process of matter.

The main objective of this thesis is to improve the removal of PAHs and NP during anaerobic digestion of sewage sludge with the help of experimental systems that make use of direct electron exchange. In order to satisfy this objective, the result chapters of this thesis evaluate the following three aspects.

- the application of a potential to a conductive material
- the nature of the conductive material
- the specific surface area of the conductive material

The present manuscript is structured in eight chapters. The first chapter reviews the existing literature on PAH and NP transformation including biodegradation and the use of microbial electrolyzers and conductive materials. The second chapter lays down the different techniques used in this thesis together with the experimental setups that were chosen to respond to the set of objectives. The third and fourth chapters discuss the results that were obtained by graphite felt addition to PAH and NP spiked anaerobic digesters in comparison to graphite felt addition (poised electrodes) inside a microbial electrolyzer. The fifth chapter summarizes the results obtained by the use of carbon plate and platinum, two different conductive materials, during anaerobic digestion and their impact on PAH removal. The sixth chapter discusses the removal of PAHs and NP by graphite felt addition of different specific surface areas to anaerobic digesters. The seventh chapter states the overall conclusions that have been made from the different experiments and the eighth chapter gives perspectives for future research opportunities.

Chapter I: Literature Review

List of figures

List of tables

1. Environmental concern of polycyclic aromatic hydrocarbons and nonylphenol

1.1 PAH and NP structure and toxicity

Polycyclic aromatic hydrocarbons (PAHs) represent a large group of persistent organic pollutants (POPs) whose structure basically consists of carbon and hydrogen atoms that form one or more aromatic rings. 16 PAHs are classified as priority hazardous substances by the environmental protection agency of the United Stated (USA-EPA) and listed in Table 1(Bojes and Pope, 2007). They can be divided into two categories: low molecular weight compounds consisting of fewer than four rings and high molecular weight compounds of four or more rings (Kim et al., 2013). Their solubility decreases and their partition coefficient increases with the number of aromatic rings since the increasing planar aromatic structure renders them more hydrophobic. The pi-electron system of their condensed benzene rings makes them particularly stable (Musat et al., 2009).

Table 1: Structure, molecular mass, solubility and partition coefficient of 16 priority PAHs.
Defined by USA-EPA and listed according to Kim et al., (2013).

PAH	Structure	Molecular mass (g/mol^{-1})	Aqueous solubility at 25°C (mg/L^{-1})	Partition coefficient K_{OW} (octanol/water)
Naphthalene (Naph)		128	32	3.3
Acenaphtylene (Acny)		152	3.93	4.07
Acenaphthene (Acn)		154	3.42	3.98
Fluorene (Flu)	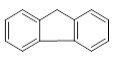	166	1.9	6.58
Phenanthrene (Phe)	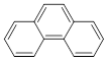	178	1	4.45
Anthracene (Ant)	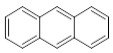	178	0.07	4.45

PAH	Structure	Molecular mass (g/mol^{-1})	Aqueous solubility at 25°C (mg/L^{-1})	Partition coefficient K_{OW} (octanol/water)
Fluoranthene (Flt)	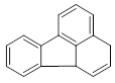	202	0.27	4.9
Pyrene (Pyr)		202	0.16	4.88
Benzo(a)anthracene (BaA)	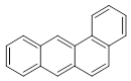	228	0.0057	5.61
Chrysene (Chry)	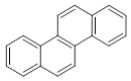	228	0.06	5.16
Benzo(b)fluoranthene (BbF)	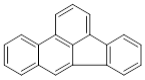	252	0.001	6.04
Benzo(k)fluoranthene (BkF)	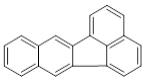	252	0.0008	6.06
Benzo(a)pyrene (BaP)	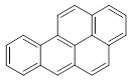	252	0.0038	6.06
Dibenzo(a.h)anthracene (DBahA)	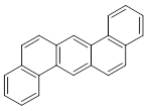	278	0.0005	6.84
Benzo(g.h.i)perylene (BghiP)		276	Insoluble	6.5
Indeno(1.2.3-cd)pyrene (Ind)	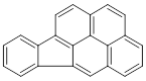	276	0.0008	6.58

PAHs are toxic and mutagenic (White and Claxton, 2004). Their carcinogenic activity is linked to their electronic structure (Manzetti, 2012) which is similar to that of hormones. In contrast to them, PAHs possess different metabolic pathways within organisms. For example, fish showed cardiac malformation, craniofacial defects and hemorrhaging upon PAH administration (Clark et

al., 2010). Diesel and petrol exhaust fine particulate matters contain PAHs which were shown to correlate strongly with oxidative stress in human cells (Wu et al., 2017). PAHs induce the uncoupling of the catalytic CYP1A1 cycle through the aryl hydrocarbon receptor to induce oxidative responses in humans (Knecht et al., 2013). The same study proved non carcinogenic PAHs, Flu, Phe, Ant, Flt, and Pyr to be cytotoxic.

Nonylphenols (NPs) are part of the larger group of alkylphenols which consist of a hydroxilized benzene ring and linear or branched saturated carbon chains as further substituents of the aromatic ring (De Weert et al., 2011). The many isomers are characterized by an amphilic behavior in case that the alkyl chain is linear and a rather hydrophobic behavior if the alkyl chain is branched since it can embrace polar groups of the molecular ($logK_{OW}$ = 4.48). Due to the lack of a point of attack for biological degradation, NP is a persistent xenobiotic in the environment with half-lives of biodegradation ranging from several days to more than 3 months (Mao et al., 2012) but is less persistent than PAHs that highly concentrated as in oil slicks exhibit half lives of many months to years (Prince et al., 2017). NP and their related nonylphenol ethoxylates NP1EO and NP2EO presented in Table 2 are most frequently found in wastewater treatment plants (WWTPs) (Gao et al., 2014; Samaras et al., 2014). These are of social concern since they cause harm as endocrine disrupting compound that can interfere with the hormonal system of numerous organisms. NPs were demonstrated not only to cause liver toxicity in rat (Kazemi et al., 2016) and reproductive dysfunctions in male fish (Sayed and Ismail, 2017) but also to be the cause of fertility loss in female and male humans who were exposed to NP in their adulthood (Noorimotlagh et al., 2017; Rattan et al., 2017).

Table 2: Structure, molecular mass, solubility and partition coefficient of NP,NP1EO and NP2EO.
(Lintelmann et al., 2003; Ying et al., 2002)

NP	Structure	Molecular mass (g/mol^{-1})	Aqueous solubility at 20°C (mg/L^{-1})	Partition coefficient K_{OW} (octanol/water)
Nonylphenol	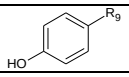	220	5,43	4,48
Nonylphenol monoethoxylate (NP1EO)	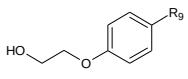	264	3,02	4,17
Nonylphenol diethoxylate (NP2EO)	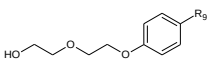	308	3,38	4,21

1.2 Sources and dissemination of PAHs and NPs

PAH derive from the incomplete combustion of fuel from vehicles (Lan et al., 2016), coal mining (Yakovleva et al., 2016) and leakages of oil pipelines, emissions of power plants and petroleum spills (Lübeck et al., 2016), surface run-off as well as other anthropogenic sources. High temperatures drive the condensation of benzene rings to give rise to PAHs' diversity. Natural sources such as forest fires and volcanic eruptions are less important sources (Srogi, 2007). However, midst diffuse pollution residential burning of wood, for instance, contributed strongly (84%) to the total Danish emissions in 2003 whereas traffic accounted for less than 5% (2006) (*Annual Danish Emission Inventory Report to UNECE,* 2003,Winther 2007).

PAH pollution is source dependent whereby macro-pollution of PAHs originates from localized sources such as industrial emissions and oil spills with high concentrations of contaminants (Lübeck et al., 2016) contrary to micro-pollution that comes from the diffuse presence of PAHs within large area extents. Diffuse pollution is characterized by low PAH concentrations and the lack of point sources (Johnsen and Karlson, 2007), for example exhaust fumes of vehicles (Wu et al., 2017). Once, released into the air by these sources, PAHs partition onto dust particle or simply stay in the gas phase (Wang et al., 2016). By wind they can be transported over long distances and by rainfall or dry deposition get transferred to soil, sediments, water bodies and surface waters. This is why they can be found at low concentrations in these recipient bodies (Srogi, 2007). They get concentrated when they are transported by rain and surface water to the sewage system, hence, the WWTP and the organic matter fraction in sewage sludge (Barret et al., 2010a). From here, they can disseminate to water bodies, soil and air again via the effluent of WWTPs (Qiao et al., 2017), sludge spreading for agricultural purposes (Stefaniuk et al., 2017) or sludge reduction via incineration (Zhang et al., 2016). An overview of possible dissemination pathways is given in Figure 1.

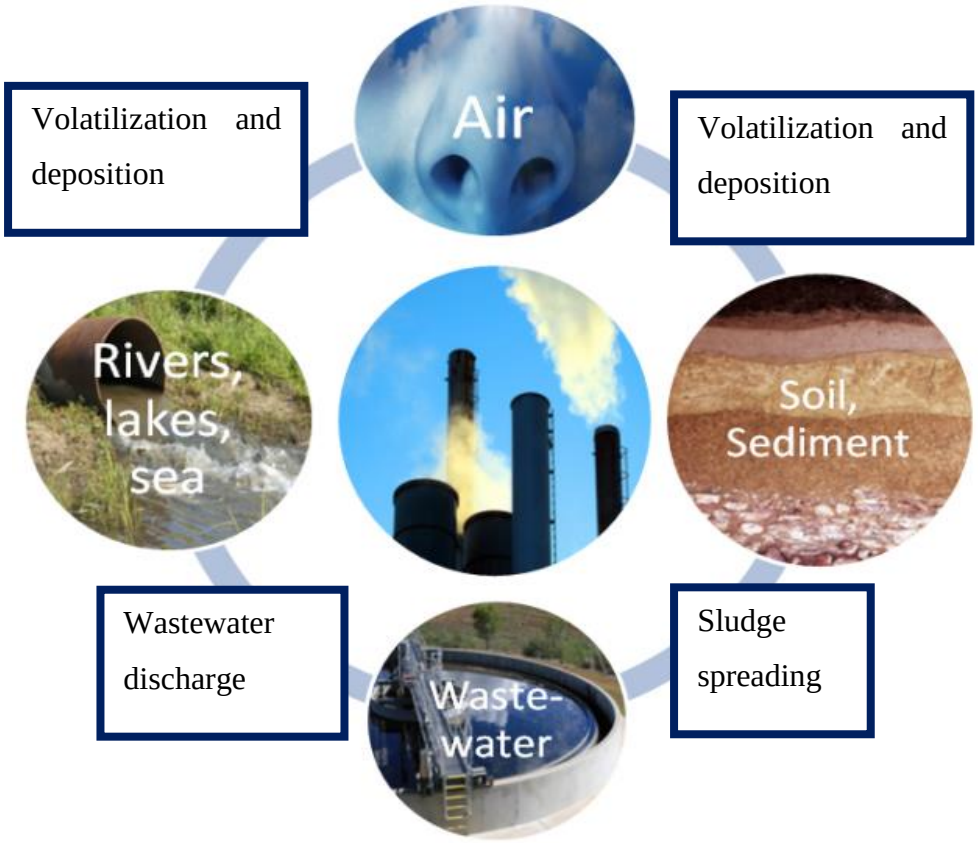

Figure 1: Incomplete combustion of fossil fuels and their transfer to different recipients

Nonylphenol polyethoxylates (NP_nEOs) are the parent molecules of NP. They are used in detergents, emulsifying agents, pesticides and other products for their quality to lower surface tensions between liquids (Nascimento et al., 2015) even if their usage was restricted in the formulation of some products by the EU Directive 2003/53/UE . Industrial wastewater as well as municipal sewage contains these molecules (Derco, 2017; Deshayes et al., 2015) which are easily transformed into NP and NP1EO or NP2EO within WWTPs (Soares et al., 2008; Ying et al., 2002). Residual concentrations of NP compounds in WWTP effluents pose risk to aquatic life and NP containing biosolids (Liao et al., 2014) can lead to dissemination of NPs to the environment (Gray et al., 2017) with detrimental health effect for organisms as described in section 1.1.

1.3 The role of wastewater treatment plants in PAHs and NPs removal

As discussed in section 1.2, PAHs (coming from urban run-off, vehicle exhaust) and NPs (present in industrial and domestic detergents) are transported into the sewer and converge in the WWTP

(Pérez-Leblic et al., 2012). WWTP play an important role in environmental protection since they can either represent a sink or a new source of these contaminants depending on treatment efficiencies within them. Influent and effluent NP concentrations of WWTPs in different countries has been reviewed by (Soares et al., 2008). The hydraulic retention time, pH and temperature are influencing NP removals as demonstrated for two different WWTPs (Samaras et al., 2013). A large amount of NPs and PAHs, however, is transferred to sludge. It was reported that more than 30 % of NPs (Janex-Habibi et al., 2009), 26 ± 15 % for NP1EO and 20 ± 10 % for NP2EO, respectively, were transferred to sludge (Stasinakis et al., 2008), adsorption being the major relocation pathways for all compounds (Bouki et al., 2010; Martin Ruel et al., 2010). NP adsorption on biomass is considered to be fast with a transfer of NP from the aqueous to the particulate phase as high as 90 % within 1 hour (Bouki et al., 2010). Removal efficiencies of six PAHs in two different MBR treatments were always higher than 97 % but their actual biodegradation varied in between 65 and 99 %, the extent of adsorption to sludge ranging from 10 to 50 % for PAHs with $\log K_{OW}$ of 4 to 5.2 (Mozo et al., 2011). After anaerobic anoxic-oxic treatment in a WWTP with total PAH concentration exceeding 15 mg/L, the overall removal of 16 PAHs was measured with 28.8 %, individual PAH removal ranging from -7.5% to 73.5%. Yet, in the grit stage 4,5,6-rings PAHs were readily adsorbed on suspending particles and sludge with removals of 22 – 25 % (Sun et al., 2012). It was remarkably high for benzo(g,h,i)perylene (50 %). Studies that report removal efficiencies of different stages of the water and sludge line also report significant removal of PAHs by adsorption in the grit stage (Tian et al., 2012). Table 3 summarizes a mass balance of NP and PAH concentrations from inlet and outlet of different WWTPs and their transfer to sludge. The values for NP removal that are reported in literature vary much in between types of sludge from different origin (municipal, industrial effluents) that underwent different treatments (anaerobic digestion, dewatering etc.) (Fernández-Sanjuan et al., 2009). In the same line, removal efficiencies between the different PAHs depend strongly on their physicochemical properties and the treatment process (Tian et al., 2012).

Table 3: PAH and NP inlet and outlet concentration of WWTP and sludge.

Inlet concentration [µg/L] average ± STD (max. – min.)			Outlet concentration [µg/L] average ± STD (max. – min.)			Removal on water line [%] average ± STD (average)			Transfer to sludge [mg/kg^{-1} TS] average ± STD (max. – min.) [adsorb.]			Author(s)
NP	NP1EO	NP2EO	NP	NP1EO	NP2EO	NP	NP1EO	NP2EO	NP	NP1EO	NP2EO	
0.23 (0.03 – 2.04)	5.8 (0.4 – 20.3)	4.0 (0.7 – 13.4)	0.18 (<0.030- 0.9)	0.89 (<0.34- 6.89)	1.84 (<0.41- 17.4)	-9	98 ± 1	91 ± 7	0.17	12.3	6.1	(Stasinakis et al., 2008)
15.7 ± 13.3	9 ± 17	2.9 ± 2.4	1.3± 1.5	0.47± 0.54	0.95± 2.6	84 ± 22 92	88 ± 11 95	- 67	9.9 ±4.3	8.9 ± 5.3	6.5 ± 4.5	(Martin Ruel et al., 2010)
11.6 (1 – 101.6)	14.3 (0.6 – 61.9)	4.4 (0.3 – 12.9)	1.0 (0.1- 7.8)	2.6 (<0.1- 35.9)	0.8 (<0.1- 4.0)	91	82	82	(3.8 _ 132.9)	(1.7 – 58.3)	(0.5 – 80.8)	(Janex-Habibi et al., 2009)
>1 (from image)	-	-	< 0.2 (from image)	-	-	82.9 – 93.5	-	-	33 [%]	-	-	(Derco, 2017)
170- 340	-	-	-	-	-	(84)	-	-	-	-	-	(Zhou et al., 2015)
PAH inlet concentration (µg/L)			PAH outlet concentration (µg/L)			Overall PAH removal on water line (%)			PAH adsorption to sludge (%) or sludge concentration before dewatering (mg/kg TS)			
> 15.1 (from figure)			~ 12 (from figure)			28.8			13.5 %			(Sun et al., 2012) ; 13 PAH
1.148 (summer) 1.157 (winter)			0.129(summer) 0.261 (winter)			88.8 (summer) 77.4 (winter)			0.15 mg/kg			(Tian et al., 2012) ; 16 PAH
800 – 80000 (from figure)			0.1- 650 (from figure)			97			10 – 50 %			(Mozo et al., 2011) ; 6 PAHs; MBR[1] industrial effluent
0.76 ± 0.57			0.05- 0.195			37 – 89			1.1 – 1.8 mg/kg			(Fatone et al., 2011) ; 16 PAHs in 5 different WWTPs

[1] Membrane bioreactor

The rise in worldwide wastewater sanitation causes an increase in sludge production from municipal sewers and studies estimate that the annual sludge production in the United States and Europe sums up to 6.5 and 11.5 million tons, respectively (Kelessidis and Stasinakis, 2012; LeBlanc et al., 2009; Venkatesan et al., 2015).

1.4 Concentrations of PAHs and NPs in sludge

The EU has suggested limits for PAHs in sludge in order to decrease diffuse pollution of such POPs in soil via fertilization with the sum of 11 PAHs (acenaphthene, phenanthrene, fluorene, fluoranthene, pyrene, benzo(b)fluoranthene, benzo(j)fluoranthene, benzo(k)fluoranthene, benzo(a)pyrene, benzo(g,h,i)perylene and indeno(1,2,3-cd)pyrene) that should not exceed a threshold of 6 mg/kg dry matter (Ju et al., 2009). Total concentrations of PAH molecules in sewage sludge range from below detection limit to 45 mg/kg dry matter in municipal sewage sludge that have been exposed to a secondary treatment (Aparicio et al., 2009; Ju et al., 2009) and range in between 218 and 3000 mg/kg for municipal sludge without treatment (Hung et al., 2015; Meng et al., 2016). NP concentrations of municipal sludge from secondary treatment vary from 0.5 to 464 mg/kg dry matter depending on the catchment area and the chosen process in the WWTP (Langdon et al., 2011). According to US EPA's 2001 National Sewage Sludge survey, the concentration of NP in sludge was 534 ± 192 mg/kg with 100 % detection frequency (Venkatesan and Halden, 2013). For NPs, yet, it is not unusual to find concentrations above 1000 mg/kg (Harrison et al., 2006). Table 4 lists concentrations of PAHs, NP, NP1EO and NP2EO that have been detected in sewage sludge in different European and non-European countries.

Table 4: PAH and NP_nEO concentrations detected in sewage sludge in different European and non-European countries.

PAH/NP	Sludge type	Concentration [mg/kg^{-1} TS]	Country	Author(s)
∑ (9 PAH) [2]	Raw, thermal dried or composted	< DL- 16	Spain	(Abad et al., 2005)
∑ 16 PAH[2]	Raw (primary)	0.4- 2.6	Poland	(Wisniowska and Janosz-Rajczyk, 2007)
	Excess	1.2- 4.5	Poland	(Wisniowska and Janosz-Rajczyk, 2007)
	Anaerobically digested	2.2- 5.2	Poland	(Wisniowska and Janosz-Rajczyk, 2007)
	Raw (primary)	< DL- max. 0.228 (Phe)	Spain	(Aparicio et al., 2009)
	Secondary	< DL – max. 0.678 (BaA)	Spain	(Aparicio et al., 2009)
	Anaerobically digested, dried	< DL – max. 2.184 (Phe)	Spain	(Aparicio et al., 2009)
	Raw (primary)	14.6- 30.9	France	(Blanchard et al., 2004)
	Different sludge types from 27 WWTPs	0.5- 11	France	(INERIS, 2014)
	Digested (anaerobic), dried	2.42 ± 1.50	Spain	(Roig et al., 2012)
	Digested (Aerobic), dried	2.96 ± 2.58	Spain	(Roig et al., 2012)
	Non-digested	1.36 ± 0.91	Spain	(Roig et al., 2012)
	Activated, precipitated, dewatered	1- 45, 10.4 (mean)	Korea	(Ju et al., 2009)
	24 municipal sewage sludge	15700 (mean, 1998); 3000 (mean 2012)	China	(Meng et al., 2016)
	Municipal, drainage system	218- 751, 456 (mean)	Vietnam	(Hung et al., 2015)
	Secondary	44- 199	Spain	(Fernández-Sanjuan et al., 2009)
	Anaerobically digested	4.8- 11.9	Spain	(Fernández-Sanjuan et al., 2009)
	13 WWTPs, different treatments	0.5- 464	Australia	(Langdon et al., 2011)

[1] Acenaphthene, phenanthrene, fluorene, fluoranthene, pyrene, benzo(b)fluoranthene, benzo(a)pyrene, benzo(ghi)perylene, indeno(1,2,3,cd)pyrene)
[2] 16 PAHs as listed by EPA, USA

NP	Anaerobically digested, dewatered	6.48 ± 2.61	Greece	(Samaras et al., 2014)
	Raw (primary)	4- 49	Spain	(Aparicio et al., 2009)
	Secondary	4.5- 18	Spain	(Aparicio et al., 2009)
	Primary, dewatered,	27.6	Greece	(Fountoulakis et al., 2005)
	Secondary, dewatered	59	Greece	(Fountoulakis et al., 2005)
	Secondary, centrifuged (4 WWTPs)	61.7- 161.4 (means)	France	(Ghanem et al., 2007)
	Activated	100	Italy	(Bruno et al., 2002)
	Anaerobically digested	40	Italy	(Bruno et al., 2002)
NP1E0	Raw (primary)	<DL – 72	Spain	(Aparicio et al., 2009)
	Secondary	< DL- 26	Spain	(Aparicio et al., 2009)
	Anaerobically digested, dewatered	1.86 ± 0.58	Greece	(Samaras et al., 2014)
	Primary, dewatered,	90.5	Greece	(Fountoulakis et al., 2005)
	Secondary, dewatered	45	Greece	(Fountoulakis et al., 2005)
	Secondary	44- 199	Spain	(Fernández-Sanjuan et al., 2009)
	Anaerobically digested	4.8- 11.9	Spain	(Fernández-Sanjuan et al., 2009)
NP2EO	Raw (primary)	<DL-47	Spain	(Aparicio et al., 2009)
	Anaerobically digested, dewatered	1.32 ± 0.55	Greece	(Samaras et al., 2014)
	Activated	242	Italy	(Bruno et al., 2002)
	Anaerobically digested	308	Italy	(Bruno et al., 2002)
$\sum$ **(NPnEO)**[3]	Raw, thermal dried or composted	659	Spain	(Abad et al., 2005)

[3] NPnEO: NP, NP1EO, NP2EO

POPs are ubiquitous contaminants that are present in all environmental compartments. Main transformations in the environment happen via volatilization, sorption and chemical or biological transformations. In order to remove these contaminants within sludge or soil, abiotic removal options include immobilization on a material, electrokinetic removal and advanced oxidation, including photolytic processes.

2. Abiotic removal of polycyclic aromatic hydrocarbons and nonylphenol

2.1 Physical removal of PAHs and NPs

Physical methods for organic contaminant removal in soil, sediment and wastewater comprise removal techniques that are based on the adsorption of contaminants to a material. Carbonaceous materials such as graphite, granular or powdered activated carbon can immobilize PAHs, NPs and a wide spectrum of other contaminants on their surface due to their hydrophobicity and large surface area (Fan et al., 2017; Guo et al., 2017). Removal mechanisms include electrostatic, polar or non-polar attraction and the sequestration or partitioning of contaminants into particulate matter as depicted in Figure 2 for the adsorption to biochar.

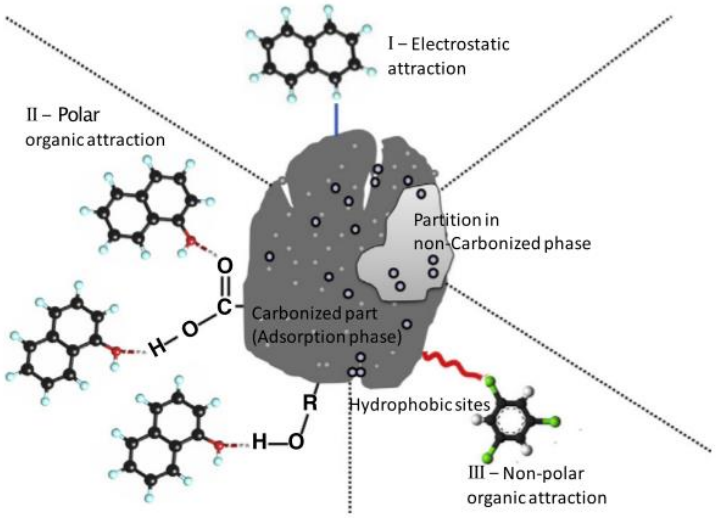

Figure 2: Postulated mechanisms of the interaction of biochar with organic contaminants. (Ahmad et al., 2014).

Polar organic attraction is excluded in the case of PAHs but can be an adsorption mechanism if PAHs are modified with polar side chains. Specifically, oxygen containing carboxyl-, hydroxyl- and phenolic side chains of the biochar surface can interact with soil contaminants (Uchimiya et al., 2011). Sorption of PAHs to graphite surfaces such as biochar (Guo et al., 2017; Tran-Duc et al., 2010) and soot (Kubicki, 2006) was reported. Subsequent desorption is judged negligible for biochar (Hilber et al., 2017) whereas it is more important for soot (Sigmund et al., 2017). Sorption capacity of biochar depends on its surface area, microporosity, and hydrophobicity. Phenanthrene was found to sequester into the meso- and micropores of biochar (Zhang et al., 2010) and PAH partitioning was observed to biochar amended sludge (BAS) for soil application (Khan et al., 2013; Stefaniuk et al., 2017). At application rates of 10 % of biochar, BAS reduced bioaccumulation of PAHs in lettuce that was grown on contaminated sites by between 56% and 67%, while sewage sludge alone reduced bioaccumulation of PAHs by less than 44%. Activated carbon addition to three soils from a coking plant area that was contaminated with 16 PAHs at 9-40 mg/kg performed better than biochar from willow and straw for PAH immobilization (Kołtowski et al., 2016). Activated carbon reduced the dissolved concentration of PAHs in soil pores by 51–98 % already at 0.5 % (w/w) whereas the two biochar amendments reached similar performances of 37–68 % (wheat-straw) and 44–86 % (willow) only at higher doses (2.5 %). The economically more advantageous biochars could not compete with activated carbon whose performances are probably due to their lower specific surface area (23 - 56 times) and lower affinity.

On the other hand, sorption of NP to cheap carbon materials such as black carbon (BC) has been described as significant and was attributed to the presence of micropores and functional groups (Jonker et al., 2005) resulting in a high desorption resistance (Cheng et al., 2017a). Sorbents that have been also tested for NP remediation comprise carbon nanotubes (Jin et al., 2015), magnetic composite adsorbent (Zhen et al., 2015) and activated carbon (Yu et al., 2008). Kaminska and Bohdziewicz (2009) tested the potential of various materials for adsorption of NP from wastewater. They also found that parameters other than SSA are decisive for contaminant adsorption. Above 90 % of NP was removed from artificial wastewater by the action of activated carbon and carbon nanotubes whereas aluminosilicates (ALS) removed less than 50 % with the same initial NP concentrations of 1500 µg/L and sorbent concentration of 100 mg/L even though

ALS possesses similar SSA to activated carbon (800- 900 m^2/g). NP adsorption was fastest for carbon nanotubes despite the fact that they exhibit half of the specific surface area of activated carbon. On the other hand, a correlation between SSA and adsorption performance was shown for in wastewater when NP removal was systematically below 50% for powdered activated carbon (PAC) doses of 15 to 50 mg/L while increasing with PAC doses of 100 mg/L (Noutsopoulos et al., 2014).

Another physical removal technique is based on the partitioning of contaminants into different solvents due to their octanol-water partition coefficient. Two-phase partitioning bioreactors (TPPB) are used in PAH bioremediation in order to increase the mass transfer of PAHs to the aqueous phase. In a first step, a water-immiscible, biocompatible and non-biodegradable liquid dissolves the water-immiscible PAHs. Through mixing and the addition of surfactants, in a second step, the total surface area between PAHs and the aqueous phase is increased. Thirdly, the higher surface leads to higher mass transfer rates of PAHs to the aqueous phase which results in improved biodegradation (Déziel et al., 1999). Such strategy has achieved very high degradation rates up to 1500 mg/day/L employing a bacterial consortium of genus *Sphingomonas* (Vandermeer and Daugulis, 2007). Similarly, soil washing in a two-phase system followed by microbial degradation with *Mycobacterium sp.* resulted in 93 % removal of total PAHs which was higher than soil washing and microbial action alone (Gong et al., 2015). Sorption of PAHs to polyurethane pellets in soil and subsequent treatment in a TPPB achieved approximately 78 %, 62 % and 36 % of phenanthrene, pyrene, and fluoranthene desorption and biodegradation after 14 days (Rehmann et al., 2008). A schematic description of the treatment process is depicted in Figure 3.

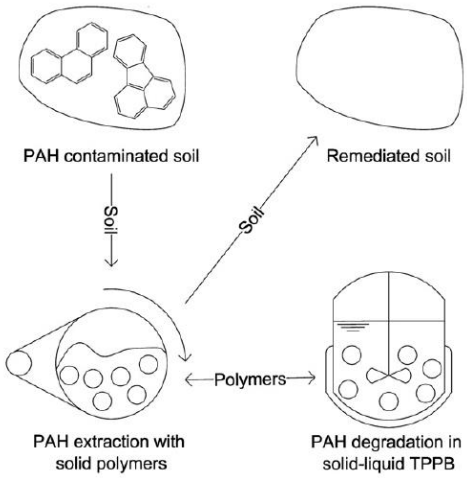

Figure 3: Extraction of PAHs or NPs from soil with solid polymers in a TPPB.
PAH and NP degradation in a two-phase partitioning reactor (TPPB) and subsequent transfer to remediated soil (Rehmann et al., 2008).

The first two phase partitioning reactor for endocrine disruptors (EDs) was developed in 2013. Ouellette et al. (2013) tested a solid polymer (Hytrel) for its capacity to extract and concentrate NP as well as five other EDs. They found that even though NP had a similar Hytrel/water partition coefficient ($K_{h/w}$= 5.10) as PAHs, it may not be sufficient to sustain microbial growth without the supply of an additional carbon source. They conclude that the tested polymer is a good choice for NP partitioning in two phase reactors since it is water-immiscible, safe to use, non-toxic to microorganisms, thermostable for sterilization and stable at different pH values and in various culture media. In the follow-up study, hytrel could extract NP and favour its biodegradation about 30 % with a ED degrading enrichment culture that was adapted to hytrel (Villemur et al., 2013). Further studies about NP removal in TPPB are not available up to this date.

2.2 Electrokinetic removal of PAHs

Another process used to remove PAHs from contaminated sites is electrokinetic treatment. It consists in a controlled application of current in order to favour electrical migration and electro-osmosis together with the electrolysis reactions at the electrodes (Chen et al., 2011). Electrokinetic treatment is used to promote the migration and osmosis of PAHs to the subsurface of soil of a contaminated environmental site where they can be concentrated and discarded. For this aim, an electrical current is applied between two electrode chambers (Alcántara et al., 2012; Chen et al., 2011) such that the resulting electric gradient favours PAH migration. Non-polar

organic pollutants are a challenge for this technique since they are weakly desorbed from soil but these low removal efficiencies can be overcome by the addition of solubilizing agents during electrokinetic treatment (Alcántara et al., 2009). For example, phenanthrene was removed to 95 % from kaoline soil with an electrokinetic approach when a co-solvent (ethanol) and a surfactant (Tween 20) were employed followed by electrochemical oxidation (Alcántara et al., 2008). The first study that assessed NP removal through electrokinetic treatment applied a current of either 10 or 20 mA in order to favour the transfer of NP to the anode (Guedes et al., 2014). Yet, NP was never detected in the anolyte but the percentage of NP remaining in the soil decreased. Therefore, the authors stipulated that photo- and electrodegradation made up for 48 -53 % removal. Electrokinetic treatment was not further developed for NP to the knowledge of the author.

2.3 Chemical and photolytic removal of PAHs and NPs

Advanced oxidation comprises remediation processes that involve the generation of hydroxyl radicals such as ozonation, UV- radiation and Fenton-like reactions (Glaze et al., 1987; Pignatello et al., 2006). Ozone is a standard oxidizing agent in current advanced treatment of wastewater and has been successfully applied in practice for sludge treatment in some European countries and Japan (Qiang et al., 2013). The OH-radical is the key reactive intermediate when ozone decomposes in water. In the presence of common water contaminants, for example, bicarbonate or humic substances, hydroxyl radicals can be trapped, forming a wide range of secondary reactive species until the radical chain mechanism is broken by radical-radical combination (Glaze et al., 1987). The process depends on the concentration of ozone, hydrogen peroxide (H_2O_2) and the pH value. The mechanisms of PAH removal by ozonation were explored recently and it was found that adsorption of PAHs on activated coking sludge strongly limited the process efficiency (Lin et al., 2016). Nonetheless, ozone pretreatment of sludge before anaerobic digestion allowed to solubilize lower and higher weight PAHs leading to 68 % more removal, on average, for the sum of 12 PAHs (Bernal-Martinez et al., 2007). As a comparison, anaerobic digesters with a high sludge retention time of 40 days that were combined with ozone addition of 0.11 g O_3/g total solids (TS) during sludge digestion enhanced PAH removal about 14 % (Bernal-Martinez et al., 2009). Ozone post-treatment enhanced anaerobic mesophilic NP removal by 48 % (Patureau et al., 2008). Recently, these removals were exceeded by the combination of ozone and electrochemical treatment with boron-diamond anodes that achieved 68 % removal of

NP from sewage sludge within an hour (de Leon-Condes et al., 2017) and by microwave peroxide oxidation that removed 95 % NP from sewage sludge at 150 °C within 3 min. Moreover, the addition of hydrogen peroxide to the ozonation of sludge could reinforce phenanthrene and anthracene degradation about 27 % and 21 % (Ning et al., 2015). Overall removals were best at an ozone flow rate of 0.4 L/min, a reaction time of 15 min, pH 7 and H_2O_2 doses of 0.60 mol/L with optimal removal rates of 89 % for fluorene, 66% for phenanthrene, 71% for anthracene and 81% for dibenzo(a,h)anthracene with respect to initial concentrations of 31, 107, 132 and 3 mg/L, respectively and a sludge moisture content of 98 %.

In the Fenton reaction, hydroxyl radicals are generated *in situ* due to the redox reaction between ferrous iron and hydrogen peroxide (Kehrer, 2000). Since the Fenton reactions needs very acidic pH, it cannot be done simultaneously to biodegradation of PAHs but only as pretreatment or polishing step (Yap et al., 2011). For instance, it was reported that biodegradation achieved the removal of low molecular weight PAHs (2-3 rings) in soil while the recalcitrant high molecular weight PAHs (4-5 rings) were subsequently removed by Fenton oxidation (Nam et al., 2001). Phenanthrene removal rates were much higher ((43 compared to 19 mg/kg/h) when a surfactant was used to increase phenanthrene bioavailability and subsequent electro-Fenton treatment (Iglesias et al., 2014). Under optimal conditions, the initial phenanthrene concentration was degraded about 92 % per day.

The comparison of different oxidation methods led to a total removal of 11 PAHs of 71 % (H_2O_2, 4.9 M) > 63 % (Fenton) > 60 % (sunlight at ambient air) > 23 % (H_2SO_4) in decreasing order (Karaca and Tasdemir, 2015) with respect to a sludge dry matter (DM) content of 22 % and total initial PAH concentrations of 1.4 mg/kg DM. Additionally, ultraviolet (UV) treatment was compared to UV-titanium dioxide (TiO_2) amendment for PAH removal from sludge and it was found that the sum of 12 PAHs was better removed with increasing amounts of TiO_2 and a temperature rise from 15 °C to 45 °C. Maximum PAH removal ratio (83%) was obtained with 20 % TiO_2 at 45 °C in comparison to 36 % with UV treatment alone (Karaca and Tasdemir, 2014) at DM content of 20 % and initial total PAH concentration of 3.3 mg/kg DM. Several other oxidation reagents have been tested for PAH and NP removal in soil and wastewater including persulphate (Usman et al., 2012) and permanganate (de Souza e Silva et al., 2009; Forsey et al., 2010; Jiang et al., 2012).

2.4 Limits of abiotic degradation of PAHs

The abiotic removal techniques of POPs that were described above intended either to augment their bioavailability for subsequent biodegradation or to favour their immobilization to a material or to break them ultimately or to generate most easily degradable transformation products. Two phase reactors and advanced oxidation processes (AOPs) are mainly ex situ techniques which is often regarded as a drawback (Jorgensen, 2011). For AOPs, there are more drawbacks such as the need of high temperatures, pressures, large amounts of reagents or complex equipment (Pera-Titus et al., 2004). Electrokinetic remediation and black carbon addition are *in situ* approaches of contaminant removal. Yet, economical alternatives to activated carbon still fall short of expected performances and the addition of synthetic surfactants to increase PAH's solubility during electrokinetic treatment can disturb the balanced ecological functions of soil biota due to their toxicity (Rosal et al., 2010). On account of the described drawbacks of abiotic POP removal, biological remediation of PAHs and NPs is an advantageous alternative since bacteria play a fundamental role in the removal of contaminants from the environment (Hatamian-Zarmi et al., 2009; Pieper and Seeger, 2008). Bioremediation describes techniques that are used to stimulate microbial communities or single strains which have already been found to degrade specific contaminants.

3. Bioremediation of polycyclic aromatic hydrocarbons and nonylphenol

Numerous aerobic bacteria that utilise PAHs as a carbon and energy source have been isolated (Venkata Mohan et al., 2006), thus revealing that PAHs containing 2 to 4 rings can be easily biodegraded in environments where oxygen is available (Cerniglia, 1993). Equally, NP is quickly degraded under aerobic conditions (Ying et al., 2003). Bioventing is a technique that supplies oxygen so as to create aerobic conditions. However, the delivery of oxygen to sediments has been criticized as ineffective (Cruz Viggi et al., 2015) since oxygen rapidly diffuses away from where it was applied (Zhang et al., 2010). Moreover, considering that most contaminated sediments and soils are oxygen depleted, *in situ* bioremediation of POPs is often associated with anoxic or anaerobic conditions. Anaerobic conditions are characterized by the absence of oxygen and the presence of other electron acceptor like nitrate, ferrous, sulphate or carbon dioxide. Such

anaerobic conditions are often present on wastewater and sludge treatment plants. They could play an important role in micropollutant removal.

3.1 Anaerobic digestion

Anaerobic digestion is a widespread biological process in nature which takes place in the digestive apparatus of many animals but can be found in many different habitats (Schink and Stams, 2006). Anaerobic digestion converts organic matter into biogas that is composed of about 60 to 70 % of methane and 30- 40 % carbon dioxide as listed in Table 5 (Arnaud and Gricourt, 2015).

Table 5: Biogas composition (dry) from anaerobic digestion (Moletta, 2015).

Gaz	CH_4	CO_2	H_2S	N_2	NH_3	Others
Percentage (v/v)	60 – 70	30 – 40	0 - 0.4	0 – 0.2	0 - 0.1	0 – 0.01

Anaerobic digestion of sewage sludge or other organic waste is used to reduce biosolids and produce methane whose energetic valorization is quantified by its inferior calorific value of 9.94 kWh/Nm^3 (8 575 kcal/Nm^3). Accordingly, biogas with a higher percentage of methane has got a higher calorific value (Camcho and Prévot, 2015, p. 214). Biogas can be used for electricity and heat cogeneration after some polishing steps. An additional advantage is the fact that biogas can be stored as an energy vector. The organic matter which is not converted by this biological process is still a valuable product used as fertilizer in agriculture since it is still rich in carbon, phosphorus and nitrogen and if sufficiently stable, free from pathogens and organic contaminants. In the WWTP, anaerobic digestion is used as one possibility of sludge treatment after primary and secondary treatment of the sewage influent as depicted in Figure 4.

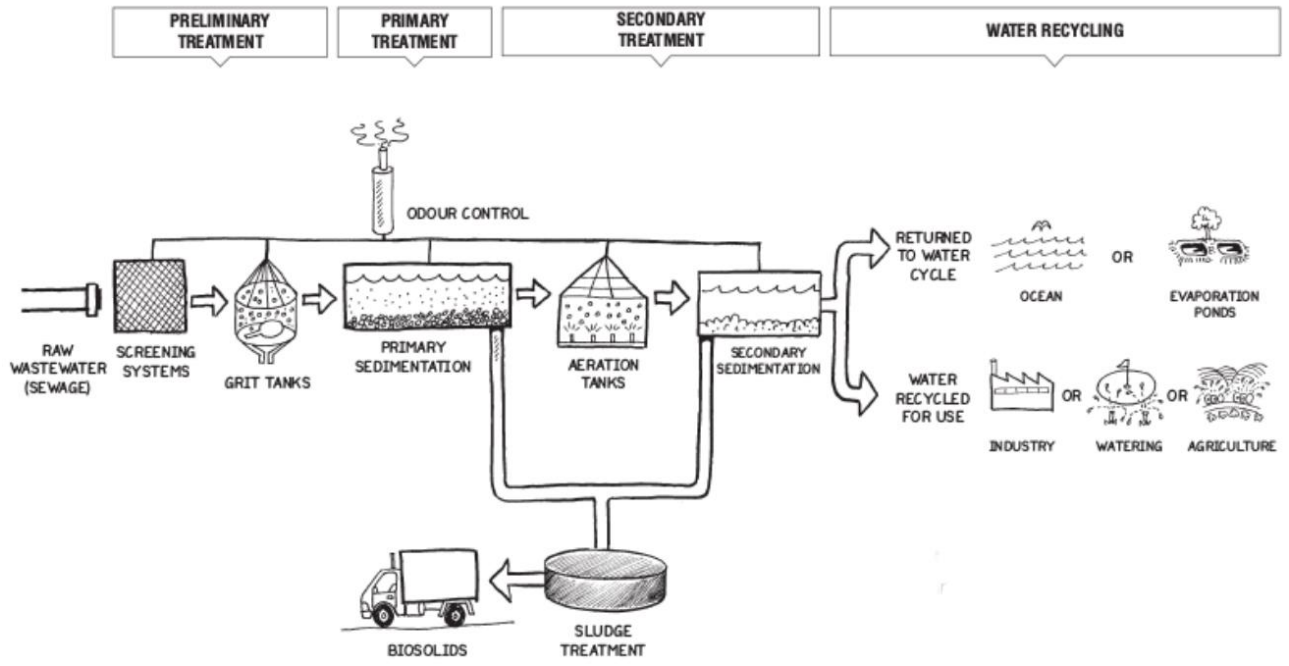

Figure 4: Wastewater treatment plant flow.
(https://www.watercorporation.com.au/home/education)

Additionally, municipal sewage sludge is a lowly contaminated but highly complex organic matter in which PAH and NP removal under methanogenic condition is a possible biological removal pathway as described in chapter 3. Therefore, anaerobic digestion offers the advantage of simultaneous production energy and biodegradation of compounds that are unwanted in the digestate. PAH biodegradation under methanogenic condition was shown to result from a combination of bioavailability and cometabolism with dry matter removal rate as the criterion for cometabolism (Barret et al., 2010a).

Anaerobic digestion consists of four different steps that are governed by the activity of different microbial communities. These are hydrolysis, acidogenesis, acetogenesis and methanogenesis. Roughly, the first three steps imply the activity of bacteria that breakdown macromolecules into proteins, lipids and sugars, then further metabolize these to carboxylic acids and then finally to acetate as the main product next to the gases hydrogen and carbon dioxide. The last step is the production of methane by the archaeal microbial community. These four steps are explained in detail in the following.

Rate limiting step of anaerobic digestion is the very first step (Vavilin et al., 1996; Zhang et al., 2007): hydrolysis. Hydrolytic bacteria excrete lipases, proteases and cellulases for enzymatic breakdown (Montero et al., 2008) of complex organic matter which consists of lipids, polysaccharides and proteins as well as nucleic acids into oligo- and monomers such as amino acids, fatty acids, pyrimidines, purines, glycerol and monosaccharides (Schink and Stams, 2006). Examples of bacteria that are responsible for hydrolysis are *Clostridium* sp., *Peptococcus* sp. (amino acids), *Acetivibrio cellulolyiticus, Staphylococcus* sp. (polysaccharides) and *Clostridium* sp. as well as *Micrococcus* sp. (lipids) (Amani et al., 2010).

Acidogenesis is 30 to 40 times faster than the previous hydrolytic step. During acidogenesis, amino acids, sugar and volatile fatty acids (VFAs) that were obtained during hydrolysis are further transformed to short chain VFAs such as acetate, propionate, butyrate, (iso)valerate and (iso)caproate as well as some short chain alcohols and lactate by acidogenic bacteria such as *Escherichia coli, Lactobacillus* and *Clostridium* sp. (Amani et al., 2010).

In acetogenesis, all metabolites from acidogenesis are consumed by microorganisms to give acetate, carbon dioxide and hydrogen. On the one hand, heteroacetogenic bacteria utilize VFAs and alcohols to produce hydrogen, carbon dioxide and acetate [ex: *Syntrophobacter wolinii, Syntrophomonas wolfei* (Amani et al., 2010)]. On the other hand, homoacetogenic bacteria use hydrogen and carbon dioxide to give acetate as the only endproduct [ex: *Clostridium aceticum* (Amani et al., 2010)].

In methanogenic step, the microbial archaeal community transforms acetate, carbon dioxide and hydrogen into methane. Acetoclastic methanogens (*Methanosaeta concilii, Methanosarcina acetivorans)* use acetate, hydrogenotrophic methanogens (*Methanobacterium bryantii, Methanobrevibacter arboriphilus)* use hydrogen and methylotrophic methanogens use methanol or methylated compounds as energy source such as methylamine (Amani et al., 2010; Garcia et al., 2000) for methane production. All methanogens belonging to the orders of *Methanomicrobiales*, *Methanobacteriales*, *Methanococcales* and *Methanopyrales* are able to catalyse hydrogenotrophic methane production. Within the order *Methanosarcinales*, only the genus *Methanosaeta* is not hydrogenotrophic according to reaction R1.

R1 $HCO_3^- + H^+ + 4\ H_2 \leftrightarrow CH_4 + 3\ H_2O$ ($\Delta\ G_0 = -139\ kJ/mol^{-1}$)

Acetoclastic methanogens transform acetate into methane and carbon dioxide according to reaction R2. They belong exclusively to the genus *Methanosarcina* and *Methanosaeta* (order *Methanosarcinales*) (Amani et al., 2010).

R2 $CH_3COO^- + H_2O \leftrightarrow HCO_3^- + CH_4$ ($\Delta\ G_0 = -31\ kJ/mol^{-1}$)

Methylotrophic methanogens belong exclusively to the genus *Methanosarcina* (order *Methanosarcinales*). They produce methane and carbon dioxide according to reaction R3 (Moletta, 2015).

R3 $4\ CH_3OH \leftrightarrow 3\ CH_4 + CO_2 + H_2O$ ($\Delta G_0 = -107\ kJ/mol^{-1}$)

The inhibition of methanogenesis can happen if products from acidogenesis for instance VFA accumulate (Hori et al., 2006). This interdependency demonstrates the complexity of anaerobic digestion since it implies syntrophic[4] cooperation between VFA producing acidogens and VFA, hydrogen and carbon dioxide consuming methanogens (Amani et al., 2010). The overall methanogenic pathway of organic matter degradation is depicted in Figure 5.

[4] '*Syntrophy is a special case of symbiotic cooperation between two metabolically different bacterial guilds which depend on each other for the degradation of a certain substrate, typically through transfer of one or more metabolic intermediate(s) between the partners.'* (Schink and Stams, 2006)

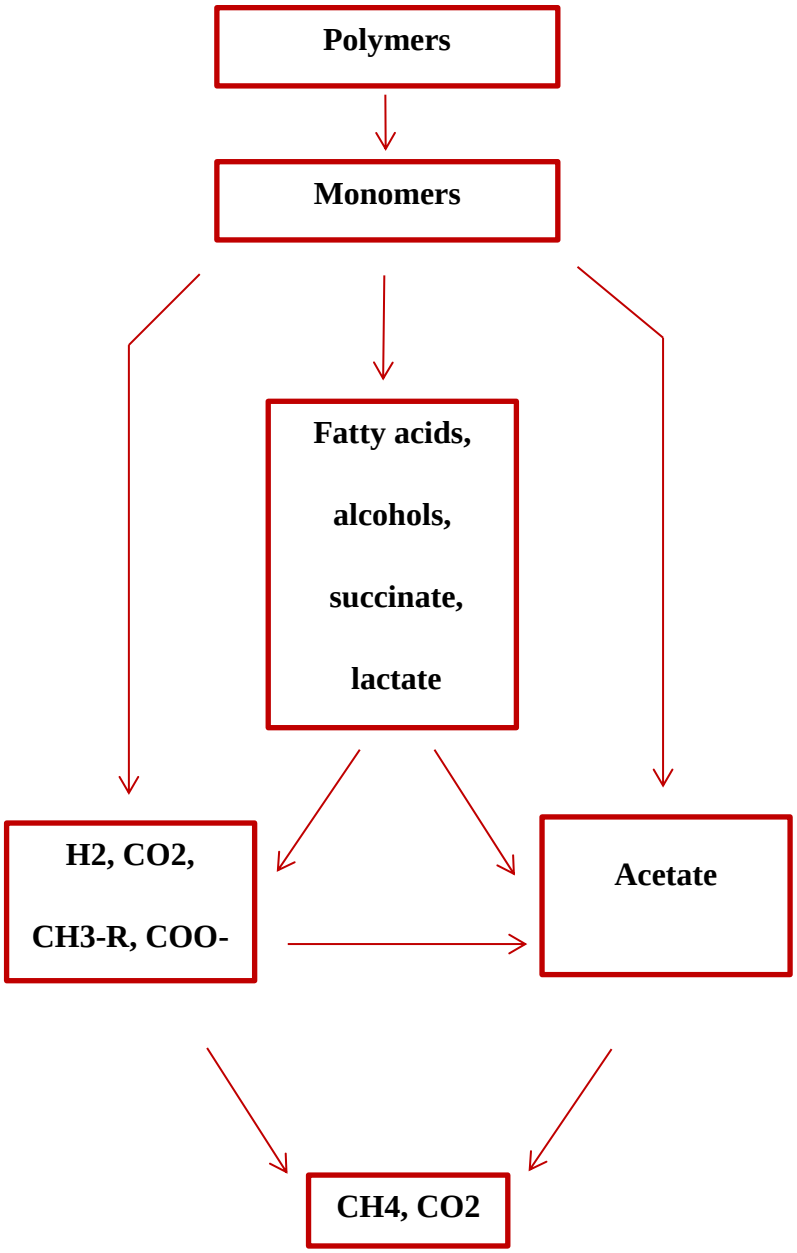

Figure 5: Methanogenic pathway of complex matter degradation.
(Schink and Stams, 2006).

3.2 Anaerobic bioremediation of PAHs and NPs

The redox potential of methanogenic environments is comprised in between -300 to - 500 mV (Godon, 2015, p. 16). Successive redox-reactions are possible according to the redox potential (Eh) of the environment since there is a direct relationship between Eh and the fact that a

reduction or oxidation is exergonic (thermodynamically feasible) with Gibbs free energy adopting a negative value ($\Delta G < 0$). Figure 6 shows redox potentials with their equivalent Gibbs free energy and corresponding possible electron acceptors.

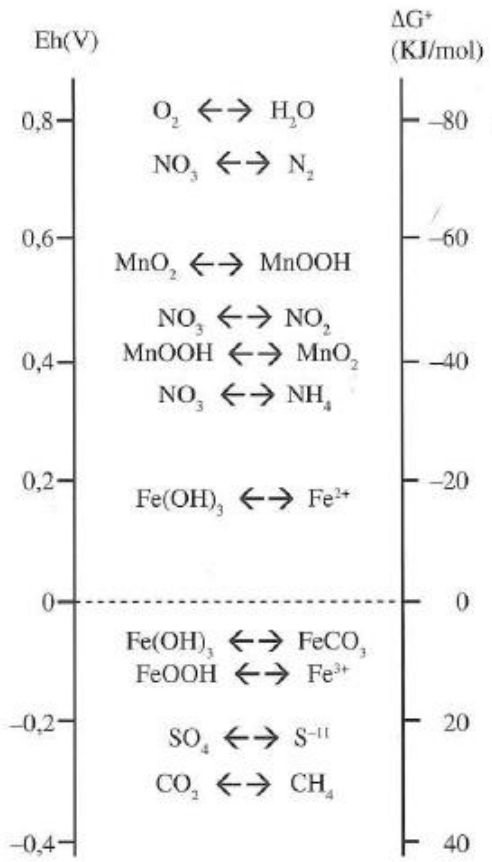

Figure 6: Redox potential (Eh) for reduced/oxidized species and corresponding Gibbs free energy (ΔG^0).

Successively, nitrate, manganese, iron and sulphate can take up electrons with decreasing redox potential and increasing Gibbs free energy. Carbon dioxide is the final electron acceptor for methane generation with hydrogen and acetate as the main electron donors. Most of the publications focus on anaerobic PAH degradation by mixed cultures under nitrate, sulphate or iron reducing conditions(C.-H. Li et al., 2010; Winderl et al., 2010; Xu et al., 2015) (Table 6). Yet, naphthalene, phenanthrene, pyrene and anthracene removal was also observed within methanogenic enrichments (Berdugo-Clavijo et al., 2012; Chang et al., 2006; Christensen et al., 2004; Maillacheruvu and Pathan, 2009; Wan et al., 2012; S. Y. Zhang et al., 2012) or methanogenic environments (Chang et al., 2003 ; Trably et al., 2003). However, there is

disagreement about choosing the best redox conditions since Chang et al. (2003) found sulphate reducing conditions to accelerate PAH degradation rates compared to methanogenic conditions whereas PAH removal was disputed in both conditions by Leduc et al. (1992). Most convincingly, stable isotope probing confirmed the presence of anthracene degraders under methanogenic conditions (Zhang et al., 2012) and thermodynamic calculations demonstrated that PAH removal during methanogenesis is possible if the hydrogen partial pressure stays sufficiently low and there is no lack of specific microbes (Christensen et al., 2004).

Table 6: Anaerobic strains and mixed cultures for PAH bioremediation.

Anaerobic strains or mixed cultures for PAH removal	Pollutant	Removal [%]	Author
Deltaproteobacteria: NaphS3, NaphS6 (sulphate-reducing)	Naphthalene	-	(Musat et al., 2009)
d-subclass of the *Proteobacteria* NaphS2 (sulphate-reducing)	Naphthalene	-	(Galushko et al., 1999)
Sulphate reducing enrichment culture	Naphthalene	-	(Annweiler et al., 2000; Meckenstock et al., 2000)
Sulfidogenic consortia	Naphthalene, Phenanthrene	89.3 (24 days) 92.1 (42 days)	(Zhang and Young, 1997)
Sulphate, iron reducing	Naphthalene	~ 23 (from figure), ~ 170 days	(Coates et al., 1996)
Sulphate reducing enrichment	Anthracene, Phenanthrene	-	(Selesi and Meckenstock, 2009)
Sulphate reducing enrichment	Phenanthrene	20– 45 (196 days)	(Davidova et al., 2007)
Bacterial isolates: *Sphingomonas*, two unidentified strains (Sulphate, iron reducing conditions tested)	Fluorene, Phenanthrene, fluroanthene, Pyrene	Flu, Phe: 50 % (41- 55 days) Flt, Pyr: 50 % (66- 108 days)	(Li et al., 2010)
Halophile bacterial consortium (potential degraders: *Achromobacter* sp. AYS3 (JQ419751), *Marinobacter* sp. AYS4 (JQ419752), *Rhodanobacter* sp. AYS5 (JQ419753)	benzo(e)pyrene co-metabolically with phenanthrene	BeP: 80 (7 days) Phe: 99 (5 days)	(Arulazhagan et al., 2014)
Humus-reducing bacterium, *Pseudomonas aeruginosa* strain PAH-1	Phenanthrene	46.5- 56.7 (30 days)	(Ma et al., 2011)

Facultative anaerobe *Pseudomonas* sp. JP1	benzo(a)pyrene, fluoranthene, phenanthrene	B(a)P: 30 Fla: 47 Phe: 5 (40 days)	(Liang et al., 2014)
Paracoccus denitrificans (nitrate/nitrite reducing conditions)	Pyrene	50.9 (10 days)	(Yang et al., 2013)
Nitrate reducing	Naphthalene, Phenanthrene	17± 1 (60 days) 96 ± 5 (20 days)	(Rockne and Strand, 2001)
Nitrate reducing	Naphthalene	70- 90 (57 days)	(Rockne et al., 2000)
Nitrate reducing	Naphthol, naphthalene, acenaphthene	100 % (16, 45, 40 days)	(Mihelcic and Luthy, 1988)
Potential degraders: bacteria (genera *Citrobacter, Pseudomonas*) *Archaea* (genus *Methanosarcina*)	Phenanthrene	84-87 (120 days)	(Zhang et al., 2012)
Methanogenic conditions (potential bacterial genera *Bacillus*, *Rhodococcus*, *Herbaspirillum*)	Anthracene	43.6 (60 days) 80.7 (120 days)	(Wan et al., 2012).
Phylum *Proteobacteria*: genera *Methylibium*, *Legionella*, *Rhizobiale*s spp. (methanogenic)	Anthracene	54- 60 (60 days) 82- 86 (120 days)	(Zhang et al., 2012)
Crude oil-degrading methanogenic enrichment	Naphthalene, 1-methylnaphthalene, 2-methylnaphthalene,, and 2, 6-dimethylnaphthalene	Naph, 1MethNaph: 0 (140 days), 2MethNaph, 2.6MethNaph: 100 (110 days)	(Berdugo-Clavijo et al., 2012)
Sulphate reducing conditions > methanogenic conditions > nitrate-reducing conditions	Acenaphthene, fluorene, phenanthrene, anthracene and pyrene	100 (41, 27, 11 17, 15 days for Ac, Flu, Phe, Ant, Pyr) with phenanthrene adapted consortium in municipal sludge, degradation rates at least double in methanogenic and sulphate reducing cond. (RC), inhibited in nitrate RC	(Chang et al., 2003)
Methanogenic	13 PAHs	46 ±4 (HRT: 40 days)	(Trably et al., 2003)
Methanobacteriales	Naphthalene	8- 26 (from figure) (41 days)	(Christensen et al., 2004)

Acetate-fed methanogenic	Naphthalene, Phenanthrene, Pyrene	PAH metabolized mg/(mg cell*d) (max.), Naph: 0.57, Phe: 0.09, Pyr: 0.07	(Maillacheruvu and Pathan, 2009)
Methanogenic	Naphthalene, Phenanthrene	50 (130 days) 40 (130 days); data from figure	(Chang et al., 2006)
Methanogenic	Pyrene, Phenanthrene	50 (77- 231 days), 50 (50- 139 days)	(Chang et al., 2008)
Methanogenic	Nonylphenol	100 (sewage sludge) 85.5 (petrochemical sludge) (both 84 days)	(Chang et al., 2009)
Methanogenic	Nonylphenol(di)ethoxylate, Nonylphenol(mono)ethoxylate Nonylphenol	25 ± 6 (NP, NP1EO, NP2EO)	(Patureau et al., 2008)
Methanogenic	Nonylphenol(di)ethoxylate, Nonylphenol	NP2EO: 90 (53 days), NP1EO, NP accumulation	(Murdoch and Sanin, 2016)
Methanogenic	Nonylphenol Alkylphenolpolyethoxylates	NP: + 463 (sludge), also NP1EO, NP2EO accumulation (sludge), NP1EO: 91 (median value, aqueous phase)	(Janex-Habibi et al., 2009). 13 WWTPs with different treatments
Methanogenic	Nonylphenol, Nonylphenolethoxylates	NP: 50 (thermophilic sludge, 90 days) NP1EO, NP2EO: 88 (mesophilic sludge, 90 days)	(Paterakis et al., 2012).
Sulphate- > no additional electron acceptor > methanogenic- > nitrate-reducing conditions	Nonylphenol	50 (19.3 > 23.9 > 28.9 > 31.5 days)	(Chang et al., 2005)
Bacterial isolates: *Bacillus cereus* (Firmicutes), *Acinetobacter baumannii* (Proteobacteria)	Nonylphenol (as carbon source)	50 (14.8- 77 days)	(Chang et al., 2005)

Only few anaerobic strains degrading PAHs have been isolated to date. Most of them belong to the *Beta*- and *Deltaproteobacteria*. Examples are sulphate reducers of the genus *Desulfobacterium* (Galushko et al., 1999; Musat et al., 2009) and a few *Geobacteraceae* (Kunapuli et al., 2010; Lovley et al., 1993; Mclnerney et al., 2001). As for gram-positive bacteria, aromatic hydrocarbon degraders belong to genera *Desulfitobacterium* (Kunapuli et al., 2010),

Desulfotomaculum (Morasch et al., 2004) and the family of the *Peptococcaceae* (Kunapuli et al., 2007). Three pure sulphate-reducing strains can anaerobically degrade naphthalene (Galushko et al., 1999; Musat et al., 2009) and three more can anaerobically degrade fluorene, phenanthrene, fluroanthene and pyrene (C.-H. Li et al., 2010) while naphthalene and phenanthrene were shown to be removed under sulphate reducing conditions (Annweiler et al., 2000; Meckenstock et al., 2000; Zhang and Young, 1997). The only isolate, so far, that can anaerobically degrade pyrene under nitrate reducing conditions is *Paracoccus denitrificans* (Yang et al., 2013). Other denitrifying enrichment cultures were found to deplete naphthalene, acenaphthene and phenanthrene (Mihelcic and Luthy, 1988; Rockne et al., 2000; Rockne and Strand, 2001). In sulphate, nitrate and methanogenic reducing conditions, minimal and maximal removals for PAHs are reported from 20 to 92 %, 17- 100 % and 8- 100 % with incubation times ranging from 24 to 196 days, 10 to 60 days and 27 to 231 days, respectively.

For NP anaerobic degradation it was demonstrated that the order of degradation rates follows sulphate- > methanogenic- > nitrate-reducing conditions (Chang et al., 2005). Also for this molecule, contradictory results have been reported with degradation rates ranging in between 0 to 100 % (Janex-Habibi et al., 2009; Paterakis et al., 2012; Patureau et al., 2008). Nonylphenol ethoxylates are decomposed to NP2EO and NP1EO during anaerobic digestion until complete deethoxylation (Lu et al., 2008) with NP as the main degradation product of NP1EO (Fountoulakis et al., 2005). Yet, NP2EO was removed to 90 % in anaerobic digesters after 52 days whereas NP1EO and NP accumulated in the sludge (Murdoch and Sanin, 2016). Redox potential, however, is not the only influencing factor since temperature, pH and sludge source (Chang et al., 2005) as well as the duration of treatment (He et al., 2015) are also important criteria that influence NP and PAH removal under various conditions. Importantly, bioavailability of the compounds often limits their bioremediation (Barret et al., 2010a).

3.3 Metabolic pathways of anaerobic PAH and NP removal

Anaerobic bioremediation of aromatic hydrocarbons is known to proceed via two activation pathways which are methylation or carboxylation. They were identified at the example of two ring PAH naphthalene and its carboxylized derivative naphtoate, respectively (Safinowski and Meckenstock, 2006; Zhang and Young, 1997). The activation pathways proceed via 2-naphtoate as hypothetical intermediate and from there either to ring cleavage of the aromatic ring to give 2-

carboxycyclohexylacetate or being sequentially dehydrogenated from octahydro-2-naphtoate to decahydro-2-naphtoate (Annweiler et al., 2002). Degradation intermediates further comprise tetrahydro-2-naphtoate (Meckenstock et al., 2000). The lack of pure cultures hinders a deepened understanding of bioremediation pathways of higher weight PAHs. A PAH degrading strain from *Clostridium* species, namely, ER9 (Yuan and Chang, 2007) showed removal of acenaphthene, fluorene, phenanthrene, anthracene and pyrene; yet, signature metabolites of PAH bioremediation were not detected. If PAHs, however, are not radiolabeled, the bioremediation hypothesis through complete mineralization is opposed to the possibility of partial oxidation through co-metabolism (Foght, 2008; Meckenstock et al., 2004). Therefore, the quantification of gaseous $^{13}CO_2$ and $^{13}CH_4$ as already tested for anaerobic digestion (Gehring et al., 2015; Keppler et al., 2010) is indispensable for the elucidation of PAH bioremediation under varying reducing conditions.

The biodegradation of nonylphenol ethoxylates assumedly starts with the degradation of the ethoxylate chain with nonylphenol(di)- and (mono)ethoxylate as intermediate products (Ying et al., 2002). Complete deethoxylation with formation of nonylphenol has been observed under anaerobic conditions (Patureau et al., 2008). Eubacteria, methanogens and sulphate reducers seems to take part in anaerobic NP degradation but they microbial key players still remain largely unknown.

3.4 Efforts to circumvent the constraints of anaerobic bioremediation

Even though certain strains for PAH removal under anaerobic conditions have been identified, the microbial degradation of PAH is still limited by five factors: (i) low abundance, diversity and activity of indigenous PAH degrading bacteria (Fagervold et al., 2005), (ii) slow growth rates of the organisms with doubling times ranging from several weeks to months (Kazumi et al., 1997; Meckenstock et al., 2004), (iii) high partial pressure of hydrogen (Christensen et al., 2004), (iv) undershot threshold concentrations of pollutants and/or pollutant specific microorganisms (Cho et al., 2003; Rhee et al., 2001) and (v) rare bioavailability of PAHs in the aqueous phase (Barret et al., 2010b; Venkata Mohan et al., 2006). These factors can result in a decreased removal rate of bioremediation or no bioremediation at all (Aulenta et al., 2011). Since the readiness of indigenous bacteria to anaerobically degrade PAH is low (Chang et al., 2003; Coates et al., 1996), research efforts consist in accelerating the indigenous microbial turnover of PAHs (Chang et al., 2003; Coates et al., 1996). On the one hand, bio-stimulated growth of naturally occurring

pollutant-degrading microorganisms can be achieved by the addition of electron acceptors, co-substrates and nutrients. Electron acceptors such as nitrate, ferric ion and sulphate are used by anaerobic microbes for the discharge of electrons that they obtain from organic matter utilisation. It has been observed that nitrate amendment enriches microbial functional genes allowing for *in situ* PAH bioremediation (Xu et al., 2014). Nutrients and co-substrates, additionally, promote microorganism cell growth and enhance their bioremediation capacity. Examples include methanol and acetate that have been employed as additional carbon sources for microorganisms in order to increase the natural attenuation of PAHs in a marine sediment (Zhang and Lo, 2015).

Biostimulation, on the other hand, is another common approach for removing organic pollutants. However, in the case of nitrates, biostimulation leads to secondary pollution issues (Pandey and Fulekar, 2012). A limited dispersion of chemicals through the soil matrix (Anneser et al., 2010), their consumption via abiotic reactions or their diffusion away from PAHs can decrease the efficiency of biostimulation (Jobelius et al., 2011). This implies that a periodic replenishment of chemicals renders biostimulation economically unfavourable (Mittal and Rockne, 2010). Bioaugmentation represents a third option for PAH bioremediation. This technique is based on the application of indigenous or exogenous microorganisms such as fungi (Yanto et al., 2017) or bacteria (Song et al., 2017; Trably et al., 2003) to polluted and hazardous wastes in order to accelerate the removal of PAHs (Ma et al., 2015). Nevertheless, as the preparation of the inoculum and the loss in microbial activity during inoculation are energy and time consuming, bioaugmentation appears to be an even less economical solution (Laszlova et al., 2016).

The revisited literature points to the fact that abiotic degradation and bioremediation of PAHs and NPs is a challenging topic. Therefore, different solutions and combined techniques have to be considered in order to improve organic contaminant remediation. The use of conductive materials and bioelectrochemical systems are two new technologies for this purpose.

4. Bioelectrochemical systems and conductive materials

The use of bioelectrochemical systems and/or conductive materials are possibilities to increase methane yield in anaerobic digesters. They are of special interest for the biodegradation of micropollutants since, as discussed in section 3.1, an increase in matter degradation and methane

production was found to be beneficial for PAH and NP degradation. The increase in methane production supposedly relies on the fact that the electron transfer between microorganisms is facilitated through the presence of conductors. Most recent research about possible electron transfer pathways between these materials and biota are presented in the following.

4.1 Direct extracellular electron transfer between species and solid conductive materials

Mediated interspecies electron transfer, also known as interspecies hydrogen transfer, occurs across a wide spectrum of engineered and natural systems, including anaerobic digesters, landfills, and freshwater/marine sediments. It is a well-studied mechanism of electron transfer (Stams et al., 2006; Stams and Plugge, 2009) in which hydrogen, formate or another mediator metabolite is produced intracellularly and diffuses to the outside of the cell where it can be consumed by a syntrophic partner (Cheng and Call, 2016). In contrast, direct extracellular electron transfer (DEET) has been reported only recently. DEET needs membrane-bound structures to physically connect and transfer electrons between cells or between cells and an inorganic electron acceptor or donator. Thus, the electron transfer takes place directly from cell to cell or electron transfer partner instead of using hydrogen or formate as electron shuttles (Rotaru et al., 2014a; Shrestha et al., 2013).Microorganisms capable of DEET with a non-biologic partner are called exoelectrogens. Exoelectrogens can undergo extracellular electron transfers with electrodes or metals in three different ways that are (a) long-range direct electron transfer via conductive pili (Reguera et al., 2005), (b) mediated electron transfer via electron shuttling molecules (methylviologen (Aulenta et al., 2007), neutral red (Park and Zeikus, 2000), flavins (Lee et al., 2015) and (c) short-range direct electron transfer via redox-active proteins (c-type cytochromes) (Wrighton et al., 2011) as depicted in Figure 7.

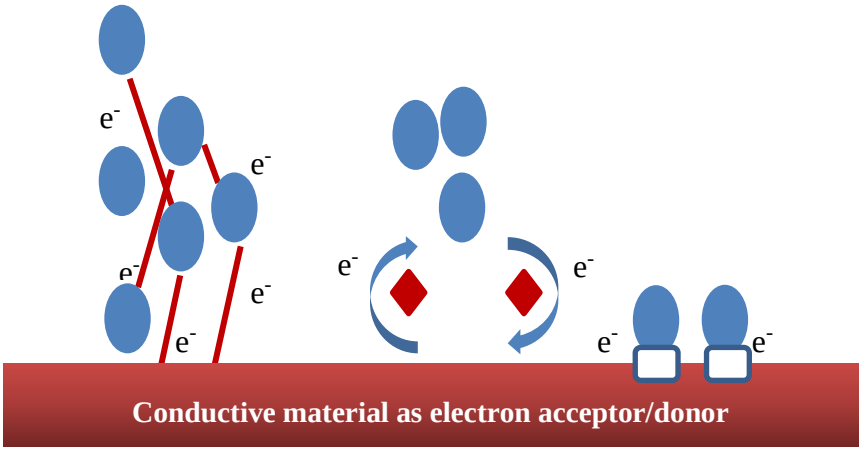

Figure 7: Strategies for extracellular electron exchange by electroactive bacteria with a conductive material.
According to Sure et al., (2016). Blue circles: electroactive bacteria. Left: long-range electron transfer via conductive pili (red lines); middle: electron transfer via electron shuttling molecules (diamonds); right: short-range direct electron transfer via redox-active proteins (white rectangles).

Conductive pili have been investigated only recently. Evidence on their existence is convincingly given by microscopic imaging techniques such as scanning electron micrographs of methanogenic co-culture as depicted in Figure 8.

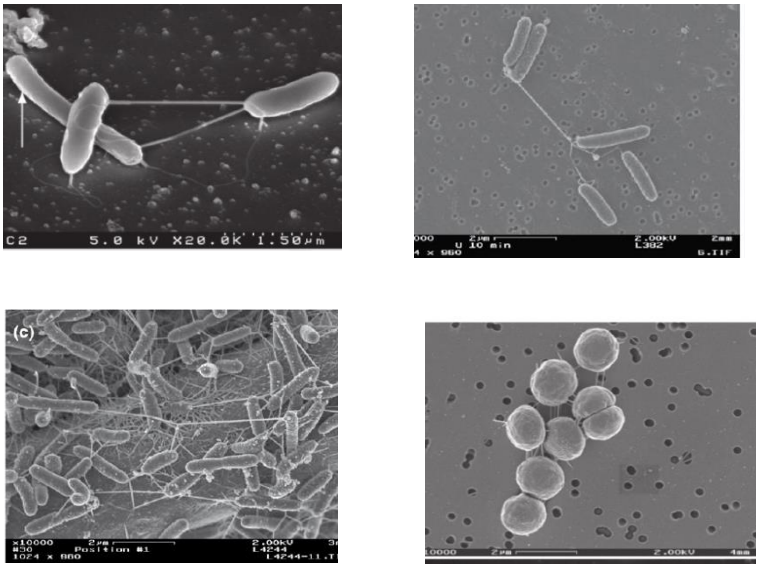

Figure 8: Evidence of conductive nanowires (pili).
Showing P. thermopropionicum and *M. thermoautotrophicus* according to Gorby 2006 and Logan 2009.

Pili conductivities from 37 μS/cm (pH 10.5) up to 188 mS/cm (pH 2) have been determined for *Geobacter sulfurreducens* which is similar to synthetic organic metals (Adhikari et al., 2016; Malvankar et al., 2011). Exceptional pili conductivities of 277 S/cm were obtained by heterologeously expressing PilA gene of *Geobacter metallireducens* in *G. sulfurreducens* (Tan et al., 2017). There is no agreement, yet, concerning the molecular mechanisms of electron flow along these microbial nanowires. Basically, two electron flow models are proposed: the electron hopping model for filaments of *Shewanella oneidensis* and the metallic-like conduction for pili of *G. sulfurreducens*. The first one is based on electron transfer from adjacent redox proteins (c-type cytochromes) of the nanowire to the electron acceptors (another cell or electrode) (a) (Malvankar et al., 2012; Strycharz-Glaven et al., 2011), the latter explains electron flow by the delocalization of charges across tightly packed aromatic amino acids based on overlapping π-orbitals through the entire nanowire (b) (Malvankar et al., 2011; Malvankar and Lovley, 2014) as depicted in Figure 9.

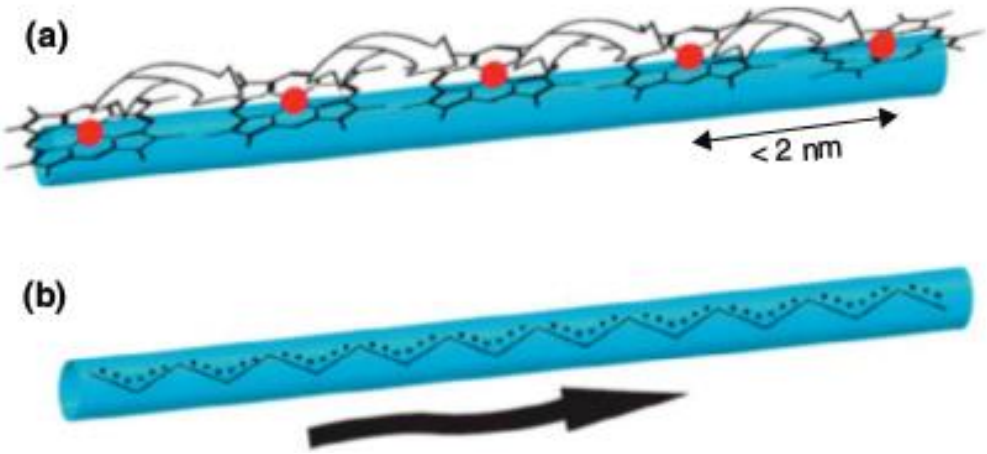

Figure 9: Electron flow models through microbial nanowires.
Electron hopping through cytochrome-c type proteins in the conductive pilin (a). Electron conduction via aromatic amino acids which form overlapping π-orbitals through the pili (b) (Malvankar and Lovley, 2014).

Extracellular direct interspecies electron transfer (DIET) though nanowires has been observed in co-culture of *Methanosarcina barkeri* and *G. metallireducens* (Rotaru et al., 2014b) but equally between the latter and other methanogens such as *Methanosaeta* (Rotaru et al., 2014a) and in methanogenic digesters (Liu et al., 2012). *Methanosaeta* are strict acetoclastic methanogens and could potentially undergo DIET since genes for CO_2 reduction to methane were highly expressed

in *Methanosaeta harundinacea* when pili expressing *G. metallireducens* was the only electron donor (Rotaru et al., 2014a, 2014b).

On the other hand, conductive materials such as biochar (Chen et al., 2014a) and granular activated carbon (GAC) (Liu et al., 2012) have been recently found to accelerate rates of anaerobic carbon metabolism. The improvements were attributed to the stimulation of indigenous microorganisms, namely the accelerated exchange of electrons by DIET (Kato et al., 2012; Liu et al., 2012). DIET via electrically conductive materials was proven when ethanol degradation was accelerated by granular activated carbon even if the genes for conductive pili or membrane protein for DIET OmcS were deleted in co-cultures of electron-donating *G. metallireducens* and electron-accepting *G. sulfurreducens* (Chen et al., 2014a, 2014b; Liu et al., 2012). DIET during methanogenesis proceeds in between syntrophic, organic matter-oxidizing bacteria and CO_2-reducing methanogens (Cruz Viggi et al., 2014). Authors observe more stable anaerobic digestion with respect to VFA accumulation when conductive particles are added to food waste digestion suggesting that the material promoted DIET processes between acetogens and methanogens (Dalla Vecchia et al., 2016). It is stipulated that microbial cells can attach to conductive materials that, in turn, serve as conduit for electron transfer between electron-donating and electron accepting cells (Malvankar and Lovley, 2014). Microbial ethanol oxidation to acetate supplies, for instance, the electron that are further used by methanogens for the reduction of carbon dioxide to methane as depicted in Figure 10.

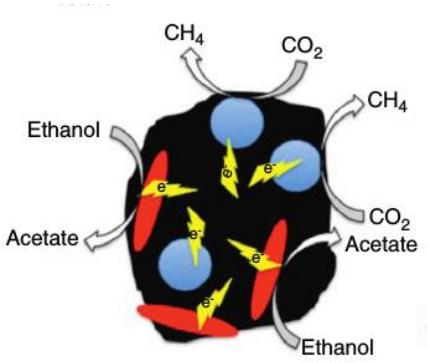

Figure 10: Interspecies electron exchange in anaerobic digesters through conductive materials.
Ethanol is biodegraded to acetate by electron-donating cells (red), electrons are transported through conductive activated carbon (yellow), electron-accepting cells (blue) use these for carbon dioxide reduction to methane according to Malvankar and Lovley (2014).

Nevertheless, it is reported that co-cultures consistently showed better performance with respect to maximum methane production rates and decrease in the lag phase than natural mixed cultures after addition of such materials (Cheng and Call, 2016). These results point to the fact that the detailed mechanisms explaining how these materials contribute to the observed performances in complex environments such as in anaerobic digesters with changing electron acceptor concentrations and evolving microbial communities still have to be determined (Kouzuma et al., 2015).

4.2 Microbial bioelectrochemistry

When one of the microbial electron transfer partners (the electron donating or electron accepting cell) as discussed in section 4.1 is replaced by an electrode, the respective electron transfer mechanisms is based on microbial bioelectrochemistry. Microbial bioelectrochemical systems (BESs) are one or two compartment electrochemical devices in which an anode and a cathode favour redox-reactions that are catalysed by microorganisms (Allen and Bennetto, 1993): this is the electroactive biocatalyst. Some microbial species are capable of interchanging electrons directly with a solid electrode (Gregory et al., 2004) and thus, they can transfer electrons that they produced from organic matter oxidation to the anode of a BES. These electrons pass through a conductive wire to the cathode where they are consumed by a reduction reaction, most often by oxygen (Logan et al., 2006) such as depicted Figure 11.

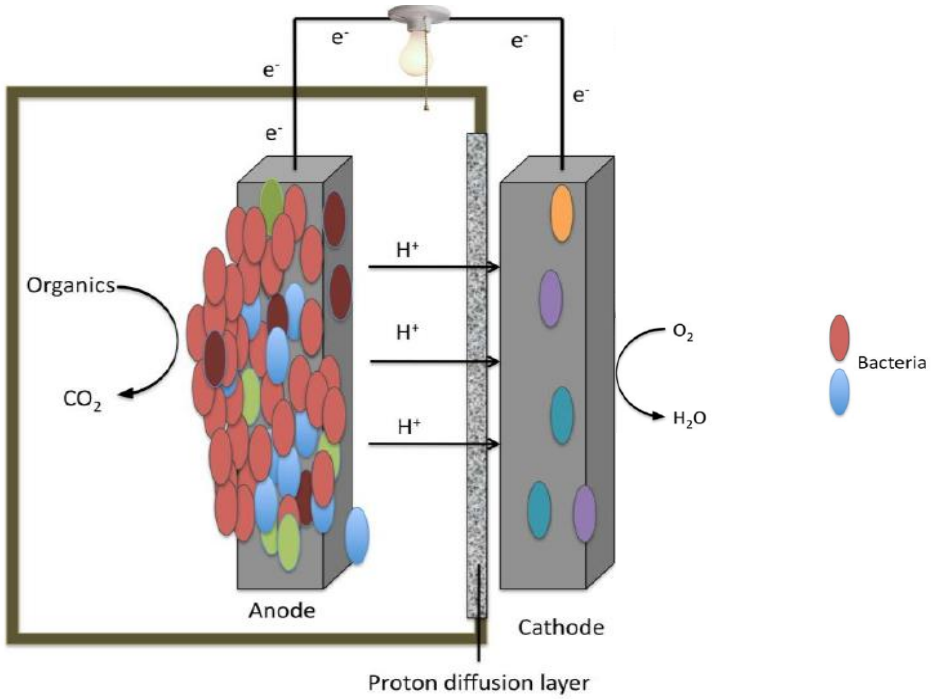

Figure 11: Microbial fuel cell (single chamber).
Catalytic oxygen reduction at cathode (Franks and Nevin, 2010). Organics oxidation to carbon dioxide by an electroactive biofilm attached to the anode, electron transfer through an external circuit generates electricity (light bulb), protons diffuse through the membrane for charge equalisation, and oxygen is reduced to water at the cathode.

In this way, microbes convert organic matter into electric current (Kiely et al., 2011) which can be used to drive an electrical load. The principle of bioelectrochemistry is the ability of certain microorganisms to interchange electrons with insoluble conductive materials via extracellular electron transfer (Reimers et al., 2001; Tender et al., 2008). On the anode side, these are called anode-respiring bacteria or exoelectrogens (Logan, 2008). Some electroactive microorganisms can serve as catalysts for oxygen reduction also at the cathode of a BES resulting in a microbial biocathode (Figure 11) (Roustazadeh Sheikhyousefi et al., 2017).

4.3 Microbial fuel cell and microbial electrolysis cell

The prototype of a BES is the microbial fuel cell (MFC) that generates electricity based on organic matter oxidation in the anode chamber (Venkata Mohan et al., 2014). Oxygen is traditionally used as electron-acceptor in the cathode compartment or at the air-cathode due to its unlimited availability and high standard redox potential (Bond and Lovley, 2003; Hou et al., 2012). Depending on the complexity of the substrate, typical maximum power densities of MFCs lie between 2 and 3 W/m^2 of projected electrode surface (mostly cathode) at optimum conditions (30°C, neutral pH, 20 mS/cm conductivity, buffered solution) (Logan and Rabaey, 2012). A rise

in electrode area per volume of reactor running on wastewater achieved power densities up to 1.55 kW/m^3 (2.77 W/m^2) (Reimers et al., 2001). MFCs can be run on inexpensive organic wastes such as wastewater, sludge and biowastes (Venkata Mohan et al., 2014), in which PAHs can be found at low concentrations. The second type of BES is the microbial electrolysis cell (MEC) that uses a small amount of energy to fuel chosen reactions in the cathode chamber. In a MEC, oxygen is eliminated from the cathode chamber so that electrons released from the cathode can be exploited for other uses than oxygen reduction (Logan, 2008). Mostly, protons from aqueous solutions are reduced to hydrogen gas (Villano et al., 2010) although other terminal electron acceptors have also been suggested. These comprise chlorophenols (Kong et al., 2014), nitrobenzene (Mu et al., 2009; Wang et al., 2011), polychlorinated ethenes (Aulenta et al., 2008; Strycharz et al., 2008) and cobalt(II) (Huang et al., 2014). In most studies, it is assumed that electroactive microorganisms catalyse the oxidation and reduction reactions in the anode and cathode chambers (Jafary et al., 2015; Rozendal et al., 2008). Nevertheless, the thermodynamic reaction barrier of these reactions still needs to be circumvented with a small external voltage delivered by a power source (Sun et al., 2008) or by setting an electrode potential using a potentiostat (Logan and Rabaey, 2012). A schematic overview of MFC and MEC setup with respective standard potentials versus the normal hydrogen electrode (NHE) is given in Figure 12.

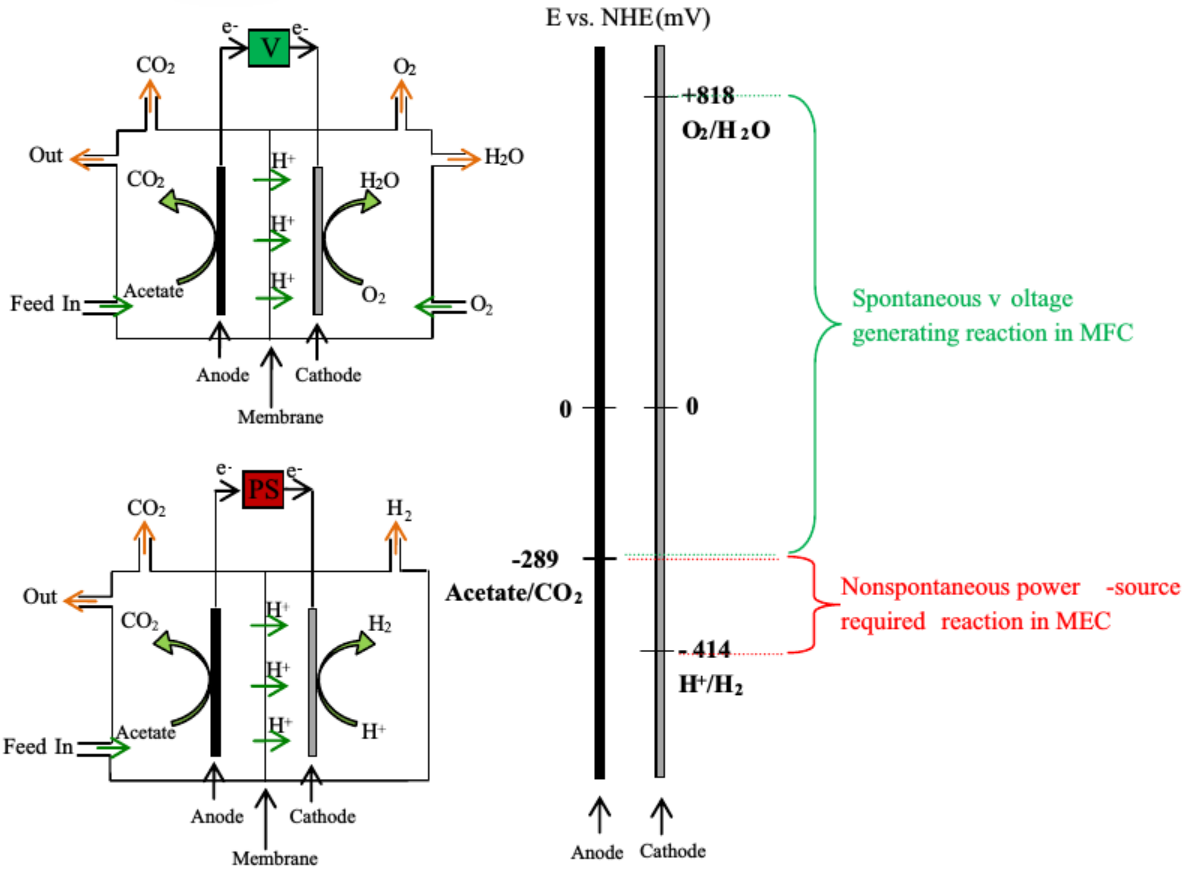

Figure 12: Schematic overviews of MFC and MEC by demonstration of standard potentials (vs. NHE) of oxidation and reduction reactions in anodic and cathodic chambers.
PS: Power Source. V: Voltage generation. The presence of oxygen in the cathode chamber of the MFC leads to a voluntary reaction which fuels the complete oxidation of acetate in the anode chamber (above). The half reaction of protons to hydrogen in the absence of oxygen in the cathode chamber is not sufficient to fuel acetate oxidation in the anode chamber. The biocatalysed process is made possible by a small energy input (below) (Jafary et al., 2015).

4.4 Methane formation through electromethanogenesis

Microbial electrolysis cells have been used to enhance methane generation since hydrogen development on the cathode side of a MEC is advantageous for hydrogenotrophic methane generation (Jafary et al., 2015). Cheng et al. (2009) proposed the use of methanogens as biocathodic catalyst to reduce CO_2 into CH_4 with a standard potential (E^0) below -0.44 V (NHE)[5] based on the following reactions:

[5] NHE : Normal hydrogen electrode

Anode: $Ac^- + 2H_2O \xrightarrow{yields} 2CO_2 + 8H^+ + 8e^-$ $E^0 < -0.2$ V (NHE)

Cathode: $CO_2 + 8H^+ + 8e \xrightarrow{yields} CH_4 + 2H_2O$ $E^0 < -0.44$ V (NHE)

Voltage E^0 imposed: -0.44 V – (-0.2 V) = -0.24 V (pH=7)

Voltage E^0 imposed: -0.41V – (-0.2 V) = -0.21 V (pH=7) for hydrogen production from acetate

As a comparison, the voltage imposed in order to produce methane inside a MEC is lower than that for electrohydrogenesis (-0.24 V < -0.21 V). For that reason, electromethanogenesis is less energy consuming than electrohydrogenesis (Cheng et al., 2009) without being in need of an organic substrate if carbon dioxide is used directly. A second advantage of methane compared to hydrogen generation in MECs is that it can be carried out in a single-chamber anaerobic system without the need of an ion exchange membrane (Clauwaert et al., 2008; Clauwaert and Verstraete, 2009). A methane producing MEC is easily designed by inserting electrodes into an anaerobic digester. In this system, organic acids can be decomposed both through acetoclastic methanogenesis and anodic oxidation (Zhao et al., 2014). Rates of methane generation were enhanced by a co-culture of *Geobacter* and *Methanosarcina* in MECs (Yin et al., 2016) but were also enhanced in mixed culture: anaerobic digestion in a MEC achieved higher methane yields (Asztalos and Kim, 2015; Guo et al., 2013), higher VSS and COD removals (Asztalos and Kim, 2015) and accelerated kinetics (Cai et al., 2016).

4.5 Removal of polycyclic aromatic hydrocarbons and NPs by microbial fuel cells

The biocatalytic principle of a MFC contributes to drive thermodynamically unfavourable reactions and can thus be an alternative electron source for improving PAH removal. Recalcitrant PAHs may be more easily transformed to less complex compounds if the metabolism of PAH degraders is directly or indirectly boosted by a bioelectrochemical activity in the vicinity of the electrodes (Chandrasekhar and Venkata Mohan, 2012). As an example, in an experiment, the number of hydrocarbon-degrading bacteria (HDB) close to the anode of a MFC increased in

comparison to an open circuit control when an electric current was applied (Wang et al., 2012). When research on BES began 15 years ago, scientists focused on the production of energy vectors (hydrogen or electricity) while evidence of aromatic hydrocarbon removal by BESs only appeared in 2010 (Zhang et al., 2010). Using ^{14}C-labeling, Zhang et al. demonstrated that toluene

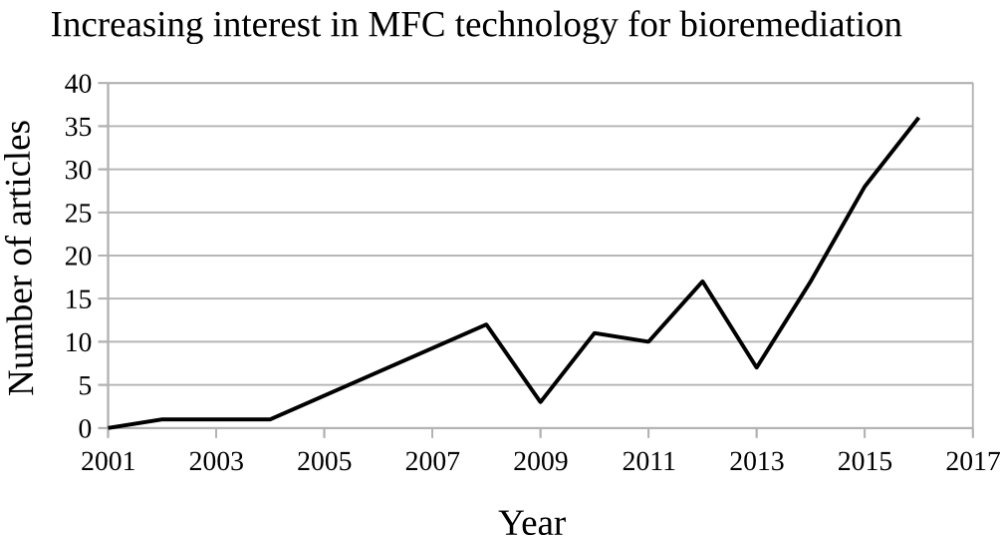

Figure 13: Number of relevant articles per year.
Web of Science search with the key words 'bioremediation' and 'microbial&fuel&cell'.

could be quantitatively oxidized to carbon dioxide in a MFC in the presence of *G. metallireducens*, a popular exoelectrogenic bacteria found in numerous MFC publications. Since the oxidation of toluene was achieved in the absence of an electron acceptor other than the anode, this discovery allowed them to ascertain that electrodes can stimulate the degradation of aromatic hydrocarbons in contaminated anaerobic sediments. As depicted in Figure 13 research on biocatalysed remediation in MFCs only accelerated in 2014.

Venkata Mohan & Chandrasekhar (2011) found further evidence of PAH removal in BESs: they observed that a soil MFC was capable of easily attacking 5-6 ring aromatics within petroleum sludge while anaerobic degradation was only restricted to 2-3 ring aromatics (Venkata Mohan and Chandrasekhar, 2011). Since then, within six years, only about 23 publications (Table 7) focus on the potentials of PAH remediation within bioelectrochemical systems, first and foremost from total petroleum hydrocarbon (TPH) contaminated soil, diesel and engine oil which contain hydrocarbon mixtures of alkanes, aromatic hydrocarbons and resin-asphaltenes as sole carbon

sources. In these studies, co-substrates were never used except for one study in which electricity generation and PAH degradation were improved after glucose addition to a saline soil MFC (Li et al., 2016a).

9 out of 26 studies use sediment microbial fuel cells (SMFCs) for PAH biodegradation. In these studies, the anode and cathode are not separated by a membrane since they are already segregated by the overlying air. The same separation holds true for all MFCs that are used in soil with the exception of Zhou et al. who uses a cation exchange membrane to separate cathode and anode chambers.

Table 7: Bioelectrochemical PAH degradation.

Author	Type of BES	Matrix	Pollutant	Start Concentration	Removal [%] (Degradation rate if indicated)	Controls (types and performances)	Experiment length (days)	Max. current density (CD) / max power density (PD)* normalized by anodic or cathodic surface area
(Adelaja et al., 2014)	MFC	Synthetic medium	Benzene, phenanthrene	200 mg/L benzene, 30 mg/L phenanthrene	> 96 (for all inocula) best: mixed culture+ *P. aeruginosa*: 27.3 µM/d (phenanthrene), 65.6 (COD) Others: Co-culture and pure strains (*P. aeruginosa*, *S. oneidensis*), same strains mixed with digested sludge	For each inoculum: abiotic MFC, disconnected MFC, anaerobic control using the same inocula	60	1.25 mW/m^2 (normalized to the projected total surface area of the anode (40 cm^2), 18 mA/m^2 (data from figure), max. voltage: 65 mV (data from figure)
(Adelaja et al., 2015)	MFC	Minimal medium	Benzene, phenanthrene	100 mg/L benzene 100 mg/L phenanthrene	91.6 (benzene +phenanthrene) 79.1 (COD)	Abiotic: 20 (benzene), 10 (phenanthrene)	60	4.89 mA/m^2, 0.72 mW/m^2
(Chandrasekhar and Venkata Mohan, 2012).	MFC	Domestic wastewater	Real field petroleum sludge	3000 (OL1), 9000 (OL2), 15000 (OL3), 30000 (OL4) mg TPH/L sewage	58 (aromatics at 30 g TPH/L) 70 (aromatics at 3 g TPH/L)	Four Organic Loading (OL) conditions: Low load better for power generation, high load better for substrate degradation	17	20.6 mW/m^2, 198.3 mA/m^2 for OL1, 11.8 mA/m^2 for OL4
(Li et al., 2016b)	SMFC	Saline Soil	TPHs, n-alkanes, PAHs	Max: 0.484 mg/kg (PAH), Max:20.181 mg/kg (n-alkanes)	153-484 % higher TPH degradation rate in all MFCs compared to CK, RM>MC>RS>CK RM: 60+-9 (TPH), OSOC: 3 (TPH), PAH removal: 59 -92, n-alkanes: 44 -88, 4-6 ring PAHs particularly removed in RM	CK: unmodified soil MFC RS: rinsed soil MFC MC: carbon fiber (2 %) + original soil MFC RM: carbon fiber (2 %) + rinsed soil MFC RMOC, RSOC, OSOC, MCOC: open circuit configurations of RM, RS, CK and MC	65	299 mA/m^2 (RM): 595 % higher than CK

(Li et al., 2016a)	SMFC	Saline soil	TPHs, n-alkanes, PAHs (phenanthrene, fluoranthene, pyrene, chrysene accounting for 70 % of all PAHs)	Contaminated soil: 945 mg/kg PAHs 28.322 mg/kg (n-alkanes), LG (low glucose 0.1 % w/v) HG (high glucose 0.5 % w/v)	TPH: 21 (LG, Layer 1, 62 % higher removal than CK) TPH removal: LG > HG > CK > LGOC > HGOC > OC PAH: 34 (LG) 44 (HG)	CK: closed circuit OC: open circuit LG: soil + current + low glucose HG: soil + current + high glucose LGOC, HGOC: open circuit controls	135	HG: 43 mW/m^2, ca. 108 mA/m^2 (with U= 0.4 V data from figure), LG: 35 mW/m^2, 79 % and 46 % higher than that of CK, CK: 24 mW/ m^2
(Li et al., 2014)	SMFC	Saline Soil	C8-C40 n-alkanes, 16 PAHs	5.653 mg/kg (total PAHs) 609 mg/kg	Max. in soil layer four: 18 (TPH), 36 (PAH), 29 (n-alkane) compared to control with natural attenuation, degradation rates depending on soil layer [SL] in distance to anodes (SL 4 > SL 1 > SL 2 > SL 3), SL4 closest to air-cathode	open circuit	180	37 mW/m^2, 366 mV, 102 mA/m^2 on day 5
(Li et al., 2015)	MFC	Aged soil	TPHs, n-alkanes, 16 PAHs	Max: 945 mg/kg (PAH) Max: 27.891 mg/kg (n-alkane)	22 (TPHs) in high ratio sand/soil MFC, (+52 % versus LS), (+84 % HS versus CK), (+268 % HS versus OC), higher removal for PAH with sand addition	Soil only (OC); soil + current (CK); sand + soil +current: low sand/soil and high sand/soil ratio= (LS)=5:1 (HS)=2:1, 15 (less sand MFC) 12 (without sand but connected electrodes) 6 (OC)	135	0.28 mA/m^2 /g soil 2.76 mW/m^2/g soil
(Li et al., 2016c)	MFC	Soil	16 PAHs, 30 n-alkanes	7942 ± 7476 ng/g (PAHs), 701 ± 736 µg/g (n-alkanes)	5 % (CKOC), Compared to CKOC: CK showed 5-fold removal, MC showed 7.4-fold removal, MCOC 4.4 times higher than CKOC	Original soil (OS), OS + carbon fiber (MCOS), Carbon fiber MFC (CK), OS-MFC (MC), Open circuit controls : CKOC, MCOC	144	203 mA/m^2, 0.8 mW/m^2, 100 Ω, Average over 144 days: 120.5 mA/m^2 for CK, 7.5 mA/m^2 for MC

(Lu et al., 2014b)	MFC	Soil	Hydrocarbons from raw diesel	12300 mg/kg dry soil	82-90 (1-34 cm radius)	68	120	70.4 mA/m^2
(Lu et al., 2014a)	MFC	Soil	TPHs	11460 mg/kg dry soil	78.7 (BCA) 73.1 (CCA) 62 (CCA-S; taken from figure)	41.6 (OC of BCA) 40.7(OC of CCA) CCA-S: CCA with surfactant addition	64	85.9 mA/m^2, 39.1 mW/m^2 (BCA) 73.0 mA/m^2, 17.7 W/m^2 (CCA), 21.2 mA/m^2, 2.9 mW/m^2 (CCA-S)
(Morris and Jin, 2012)	MFC	Sediment	TPHs	16000 mg/kg sediment	24 (closed circuit)	2 (open circuit)	66	190 mV, 2.2 mW/m^3
(Morris et al., 2009))	MFC	Ground-water	Diesel range organics (DRO) C10-C28 aliphatics	176-241 mg/L	82 (DRO) 6.9 mg DRO/(L day) (or 34.5 µmol/day)	31 (cathode removed)	21	32 mW/m^2 Data from figure: ~175 mA/m^2 average 160 mV (CD and PD calculated per cathode surface)
(Venkata Mohan and Chandrasekhar, 2011)	MFC	Soil	TPHs	2-480 mg/L soil (calculated by us: 480000 mg/kg soil)	41 (Total TPH), 98 (benzo(g,h,i)perylene), 96 (dibenzo(a,h)anthracene)	Anaerobic controls: 21 (total) 68 (Benzo(g,h,i)perylene) 56 (Dibenzo(a,h)anthracene)	17	20.62 mW/m^2, 198.31 mA/m^2, 104 mV
(Sabina et al., 2014)	MFC	Saline water	Waste engine oil (branched, long-chain & cyclic hydrocarbons)	1 % (v/v) (100ml/L)	70.1 in desalination MFC (gravimetrical decrease in engine oil)	62.9 % (gravimetrical; shake flask study with Bacillus subtilis moh3)	14	3.1 mW/m^2 (based on the cross-sectional area of anode)
(Sherafatmand and Ng, 2015)	SMFC	Sediment	PAHs, naphthalene, acenaphthene, phenanthrene	50 ppm for all three PAHs (50 mg/kg)	Anaerobic cathode: 76.9 Naphthalene, 52.5 acenaphthene, 36.8 phenanthrene	Natural attenuation: 29 (Naphthalene), 29 (acenaphthene), 12 (phenanthrene), Aerobic cathode: 41.7 (Naphthalene), 31.4 (acenaphthene), 36.2 (phenanthrene)	45	2 mW/m^2 in anaerobic, 5.8 mW/m^2 in aerobic
(Venkidusamy et al., 2016)	MFC	Synthetic medium	Diesel	800 mg/L	100 (1 year selected biofilm anode)	83 (freshly inoculated anode)	30	90.8 mW/m^2, 115mA/m^2 normalized to cathode surface

(Cruz Viggi et al., 2015)	SMFC	Sediment	Spiked crude oil (TPH)	11300-12300 mg/kg dry sediment	After 200 d: 12 (S) 21 (S3) 0 (C)	S: One graphite rod, S3: three graphite rods, C: biotic without graphite rod, B: autoclaved+ one graphite rod, B3: autoclaved+ three rods,	417	No external electrical charge input or output
(Wang et al., 2012)	MFC	Saline soil	TPHs, 16 PAHs (phenanthrene, chrysene, pyrene and phenanthrene representing 75 %)	0.5- 0.8 mg/kg soil	15.2 (TPH), 120 % higher degradation rate in CC (TPH) than OC in 1 cm distance of the anode	6.9 (open circuit), CC: closed circuit	25	0.85 mW/m^2
(Xia et al., 2015).	SMFC	Sediment	PAHs, cylohexanes, cyclopentanes	ca. 3 µg/g sediment (PAHs)	< 15 %	Mainly < 10 % (open circuit)	20	0.6 V 4.32 mW/m^2 9.29 mA/m^2
(Yan et al., 2012)	SMFC	Sediment	Phenanthrene, pyrene	10 and 5 mg/kg dry sediment for phenanthrene and pyrene	94.8 (Pyrene), 99 .5 (phenanthrene) (SMFC + FeOOH); combined treatment best for all anaerobic conditions except methanogenic	Open circuit: 80.3 (phenanthrene), 74.5 (pyrene); ferric hydroxide (FeOOH): 87.6 (phenanthrene) , 79.9 (pyrene); SMFC: 96.1 (phenanthrene), 92.1 (pyrene)	240	16-17 mV, average CD not reported (average per anode surface: 170 mA)
(Yan et al., 2015)	SMFC	Sediment	Benzo(a)pyrene, pyrene	2 mg/kg dry sediment (benzo(a)pyrene), 4 mg/kg dry sediment (pyrene)	87 (Macrophyte +SMFC) Combined treatment degradation rates are 70% higher than control treatments	68 (Macrophyte alone), 56 (SMFC alone), 27 (control)	367	61 -65 mV, average CD not reported directly (average given with: 650 mA/anode surface, 17 A/m^2)
(Yang et al., 2015)	SMFC	Sediment	PAHs	PAH: 1.2 mg/kg wet weight, PBDE: 178µg/kg wet weight	22.1 (TOC removal in closed circuit)	3.8 (TOC removal in open circuit)	2 years	0.4 -0.6 V

(Yeruva et al., 2015)	MFC/ MFC + anoxic cathode	Waste-water	Petrochemical wastewater (BOD 5 /COD: 0.36).	9.68 kg COD/m^3*day	55 (COD in anoxic SBR-BET), 49 (COD in aerobic SBR-BET) SBR: Sequential batch reactor BET: Bioelectrochemical treatment	34.6 (COD anoxic SBR), 30 (COD removal in aerobic SBR); both of these without BET	HRT: 48 h	17.1 mW/m^2 (anoxic), 14.3 mW/m^2 (aerobic) OCV: 248 and 280 mV
(Zhang et al., 2010)	MEC	Sediment	Naphtalene	100 µM (naphthalene) mixed with seawater and sediment	100 (Naphthalene)	0 (Naphthalene if heat treated) 0 (Naphthalene without electrode)	9	-
(Zhang et al., 2015)	MFC	Soil	TPHs, 16 PAHs, C8-C40 n-alkanes	25700 mg/kg dry soil	12.5 (Horizontal anodes HA),	8.3 (Vertical anodes VA) 6.4 (open circuit)	135	HA max. 0.282 V, VA max. 0.285 V, 833 coulomb accumulated for VA over the whole duration: 9 % more than in VA, current and power densities not indicated
(Zhou et al., 2016)	MFC	Soil	Petroleum hydrocarbons	20 mM	-	-	7	600 µA/cm^2 (6 A/m^2), 220 mW/m^2

The relationship between power density of a MFC and biodegradation efficiency is poorly investigated. Still, a correlation between current or power density and the extent of PAH biodegradation inside BESs could be an easy way to monitor *in situ* approaches for PAH removal. In some electrokinetic studies, authors proved higher degradation of diesel (Mena et al., 2014) and petroleum hydrocarbons (Li et al., 2010) with an augmentation of current intensity. Petroleum was mixed to soil at a level of 50 g/kg dry soil and electric current was constantly supplied at a voltage of 1 V/cm. Two reasons were attributed to accelerated removal of petroleum hydrocarbons. The supplied current would support microbial activity, in general; and particularly, boosted the metabolism of HDB that use oil as the sole carbon. In fact, also in MECs a small current is applied to the existing microbial community. However, until now, there are few studies on anaerobic cathodes (MEC setups) as described before. The suggestion that hydrocarbons are better removed by the assistance of an anode in MFCs, however, is backed up by the relationship between charge output, the presence of HDB and PAH removal. The increase in number of HDB in soil close to the anode (1cm) was found in different studies. Wang et al. tested anodes that were precultured with exoelectrogenic bacteria for TPH removal in petroleum in contaminated soil (Wang et al., 2012). Consequently, the number of HDB within 1 cm close to the anode increased by almost two orders of magnitude from $8*10^3$ CFU/g-soil to $373*10^3$ CFU/g-soil in comparison with the open circuit control. As a result, the net biodegradation of 16 PAHs increased from 30 to 42 % within 25 days when the soil MFC had a water content of 33 %. The substantial increase in number of HDB gives evidence on the biostimulation of their growth by the colonization of exoelectrogenic bacteria in the same system. The authors stipulate that the limited biostimulation far from the anode is due to the fact that exoelectrogenic bacteria need either to connect to the anode through direct contact or through a conductive network which is limited in length (Wang et al., 2012). The study that testified highest current density (299 mA/m^2) also reported highest improvement of removal with 153-484 % higher TPH degradation rate after 65 days than the control. However, some authors found no correlation between power densities and biodegradation rates; a fact that they explain with oxygen intrusion (Adelaja et al., 2015), substrate to biomass conversion (Hu et al., 2011) and electron losses due to the electron transfer from the substrates to other electron acceptors such as sulfate in solution and/or assimilation of electrons for bacterial growth (Liu et al., 2005).

Down to the present day, there is no available data for the treatment of NPs within microbial fuel cells.

4.6 Removal of polycyclic aromatic hydrocarbons and NPs by bioelectrochemical systems with an anaerobic cathode

Only two scientific articles are published to this date that considered PAH removal in a BES with an anaerobic cathode. The first study used an anaerobic cathode for the bioremediation of naphthalene (100µM) in a dual chamber BES where both electrode chambers were flushed with a mixture of nitrogen and carbon dioxide (95/5) to maintain anaerobic conditions (Zhang et al., 2010). Naphthalene was completely removed after only 9 days while the sterile and open circuit controls did not show any removal. This outcome was the first evidence that an electrode as electron acceptor can stimulate the anaerobic oxidation of aromatic hydrocarbons in contaminated sediments. In the second study, Sherafatmand and Ng tested the action of a SMFC on naphthalene, acenaphthene and phenanthrene removal with either an aerobic or an anaerobic cathode that they obtained by diffusing air in the overlying water column of the SMFC or by sealing the reactor (Sherafatmand and Ng, 2015). Interestingly, results for the anaerobic cathode removal were much higher for two of the PAHs (76.9 % naphthalene, 52.5 % acenaphthene, 36.8 % phenanthrene) than results for the degradation with an aerobic cathode (41.7 % naphthalene, 31.4 % acenaphthene, 36.2 % phenanthrene). Nevertheless, both treatments exceeded the natural attenuation of all PAHs, some by a factor of three (natural: 29 % naphthalene, 29 % acenaphthene, 12 % phenanthrene). The authors stipulated that the potential difference between anode and cathode led to a change in the physical and chemical properties of soil that consequently stimulated the prevailing microorganisms. These pioneering studies exemplify that there is a significant opportunity to degrade PAHs in BESs where oxygen is completely absent from both electrode chambers.

The relationship between the supplied current and the degradation efficiency of PAHs in MECs is not yet proven. Nevertheless, a positive correlation between the bioremediation of PAHs and the amount of supplied current has been demonstrated in several electrokinetic studies (Li et al., 2010; Mena et al., 2014). Examples of positive correlations between current density and PAH bioremediation in MFCs have been put forward although, it is yet unclear whether the success of

bioremediation through the application of current in MECs is due to a change in soil properties or whether the metabolism of HDBs is accelerated more directly.

Down to the present day, there is no available data for the treatment of NPs within microbial electrolysis cells.

4.7 Removal of polycyclic aromatic hydrocarbons and nonylphenols enhanced by conductive materials

Materials such as graphite and biochar inhere conductive properties based on their aromaticity since the delocalization of pi electrons throughout the planes of aromatic rings causes electron to flow (Bourke et al., 2007). Conductive materials were shown to enhance methane production in anaerobic digesters (Dang et al., 2016) suggesting their potential to increase the removal of PAHs and NPs during methanogenesis based on cometabolism. Improved biogas yields are proposed to rely on enhanced DIET or enhanced interspecies hydrogen transfer (Xu et al., 2016). Conductors have been, therefore, tested as electron shuttles separate from and inside bioelectrochemical systems with the hope to increase direct interspecies electron transfer and/or direct electron transfer between solid electrodes and microorganisms. For instance, carbon materials served as electron shuttles for the biological and chemical reduction of organic pollutants such as azo dyes (Pereira et al., 2017) and it was demonstrated that carbon felt as conductive carrier for biofilms enhanced phenol removal from wastewater in BES (Ailijiang et al., 2016). Only recently, conductive carbon materials enhanced bioelectricity generation along with PAH removal in MFCs (Li et al., 2016b, 2016c). Hydrocarbon degrading MFC in soil was optimal both in terms of current density (299 mA/m^2) and remediation efficiency (484 % higher degradation rate than the control) when carbon fibre was added after having rinsed saline soil with distilled water (Li et al., 2016b). Accordingly, net PAH removal in the connected MFCs ranged between 44 and 88 %. While 1-3 ring PAHs were removed very efficiently the concentration of 4-6 ring PAHs also decreased. This bioremediation success resulted from electron transfer promotion and current collection by the conductive carbon material. The soil electrical conductivity of the control MFC without carbon fibre addition was 0.61 mS/cm whereas the carbon fibre supplemented soil MFC showed a 2.5 fold higher electrical conductivity of 1.5 mS/cm. The corresponding open circuit controls had 110 % and 419 % lower conductivities. In this study, the authors correlated strong degradation rates of hydrocarbons with stronger naphthalene dioxygenase and xylene

monooxygenase activities in comparison relative to the non-carbon fibre control. Interestingly, even the high molecular weight fractions of hydrocarbons (C28-C36, 4-6 ring aromatics) could be degraded in this MFC. Moreover, the easy recovery of the carbon fibre could allow for its reuse. As a comparison, the soil conductivity of another saline soil MFC that processed petroleum hydrocarbons ranged between 7 and 14 mS/cm. The MFC with the highest water content (33 %) and highest conductivity achieved a 120 % higher TPH degradation rate than the open circuit control (Wang et al., 2012). A comparison between conductivities indicates that even though conductivity appears to enhance microbial electron transfer reactions, the measurement of conductivity alone cannot be a sufficient indicator of removal success. For example, salts such as sodium chloride can cause microbial inhibition in spite of enhanced soil conductivity. On the contrary, conductive materials such as carbon fibre act as electron transport promoters without inhibiting microbial metabolisms. Interspecies electron transfer (IET) via electric currents through carbon materials and other conductors exhibits faster electron transfer mechanisms compared to interspecies hydrogen transfer (Cruz Viggi et al., 2014) and could therefore explain enhanced bioremediation of PAHs. As another example, the addition of 1 % (w/w) carbon fibre to a soil MFC could further enhance PAH removal compared with the MFC without carbon fibre. In open circuit controls without carbon fibre, the net concentration of 16 PAHs decreased by 5% whereas the equivalent closed circuits showed a 5 fold removal. However, the carbon fibre MFC outcompeted the classic MFC with a 7.5 times higher removal rate than in the open circuit (Li et al., 2016c). Interestingly, the open circuit control containing carbon fibre similarly outcompeted the open circuit control without carbon fibre. This confirms that the sole presence of carbon fibre can enhance PAH removal even if electrodes are not connected. Yet, the experimental conditions are specific to the employment of MFCs which use the anode as electron acceptor for organics oxidation and associated hydrocarbon removal. Even though oxygen is not present in the anode medium, in principal, it is the terminal electron acceptor of the MFC. Therefore, this removal can be considered aerobic-like.

On the other hand, activated carbon is used as additive to soils in agriculture since it can not only enhance the soil's water-holding capacity and remediate soil acidification (Sigmund et al., 2017) but also remove PAH in water, sediment and soil (Ahmad et al., 2014). As described in section 2.1 most studies that concern bioremediation with conductive materials investigate PAH removal

with respect to sorption. Experimental setups that combine the questions whether hydrophobic organic contaminants are bioavailable with the study of microbial ecology are rarely documented (Cheng et al., 2017b). Nonetheless, there are some studies that also explore the microbial activation capacity of the conductive material which was employed. For instance, (Liu et al., 2015) found that the number of gene copies related to aerobic PAH degradation was enhanced after biochar addition (Liu et al., 2015) and the soil microbial community changed its composition. It was, hence, concluded that the addition of biochar has a positive effect on PAH-metabolizing bacterial activity leading to increased PAH dissipation (Liu et al., 2015). Interestingly, biochar of different sources were used by different biota. For instance, yeast-derived biochar promoted fungi in the soil, while glucose-derived biochar was utilized by Gram-negative bacteria (Steinbeiss et al., 2009). Consistent with this study, substantial biochar addition changed the community structure of soil samples towards a more gram negative dominated community (Gomez et al., 2014). In contrast to these results, biochar which was produced at 700°C did not affect microbial activity or biomass no matter the feedstock source (Zhang et al., 2014). This result was explained by the fact that biochar derived at such high temperature does not contain available carbon or nitrogen substrates. Finally, biochar was also found to decrease microbial abundance when amended to mangrove sediments (Luo and Gu, 2016). One of the rare studies which investigated NP removal in view of both, enzyme activity and microbial abundance showed that biochar had an impact on microorganisms by changing NP toxicity as well as microbial quantity and activity, rather than by changing microbial community structure (Cheng et al., 2017b).

Conductive materials are considered to provide an ecological advantage for species that employ DIET (Zhao et al., 2016). Surprisingly, it was not yet proposed that the conductive materials could accelerate DIET with respect to PAH removal. The addition of conductive materials in methanogenic conditions is a hot topic in recent research papers. Conductive materials were used to improve performances of anaerobic digesters (Chen et al., 2014a; Liu et al., 2012) as described in section 4.1 but did not focus on the removal of specific micropollutants. To the best knowledge of the author, there are only two studies which suggest a DIET mechanism for the enhanced biodegradation of an aromatic compound during methanogenesis based on the characteristics of conductivity iron minerals (Wang et al., 2017; Zhuang et al., 2015). The first showed that the

presence of hematite and magnetite in methanogenic benzoate degradation led to 25 % and 53 % more removal compared to the iron-free controls (Zhuang et al., 2015). The second study demonstrated that dichloronitrobenzene can be more efficiently removed by magnetite addition to a bioelectrode-upflow anaerobic sludge blanket (UASB) reactor, combining a BES with the addition of conductors (Wang et al., 2017).

Overall, the finding that petroleum hydrocarbons (including PAHs) within MFCs and benzoic acid under methanogenic conditions can be better removed by the addition of conductive materials points to a huge bioremediation potential also for PAHs. Therefore, PAH and NP bioremediation under such conditions should be explored in more detail.

5. Microbial insight in PAH bioremediation with bioelectrochemical systems or conductive materials

5.1 Electroactive species

Electroactive species are interesting candidates for the enhanced removal of organic matter and possibly the degradation of organic contaminants since their growth is favoured by conditions in which they can perform DIET. Exoelectrogens can be found in diverse habitats and are affiliated to many different microorganisms such as *Clostridia*, *Bacilli* and different *Proteobacteria*, thus pointing to the absence of an ecological niche for exoelectrogens (Koch and Harnisch, 2016). In electroactive biofilms that were established from sediment, it is the *δ-Proteobacteria* that are predominant but a great diversity of *α-,β-, γ-Proteobacteria* and *Firmicutes* is found in different MFC architectures and operating conditions (Logan and Regan, 2006). Few exoelectrogens are able to exchange electrons with electrode in both directions. Notably, bidirectional electron exchange has recently been observed for *Geobacter soli* biofilms from and to a graphite electrode (Yang et al., 2017). *Geobacter* and *Shewanella* are two of the most important exoelectrogens in bioelectrochemical systems that can accept or donate electrons from and to anodes or cathodes of a bioelectrochemical system (Choi and Sang, 2016; Yang et al., 2017). High power densities from complex sources of organic matter in MFCs are typically associated with the presence of *Geobacteraceae* in the anodic community (Kiely et al., 2011) since through nanowires, they facilitate substrate degradation (Bond and Lovley, 2003; Shu et al., 2016). *Geobacter* is capable

to exchange electrons via mediated electron exchange using self-produced flavins (Park et al., 2016; TerAvest and Angenent, 2014) but also via direct interaction with an electrode (Ding et al., 2016; Malvankar and Lovley, 2014). *Geobacter* sp. is gram negative and strictly anaerobic bacteria. They are ubiquitous in sediments and aquatic environments. As a result, they can metabolize a broad range of organic substrates such as VFAs, alcohols, phenols and benzene (Lovley et al., 2011). Moreover, *Geobacter* is able to produce current from acetate, starch, glucose (Eyiuche et al., 2017), lactate and formate consumption (Speers and Reguera, 2012). In particular, with respect to PAH biodegradation, *G. metallireducens* can initiate the degradation of benzene (Zhang et al., 2013) and *G. sulfurreducens* was isolated from a petroleum hydrocarbon degrading MFC (Zhou et al., 2016).

5.2 Microbial syntrophy for PAH bioremediation

The complex nature of organic waste requires a diverse microbial community for dissembling its chemical components (Logan and Rabaey, 2012), thus giving rise to syntrophic degraders. The positive effect of electricity generation or input in PAH bioremediation is probably related to bioelectrochemical catalysis in which HDB are favoured by the presence of electroactive microorganisms. A syntrophic relationship between exoelectrogens and various bacterial phyla has already been determined by various scientists (Kiely et al., 2011; Kimura and Okabe, 2013; Lu et al., 2012). Fermentative bacteria and acetate consuming anode respiring bacteria (Parameswaran et al., 2009) as well as methanogenic communities and exoelectrogens (Rotaru et al., 2014b) have been observed to interact on the basis of cooperative metabolite production and consumption. This is no surprise since syntrophic bacteria drive the anaerobic degradation of certain fermentation products (e.g., butyrate, ethanol, propionate) into intermediary substrates (e.g., H_2, formate, acetate) (Schmidt et al., 2016) that can eventually be used by exoelectrogens and/or methanogens. Although a syntrophic relationship between HDB and an exoelectrogen has not yet been proven, a metabolic cooperation could be imagined between heterotrophs in soil from the *α*- or *β-Proteobacteria* phylum such as *Sphingomonas* or *Burkholderia* genus. Indeed, these organisms use diverse substrates among other recalcitrant aromatic and phenolic compounds as carbon sources (Aislabie et al., 2013). Interestingly, *Burkholderia cenocepacia* was identified as the microorganism that produced an unidentified bacterial oxidant in the cathode chamber of an acetate fuelled MFC which caused an 11 times increase in cell voltage

compared to oxygen as electron acceptor (Hunter and Manter, 2011). *Burkholderia species* were also acknowledged as one of the dominant members of an anode chamber microbial community in a MFC using acetate as anodic substrate (Quan et al., 2012). The results described in chapter 4.5, suggest that electricity generating bacteria enhance HDB activity (G. Zhang et al., 2012) through a syntrophic metabolism, namely by accepting additional electrons from the metabolites of HDB degradation. By shuttling them to the anode, they supposedly alleviate thermodynamic limitations of PAH removal similar to those described under methanogenic conditions (Christensen et al., 2004) when *Archaea* consume hydrogen to keep hydrogen partial pressure low enough for an exergonic reaction to occur (Gieg et al., 2014). Furthermore, microbial community analysis from an olive mill wastewater treating MFC has shown that both exoelectrogenic and phenol-degrading microorganisms from the *Sphingomonas* phylum were concentrated in the anode biofilm (Bermek et al., 2014).

Syntrophy of microbial PAH degraders with bacteria or *Archaea* by the addition of conductive materials is not yet investigated. However, sequencing results of a benzoate degrading microbial community under methanogenic conditions showed that *Bacillaceae*, *Peptococcaceae*, and *Methanobacterium* are potential partners in syntrophic benzoate degradation that is promoted by DIET (Zhuang et al., 2015). Since benzoate is a common intermediate in the anaerobic metabolism of aromatics, these species could constitute potential syntrophic degraders in PAH metabolizing microbial communities.

5.3 Promising microbes for PAH removal with BES and conductive materials

Several studies cite the *Proteobacteria*, *Firmicutes* and *Bacteriodetes* phyla comprising bacteria belonging to the *Enterobacteriaceae* and *Pseudomonadaceae* families that could be potential key players of PAH removal in BESs. *Geobacteraceae* have been found in two petroleum removing MFCs (Li et al., 2014; Zhou et al., 2016) and one toluene removing MEC (T. Zhang et al., 2010), thus representing three out of nine publications that investigated the presence of specific microbial phyla in PAH degrading BESs (Table 8). Interestingly, the capacity of a soil-MFC to selectively enrich exoelectrogenic hydrocarbon degraders was convincingly demonstrated by the isolation of two exoelectrogens from *Geobacter* and *Ochrobactrum* species that used petroleum hydrocarbons as a sole carbon source (Zhou et al., 2016). Likewise, *Escherichia* species (Li et al., 2014; Lu et al., 2014a) and the *γ*- and *δ-Proteobacteria* as well as *Negativicutes* and *Bacilli*

(*Firmicutes*) classes are possible candidates for successful PAH bioremediation in MFCs (Table 8) since their abundances have shown positive correlations with hydrocarbon degradation (Li et al., 2016a; Venkidusamy et al., 2016). Differences in functional bacteria can be observed for crude oil and diesel degradation. Accordingly, 71 % of the predominant γ-*Proteobacteria* in a crude oil degrading MFC were *Escherichia spp.* (Li et al., 2016a) whereas the dominant phylum following bioremediation of diesel contaminated soil was *β-Proteobacteria* including mainly genera of *Achromobacter*, *Alcaligenes*, *Bordetella*, *Comamonas*, and *Pusillimonas* (Lu et al., 2014a). As an example for microbial selection during bioelectrochemical treatment, the abundance of *Firmicutes* increased by 346 % on average during the BES-treatment of a petroleum contaminated soil, at a much higher degree than for conventional bioremediation (Popp et al., 2006). Furthermore, the study by Lu et al. (2014a pointed out that all exoelectrogens observed in their study belonged to *Proteobacteria*. More specifically, exoelectrogens that could also degrade hydrocarbons belong to the *Enterobacter* and *Pseudomonas* genera. The recognised hydrocarbon degraders and exoelectrogenic bacteria *Pseudomonas putida* and *Pseudomonas aeruginosa* were also part of the anode biofilm. *Pseudomonas* species respire anaerobically via the production of phenazines and pyocyanin. These electron shuttling compounds can in turn help microbial co-oxidation of contaminants such as phenanthrene via electron transfer to the anode (Qiao et al., 2015). In addition, Venkidusamy et al. reported sequence similarities with *Geobacillus* and *Megasphaera* species that both participate in current generation of mediator-less MFCs and diesel degradation (Liu et al., 2009; Venkidusamy et al., 2016). The anode biofilm of another diesel degrading MFC contained *Shewanella* and *Dechloromonas* species. Certain *Dechloromonas* species such as *Dechloromonas aromatica* are capable of degrading aromatics, (Salinero et al., 2009). They can use toluene, benzene and xylene as electron donors under anaerobic conditions coupled to nitrate reduction (Chakraborty et al., 2005). The discovery of the *Shewanella* species is promising since *Shewanella oneidensis* and *Shewanella putrefaciens* are part of many MFC anode biofilms (Gorby et al., 2009). Moreover, *Shewanella* species have been found to possess nanowires which are believed to improve the utilization of the anode as an electron acceptor (Gorby et al., 2009). Table 8 lists the microbial communities that were already detected in PAH degrading MFCs.

Table 8: MFC microbial communities involved in PAH removal.

References	Genera	Phylum, Class, Order, Family	Hypothetical role proposed by author
(Li et al., 2014)	*Geobacteraceae* spp.	*Proteobacteria, δ- Proteobacteria, Desulfuromonadales, Geobacteraceae*	Electricity generation, hydrocarbon degradation
	Escherichia spp.	*Proteobacteria, γ-Proteobacteria, Enterobacteriales, Enterobacteriaceae, Escherichia*	
(Li et al., 2016b)	No genera indicated	*Negativicutes, δ- Proteobacteria, Bacilli*	Hydrocarbon degradation (TPH, alkane, PAH)
(Li et al., 2015)	*Alkanivorax*	*Proteobacteria, γ-Proteobacteria, Oceanospirillales, Alcanivoracaceae*	Hydrocarbon degradation
	No genera indicated	*Proteobacteria* (88% *γ-Proteobacteria*)	
	Escherichia spp.	*Proteobacteria, γ-Proteobacteria, Enterobacteriales, Enterobacteriaceae, Escherichia*	
(Lu et al., 2014a)	*Enterobacter cloacae*	*Proteobacteria, γ-Proteobacteria Enterobacteriales, Enterobacteriaceae, Enterobacter*	Oxidation of hexadecane and diesel
	Pseudomonas aeruginosa, Pseudomonas putida	*Proteobacteria, γ-Proteobacteria, Pseudomonadales, Pseudomonadaceae, Pseudomonas*	Electricity generation, hydrocarbon degradation
(Morris et al., 2009)	*Shewanella* spp.	*Proteobacteria, γ-Proteobacteria, Alteromonadales, Shewanellaceae, Shewanella*	Diesel range organics degradation
(Sabina et al., 2014)	*Bacillus subtilis moh3*	*Firmicutes, Bacilli, Bacillales, Bacillaceae, Bacillus*	Waste engine oil: long-chain, branched and cyclic hydrocarbons

(Venkidusamy et al., 2016)	*Clostridium*, *Shewanella*, *Rhodopseudomonas*	*Firmicutes*, *Clostridia*, *Clostridiales*, *Clostridiaceae*; *Proteobacteria*, *γ-Proteobacteria*, *Alteromonadales*, *Shewanellaceae*; *Proteobacteria*, *α-Proteobacteria*, *Rhizobiales* *Bradyrhizobiaceae*	Electricity generation
	Geobacillus spp.	*Firmicutes*, *Bacilli*, *Bacillales*, *Bacillaceae*, *Geobacillus*	Diesel degradation, current generation in mediator-less MFC
	Megasphaera spp.	*Firmicutes*, *Negativicutes*, *Selenomonadales*, *Veillonellaceae*	
	Flavobacterium, *Stenotrophomonas*, *Geobacillus*, *Gordonia*	*Flavobacteria*, *Flavobacteriaceae*, *Flavobacterium*; *Proteobacteria*, *γ- Proteobacteria*, *Xanthomonadales*, *Xanthomonadaceae*; *Firmicutes*, *Bacilli*, *Bacillales*, *Bacillaceae*; *Actinobacteria*, *Actinomycetales*, *Gordoniacea*	Diesel degradation
(Zhang et al., 2010)	*Geobacter metallireducens*	*Proteobacteria*, *δ-Proteobacteria*, *Desulfuromonadales*, *Geobacteraceae*	Toluene degradation
(Zhou et al., 2016)	*Ochrobactrum cicero* *Ochrobactrum intermedium*	*Proteobacteria*, *α-Proteobacteria*, *Rhizobiales*, *Brucellaceae* *Ochrobactrum*	Electricity generation, petroleum hydrocarbon degradation
	Geobacter sulfurreducens	*Proteobacteria*, *δ-Proteobacteria*, *Desulfuromonadales*, *Geobacteraceae*	

6. Conclusions of the literature review

Firstly, the literature survey demonstrated that PAHs and NP are ubiquitous and recalcitrant organic micropollutants that pose threat to the future well-being of eco-systems and human's health. It was shown that the wastewater treatment plant represents a sink and source of these contaminants. It was, therefore, argued that micropollution should be addressed by finding innovative solutions for the removal of NP and PAHs in sewage sludge where they are concentrated, thereby limiting their diffusion to the environment. Secondly, anaerobic biodegradation of PAHs and NP was portrayed as an alternative to abiotic treatments and aerobic biodegradation with the advantage of being less expensive and already employed as removal pathway in existing wastewater treatment facilities; this latter points to the relevance of PAH removal that will be achieved during anaerobic digestion within the framework of this doctoral research study. Thirdly, it was pointed out that anaerobic biodegradation is limited by several factors, most importantly, the lack of terminal electron acceptors and the reduced bioavailability of PAHs and NP in complex organic matter due to their hydrophobicity. As a solution to these limitations, bioelectrochemical systems and conductive materials were, fourthly, presented showing their huge potential as accelerators of electron transfer between microorganisms and accordingly the syntrophic biodegradation of organic macro- and micropollutants. To this date, no studies can be found that investigate the use of a microbial electrolyser in order to decompose PAHs inside sludge. However, PAHs have been degraded inside sediment microbial fuel cells (SMFCs). These systems also make use of electroactive bacterial species but use of oxygen as terminal electron acceptor in the cathodic compartment (oxygenated water or the surrounding air). The fact that the system works in aerobic condition and that the polluted matrix is different (sediment instead of sludge) will change experimental parameters a lot. Two examples of enhanced PAH biodegradation with anaerobic cathodes (microbial electrolysers) in sediment showed that there is, nevertheless, a huge potential for PAH biodegradation in anaerobic conditions. One of these studies compared aerobic condition to anaerobic condition for the removal of phenanthrene, acenaphthene and naphthalene in a highly contaminated sediment. The anaerobic condition showed even higher removals for the degradation of naphthalene and

acenaphthene. Surely, the PAHs were present in higher concentrations compared to micropollution inside sewage sludge but these experiments point to the fact that different terminal electron acceptors than oxygen can have a positive impact on biodegradation of such recalcitrant components as PAHs inside bioelectrolysers. Lastly, the enhanced biodegradation of benzoic acid due to the addition of conductive iron minerals during methanogenesis was taken as an example for the acceleration of direct interspecies electron transfer with conductive materials in order to decompose a common aromatic's metabolite in methanogenic conditions. Based on these encouraging results, the focus of this dissertation comprised the use of conductive graphite felt or a MECs with graphite felt electrodes to stimulate PAHs and NP degrading organisms during anaerobic digestion and achieve higher removal rates from lowly contaminated municipal sewage sludge. The scientific ambition is to shed light on the underlying removal pathways including sorption, volatilization, biodegradation and electrochemical removal of PAHs and NP.

Chapter II: Materials and methods

List of tables

List of figures

1. Spiking of municipal sewage sludge

Dewatered sludge was obtained from a WWTP of 285,000 population equivalent (Limoges, France). The sludge from the secondary treatment (activated sludge) was dewatered and kept in a storage tank until anaerobic digestion. The properties of the initial sludge are shown in Table 1.

Table 1: Properties of the initial dewatered sludge. Aqueous and particulate phases were separated thanks to centrifugation at 18600 g at 4 °C for 20 min.

	Sludge phase	Total solids [g/L] (% of bulk)	Chemical oxygen demand [g/L] (% of bulk)	Volatile Fatty acids (VFA) [g/L]
Aliquot A	Bulk	59	67	-
	Aqueous	(25)	(0.2)	0.9
	Particulate	(75)	(98.8)	-
Aliquot B	Bulk	45	57	-
	Aqueous	(20)	(0.2)	0.45
	Particulate	(80)	(98.8)	-

A decontaminated (acetone washed) plastic recipient was filled with the dewatered sludge and diluted 2.5 times with distilled water. This sludge with chemical oxygen demand (COD) of 29.0 g/L and total solids content of 23 g/L served as both, inoculum and substrate for the various experiments, and was spiked with a mix containing 12 PAHs and NP in acetonitrile (ACN). The targeted spiking concentrations were 5, 1.25 and 100 mg/kgTS for 11 PAH, indeno(1,2,3,c,d)pyrene and NP, respectively. For this aim, each molecule was weighed in a glass vessel and diluted in dichloromethane before joining volumes of known PAH and NP concentrations to a micropollutant mix which was evaporated and taken up with 5 ml of ACN. 4.975 ml of the spiking solution were added to 8.5 L sludge that was continuously mixed. After 20 minutes, the spiked sludge was portioned into 1 L and 2 L acetone washed polypropylene

containers and stored at -20°C. For sludge sterilization, spiked sludge was slowly defrosted and underwent heat treatment at 121°C for 20 min before its use in the digesters. 25 µl of the spiking solution was stored at 5°C for five months before detection of its concentration with a dilution factor of 3460 in order to fit the range of calibration. The measured initial concentrations in the total phases of sludge are listed in Table 2.

Table 2: Initial concentrations of 12 PAHs and NP after diluting and spiking the dewatered municipal sewage sludge.

Molecule	Theoretical concentration in sludge via the spiking solution [µg/kg TS]	Concentration measured in sludge after spiking [µg/kg TS]	Recovery of theoretical concentration [%]	Concentration measured in sludge after spiking & heating [µg/kg TS]	Recovery of theoretical concentration [%]
Fluorene	5906	1709 ± 4	29	612	10
Phenanthrene	5718	3089 ± 92	54	1434	25
Fluoranthene	4985	2867 ± 7	58	2325	47
Pyrene	5144	3118 ± 82	61	2126	41
Chrysene	5506	3682 ± 88	67	3269	59
Benzo(a)anthracene	6842	4057 ± 55	59	3688	54
Benzo(b)fluoranthene	5489	3766 ± 82	69	3504	64
Benzo(k)fluoranthene	10090	6729 ± 149	67	6346	63
Benzo(a)pyrene	6231	3238 ± 88	52	3322	53
Benzo(g,h,i)perylene	3921	3772 ± 82	96	4068	104
Indeno(1,2,3,c,d)pyrene	1090	833 ± 11	76	823	76
Dibenzo(a,h)anthracene	5870	5468 ± 82	93	5760	98
Nonylphenol	Not measured	35669 ± 42	-	Not measured	-

The spiked sludge was stored at – 20°C in order to keep the inoculum unchanged. It was used at different points of time in 2015 and 2016. In 2017, the inoculum source was renewed (same WWTP as before) and diluted with distilled water in order to obtain a similar TS concentration of 25.3 g/L as in previous experiments. Another strategy was used to spike and fill the aliquot B of sludge in the various reactors as shown in Figure 1.

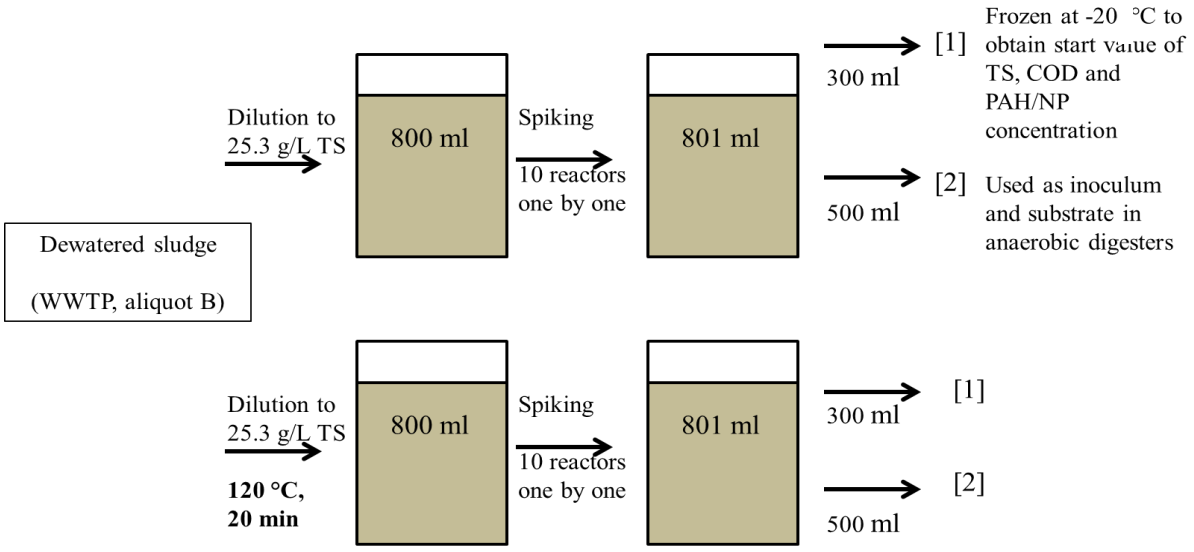

Figure 1: Spiking strategy of reactors for sludge aliquot B.

800 ml diluted sludge was firstly portioned in 20 reactors of 1L. 10 of these reactors were heat treated at 121°C for 20 min and spiked subsequently in order to avoid volatilization of micropollutants. Spiking was achieved with concentrations of 100 and 2000 µg/L ACN for each of 12 PAHs and NP after the sludge had cooled down to ambient temperature. The 10 other reactors were spiked directly with the same spiking solution. The individual spiking of the reactors was done by pipetting 0.5 ml to each reactor and gravimetrically verifying the volumetric addition (Table 3). 300 ml sludge of each reactor were, then, taken aside and frozen at -20°C until contaminant extraction to obtain individual start concentrations of NP and PAHs. The remaining 500 ml were used as inoculum and substrate for 20 anaerobic digesters. The theoretical micropollutant concentrations of start sludge were calculated as follows:

Equation 1:
$$\frac{Micropollutant}{start\ sludge}\left[\frac{\mu g}{L}\right] = \frac{conc\left(\frac{Micropollutant}{ACN}\right)\left[\frac{\mu g}{L}\right] \times \frac{mass\ (spiking\ solution)\ [g]}{\rho(ACN)\ [\frac{g}{L}]}}{V(sludge)0.801\ [L]}$$

Table 3: Gravimetrically verified addition of spiking solution into 0.8 L of sludge.
Calculated (density of ACN= 0.873 g/ml) PAH and NP concentrations.

	Mass added [g]	Volume added [ml]	Theoretical concentrations in start sludge [µg/L]	
Sample	Spiking solution	Spiking solution	NP	12 PAHs (each molecule)
Cont_a	0.4255	0.5434	1357	67.8
Cont_b	0.4004	0.5114	1277	63.8
GF_INT1a	0.3947	0.5041	1259	62.9
GF_INT1b	0.3893	0.4972	1241	62.1
GF_INT2a	0.4017	0.5130	1281	64.0
GF_INT2b	0.3995	0.5102	1274	63.7
GF_DES1a	0.3934	0.5024	1254	62.7
GF_DES1b	0.3887	0.4964	1240	62.0
GF_DES2a	0.4005	0.5115	1277	63.9
GF_DES2b	0.394	0.5032	1256	62.8

	Mass added [g]	Volume added [ml]	Theoretical concentrations in start sludge [µg/L]	
Sample	Spiking solution	Spiking solution	NP	12 PAHs (each molecule)
Cont_a__HT	0.3558	0.4544	1135	56.7
Cont_b__HT	0.3569	0.4558	1138	56.9
GF_INT1a__HT	0.3563	0.4550	1136	56.8
GF_INT1b__HT	0.3564	0.4552	1137	56.8
GF_INT2a__HT	0.3599	0.4596	1148	57.4
GF_INT2b__HT	0.3586	0.4580	1144	57.2
GF_DES1a__HT	0.3605	0.4604	1150	57.5
GF_DES1b__HT	0.36	0.4598	1148	57.4
GF_DES2a__HT	0.357	0.4559	1138	56.9
GF_DES2b__HT	0.3589	0.4584	1144	57.2

2. Design of experiments

2.1 Anaerobic digester operation with graphite felt and potentiometric control

In order to start the anaerobic digesters in parallel, the dewatered and spiked sludge (aliquot A) was defrosted at 5°C and triplicate reactors with working volumes of 500 ml were prepared as follows. Three anaerobic digesters (3 x Cont) served as controls (no material). Three more reactors contained two pieces of 1.36 g graphite felt (GF) (Mersen grade RVG 4000 with dimension of 4.7 cm x 2.7 cm x 1.2 cm) as conductive material with a specific surface area (SSA) of nearly 2 m^2 (3 x GF_INT2). The three last reactors contained the same amount and dimension of GF to constitute two electrodes in a single chamber MEC at closed circuit with a polarized working electrode at an electric potential of +0.8 V vs. the Standard Hydrogen Electrode (SHE) (3 x BES as bioelectrochemical systems). Equivalent reactors were run on the same spiked sludge that was heat treated in an autoclave at 120°C for 20 min. to obtain abiotic control reactors (2 x Cont_HT, 1 x GF_HT, 3 x BES_HT). A schematic overview of the reactor configurations of anaerobic digesters with graphite addition and potentiometric control is given in Figure 2 along with digital illustrations (Figure 3).

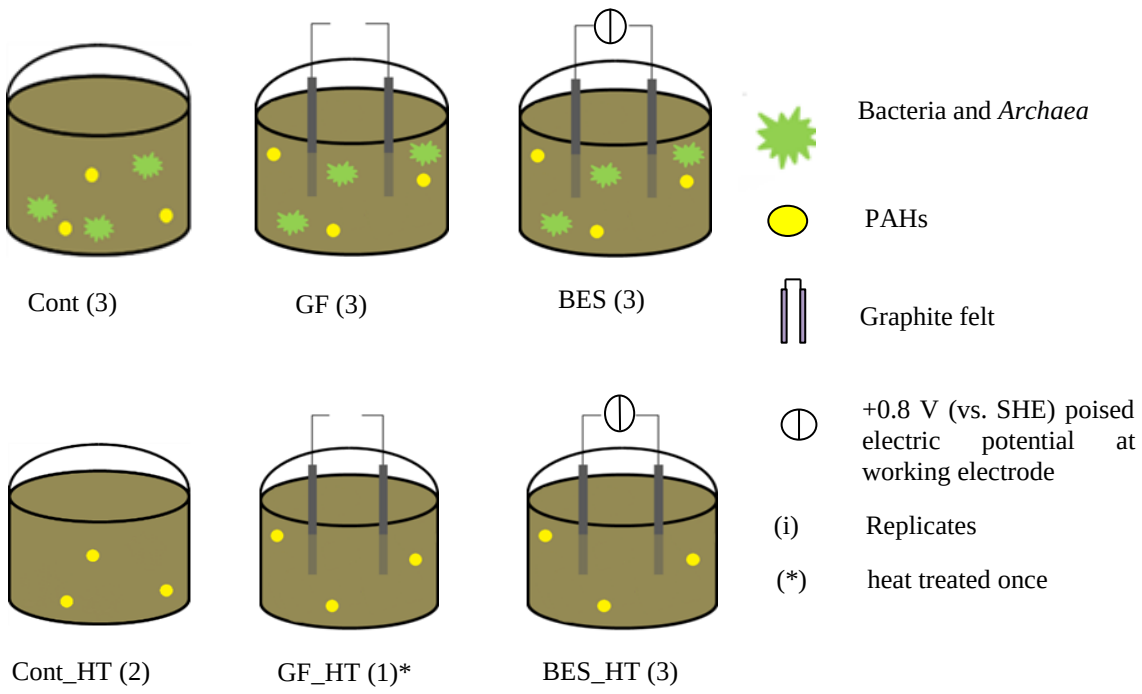

Figure 2: Reactor configurations of graphite felt supplemented reactors with or without potentiometric control.
Cont=anaerobic control digester; GF= graphite felt digester; BES= bioelectrochemical digester; below: HT= heat treated controls.

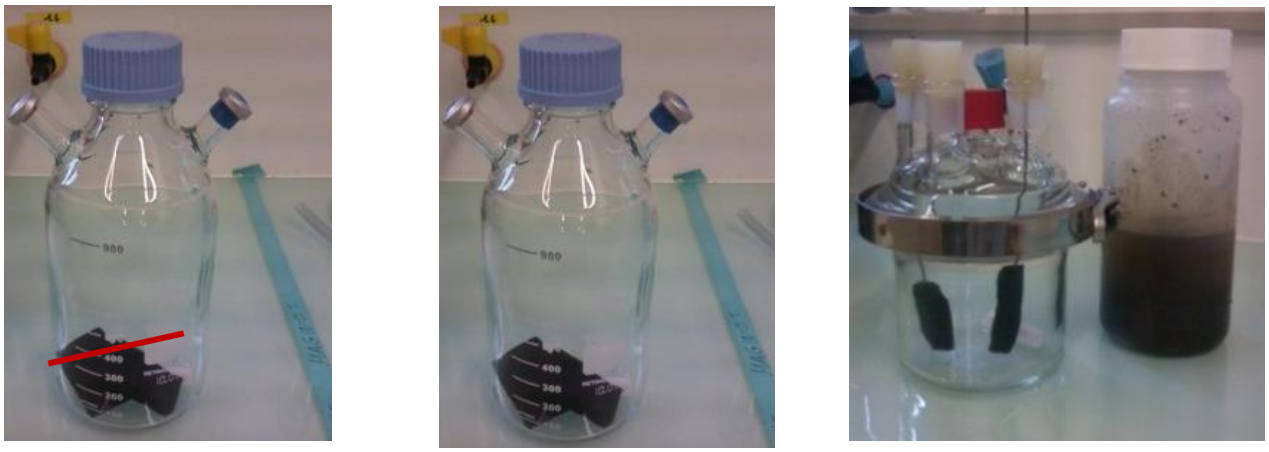

Figure 3: Reactor configuration.
Left=anaerobic digester without graphite felt; middle= graphite felt digester with graphite felt pieces; right= bioelectrochemical digester with the same amount of graphite felt, each piece connected to a titanium rod for subsequent connection to a potentiostat.

The reactors were operated at 37°C, 650 rpm (magnetic agitation) and initial pH 7 during the experiment length of 42 days under anaerobic conditions (100 % nitrogen in headspace at t_0).

After 42 days, sludge samples were either centrifuged at 18,600 g for 20 min. and frozen (aqueous and particulate phases separately stored) or directly frozen at -20 °C. Particulate and bulk samples were, then, freeze-dried, grinded and stored in the dark before PAH extraction.

2.2 Anaerobic digester operation with conductive materials of different conductivity

This experiment was realized using the same aliquot A of the dewatered and spiked sludge. The sludge was slowly defrosted (5°C). Triplicate anaerobic digesters were prepared to distinguish between two different conditions. A projected surface area of 13 cm^2 of platinum (Pt) was added to three anaerobic reactors (3x Pt) filled with 160 ml of spiked sludge (working volume). Two carbon plates (Cp) with a similar projected surface area of 15 cm^2 were added to three other reactors (3x Cp) with the same working volume. The planar plates consisted of rigid graphite with the dimension 2.5 cm*2.5 cm*0.25 cm (C000440/15, Goodfellow SARL, 229 Rue Solférino, F-59000 Lille, France). Electrical conductivity data were not indicated by the manufacturer. According to values reported in literature synthetic graphite is 1000 times less conductive than Pt and 10-1000 times more conductive than GF (Bourke et al., 2007; Coeuret, 2007; Macijauskienė and Griškonis, 2015; Pauleau and Barna, 1997). The platinum-iridium material was manufactured according to Carmona-Martínez et al. (2013) and consisted of 90% Pt and 10% iridium (Heraeus PSP S.A.S., Contact Materials Division, 526, Route des Gorges du Sierroz, 73100 Grésy-sur-Aix, France). Equivalent reactors were run on the same spiked sludge that was heat treated in an autoclave at 120°C for 20 min. to obtain abiotic control reactors (2 x Cont_HT, 1 x Cp_HT, 1 x Pt_HT). Since remaining sludge quantities were limited, these reactors were operated only as unicates. Control reactors without conductive material addition were already operated with the same spiked sludge in the previous experiment. Results from the initial heat treated sludge as well as Cont and Cont_HT digesters are, however, presented in the result chapter along with the results obtained for heat and non-heat treated sludge that was supplemented with Cp and Pt.

A schematic overview of the reactor configurations of anaerobic digesters with Pt and Cp addition is given in Figure 4. The reactors were operated at 37°C, 650 rpm and initial pH 7 during the experiment length of 42 days under anaerobic conditions (100 % nitrogen in headspace at t_0). When methane production reached the stationary phase, sludge samples were either centrifuged

at 18,600 g for 20 min. and frozen (aqueous and particulate phases separately stored) or directly frozen at -20 °C. Particulate and bulk samples were, then, freeze-dried, grinded and stored in the dark before PAH extraction.

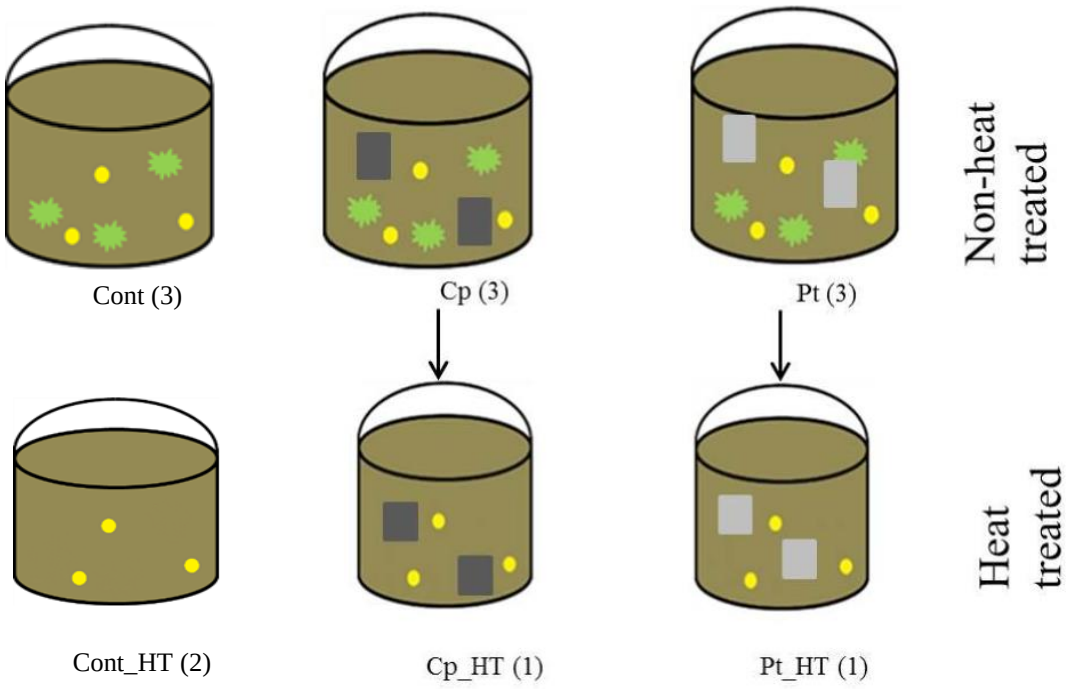

Figure 4: Reactor configurations for carbon plate and platinum supplemented anaerobic digesters. Above: Anaerobic digesters supplemented or not with carbon plate (Cp) and platinum (Pt), below: heat treated reactors (HT).

An overview of the conductivities of Pt and Cp together with the added quantities of conductors is given in Table 4. As a comparison, the same data are given also for GF which was used as conductive material in the former experiment. The SSA was only reported by the manufacturer for GF via nitrogen adsorption (0.7 m^2/g) leading to a SSA of 1.9 m^2 (2.72 g added to each reactor). In comparison to the SSA of activated carbon fibers, GF exhibits 1000- 3000 lower values (Fung et al., 1993). It is assumed that Pt and Cp SSAs are much smaller since both are rigid, non-porous materials and the SSA increases with smaller particle size as shown for graphite (Lowell et al., 2004) and higher porosity as confirmed experimentally by nitrogen adsorption isotherms and the use of the Brunauer, Emmett and Teller equation (Kruk et al., 1999; Ustinov, 2016).

Table 4: Main characteristics of materials added to anaerobic digestion.

Material	Conductivity at 20 °C [S/m]	Projected surface area [cm^2]	Experiment photos	Reference for conductivity
Materials used in experiments				
Platinum	$9.43*10^6$	13		(Pauleau and Barna, 1997) (Wilf and Dawson, 1976)
Carbon plate (99,95 % C)	$3.3*10^3$ (values for synthetic graphite), 2.0- $3.0*10^5$ (parallel to basal plane)/ $3.3*10^2$ (orthogonal to basal plane)	15		(Bourke et al., 2007), (Pierson, 1994)
Graphite felt (99,9 % C)	1.2	14		(Coeuret, 2007)
Materials listed as a comparison				
Graphite	$6.6 \pm 0.5*10^2$	-	-	(Macijauskienė and
Activated	$2.9\text{-}5.5*10^2$	-	-	(Fung et al., 1993)
Amorphous carbon	$2*10^3$	-	-	(Pauleau and Barna, 1997)

2.3 Anaerobic digester operation with graphite felt of different size

This experiment was conducted with the aliquot B of the dewatered sludge with characteristics as in Table 1. Previously sampled municipal sewage sludge was defrosted and twenty anaerobic

digesters were individually spiked as described in section 1. Duplicate reactors with 500 ml spiked sludge (working volume) were provided with different amounts of powdered or intact GF as depicted in Figure 5 with the corresponding nomenclature of samples given in

Table 5. Pieces of GF with SSAs of 1 m^2 and 2 m^2 were added as intact pieces (1.43 g and 2.86 g) constituting four anaerobic digesters with intact material (2x GF_INT1, 2x GF_INT2). GF pieces of the same SSA were destroyed with a mortar to increase its SSA as reported by Kuila and Prasad (2013). Values of the SSA of the obtained powder were not measured but are assumed to be at least ten fold higher (Lowell et al., 2004, p. 1) when descending from GF dimension of cm to mm or smaller. The obtained powder was added to four other reactors (2 x GF_DES1, 2x GF_DES2). Two controls without material addition were also operated in parallel. Equivalent reactors were run on the same spiked sludge that was heat treated in an autoclave at 120°C for 20 min. to obtain ten heat treated control reactors and spiked individually after heat treatment to avoid volatilization of PAHs and NPs as described before in section 0. (2 x Cont_HT, 2 x GF_INT1_HT, 2 x GF_DES1_HT, 2 x GF_INT2_HT, 2 x GF_DES2_HT).

The twenty digesters were operated at 35°C (constant room temperature) on a shaking device at 90 rotations per min with initial pH 7 during the experiment length of 83 days under anaerobic conditions (100 % nitrogen in headspace at t_0). When methane production reached the stationary phase (when the increase in methane production was only 2 % of the total accumulated normo-litre of methane), sludge samples were either centrifuged at 18,600 g for 20 min. and frozen (aqueous and particulate phases separately stored) or directly frozen at -20 °C. Particulate and bulk samples were, then, freeze-dried, grinded and stored in the dark before PAH/NP extraction.

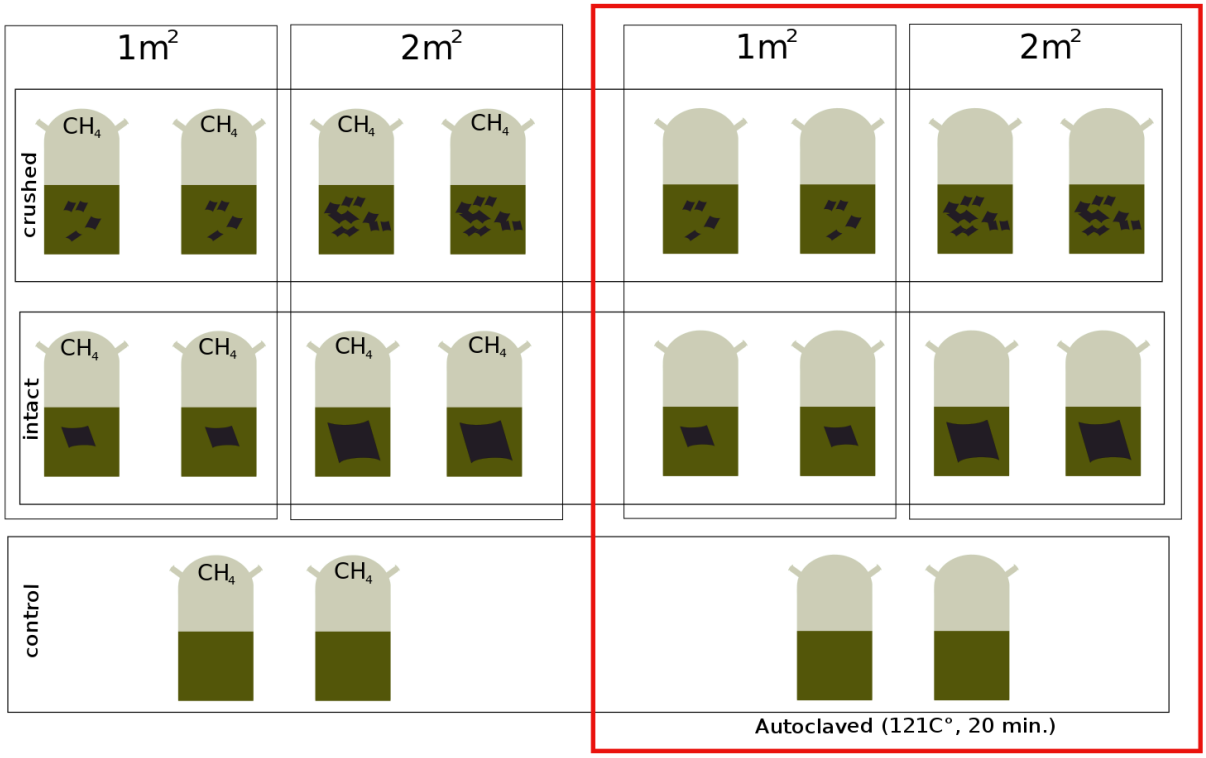

Figure 5: Schematic overview of 20 reactors that were provided with different amounts and structure of graphite felt. Left: Non-heat treated. Right: Heat treated.

Table 5: Nomenclature of experiment with powdered and intact graphite felt.
DES: destroyed, INT: intact. Cont: control, GF: graphite felt.

GF_DES1a,	GF_DES2a,	GF_DES1a_HT,	GF_DES2a_HT,
GF_INT 1a,	GF_INT2a,	GF_INT 1a_HT,	GF_INT2a_HT,
CONTa, CONTb		CONTa_HT, CONTb_HT	

3. Matter analysis

3.1 Methane quantification

Biogas volume was periodically measured using water displacement method. For the experiment with different added amounts of GF, biogas quantity was measured by inferring volumes from the difference in gas pressure that was detected in the headspace of reactors from one measuring event to the other. The biogas composition (CH_4, CO_2, H_2 N_2) was measured using a gas chromatograph (GC) (Clarus 580, Perkin Elmer) coupled to a thermal conductivity detector (TCD) operating according to a former study (Laperrière et al., 2017) except flow rate (35.5

mL/min). The norm-volume of methane was calculated by using the ideal gas equation at standard conditions (T= 273.15 K) with the ideal gas constant R= 8.314 J/(K*mol).

Equation 2: $$V = \frac{n \times R \times T}{p}$$

3.2 Volatile fatty acids quantification

Volatile fatty acids (VFAs) i.e. acetate, propionate, butyrate, isobutyrate, valerate and isovalerate were quantified using a gas chromatograph (Perkin Clarus 580) with capillary column [Elite-FFAP crossbond®carbowax® (15 m), 130 °C, N_2 as gas vector with flow rate of 3 mL/min] and equipped with a flame ionization detector maintained at 250°C. Before use, 500 µL of centrifuged bulk sludge (20 min., 18600 G) were mixed with 500 µL of internal standard (ethyl-2-butyric acid, 1 g/L).

3.3 Solids and suspended solids analysis

Total solid (TS) analyses of particulate and bulk phases were performed for the start and final sludge samples of reactors by gravimetric method with a sampling volume of 20 – 40 ml sludge. Mass of porcelain crucibles with sludge content were weighed before and after 24 hours of drying at 105 °C and calcination at 550 °C. The initial mass of the empty crucible after 2 h of drying at 105 °C (m_0) is deducted from the masses of sludge before (m_1) and after drying (m_2) and the quotient of these differences is calculated as the total solids per litre of raw sludge (Eq. 1).

Equation 3: $$TS\ (g\ TS/L) = 1000 * \frac{m_2 - m_0}{m_1 - m_0}$$

For volatile solids (VS), the difference of mass between drying (m_2) and calcination (m_3) is divided by the mass of sludge after drying (m_1 - m_0) to obtain the volatile solids per litre of raw sludge (Eq. 2).

Equation 4: $$VS\ (gVS/L) = 1000 * \frac{m_2 - m_3}{m_1 - m_0}$$

For the analysis of suspended solids, 20 ml of sludge was weight and subsequently centrifuged at 18600 g at 4 °C for 20 min. The supernatant was discarded and the retrieved precipitate subjected to drying at 105 °C and 550 °C. The suspended solids (SS) and volatile suspended solids (VSS) are calculated analogously to equations 3 and 4.

3.4 Chemical oxygen demand quantification

The COD expresses the amount of oxygen originating from potassium dichromate that reacts with the oxidizable substances that are contained in 1 L of water. It is measured in total and aqueous phases of sludge samples with kit Spectroquant (Merck) according to ISO 15705. 2 ml of diluted raw sludge/ undiluted aqueous sludge phase is added to the prepared test tube with potassium dichromate $K_2Cr_2O_7$ (orange) that oxidizes the present organic matter in acidic solution with silver sulphate as the catalyst while being reduced to chromate $Cr\ 3^+$ (green) during a contact time of 2 h at 150 °C. The obtained colour is measured photometrically in a range of 0 to 1500 mg O_2/L of prepared sample with MultiDirect Spectrophotometer (Aqualytic). 1 mol $K_2Cr_2O_7$ corresponds to 1.5 mol oxygen. The obtained value is referred to the total solids of the sludge sample as follows:

Equation 5: $$COD\ (mg\ O_2/TS) = \frac{COD_{undiluted}(mg\ O_2/L)}{TS_{sample}(gTS/L\ )}$$

The supplier indicates a standard error (STD) of 4.9 mg/L (0.3 %). This may be the case for a homogeneous aqueous sample without many particles or colloids. However, sludge and wastewater samples, on the contrary, are complex in composition. Thus, the standard error of the measurement of aqueous samples from sludge is about 5 % on average whereas the STD of the total sludge can attain more than 10 % since (i) the sampled sludge is heterogeneous, (ii) particles may not be completely oxidized (entrapped organic matter) and (iii) the dilutions made for samples that are highly charged in COD lead to the propagation of uncertainty.

4. PAH and NP analysis

4.1 PAH and NP extraction by accelerated solvent extraction

Frozen samples are freeze-dried with HetoPowerDry PL 3000 (ThermoElectron Corporation) at –55 °C and 1 mbar and subsequently crushed with a mortar to obtain a fine powder. Until extraction, these samples are stored in the dark at room temperature. The 12 PAHs and NP are extracted from 0.15 g dried sample (particulate and total phases) in duplicates using Accelerated Solvent Extraction (ASE 200, Dionex) with a hexane/acetone mixture (50:50 v:v). Inside the extraction cell, 1 g aluminium oxide (Sigma Aldrich) absorbs water traces from the sample and 1

g of hydromatrix (Varian) for a homogenous dispersion of samples, solvent flow and extraction. The extraction procedure consists in heating the cell to 120 °C, keeping the temperature and pressure of 100 bars for 5 min and purging 60 % of the cells volume to replace it by new solvent. Two extracts are obtained which are evaporated in Multivapor P-12 (Buchi) with vacuum pump V-700 (Buchi) at 45 °C, 350 mbars and constant agitation for a homogenous evaporation. Solvent evaporation to dryness is done under nitrogen flux. The dry extract is incorporated in 2 ml of ACN for PAH analysis (HPLC) and 1 ml of this extract is evaporated after weighing in order to obtain a quantified mass of extract in 1 ml of hexane for NP analysis (HPLC). These dilutions are stored at -20 °C.

In addition to each series of extraction, a reference sludge with known PAH and NP concentrations is extracted in order to guarantee that the series of extraction is in accordance with the standard extraction procedure. The results obtained from the extraction of NP and PAHs in the reference are given in Figure 6 and Figure 7 with micropollutant concentration in mg/kg TS and µg/kg TS, respectively. The upper and lower values indicate the range in which concentrations were measured by different laboratories in France and serve as standards. For NP extraction one observes that its concentrations always fall below the lower reference value (< 40 mg/kg). This extraction behavior has been observed for several years in the laboratory for extractions by different manipulators using the same reference sludge and analytical equipment. Therefore, these values are considered as a standard for NP concentrations in the present study.

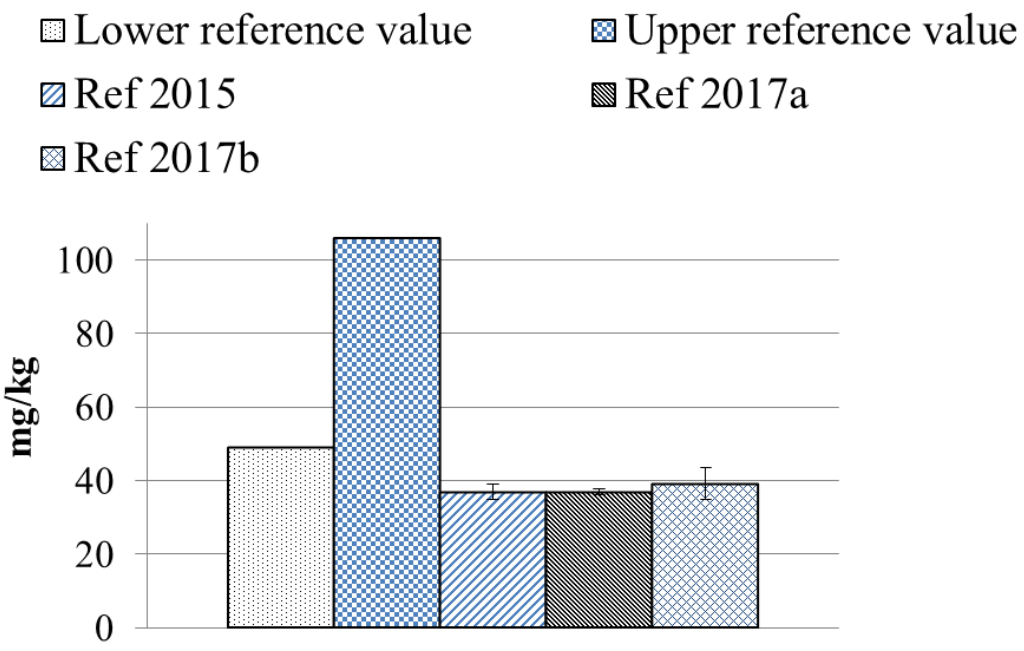

Figure 6: Results of NP extraction from the reference sludge that was extracted along with the different experiments in 2015 and 2017.
The upper and lower reference values were detected for the same sludge reference by different laboratories and are shown for comparison.

The average concentrations for 12 PAHs in the reference sludge that was extracted during the period of the PhD grant (2015, 2016 and 2017) lie in the range of the upper and lower PAH concentrations detected in different laboratories. Phenanthrene, Chrysene, Benzo(a)pyrene and Benzo(g,h,i)perylene are depicted in Figure 7 as representatives of 3,4,5 and 6 ring containing PAHs. The extractions that were performed in 2017 show a higher trend for extraction of all PAHs. This could be due to the fact different operators performed PAH extraction in 2016 and 2017.

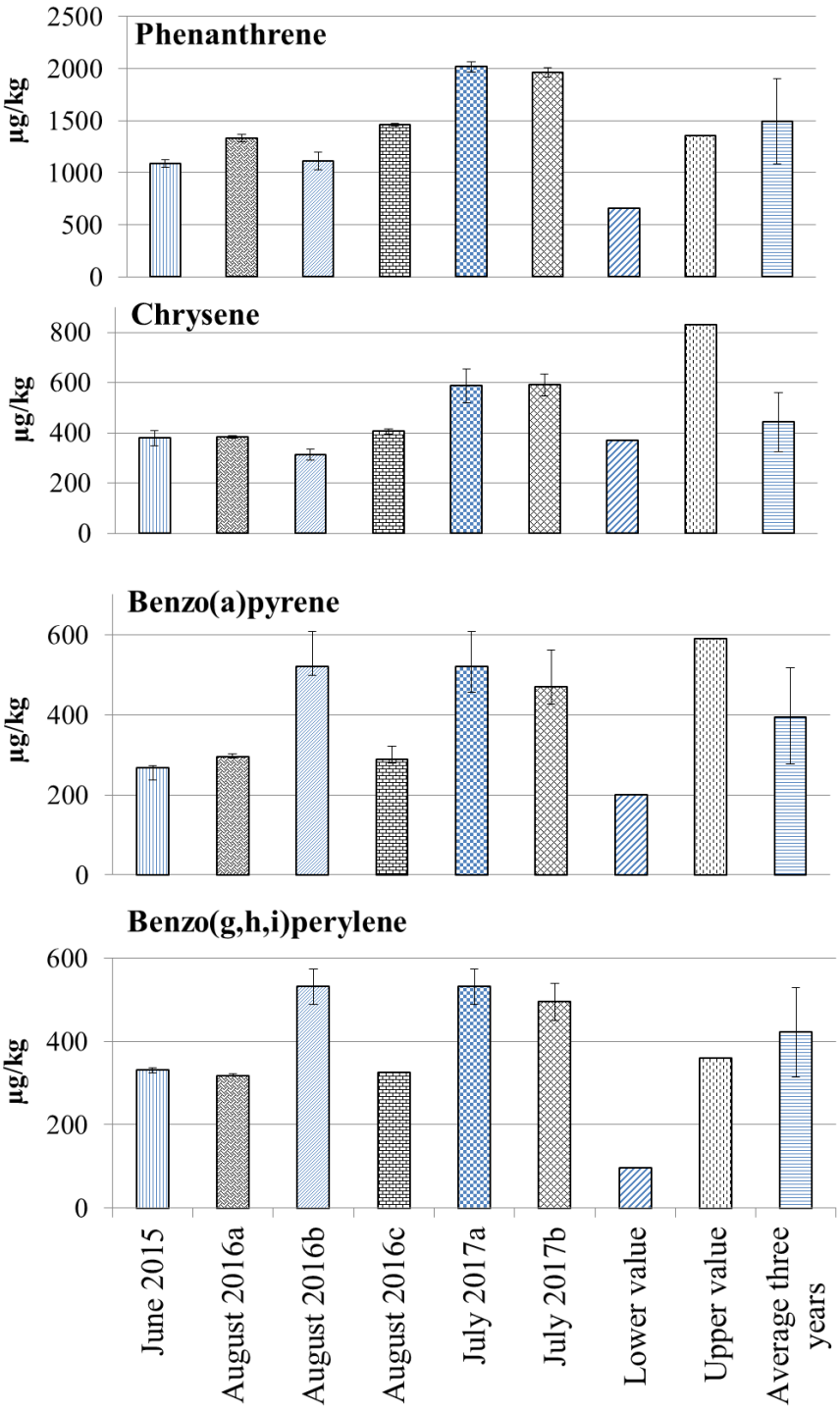

Figure 7: Results of PAH extraction from the reference sludge that was extracted along with the different experiments in 2015, 2016 and 2017.
The upper and lower reference values were detected for the same sludge reference by different laboratories and are shown for comparison.

.

4.2 PAH and NP quantification via HPLC

PAH and NP quantification is done *by liquid chromatography (HPLC Alliance Waters 2695) with* fluorescence detector *(Waters 2475)*. The column (EC 4/3 Nucleodur C18 PAH, 3µm, Macherey Nagel) is maintained at 30 °C during chromatrographic separation. 20 µL of sample are injected at a constant flow rate of 0.6 ml/min with a water/ACN mixture (40/60 v/v) during 2 min. The percentage of ACN is gradually increased until it reaches 100 % (15 min). It remains 4 min at 100 % and then the percentage is decreased to 60 % during 1 min where it remains 14 min. Optimal excitation and emission wavelength used for PAH and NP detection are listed in Table 6.

Table 6: Average retention time (t_R) and their excitation/ emission wavelengths (λ_{Ex} /λ_{Em}).
t_R and λ_{Ex} /λ_{Em} of PAHs and NP in the two different liquid chromatographic column for fluorimetric detection.

PAH	Flu	Phe	Ant	Flt	Pyr	BaA	Chry	BbF	BkF	BaP	DBahA	BghiP	Ind	NP
t_R	5.2	6.0	6.9	7.8	8.5	11.1	11.8	13.9	15.0	15.8	17.3	17.9	18.6	14
λ_{Ex}	266	250	250	280	260	280	268	234	270	270	300	300	300	228
λ_{Em}	312	370	400	430	410	430	384	420	400	400	407	407	500	305

Eight standards are used for PAH calibration with concentrations 5, 10, 25, 50, 100, 250, 500 and 750 µg/L obtained by diluting a concentrated stock solution of 10 mg/L (PAH MIX 9, CIL Cluzeau). Each ten samples (extracts in ACN), a standard of 50, 100 or 250 µg/L is injected in order to verify the instrument stability. Each extract is injected two times. A recalibration is done with respect to the obtained STDs of the control samples.

The column for NP quantification (Purospher STAR NH_2 (5 µm), LiChroCART 250-4, Merck) is used with the same HPLC and is maintained at 30 °C during chromatrographic separation. 40 µL of sample are injected at a constant flow rate of 1.5 ml/min with an isocratic mixture of hexane and isopropanol (98.5/1.5). Four standards injected at the beginning and the end of a sequence are used for NP calibration at concentrations of 0.1, 0.5, 1, 3, 5 mg/L (0.1 mg/L is used to assess the detection limit). These were obtained by diluting a concentrated stock solution of 100 mg/L (CIL Cluzeau). A sequence consists in measuring 4 standards (calibration) 1 control, 10 samples (extracts in hexane), 1 control, 10 extracts, 1 control and 4 standards (calibration). Each extract is injected two times. The control solution is made of a commercial mixture of NP, NP1EO and

NP2EO with known concentrations. The limit of quantification of each PAH varies between experiments but is about 10 µg/L in ACN which corresponds to 134 µg/kg dry matter and can attain concentrations as low as 100 µg/L for NP. Aqueous PAH and NP concentrations were obtained by calculating the difference of concentrations in bulk and particulate matter.

4.3 Calculations for NPnEO transformations to NP during anaerobic digestion

Since nonylphenol diethoxylate can be biodegraded to nonylphenol monoethoxylate during anaerobic digestion which can further decompose to nonylphenol (Ahel et al., 1993), the biotransformation of these compounds had to be taken into account in order to establish a correct mass balance of the system. These calculated concentrations are further interpreted as corrected initial concentrations based on which the overall removal of nonylphenol will be discussed. The following equation is used to calculate the corrected NP1EO concentrations of the start sludge knowing that 1 mol NP2EO corresponds to 1 mol NP1EO after de-ethoxylation:

Equation 6: $$n\,(NP1EO_{produced})\,[mol] = n\,(NP2EO_{degraded})\,[mol]$$

The degradation of NP2EO in mol is calculated by substracting the concentrations after 42 days from the initial sludge:

Equation 7: $$NP2EO_{degraded}\left[\frac{mol}{L}\right]$$

$$= NP2EO_{start}\left[\frac{mol}{L}\right] - NP2EO_{final}\left[\frac{mol}{L}\right]$$

$$= \frac{c(NP2EO_{start})\left[\frac{g}{L}\right]}{M(NP2EO)\left[\frac{g}{mol}\right]} - \frac{c(NP2EO_{final})\left[\frac{g}{L}\right]}{M(NP2EO)\left[\frac{g}{mol}\right]}$$

This molar amount of NP2EO is transformed back to the corresponding mass of NP1EO with the help of the molar mass M (equations 8 and 9) and then added to the measured amount of NP1EO by HPLC to correct the initial concentration of NP1EO.

Equation 8: $$NP1EO_{produced}\left[\frac{g}{L}\right] = NP1EO\,[\frac{mol}{L}] \times Molar\ mass(NP1EO)\left[\frac{g}{mol}\right]$$

Equation 9: $$NP1EO_{measured} + NP1EO_{produced} = NP1EO_{corrected\ start}$$

The same calculations as before are done in order to obtain the correct initial concentrations of NP in the start sludge of reactors with different treatments and to calculate the actual removal of NP from the sludge. This time the underlying hypothesis says that the dissipated amount of NP1EO is biodegraded to NP [n (NPproduced) = n (NP1EOdegraded)] since this biodegradation of NP1EO to NP is documented in existing literature (Ahel et al., 1994; Giger et al., 1984; Patureau et al., 2008).

4.4 Calculations of PAH/NP sorption on graphite felt

The total solids of sludge samples from reactors GF_DES1a/GF_DES1b and GF_DES2a/GF_DES2b contained finely grinded GF which was extracted by accelerated solvent extraction (ASE) together with the sludge. Therefore, it is assumed that all PAHs were extracted from these reactors including the amount of PAHs that could have sorbed onto GF due to hydrophobic interactions. On the contrary, intact GF that was added to anaerobic digesters was taken out of the sludge after 83 days and analysed apart to be able to perform different analysis. Therefore, it must be assumed that PAH concentration of bulk sludge of GF_INT1a/GF_INT1b and GF_INT2a/GF_INT2b is underestimated. It must be corrected by adding the amount of sorbed PAHs to intact GF to the bulk concentrations. Therefore, intact GF was weighed after digestion and pieces of GF were attributed to microbiological analysis (PCR & sequencing), dry matter analysis and PAH quantification (Table 7).

Table 7: Quantified mass of the intact graphite felt after anaerobic digestion for analytical uses.

Mass $_{GF}$ used for different purposes [g]	GF_{total} after digestion	GF for PAH/NP extraction	GF for TS analysis	GF for PCR & sequencing
GF_INT1a	23.7652	14.88	7.4367	1.4485
GF_INT1b	10.6126	7.4775	1.7254	1.4097
GF_INT2a	30.4794	13.5248	14.4619	1.5227
GF_INT2b	28.7001	12.4458	12.9273	1.9843

GF_INT1a_HT	22.0537	11.2316	9.4965	1.3256
GF_INT1b_HT	20.9755	10.7356	8.536	1.7039
GF_INT2a_HT	34.1647	17.76	15.3187	1.086
GF_INT2b_HT	32.3813	47.7525	13.6928	1.6784

For PAH and NP quantification, a quantity of GF as indicated in Table 7 was freeze-dried and crushed to pieces. Accelerated solvent extraction was performed as for bulk samples of sludge to obtain extracts of PAH and NP in acetonitrile and hexane, respectively. PAH and NP concentrations were, then, detected by HPLC. The PAH and NP concentrations on the GF material were calculated according to the following equation:

Equation 10: $$Micropollutant_{GF\ intact}\ \frac{\mu g}{kg} = \frac{Total\ solids}{GF\ intact}\left[\frac{g}{kg}\right]_{GF} \times \frac{Micropollutant_{GF}}{Total\ solids}\left[\frac{\mu g}{g}\right]$$

These PAH and NP concentration onto GF were further compared to the PAH concentrations found in the bulk sludge of the respective reactors in order to evaluate the extent of sorption of PAH onto GF. Concentration of NP and PAHs, respectively, inside the reactor with a sludge volume of 500 ml were calculated by adding the amount of pollutants sorbed onto GF and the pollutant concentrations of the bulk sludge as follows:

Equation 11:

$$Micropollutant_{reactor}[\mu g] = Micropollutant_{GF}\ [\mu g] + 0.5\ L\ \times\ Micropollutant_{bulk}\ [\mu g]/L$$

The results are expressed as fractions of sorbed pollutants with respect to total PAH and NP concentrations inside the reactor according to the following equation:

Equation 12: $$Fraction_{sorbed} = \frac{conc(micropollutant)_{GF}}{conc(micropollutant)_{reactor}}$$

5. Bioelectrochemical operation and data analysis

Bioelectrochemical experiments were conducted in single chamber MECs under potentiostatic control (BioLogic Science Instruments, France) with EC-Laboratory v.10.1 software. Carbon felt

electrodes were completely immersed in sludge with a distance of 6 ± 1cm from each other and were fixed onto a 2 mm diameter titanium rod (T1007910/13, Goodfellow SARL, France) as electron collector. The reactors were hermetically closed with a silicone seal and a stainless steel ring. Current density was measured at all times. Chronoamperometric curves were recorded during the experiment length. Plots of cyclic voltammetry were obtained at the start and at the end of experiments that used polarized electrodes with a scan rate of 2 mV/s. The working electrodes were polarized at a voltage of +0.8 V vs. the standard hydrogen electrode (SHE). An illustration of the reactor configuration is given in Figure 8 together with a schematic view on how the working electrode was polarized in the described experiment.

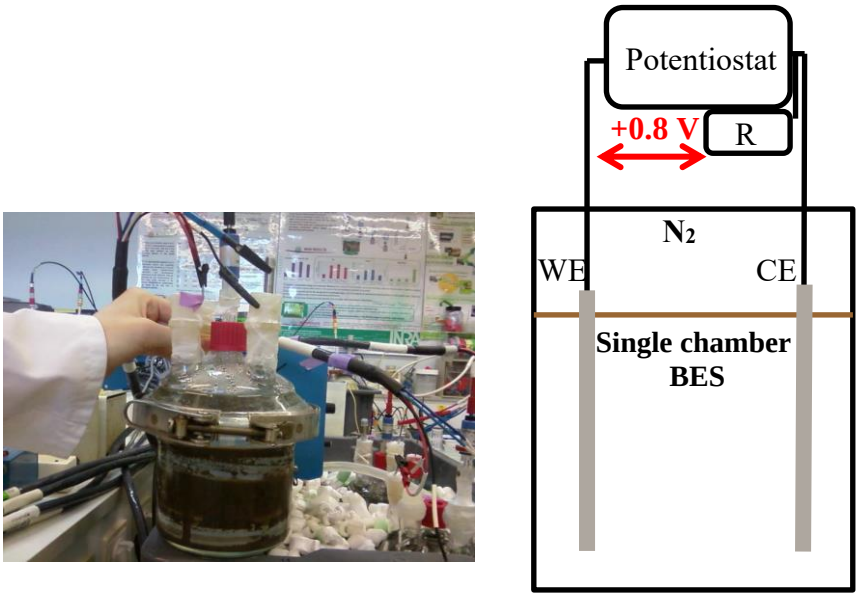

Figure 8: Left: Anaerobic digester with graphite felt electrodes that are polarized with the help of a potentiometer.
Anode in red, cathode in blue. Reference electrode in the middle. Right: Three electrode configuration in a single chamber bioelectrochemical system (BES) with working electrode (WE) and counter electrode (CE) under nitrogen (N_2) atmosphere. The reference electrode (R) measures the potential difference to WE and CE.

6. Microbiological analysis

6.1 Microbial community analysis

Microbial analysis was performed on communities from the bulk sludge and from the biofilm attached to GF surface. 1 cm x 1 cm pieces of GF were sampled with a sterile scalpel and biofilm communities were extracted with PBS buffer by agitation and subsequent centrifugation (15 min,

13400 rpm). Bulk sludge was centrifuged and all precipitates were retained. Firstly, DNA was extracted and purified with the Fast DNA SPIN kit for soil in accordance with the manufacturer's instructions (MP Biomedicals). DNA quantity and purity were assessed by spectrophotometry (Infinite NanoQuant M200, Tecan). The V4-V5 region of 16S rRNA gene was amplified using primer pair and linkers as described before (Venkiteshwaran et al., 2016), targeting both archaeal and bacterial 16S rRNA genes. An index sequence was added in a second PCR of 12 amplification cycles and the purified results were loaded onto the Illumina MiSeq (v3) cartridge for sequencing of paired 300 bp reads at the GenoToul platform, Toulouse, France (http://www.genotoul.fr). Final community composition was obtained after assembly of forward and reverse sequences, chimera checking, alignment, clustering (97 % similarity) and assignment of taxonomic affiliations using mother as described before (Schloss et al., 2009). All corresponding figures of taxonomic distributions classify sequences accounting for less than 2% of the population as ''Others". Sequences have been submitted to NCBI GenBank under the accession numbers MF794208-MF794703 and MF784615-MF784637.

6.2 Quantitative PCR (qPCR)

PCRs were prepared using 96-well real-time PCR plates (Eppendorf, Hamburg, Germany) and Mastercycler CFX96 (Biorad, California, USA). Then, 6.5 µl of SsoAdvanced™ Universal Probes Supermix (biorad), 2 µl of DNA extract with two dilutions, for Bacteria 100 nM forward primer F338-354 (5′-ACTCC TACGG GAGGC AG-3′), 250 nM reverse primers R805-785 (5′-GACTA CCAGG GTATC TAATC C-3′), 50 nM TaqMan probe (5'YakimaYellow-TGCCAGCAGCCGCGGTAATAC-TAMRA-3'), for *Archaea* 200 nM forward primer F787 (5'-ATTAG ATACC CSBGT AGTCC-3'), 200 nM reverse primers R1059 (5'-GCCAT GCACC WCCTC T-3'), 50 nM TaqMan probe (5'FAM-AGGAATTGGCGGGGGAGCAC-TAMRA-3') and water were joined to obtain a final volume of 12.5 µl for all analyses. Conditions of PCR were described before (Moscoviz et al., 2016). Absolute abundances of 16s rDNA were calculated by multiplying relative abundances obtained from sequencing times the number of gene copies found by qPCR for Bacteria and Archaea, respectively. This rough calculation was done even though some bacteria possess several regions of 16s rDNA in their genome. In a sample with only few richness, the results obtained by qPCR would be divided by a factor that is species dependent in order to correct the overestimated gene copy number. Yet, with respect to

the richness of species in all of the sewage sludge samples in the present study the number of individual cells with multiple regions of the target gene will be equivalent. Therefore, the number of gene copies obtained by qPCR is taken to be the number of individual bacterial and archaeal cells that were present in the samples.

7. Analytical problems

When the first spiking strategy was employed, all PAH initial concentrations were below the targeted theoretical value except for Benzo(k)fluoranthene and Dibenzo(a,h)anthracene. It is known that measured PAH values can diverge from theoretical values since sludge is a complex substrate and PAHs can get entrapped in the matter which makes them non-extractable. However, previous spiking concentrations showed better recovery even though the extraction method exhibits a STD of 5- 10 %. Yet, most of the molecules found in sludge, in this study, attained only 52-69 % of the theoretical concentrations, fluorene exhibiting lowest recovery (29 %) which is probably due to evaporation during sludge preparation (spiking and transfer to containers) and freeze-drying. The constantly low recoveries indicate that there must be a different reason. During the spiking it was noted down that 5 ml of ACN could not completely dissolve the contaminant mixture. Therefore, 0.281 g of dichloromethane was used to dissolve the remaining contaminants in the vessel containing the spiking solution. Furthermore, already spiked sludge was used to rinse the vessel. Yet, it is possible that contaminant losses occurred. The NP concentration of the spiking solution could not be measured since ACN evaporated during long-term storage at 5°C. The recoveries of PAH concentrations in heat treated sludge were also low except for BghiP but exhibited similar recoveries as the non-heat treated sludge for HMW PAHs with molecular masses above or equal to 228 g/mol with an average of 98 ± 6% (Table 2). On the contrary, all PAHs below or equal to a molar mass of 202 g/mol (Pyr, Flt, Phe, Flu) showed high discrepancies to their concentrations in sludge before the heat treatment (34, 46, 81, 67 % of values before heating for 20 min) meaning that they are volatilized at 120°C. In a different study, PAH penetration into air during sludge treatment did not exceed 15% at 38 and 53 degrees but confirmed that 3 ring PAHs migrated to the air in the largest extent (80% of all PAHs detected in air) (Karaca et al., 2014). However, since the initial spiking concentrations of PAHs and NP are measured in this study, the divergence of theoretical initial and actually measured initial

concentrations does not impact on the result of contaminant removal calculation in the anaerobic digesters.

For the new spiking strategy in the experiment that employed GF of different surface area, the comparison between theoretical (based on spiking) and measured concentrations of NP and PAHs showed recoveries ranging from 23 to 142 % which strongly points to the fact that the 300 ml sludge samples that were taken for TS analysis in the beginning of the experiment were not homogenous and, therefore, micropollutant concentrations could not be determined correctly (TS values are needed since micropollutants are extracted from TS). Therefore, the results in chapter VI will discuss micropollutant biodegradation based on the comparison of the final NP and PAH concentrations only. The start concentrations that were calculated (Table 3) can only be taken as approximate values and should be similar in each start sludge since all reactors were prepared in the same way.

Chapter III

List of figures

1 Testing conductive graphite felt and MECs with graphite felt electrodes for PAH removal during anaerobic digestion of sludge

As discussed in chapter I, conductive materials were found to enhance methane production in anaerobic digesters (Clauwaert and Verstraete, 2009; Kato et al., 2012; Zhao et al., 2015) and the addition of a conductive iron mineral led to an increase in methanogenic benzoate degradation (Zhuang et al., 2015). Moreover, an MEC was used for the bioremediation of naphthalene (Zhang et al., 2010) inside a two chamber BES. Based on these encouraging reports, we evaluated the potential of graphite felt addition (GF_INT2) or the use of a MEC with GF electrodes (BES) with the same specific surface area (2 m^2) on PAH degradation during anaerobic digestion (AD) of lowly contaminated municipal sewage sludge. The results of methane production, organic matter and PAH removal as well as microbiological composition of samples are presented for heat treated and non-heat treated digesters which employ sewage sludge as inoculum and substrate in the following chapter.

1.1 Kinetics of methane production

Methane production is depicted in

Figure 1 in normo-liters for duplicate or triplicate reactors that were inoculated with sludge of the same dry matter content (23.2 ± 1.0 g/L).

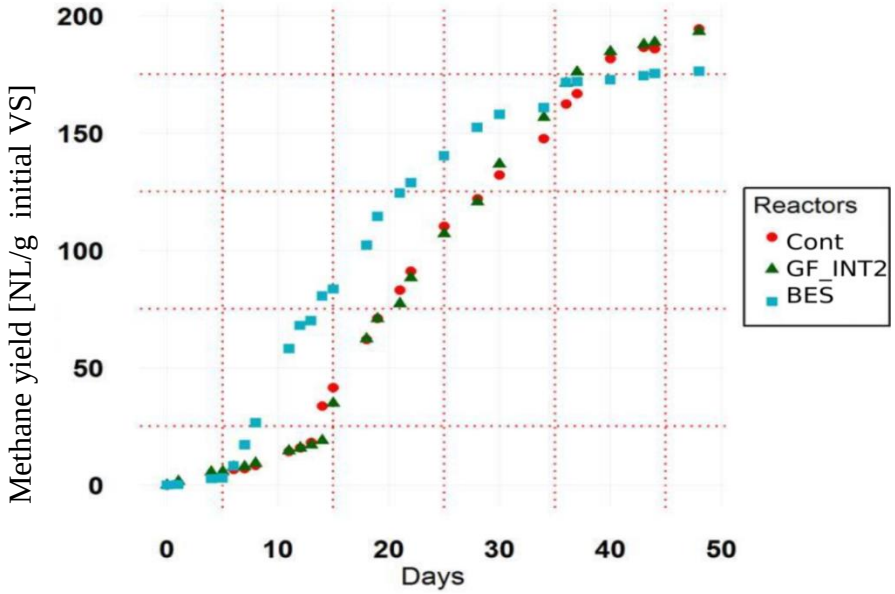

Figure 1: Mean methane production.
Methane yield per initial volatile solids. (Cont=anaerobic control digester; GF_INT2= graphite felt digester with specific surface area of 2 m^2; BES= bioelectrochemical digester).

All the reactors presented similar methane yields. Nonetheless, the two BES reactors started to produce methane five days earlier than the triplicate reactors of Cont and GF_INT2. The application of the electric potential (+0.8 V vs. SHE) at the working electrode had an accelerating effect on methane production. This was reported in other studies likewise [14, 22]. In contrast, heat treated reactors did not produce methane. A mass balance of methane, VFA and final COD (bulk sludge) was calculated and is depicted in Figure 2.

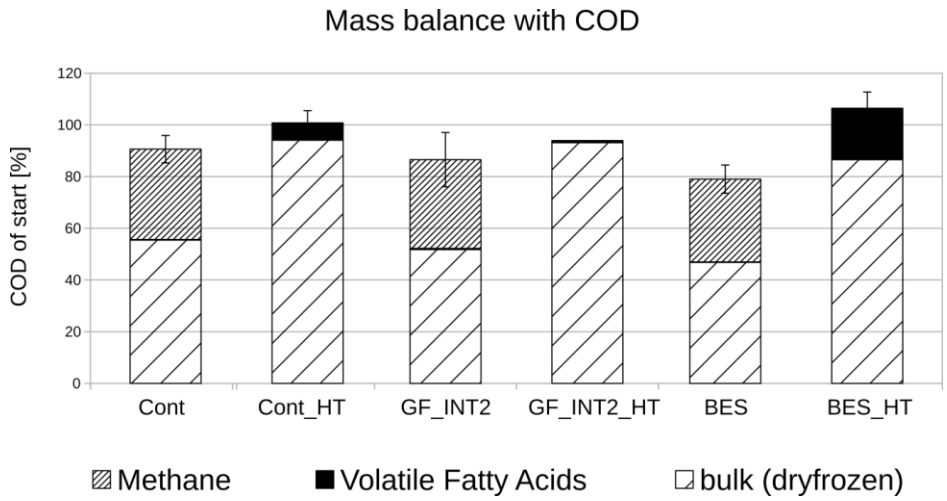

Figure 2: Mass balance of chemical oxygen demand (COD) as percentage of the initial COD.
Cont=anaerobic control digester; GF_INT2= graphite felt digester with intact surface of 2 m^2; BES= bioelectrochemical digester, HT: Heat treated). Error bars represent standard deviations of two (BES) and three (GF_INT2, Cont) replicates.

For heat treated reactors the mass balance rounded up to 100 % ± 6 %, but with changes in the COD distribution. Indeed, Cont_HT and BES_HT presented higher acetate concentration (1.0 ± 0.5 g/L and 2.7 ± 0.1 g/L, respectively) compared to the start sludge (acetate 0.613 g/L, propionate 0.366 g/L, isobutyrate 0.051 g/L). It indicates that electrochemical decomposition of organic matter took place in BES_HT and that some weak anaerobic respiration of fermenters but no further consumption of fermentation products took place in Cont_HT. GF_INT2_HT showed VFA consumption (0.1 g/L acetate at the end) but as the other heat treated reactors did not produce methane. Hence, heat treated reactors were not completely sterile but the remaining biological or chemical activities were very low. For non-heat treated reactors, all the VFAs were consumed. In between 10 to 21 % COD are missing to keep up the initial COD value. These missing percentages are explained by gas leakages when biogas was quantified with water displacement method and the uncertainty of COD measurement for freeze-dried sludge.

1.2 Organic matter removal and PAH reduction in heat treated reactors

The removals of three PAHs were chosen as representative of 4, 5 and 6 ring PAHs (Figure 3B). The remaining results are presented in the supplementary information (SI). Pyrene and fluoranthene as very compact, hence, more volatile 4 ring PAHs and three ring PAHs show some removal in heat treated control reactors due to which the interpretation for these molecules is not straight forward (SI). There could have been some volatilization during the heat treatment.

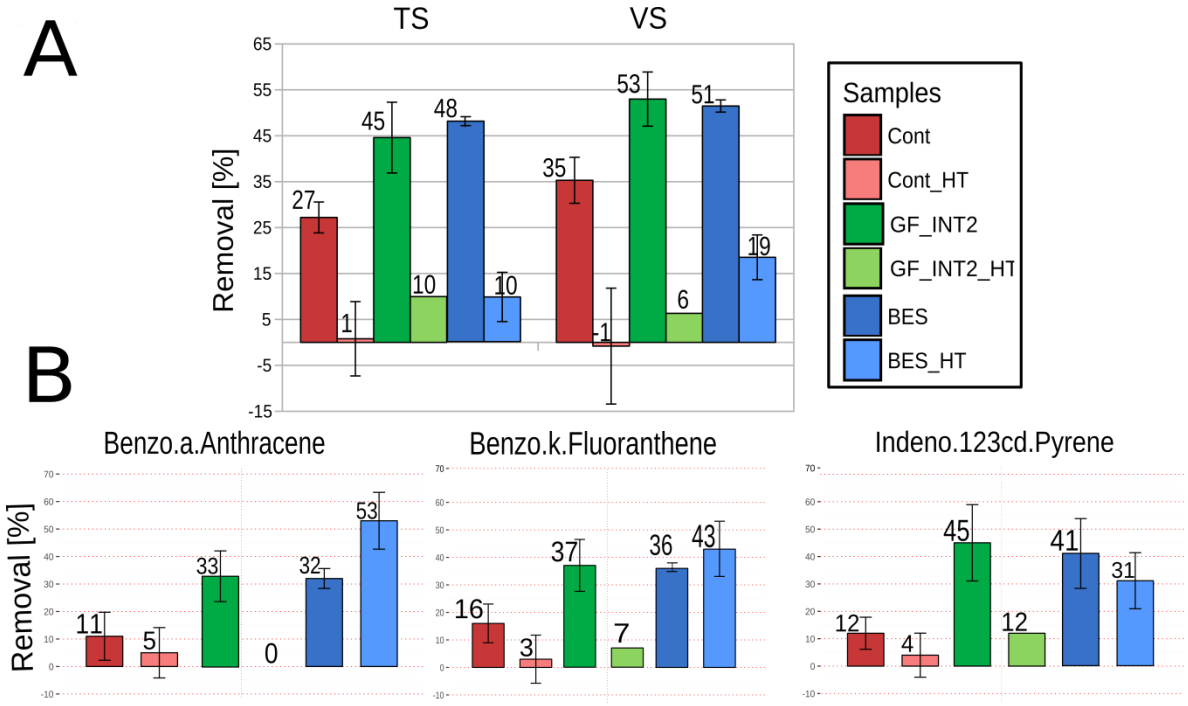

Figure 3: (A) Removal of total solids and volatile solids during anaerobic sludge digestion for heat treated and non-heat treated digesters.
Control (Cont), graphite felt supplemented digester (GF_INT2) with specific surface area of 2 m^2 and bioelectrochemical digester (BES). Error bars represent standard deviations (STDs) of four or six measured values for duplicate or triplicate reactors respectively. (B) Total removal of indeno(123cd)pyrene, benzo(k)fluoranthene and benzo(a)anthracene in anaerobic sludge. Error bars represent standard deviations (STDs) of 12 or 18 measured values for duplicate or triplicate reactors, respectively.

In general, heat treated reactors Cont_HT and GF_INT2_HT showed little organic matter (TS, VS) and PAH removal, which indicates that abiotic processes such as volatilization or sorption onto GF were minor mechanisms by which four or more cycle possessing PAHs are removed under such conditions (Figure 3A). The heat treated electrochemical reactor (BES_HT) showed unexpectedly high removal of PAHs that exceeded the removal for 4 and 5 ring PAHs (BaA and BkF) in non-heat treated reactors. It suggests that the experimental conditions (dead biomass after heat treatment, the presence of GF, applied voltage) favoured the electrochemical removal of PAHs (Figure 3B). Through thermal hydrolysis, aromatic compounds were transferred from particulate sludge into the aqueous phase. Their high affinity for non-polar compounds, then, presumably let them establish a close contact to the GF electrodes through Van der Waals forces (Kubicki, 2006). Indeed,

electrochemical PAH oxidation is known to proceed via direct oxidation at the anode surface or the formation of adsorbed OH-radicals on the electrode surface and subsequent attack on aromatic rings (Rubio-Clemente et al., 2014). Hydroxylation and subsequent ring opening finally leads to complete degradation to CO_2 (Tran et al., 2009) depending on the anode material. Typical applied voltages lie in between 0.1 and 1 V (Cordeiro and Corio, 2009) which supports the hypothesis that electrochemical oxidation of PAHs in the heat treated experiments is a possible mechanism of the observed PAH removal. The lower TS and VS removal in the heat treated electrochemical reactors compared to reactors without heat treatment (16 to 34 % difference) confirms that electrochemical action may play a major role for the disintegration of sludge (VFA production) and the removal of contaminants but not for solids removal. Chronoamperometric curves did not show an increase in electron transfer except for BES2_HT. It is, therefore, assumed that an electroactive species must have been present in this reactor despite heat treatment.

1.3 Organic matter removal parallel to PAH reduction in non-heat treated reactors

Total solids (TS) and volatile solids (VS) removals were enhanced by about 18% in the GF reactors with or without the application of an electric potential (BES and GF) in comparison to the control digesters (Cont) as shown in Figure 3A. GF acted positively not only on dry matter removal but also on PAH with about 21-33 % more removal for BaA, BkF and Ind (Figure 3B). Polarized GF electrode reactors did not perform better than the reactors with GF material alone. Yet, the action of BESs on sludge digestion is known to enhance organic matter degradation and methane yield (Zhao et al., 2014). Contrarily to these results from literature, a beneficial effect of GF on sludge digestion and PAH removal was proven without the polarization of electrodes in our study. An exponential rise in current density was observed in BES1 from day 10 to day 20 and in BES2 until day 11 that can be observed in chronoamperometric plot of Figure 4. The current that was generated in BES2_HT could mean that an electroactive activity is still observed after the heat treatment of sewage sludge and is discussed in detail in section 1.5.1.

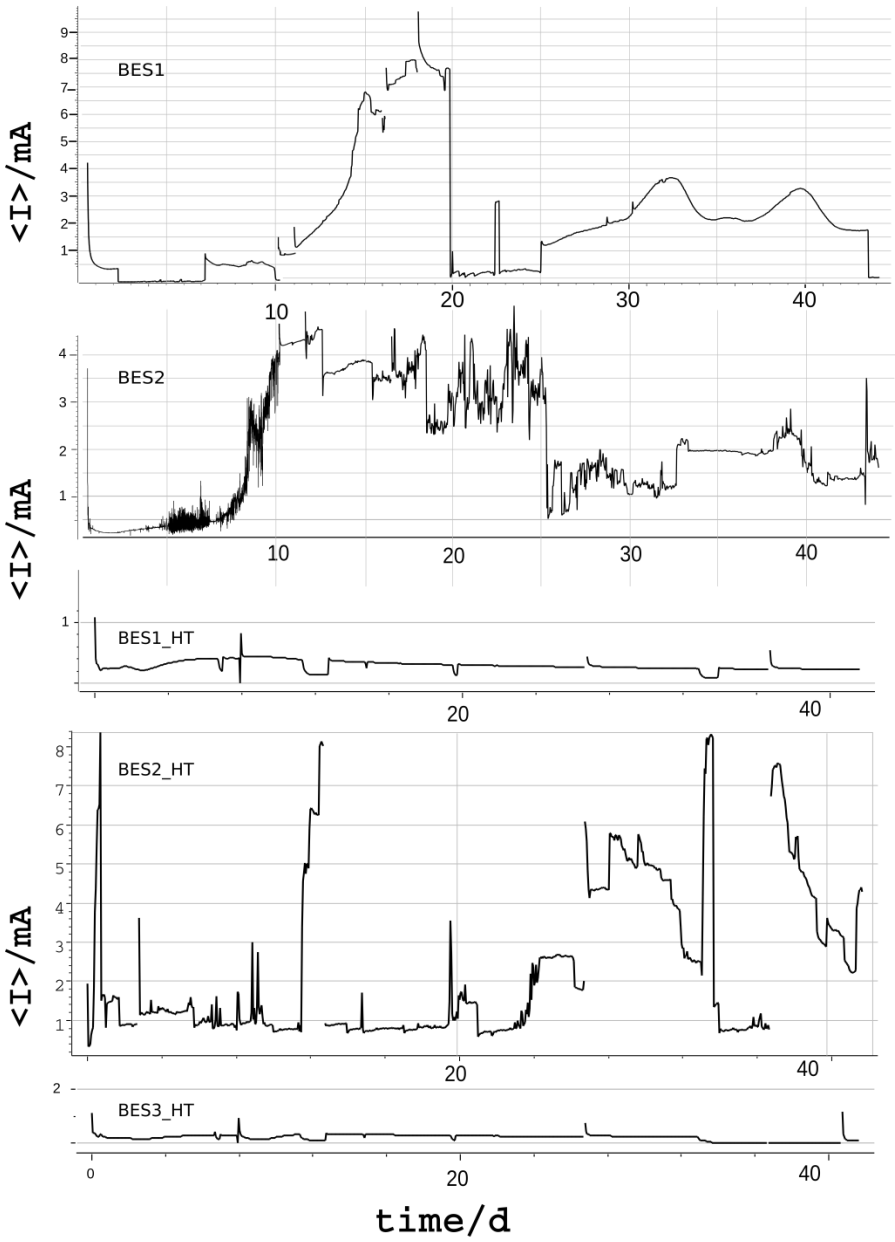

Figure 4: Chronoamperometric curve of bioelectrochemical and electrochemical reactors. BES1, BES2, BES1_HT, BES2_HT, BES3_HT with external surface area of graphite felt electrode 43.14 cm^2 and specific surface area of 2 m^2 [current density I (mA) vs. time t (days].

Current density was not disturbed although shortcuts occurred during the experiment after day 10 and day 16. When + 0.8 V (vs. SHE) was applied to the working electrode, the counter electrode's potential was measured in between -0.8 and -1 V (vs. SHE). The reason

why the current density could not be maintained all along the experiment can be that in the long run 1.8 V of applied voltage damaged cytochrome c proteins on the outer anaerobes' membrane (Schröder et al., 2015) and disturbed further stimulation of electrode interacting microbial communities. The damage to membranes could also explain why *Geobacter* sp. was not detected on all electrode surfaces and its relative abundances stayed below 5 %. The effect of materials on AD was suggested to be dependent on their conductivity; however, Chen et al. (2014) observed that the same quantities of dry GAC and biochar showed similar performances of accelerated DIET during methane generation even though GAC is 1000 times more conductive (4.4 µS/cm compared to 3000 µS/cm) (Chen et al., 2014).Uncompressed dry GF (RVG 4000) which we used in the present study exhibits electrical conductivity similar to biochar that was found to exhibit conductivities similar to pilin of *G. sulfurreducens* also known as microbial nanowires (5 mS/cm) (Malvankar et al., 2011). This finding can explain the performances of biochar and GF as microbial electron conduits. Presuming that there is a limit in accelerating AD with the help of DIET (Chen et al., 2014) via conductors, the surplus electrons that were supplied to the system in bioelectrochemical reactors were not used by microorganisms. Apparently, the sole presence of GF was sufficient to enhance AD (Figure 3A). We hypothesize that GF acted as an electron exchange facility for microorganisms to discharge the electrons that they obtained from organic matter destruction and tunnel these to microorganisms that are in need of electrons and equally capable of DIET. Accordingly, PAHs were biodegraded in co-metabolic fashion independently on the potential difference between electrodes. A continuous reactor design with a sludge retention time between 12 and 20 days could possibly shed light on the question if the enhanced methane kinetics that were observed in BES would cause an increase of PAH removal after some fed batch cycles and if this is correlated to higher abundances of *G. metallireducens* on the anodic and cathodic biofilms. Further research is necessary to investigate if BES can further enhance PAH bioremediation or if the beneficial effect on PAH removal principally comes from the conductive material itself.

1.4 Enhancement of PAH bioavailability by graphite felt addition

In order to further investigate the improved removal of PAHs with GF, their concentrations in the aqueous phase at day 42 were compared to each other and to the start. GF reactors with specific surface area of 2 m^2 exhibited 24, 31 and 37 % more PAHs (BaA, BkF, Ind) in the aqueous phase than digesters without GF addition (Figure 5).

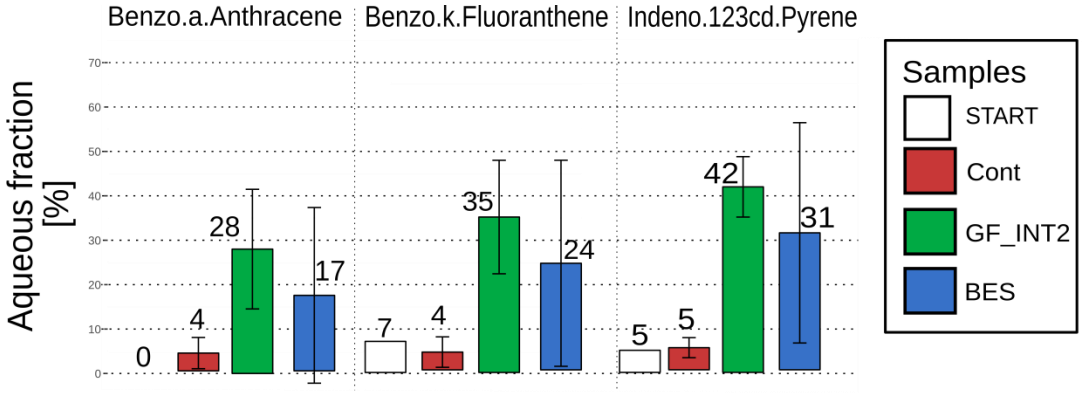

Figure 5: Percentage of indeno(123cd)Pyrene, benzo(k)fluoranthene and benzo(a)anthracene in the aqueous phase before (START) and after anaerobic digestion of l sludge at 42 days. Cont=anaerobic control digester; GF_INT2= graphite felt digester with specific surface area of 2 m^2; BES= bioelectrochemical.

BES reactors showed the same trend. Apparently, the addition of GF to anaerobic digesters relocated PAHs from the particulate to the aqueous phase. The solubilisation of PAHs could be due to an enhanced hydrolysis of organic matter due to the syntrophic cooperation between acetogens and methanogens (Dalla Vecchia et al., 2016) which can use conductive materials as a kind of solid electron shuttle replacing or rather contributing to the role of hydrogen as molecular electron shuttle (Lohner et al., 2014). The hydrolysis of particulate matter was thus facilitated by the mediatorless electron exchange between the conductive material and the anaerobic syntrophic community which led to the enhanced dry matter and PAH removal. Carbonaceous conductors such as GF seem to circumvent two limitations of bioremediation of PAHs, the lack of terminal electron acceptors as well as PAHs' limited bioavailability.

1.5 Microbial community analysis

In order to compare microbial community structure, diversity, and function in different reactors, sequencing was performed at the beginning (inoculum) and at the end of batch experiment and OTUs correspond to 16S rRNA sequences with 3 % similarity.

1.5.1 Microbial community of heat treated reactors

Archaeal 16S rRNA was absent from all heat treated reactor. The absence of methanogens is consistent with the fact that heat treated reactors did not produce any methane. Almost the same quantities of bacterial 16S rRNA was found in heat treated compared to non-heat treated reactors (ranges of 10^9 for Cont2, BES2, BES2_HT, 10^8 for Cont2 _HT, no data acquisition for GF_INT2/GF2_INT2_HT). The richness of the bacterial community was reduced through the heat treatment to main phylum *Firmicutes* wherein *Clostridiales* was the main bacterial order in all reactors except from Cont2_HT (*Thermoanaerobacterales*) Figure 6A.

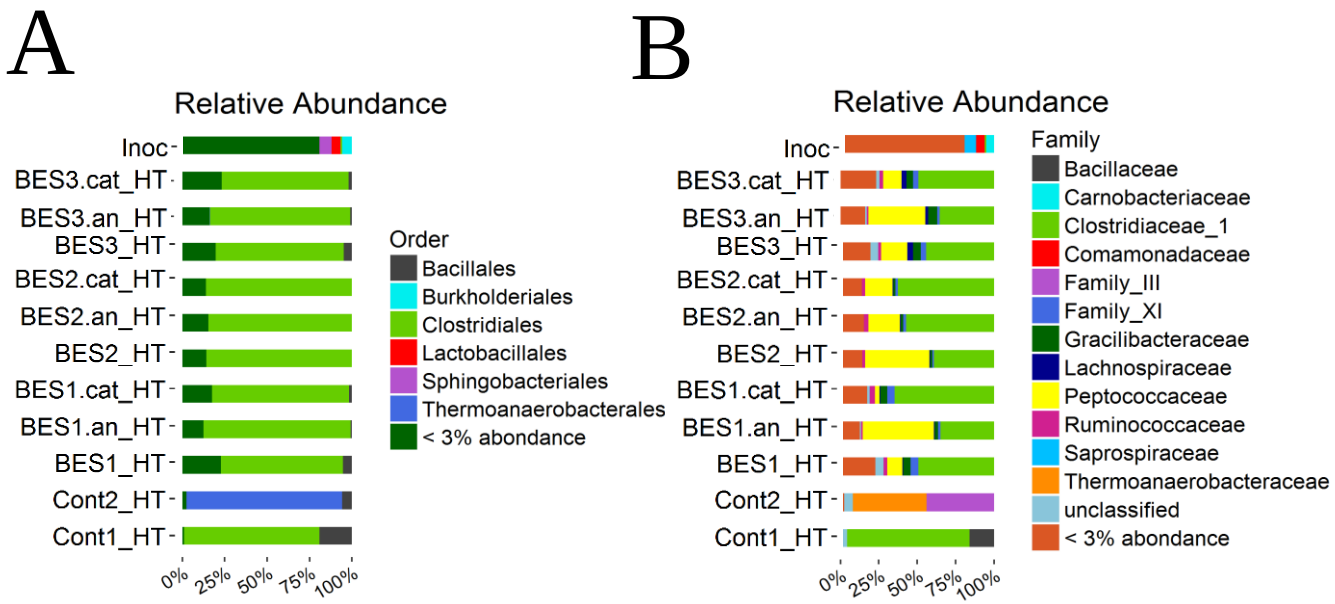

Figure 6: Relative abundances of bacterial 16S rRNA gene sequences at order (A) and family level (B) of heat treated reactors and the inoculum.

The heat treatment favoured the selection of sporulating bacteria but did not prevent their emergence. Apparently bacterial orders of spore formers (*Clostridiales, Bacillales, Thermoanaerobacterales*) were selected which make up 99 and 98 % of all bacterial rRNA found in Cont_HT and BES_HT whereas absolute abundances are only about 25 and 34 % in non-heat treated Cont 2 and BES 2 reactors. In addition, Cont_HT and all BES_HT reactors showed a clear difference in bacterial composition as observed on family level (*Peptococcaceae* presence only in BES_HT) (Figure 6B). OTU 1, most closely related to *Desulfitobacterium* [(up to 42 % absolute abundance (BES2_HT)] is only found in BES_HT samples which suggests that the voltage application selectively enriched this genus. *Desulfitobacterium* is a known electroactive bacteria (Chen et al., 2017) and syntrophy between *Clostridium* sp. and electroactive bacteria was proven in co-cultures (Moscoviz et al., 2017). Furthermore, a *Desulfitobacterium* enriched culture was capable of catalyzing H_2 production without mediators at cathode potentials lower than - 700 mV (Villano et al., 2011) confirming that the enrichment in BES_HT fits to the potential (< -600 mV) measured at the counter electrode. Moreover, gram-positive spore-forming bacteria may play an important role in the anaerobic biodegradation of non-substituted aromatic hydrocarbon (Kleemann and Meckenstock, 2011). In conclusion, the joint growth of *Desulfitobacterium* and syntrophic *Clostridium* sp. in BES_HT could likely be the reason why electrochemical control reactors removed 19 % of VS. PAH bioremediation in sludge is dependent on PAHs' bioavailability and cometabolism which was found to be correlated to the dry matter removal rate of sludge (Barret et al., 2010). On this account, the high removal of PAHs in BES_HT reactors could be partly linked to the cometabolism of PAHs along with VS removal.

1.5.2 Bacterial community structure of non-heat treated reactors

Three dominant bacterial phyla including *Firmicutes*, *Bacteriodetes* and *Spirochaetae* accounted for 64-73 % of the bacterial 16S rRNA gene sequences in the bulk sludge of all reactors and the biofilms on the surface of GF_INT2 and electrodes of BES (Figure 7A). GF_INT2 and BES biofilms showed a lower relative abundance of *Bacteriodetes* (19-21 %) compared to 28 ± 0 % for all bulk samples (Cont, GF_INT2, BES). The phyla *Chloroflexi*, *Proteobacteria*, *Actinobacteria* and *Armatimonadetes* counted midst less abundant phyla. Phyla with relative abundances less than 2 % of bacterial sequences represent 25- 37 % in all anaerobic digesters

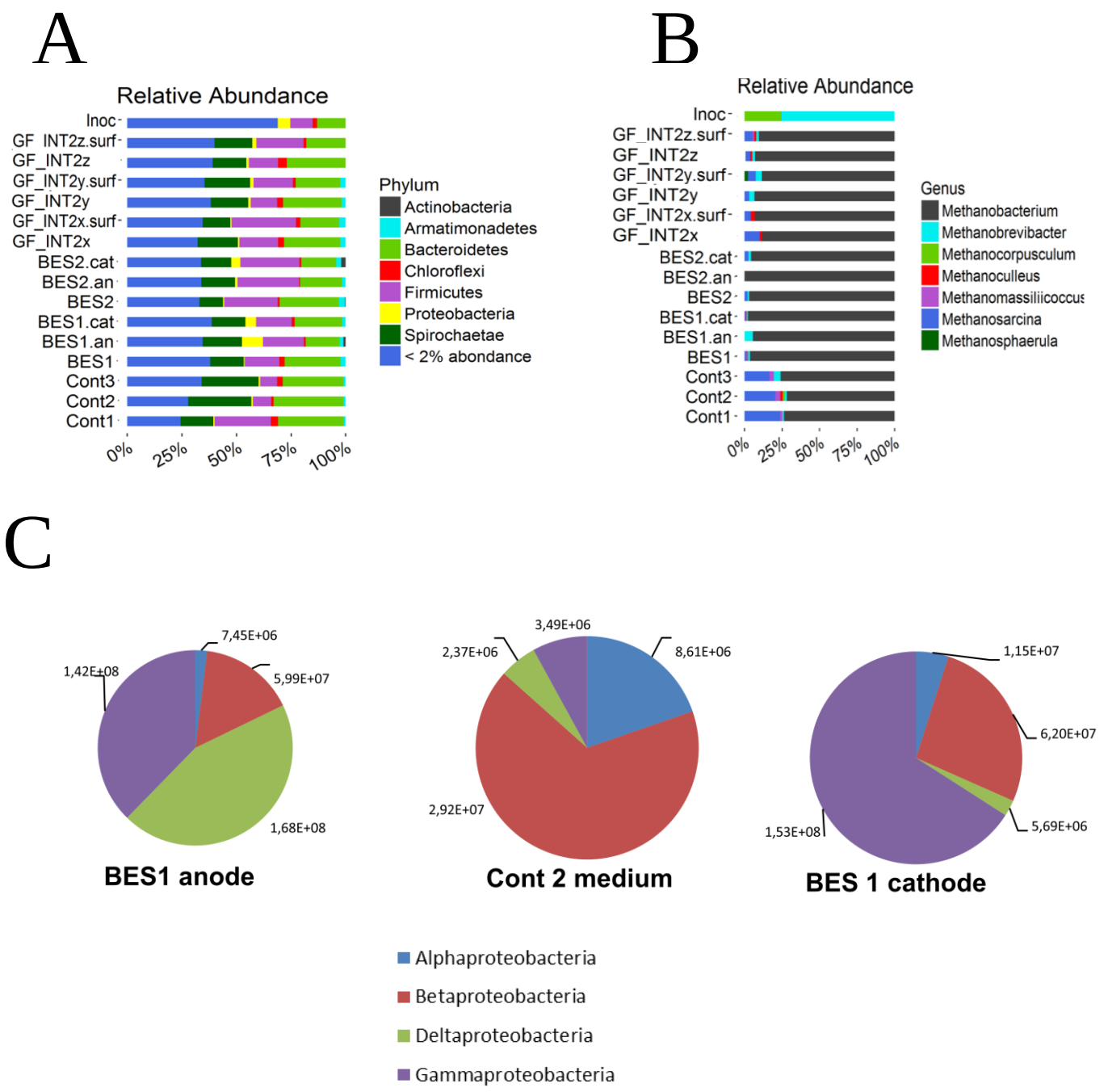

Figure 7: Bacterial (A) and archaeal (B) phylogenetic distribution on Phylum and Genus level.
(C) Absolute abundances of Proteobacteria in BES 1 biofilms and Cont 2 [number of gene copies per ml sludge]. (Cont= anaerobic control digester; GF= graphite felt digester; GF.INT2.surf= biofilm on the surfaces of GF reactors (surface area 2 m^2); BES= bioelectrochemical digester; BES.an/BES.cat= anodic and cathodic biofilm).

signifying high bacterial diversity (Shannon indices: 5 (Inoc) > 4 (BES, GF_INT2) > 3.5 (Cont) (SI). *Proteobacteria* accounted for less than 5 % relative abundance in all bulk samples. In anode and cathode biofilms of BES *Proteobacteria*' relative abundances rose to 10.9 and 6.7 %. Figure 7C shows absolute abundances on class level within BES 1 biofilms compared to Cont 2.

A clear shift from *Alpha-* and *Betaproteobacteria* to *Gamma-* (cathode) or *Gamma-* and *Deltaproteobacteria* (anode) is observed in biofilms of BES 1 with an increase in absolute abundance of 2 on logarithmic scale. More precisely, BES reactors could be distinguished from GF_INT2 and Cont reactors by the presence of OTU 59 with 99 % sequence similarity to *G. metallireducens GS-15* in the anodic and cathodic biofilms of reactors BES 1 and BES 2 both representing above 95 % of order of *Deltaproteobacteria*. Bulk sludge of both BES did not include OTU 59 which is in agreement with other studies where *Geobacter* sp. were only enriched in the anodic biofilm (Parameswaran et al., 2011). The relative abundance of *G. metallireducens* was 100 fold higher in BES 1 (3.5 %) and BES 2 (4.6 %) biofilms compared to all other reactors where relative abundances stayed below 0.4 %. Apparently, the use of a single chamber methanogenic digester favoured the presence of *G. metallireducens* not only in the anodic but also in the cathodic biofilm. Since *G. metallireducens* was found to oxidize benzene under anaerobic conditions (Zhang et al., 2013) and has been detected within the bioanode community of PAH removing MFCs (Yu et al., 2017), this bacterium could have a positive effect on PAH biodegradation when further enriched on the electrodes. The presence of *G. metallireducens* within cathodic biofilms under methanogenic regime or in a mixed culture study with sewage sludge as inoculum and substrate is reported, here, but little is known about the exact role of these microbial key players in methanogenic PAH biodegradation (Kronenberg et al., 2017). Therefore, metabolic analysis would be necessary to confirm the implication of *G. metallireducens* in PAH biodegradation. GF_INT2 reactors, on the contrary, did not show a specific enrichment of *Geobacter* sp. which is consistent with the fact that enhanced kinetics of methane production is only observed for BES. However, TS and VS removals were as high as in BES reactors which suggests that other bacteria than *Geobacter* were most probably participating in DIET through GF to decompose sludge organic matter. This hypothesis is underpinned by the fact that the low percentage of *G. metallireducens* in BES reactors cannot explain the enhanced hydrolysis of sludge organic matter and better PAH removal

alone. *G. metallireducens* is a known electroactive bacteria and its presence has been associated to enhanced methane generation during AD in MECs due to the cooperation of *Methanosarcina* and *Geobacter* sp. (Yin et al., 2016). Therefore, it is possible that the effect of the polarized working electrode (+0.8 V vs. SHE) in the employed BES favoured the presence of *G. metallireducens* and beyond that the syntrophy between methanogens and electroactive bacteria. To further explore hypothetical syntrophic relationships, the increase of abundance for less abundant bacterial species was investigated. The appearance of *G. metallireducens* coincided with the increase in relative abundance of OTU 49 in the anodic (4.1 %) and cathodic (4.2 %) biofilm of BES 1 compared to all other reactors (< 0.1 %). Four species could be identified with 100 % sequence similarity to OTU 49. These are *Pseudomonas veronii strain CIP 104663*, *Pseudomonas gessardii strain CIP 105469*, *Pseudomonas proteolytica strain CMS 64* and *Pseudomonas brenneri strain CFML 97-391*. These results indicate that *Pseudomonas* sp. may play a role in syntrophic interactions with *G. metallireducens*. *Pseudomonas* sp. have been found within anodic biofilms, for example, *Pseudomonas putida* has been found in anode communities of MFCs degrading petroleum hydrocarbons (Lu et al., 2014) and *Pseudomonas aeruginosa* was reported to be electroactive (Qiao et al., 2015). OTU 7 and OTU 13 were both enriched in GF_INT2 as well as BES reactors [relative abundances: Cont (0.9 ± 0.3 %), GF_INT2 (2.7 ± 0.5 %), GF_INT2 surface (3.3 ± 0.9 %), BES (4.0 ± 0.5 %), anodic, cathodic biofilm (2.8 ± 0.7 %)] and are both most closely related to *Clostridium sensu stricto*. Both OTUs were 12 times more abundant in BES compared to Cont in terms of absolute abundance. *Clostridia* sp. are typical exoelectrogens (Chen et al., 2017) and the increase of their abundance probably indicates that they take part into syntrophic metabolism and/or DIET with GF.

1.5.3 Archaeal community structure of non-heat treated reactors

A clear selection of archaeal species was observed in GF supplemented reactors [(Shannon indices: 1.75 (Inoc) > 1.3 (Cont) > 1.1 (GF_INT2) > 1 (BES)] in opposition to bacterial communities which are more diverse in GF and BES reactors than in AD. Shannon index is represented as box plot for archaeal and bacterial communities in Figure 8.

.

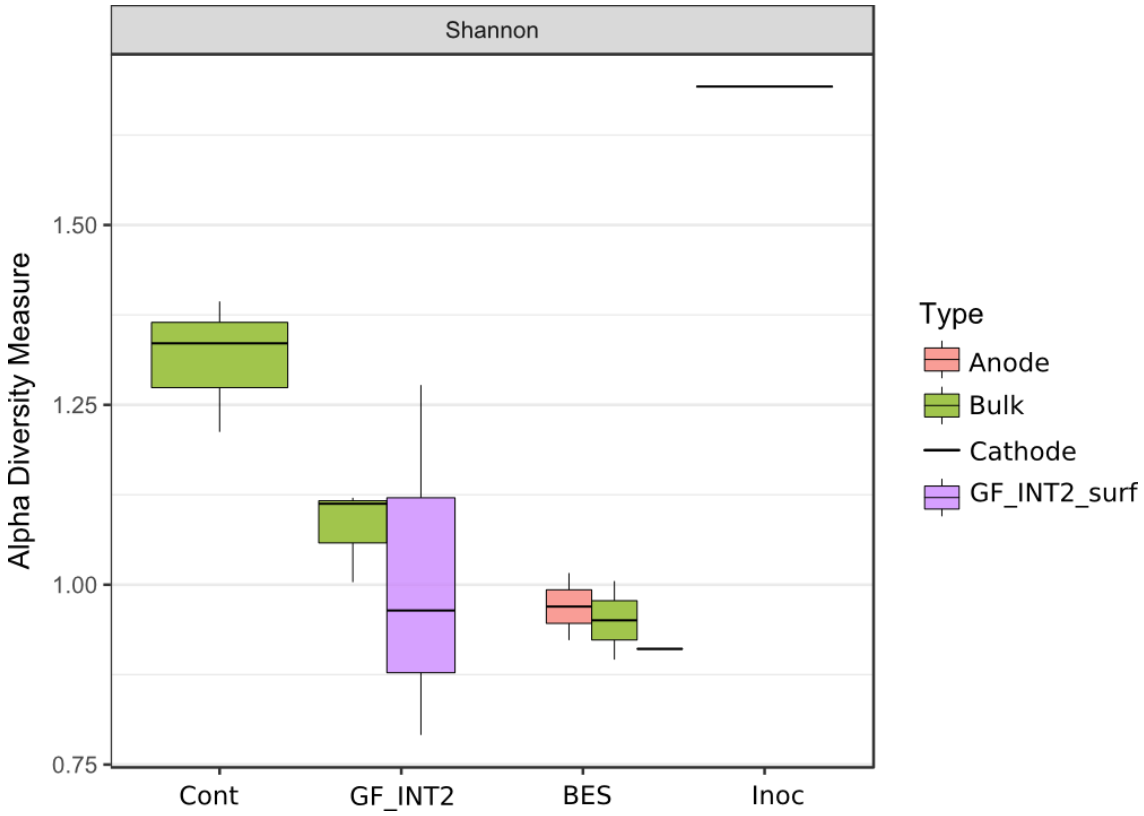

Figure 8: Shannon index as specific diversity measure of *Archaea* in bulk, anodic, cathodic and GF biofilm communities in non-heat treated reactors.
Cont=anaerobic control digester; GF_INT2= graphite felt digester with specific surface area of 2 m^2, BES= bioelectrochemical digester; Inoc= inoculum.

Archaeal community structure revealed that most dominant genera of methanogenic *Archaea* were *Methanobacterium, Methanobrevibacter (both hydrogenotrophic)* and *Methanosarcina* sp. (acetotrophic) accounting on average for 97 ± 1.6 % of the archaeal 16S rRNA gene sequences in the bulk sludge of all reactors and the biofilms on the surface of GF_INT2 and electrodes of BES, respectively (Figure 7B). OTU 1 most closely related to genus of *Methanobacterium*, a typical H_2 utilizing methanogen and responsible for interspecies H_2 transfer, was highly enriched in GF_INT2 and BES reactors (5 fold higher absolute abundance in BES 2 compared to Cont 2). Relative abundances of OTU 1 increased about 16 % ± 9.5 % for GF_INT2 and 16 % ± 4.3 % for BES anode but were equally enriched in GF_INT2 and the cathode of BES. On the other hand, OTU 3 with closest affiliation to *Methanosarcina* was much less abundant in GF_INT2 and BES reactors than in Cont (difference in absolute abundance of one logarithmic unit Cont 2 < BES 2). Relative abundances decreased about 15 ± 3.0 % in GF_INT2 material and 19 ± 3.6 in the BES

reactors. A reason might be that growth rates of acetoclastic methanogens are much lower (Cai et al., 2016) and hydrogenotrophic genera took advantage of hydrogen development at the cathode of BESs, thereby replacing acetoclastic methanogens. Since *Methanosarcina'* relative abundance decreased in all reactors employing GF, GF alone and jointly with polarized electrodes shifted, both, archaeal community composition as well as metabolic pathways. GF_INT2 reactors probably favoured hydrogen development by DIET which could explain their community structure similar to BES. The microbiology of enhanced methane development via DIET as well as PAH biodegradation is still poorly understood. The low percentages of *Geobacter* and other syntrophic bacteria capable of DIET in this study indicate that there might be other microbes participating in DIET. Further elucidation of microbial interactions via DIET in methanogenic environments and their implication in PAH degradation will be important for further improvement of methanogenic PAH removal during AD.

1.6 Conclusions

The addition of GF to anaerobic digesters relocated organic matter and PAHs from the particulate to the aqueous phase. DIET through GF apparently enhanced dry matter and PAH removal since mediatorless electron exchange between the conductive material and the anaerobic syntrophic community may have facilitated hydrolysis. GF seems to circumvent two limitations of PAH bioremediation: the lack of terminal electron acceptors and PAHs' limited bioavailability. The addition of GF to anaerobic digesters could present an effective and affordable bioremediation strategy: GF triggers the solubilisation of particulate matter, thereby rendering PAHs more bioavailable for further degradation.

Chapter IV

List of figures

1 Testing conductive graphite felt and MECs with graphite felt electrodes for NP2EO, NP1EO and NP removal during anaerobic digestion of sludge

PAH removal was shown to increase with the addition of conductive graphite felt (GF) in the preceding chapter. NP, NP1EO and NP2EO concentrations were also measured for the same experimental setup and results for their respective removals are presented in the following.

1.1 NP reduction in non-heat treated anaerobic digesters

Nonylphenol polyethoxylates had not been spiked to the sludge but were present in the raw sludge due to NPnEOs discharging households connected to the WWTP from which the sludge was obtained for experiments. The nonylphenol diethoxylate (NP2EO) concentration that was measured in the beginning of the experiment was 1.26 mg/L (Figure 1) which corresponds to 54.1 mg/kg of sludge dry matter (initial TS: 23.2 g/L) whereas the measured initial NP concentration was 35.7 mg/kg dry matter. Since the initial NP concentration was lower than for NP2EO, this means that the anaerobic transformation of NP2EO to NP probably takes place in a large extent and influences the NP concentration and biodegradation during the experiment.

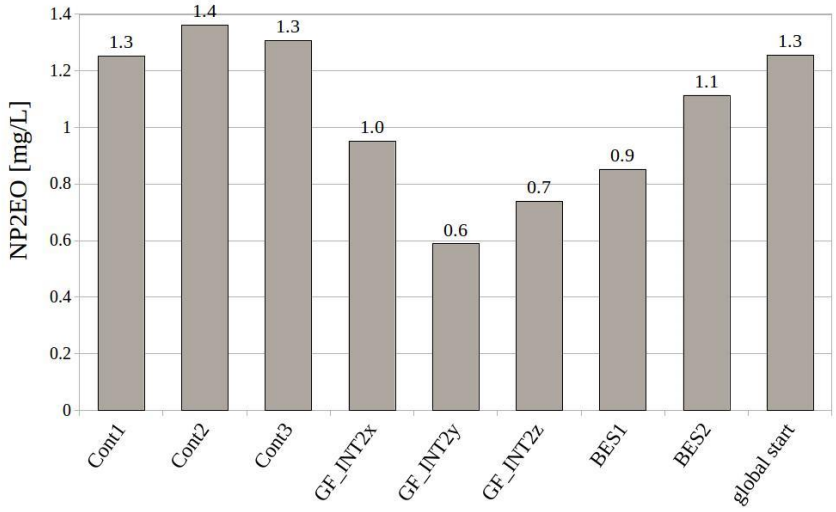

Figure 1: NP2EO concentrations in bulk sludge of anaerobic digesters with different treatments after 42 days along with the initial concentration of start sludge.
Cont= control digester; GF_INT2= graphite felt addition with specific surface area of 2 m2; BES= graphite felt + poised electrodes). Error bars represent standard deviations (STDs) of four measured values for duplicate or triplicate reactors, respectively.

Likewise, and as observed for the control digesters Cont2 and Cont3 the bulk concentrations of NP2EO increase slightly after 42 days of anaerobic digestion which must be due to the transformations of nonylphenol polyethoxylates that were present in the start sludge and that have been deethoxylated to NP2EO during anaerobic digestion (Figure 1). This deethoxylation of NP precursors complicates the discussion of NP2EO and NP1EO fate during AD as reported by several authors (Bozkurt and Sanin, 2014; McNamara et al., 2012; Samaras et al., 2014). Removals for NP2EO are therefore not precise since these precursor molecules have not been measured by HPLC. One can assume that if the final concentration is similar to the initial one, the compound is equally produced and degraded which is the case for the control reactors (Cont). For the other reactors (GF and BES), the degradation of NP2EO is higher than its production; this is reflected by a smaller final concentration. These conditions seemed to favour the degradation of NPnEO. In order to calculate the actual removal of NP1EO, one can add the degraded amount of NP2EO (in mol) of each reactor to the initial concentration of NP1EO. Since NP2EO was found not to accumulate during anaerobic digestion of mixed sludge, it is considered to be biodegraded to NP1EO that accumulated instead (Paterakis et al., 2012). On this basis, the suggested calculations as specified in chapter II, section 4.3 are defensible. Notably, the adopted hypothesis does not take into account abiotic removal processes such as volatilization or sorption of the parent compound. Therefore, calculated results must be interpreted carefully.

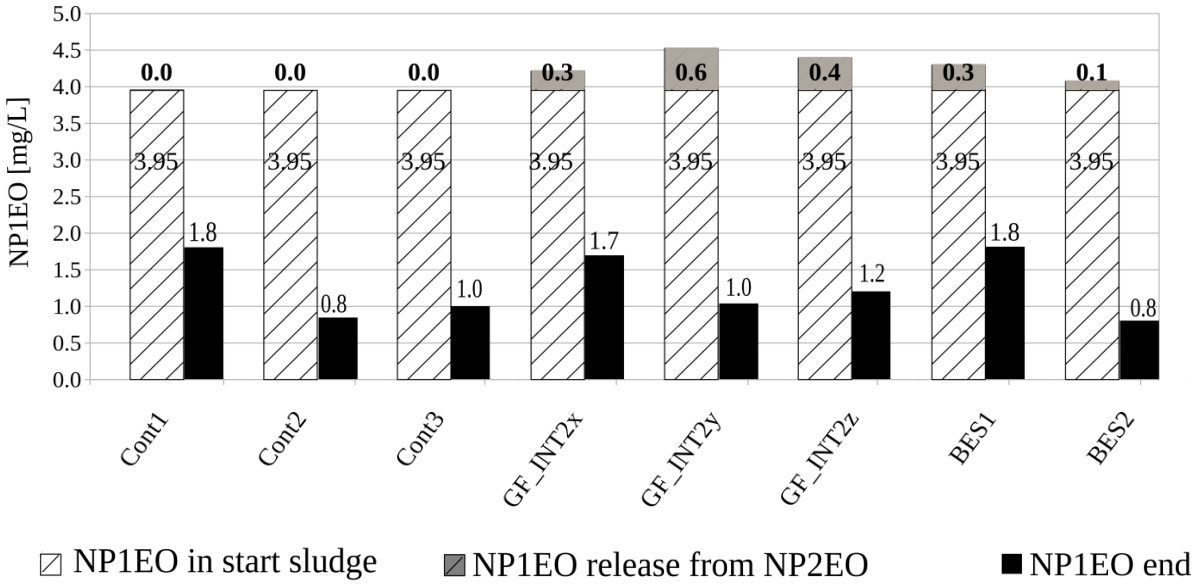

Figure 2: Total start and end concentrations of NP1EO in bulk sludge of anaerobic digesters with different treatments.
The amount of NP2EO transformed to NP1EO is indicated in grey. (Cont= control digester; GF_INT2= graphite felt addition with specific surface area of 2 m2; BES= graphite felt + poised electrodes (AD= control; GF= graphite felt addition; BES= GF + poised electrodes). Error bars represent standard deviations (STDs) of four measured values for duplicate or triplicate reactors, respectively.

Figure 2 shows these corrected concentrations of NP1EO of the start sludge (for each treatment Cont, GF_INT2, BES) where the grey parts of the bar plot indicate calculated amounts of NP1EO coming from NP2EO transformation. The measured concentrations of NP1EO after 42 days of anaerobic digestion are indicated as well.

In most cases end concentrations after 42 days are smaller than the corrected initial NP1EO concentration. Consequently, the total removal of NP1EO is positive in all digesters, as shown in Figure 3. NP1EO is removed 70 % on average from the bulk sludge irrespective of the employed conditions.

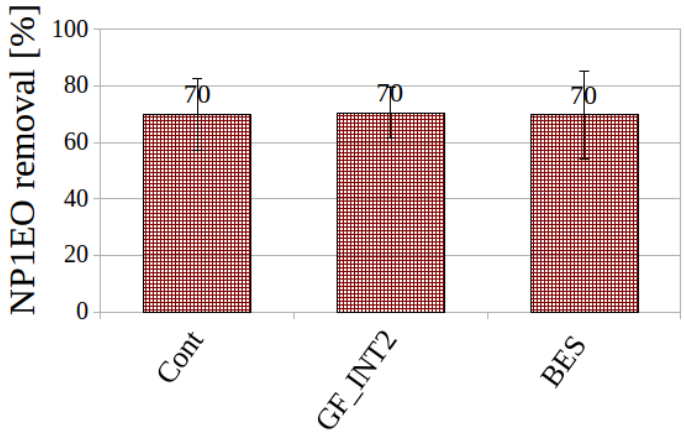

Figure 3: Average NP1EO removal in anaerobic digesters with different treatments.
Error bars represent standard deviations (STDs) of 8 or 12 measured values for duplicate or triplicate reactors, respectively.

NP1EO molecules that were removed were assumed to be biodegraded to NP with the same calculation as done for NP2EO biodegradation to NP1EO. The corrected initial concentration of NP and measured NP concentrations in different digesters after 42 days are depicted in Figure 4.

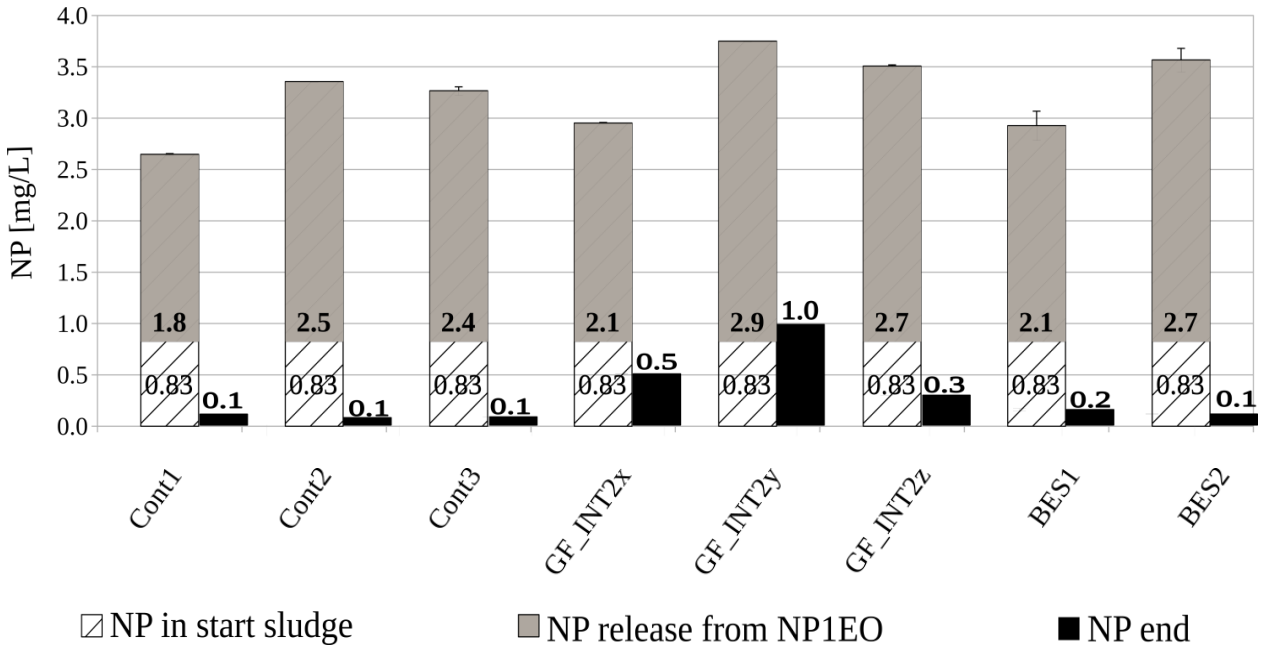

Figure 4: Total start and end concentrations of NP in the bulk of digesters with different treatments.
The amount of NP1EO transformed to NP is indicated in grey (Cont= control digester; GF_INT2= graphite felt addition with specific surface area of 2 m^2; BES= graphite felt + poised electrodes). Error bars represent standard deviations (STDs) of four measured values for duplicate or triplicate reactors, respectively.

Initial concentrations of NP range in between 2.6 and 3.8 mg/L. They decrease to less than 0.2 mg/L after 42 days of AD for all control digesters and BESs whereas GF supplemented digesters show higher end concentrations of NP in between 0.3 and 1 mg/L. More than 80 % of NP removal was observed in almost all reactors (Figure 5) but Cont and BES digesters performed exceptionally well with NP removals reaching 97 %. Such high removals have not been observed before for the sludge that was used in the laboratory during batch experiments. Therefore, we assume that the dilution of sludge from 59 g/L to 23 g/L in the beginning of the experiment already relocated NP to the aqueous phase due to the adjustment of equilibrium of NP concentrations in the aqueous and particulate phase. NP degrading bacteria could therefore have easily attacked NP leading to very high removal performances of NP in all treatments. These results were confirmed by the use of diluted sludge for NP removal in chapter VI. Reports from literature that employ NP contaminated sludge for anaerobic digestion in continuous stirred-tank reactors with similar conditions (same sludge source, similar pollutant charge, mesophilic) but employing sludge with a higher TS content (35 g/L) indicate removals that fall short of the

observed NP dissipation with 25 % removal for the sum of NP, NP1EO and NP2EO (Patureau et al., 2008) thus also pointing to the beneficial effect of sludge dilution to NP biodegradation.

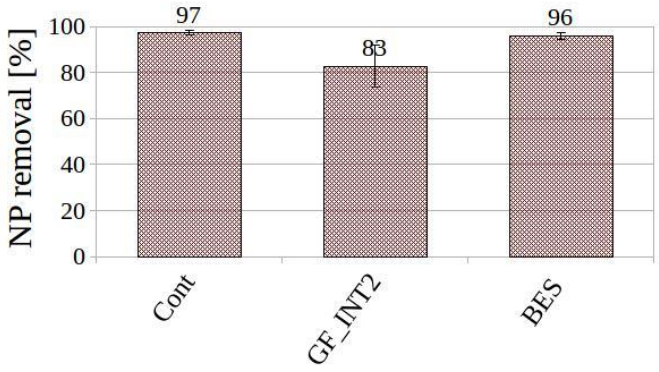

Figure 5: Average NP removal in anaerobic digesters with different treatments.
Error bars represent standard deviations (STDs) of 8 or 12 measured values for duplicate or triplicate reactors, respectively.

1.2 Conclusion

NP removal performances amounting to over 80 % were indistinguishable between the different operating conditions. Assumedly, this is due to sludge dilution and the fact that NPs are transferred from the particulate to the aqueous phase rendering them bioavailable. Thus bioavailability is not a limiting factor of NP degradation as suggested in previous studies (Patureau et al., 2008) and this can explain why NP removal is not correlated to TS removal (27-48 %, chapter III, section 1.2) in the chosen conditions.

Chapter V

List of figures

1 Conductive carbon plate and platinum enhance the removal of fluorene and phenanthrene during anaerobic digestion of sludge

It was shown in our previous experiments that conductive graphite felt (GF) improved the removal of dry matter and 12 spiked high and low molecular weight polycyclic aromatic hydrocarbons (PAHs) during anaerobic digestion of lowly contaminated municipal sewage sludge independently of an applied electric potential. We concluded that if it is not the polarization of an electrode that caused the enhanced removal performances, the improvement must be related to one of the GF's characteristics itself. Conductive materials are reported to improve methane production in anaerobic reactors due to the promotion of direct interspecies electron transfer (DIET). DIET is based on the fact that microbial pili and conductive materials serve as conduits between biota as described before (chapter I, section 4.1). A working hypothesis is that materials with higher conductivity may better promote direct interspecies electron transfer (DIET) besides other factors such as the specific surface area (SSA), porosity, micro- and macropore structure of the material. In this chapter, carbon plate (Cp) and the 1000 fold more conductive platinum (Pt) (Pierson, 1994; Wilf and Dawson, 1976) are used to test their impact on methanogenic activity and the removal of the same 12 polycyclic aromatic hydrocarbons (PAHs) during anaerobic digestion of sewage sludge. Experimental conditions are depicted in chapter II, section 2.2.

1.1 Kinetics of methane production

Methane production is depicted in Figure 1 in normo-liters for duplicate or triplicate reactors that were inoculated with sludge of the same TS content (23.2 ± 1.0 g/L).

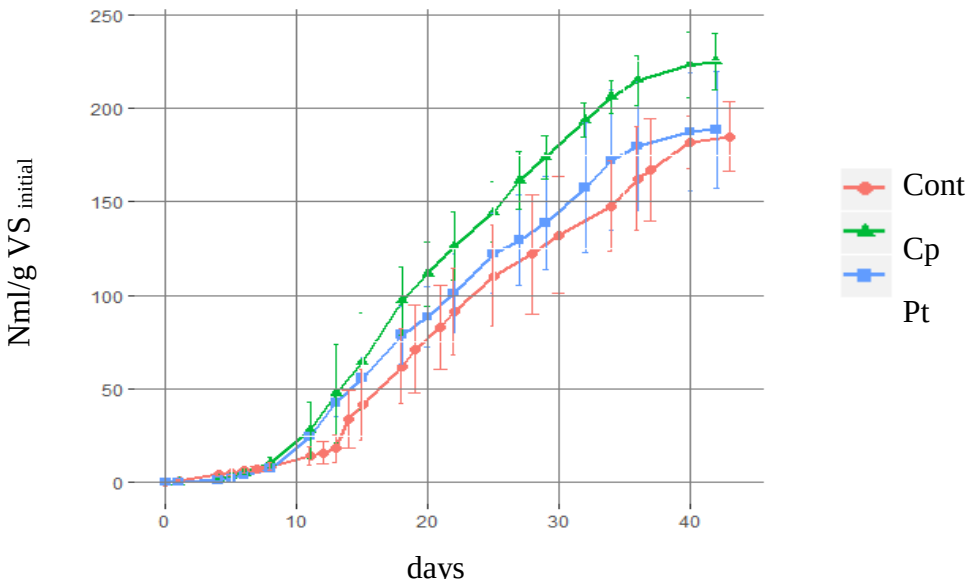

Figure 1: Methane production (NmL) normalized to the initial volatile solids concentration.
Cont= control anaerobic digester; Cp = Carbon plate digester; Pt= Platinum digester.

Platinum supplemented reactors showed the same slope of methane production as the control anaerobic digesters reaching 189 Nml similar to the control with 185 Nml. Carbon plate supplemented reactors exceeded these methane yields with a steeper slope from day eight on attaining 225 Nml after 42 days but not showing a statistical significant difference to Pt reactors. Even though, Cp showed a significant difference of methane production with respect to the control digester (p-value of 0.035, n=3, presupposing a normal distribution). However, it must be considered that the exact value of methane produced from the control is higher than depicted since the biogas volume was measured with water displacement method without acidification whereas for Cp/Pt reactors this was corrected. Methane productions for the three triplicate reactors are, therefore, considered almost the same. Nonetheless, graphene was already found to increase biomethane yield to 25 % in anaerobic digesters (Lin et al., 2017). This may be due to the fact that the authors added graphene (1g/L) in micro size (5~10 µm) in contrast to rigid Cp used in the present study (two pieces totaling 4.75 g in 160 ml sludge with TS content of 23.2 g/L for comparison) as well as the fact that they used ethanol as an easy degradable substrate instead

of sludge. Zhao et al. (2015) added solid graphite rods to enhance anaerobic digestion of ethanol leading to about 10 % higher COD removal and methane production with respect to control digesters without conductive carbon material. They used a similar quantity of graphite per working volume in terms of its projected surface area (200 cm^2/L) as in our experiments with Cp (187 cm^2/L) but used artificial wastewater as substrate instead of sludge, a 1.8 times less TS containing seed sludge and operated reactors in a continuous upflow anaerobic sludge blanket reactor with a hydraulic retention time of 24 hours instead of a single batch of 42 days. Furthermore, nano-graphene addition (30 mg/L) was demonstrated to enhance AD of glucose about 14.3 % in long term experiments under low temperature (10 °C) (Tian et al., 2017). Therefore, we conclude that methane production was not enhanced in our experiment due to the form of graphite delivered with a lower specific surface than the one used in the previous studies or due to the higher TS content and more complex substrate type. A mass balance of methane, VFA, sampled sludge and remaining chemical oxygen demand (COD) in bulk sludge was calculated and is depicted in Figure 2. No methane was produced in the heat treated reactors.

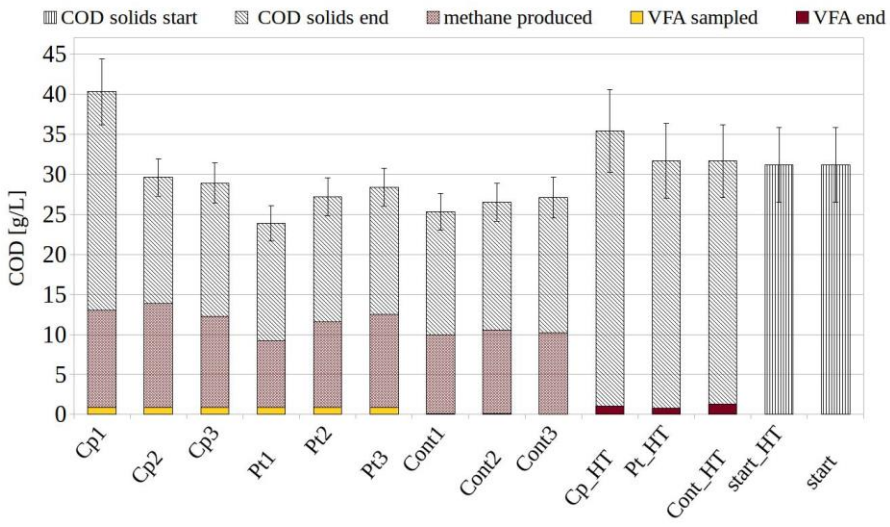

Figure 2: Mass balance of chemical oxygen demand (COD) in [g/L].
Anaerobic control digesters (Cont) with either Cp= Carbon plate or Pt= Platinum addition; Cont_HT, Cp_HT and Pt_HT= heat treated controls, start_HT/ start= heat/non-heat treated sludge before anaerobic digestion).

The CODs of the heat treated start sludge (start_HT) and the start sludge (start) are very similar and can, therefore, be taken as reference values. The measurement of COD on bulk sludge shows

standard errors (STD) below 5 % for all reactors except for Pt1 (12 %). Yet, the measured CODs on the total sludge phases are considered to vary in between 10 % in general, since mass balances often do not sum up to 100 % even though VFA and methane measurements show better accuracy. Therefore, error bars of Figure 2 represent the major error of COD with respect to bulk sludge taking an estimated error range of 10 %. The COD mass balances of all reactors, then, round up to the reference value of the start sludge's COD of 31 g/L. Heat treated reactors also fulfilled the mass balance but showed different COD composition, reaching 100 % with the COD of the remaining bulk sludge and VFAs accounting for less than 4.2 %. The presence of VFAs at the end of 42 days signifies that some organic matter must have been hydrolysed by biota that persisted during the heat treatment but that further degradation did not take place. For biotic reactors, all the VFAs were consumed at 42 days.

1.2 Organic matter removal and PAH reduction in heat treated reactors

Heat treated anaerobic digesters showed neither total solids nor volatile solids removal for the control and Cp supplemented reactor (Figure 3). Heat treated reactors were operated as single reactors and therefore, error bars are not shown. The platinum supplemented digester, yet, removed 11 % of total solids. From day one of the experiment, in between 3.0 and 3.6 % carbon dioxide accumulated in the headspace of Pt_HT reactor in contrast to the absence of CO_2 in the other heat treated reactors. It is assumed that some VFAs were oxidized to carbon dioxide in Pt_HT. The TS and VS removals were, therefore, ascribed to the microbial activity of spore formers that survived the heat treatment. Hydrogen and methane were not detected in any headspaces of heat treated reactors.

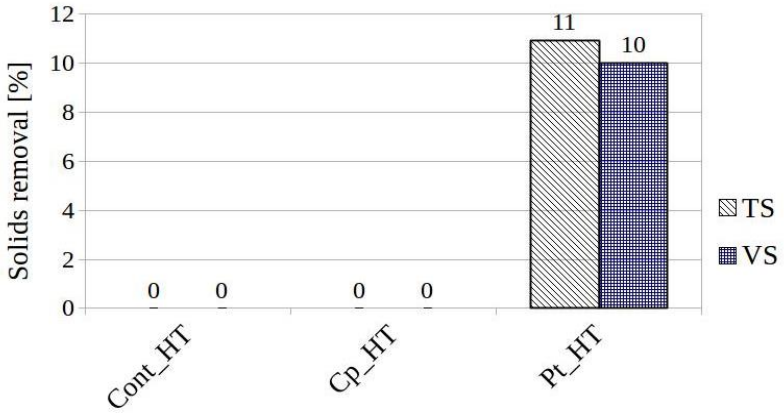

Figure 3: Total and volatile solids removal in single heat treated reactors.
Cont_HT= Heat treated control digester; Cp_HT/Pt_HT= Heat treated digester with carbon plate or platinum.

Figure 4 depicts the concentrations of the 12 PAHs before and after anaerobic digestion in the heat treated reactors. The start concentrations are the ones used for the previous experiment with Cont, GF_INT2 and BES, measured on the aliquot A after dilution, spiking and heat treatment (taking into account the losses due to volatilization during spiking/mixing and heat treatment). However Cp_HT and Pt_HT reactors were realized subsequent to Cont_HT reactors and they possessed a smaller reactor volume with less head-space. This difference in sample preparation explains why the start concentrations of more volatile PAHs (Flu, Flt, Phe and Pyr) undershoot the measured concentrations after anaerobic digestion for Cp and Pt. Moreover, the incorrectness cannot arise from incorrect extraction or incorrect measurement by HPLC since the analytical STDs of PAH concentrations of the heat treated start sludge are low. For the less volatile PAHs, the difference in reactor volume during heat treatment is less important since the start concentrations of Benzo(a)pyrene and PAHs with higher molecular weight are always higher than their final concentrations after anaerobic digestion in Cp and Pt reactors. In any case, even if the start concentration START_HT does not reflect the start concentrations for heat treated Cp/Pt, one observes a difference in treatment performance between Cont/Pt compared to Cp digesters with respect to the partition of these LMW PAHs in sludge: it is known that prior to anaerobic digestion PAHs are mainly present in the particulate phase of sludge which is confirmed by the measurement of 10 heat treated start sludge from a different experiment (79.0 ± 3.5 % in particulate phase, data not shown).

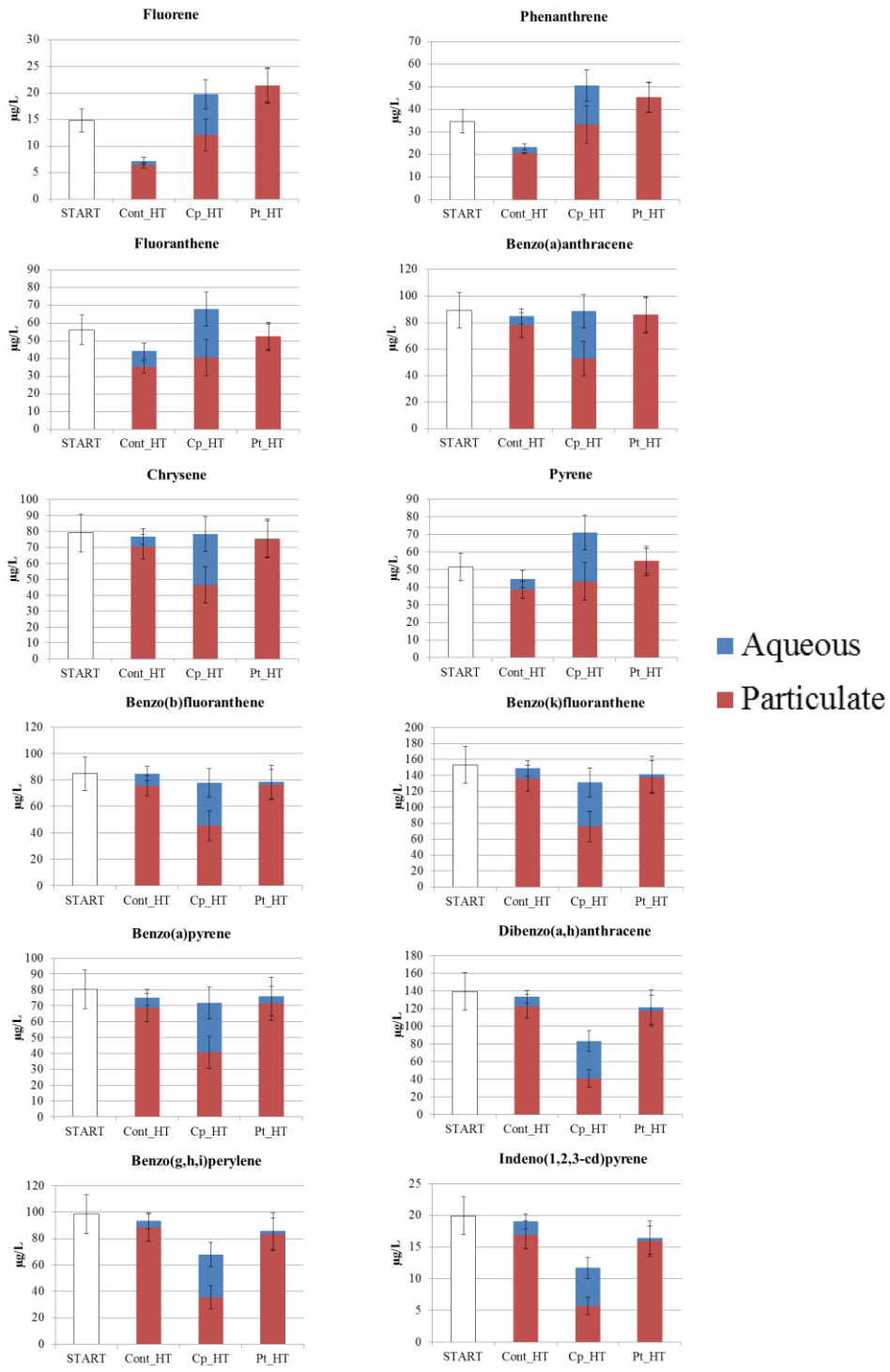

Figure 4: Partitioning of individual PAHs in particulate and aqueous phase of heat treated sewage sludge before and after anaerobic digestions with different conductors.
Standard errors correspond to four HPLC values (2 injections for two extractions of single reactors except for the control (8 injections for duplicate reactors). (Cp= carbon plate supplemented, Pt= platinum supplemented, Cont= control digester).

Control and Pt digesters show a similar partitioning of phases after AD but it seems as if Cp addition acts in favour of the transfer of the LMW PAHs from the particulate to the aqueous phase even though they may not be degraded in the aftermath. We cannot conclude on the percentage of biodegradation of these molecules since the start concentration of Cp and Pt heat treated reactors were not measured. For Chry, BaA, BaP, BbF and BkF, nonetheless, the concentrations after AD is similar for all treatment conditions but one can also observe a transfer of these PAHs from the particulate to the aqueous phase that is more severe with the addition of Cp. For the three HMW PAHs DBahA, BghiP and Ind, the final concentration is lower for Cp than the two others, suggesting a potential higher removal. The results show consistently that Cp has an effect on PAH partitioning favouring their transfer from the particulate to the aqueous phase during anaerobic digestion. The partitioning of suspended solids and total solids is nearly the same for all heat treated Cont, Cp and Pt averaging 75± 2% and, thus, cannot be the cause of PAH partitioning. Although PAH degraders could have been enriched midst spore formers in the presence of Cp, this assumption is not verifiable since sequencing was not performed for heat treated reactors.

1.3 Organic matter removal and PAH reduction in non-heat treated reactors

TS and VS removal were similar in reactors with added Cp or Pt and without conductive material. Average TS removals ranged from 27 to 30 % whereas the removals of VS were higher on average (35- 41 %) accounting for two independent measurements of each triplicate (Figure 5). There is no significant difference of TS/VS removals between the control and the conductive material digesters. Together with the observations made before for methane production, it is very probable that the methane production of the control digesters was underestimated (possible gas leakages, see chapter III, section 1.1). Theoretically, they should have produced the same amount of methane as Cp and Pt reactors which is supported by the fact that VFA concentrations are very low for all digesters after anaerobic digestion (Figure 2). Therefore, on the macroscopic level, all reactors behaved similarly.

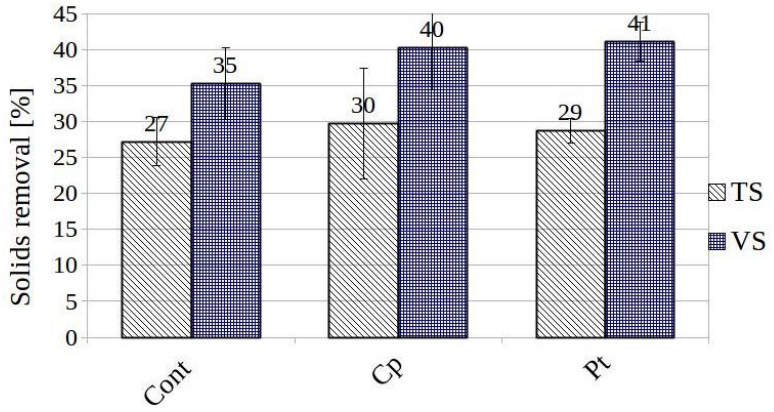

Figure 5: Total and volatile solids removal in sewage sludge after anaerobic digestion.

Figure 6 shows PAH removal performances from the bulk sludge of non-heat treated digesters during anaerobic digestion. The anaerobic control digester showed very low PAH removals in between 2 ± 5 % and 16 ± 7 % independently of the molecular weight. Reactors that were

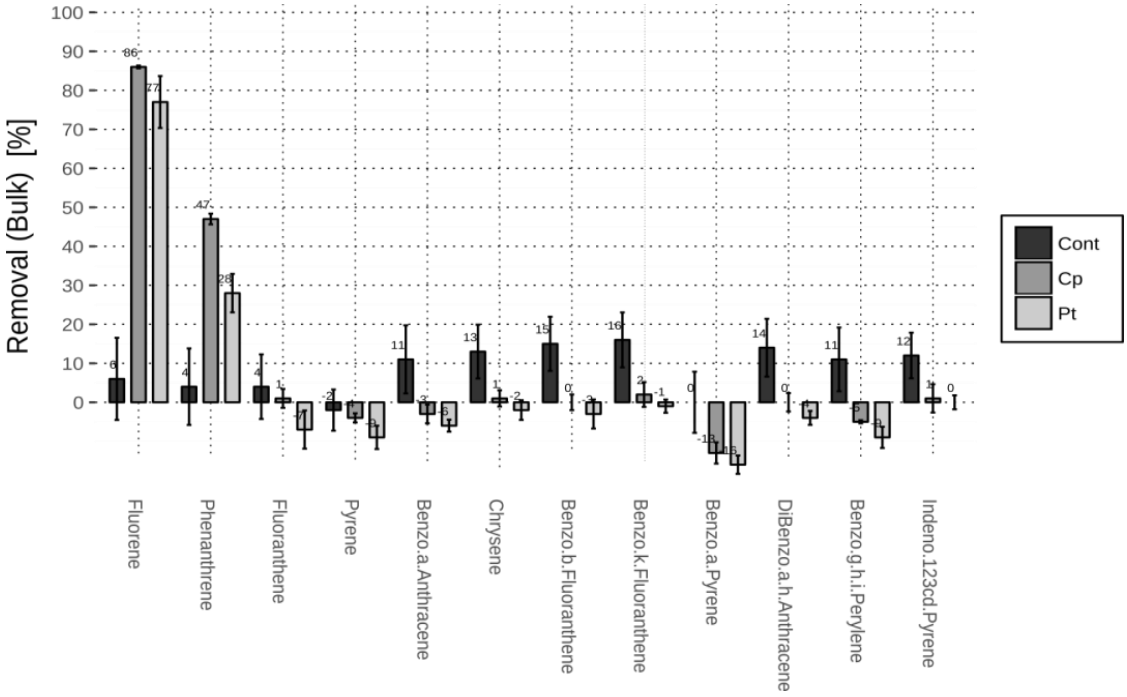

Figure 6: Removal of 12 PAHs from bulk sludge after anaerobic digestion.
Control (Cont) and material supplemented digesters with carbon plate (Cp) and platinum (Pt). Standard errors represent 12 measured values of triplicate reactors, each extracted from sludge twice and injected twice in HPLC.

supplemented with Cp or Pt showed no removal for PAHs with three or more rings but very high removal for the three-ring PAHs Flu (76.8 ± 6.7 % Pt, 85.5 ± 0.4 % Cp) and Phe (28.4 ± 5.0 % Pt, 47.4 ± 1.4 % Cp). Astonishingly, Cp being the material with a tenfold lower conductivity showed better removal for these two PAHs.

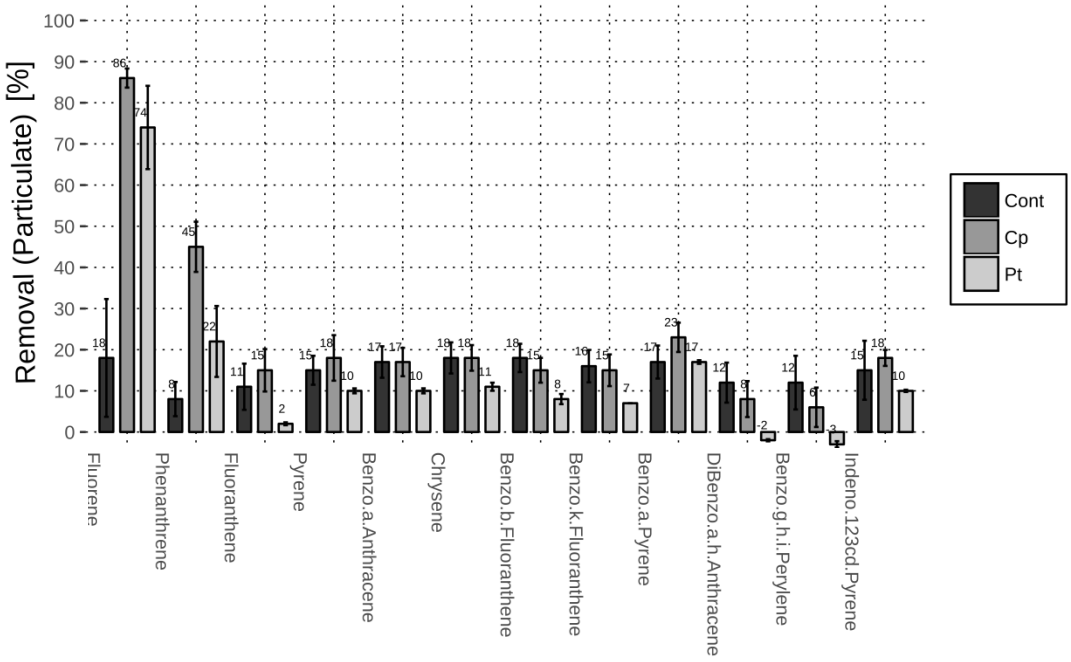

Figure 7: Removal of 12 PAHs from the particulate phase in anaerobic digesters.

Control digester (Cont) and material supplemented digesters with carbon plate (Cp) and platinum (Pt). Standard errors represent 12 measured values of triplicate reactors, each extracted from sludge twice and injected twice in HPLC

Figure 7 illustrates the removal of 12 PAHs from the particulate phase of the same reactors. Independently of the treatment, all 12 PAH concentrations in the particulate phase decrease which means that they are either degraded or relocated to the aqueous phase during anaerobic digestion (except in case of Flt, DBahA and BghiP in Pt reactors). By comparing bulk and particulate removals (Figure 6 and Figure 7), one can observe that the HMW PAHs must have been transferred to the aqueous phase (no removal in the bulk and low removal in the particulate). However, for Cp and Pt reactors, removal from the particulate phase was especially high for the

three ring PAHs Flu and Phe (86.3 ± 6.1 and 73.9 ±8.6). They may have been transferred to the aqueous phase before being degraded (Figure 6) or they may have been biodegraded while being adsorbed to particulate (Fountoulakis et al., 2006) or colloidal (Barret et al., 2010) sludge organic matter. In any case, their degradation was enhanced by the presence of Cp and Pt, respectively. Figure 8 shows the partitioning of the 12 PAHs within the particulate and aqueous phases of material supplemented reactors and the controls together with the PAH start concentrations.

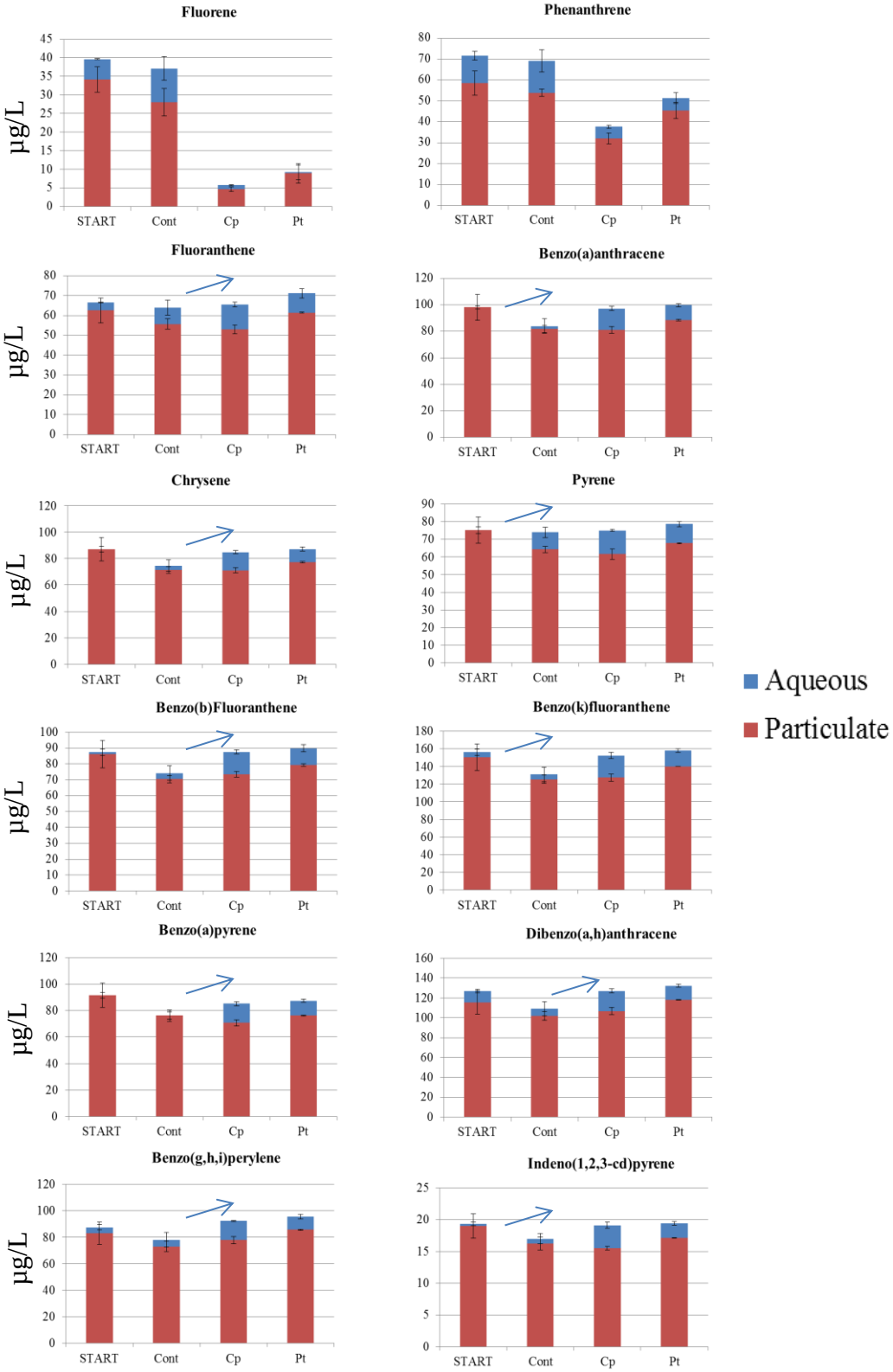

Figure 8: Partitioning of individual PAHs in particulate and aqueous phase of non-heat treated sewage sludge before and after anaerobic digestion with different conductors.
Standard errors correspond to eight and sixteen HPLC values (2 injections for two extractions of duplicate (Cp) or triplicate (Cont, Pt) reactors and six HPLC values for start sludge with three extractions. (Cp= carbon plate supplemented, Pt= platinum supplemented, Cont= control digester).

Again, highest removals are observed for Flu and Phe as seen before. Additionally, Figure 8 demonstrates the complete removal of Flu from the aqueous phase (blue) of Cp and Pt digesters after 42 days meaning that the partitioning was almost 100 % on the side of the particulate (red). On the contrary, for all other PAHs the partitioning in Cp and Pt digesters was distributed (20:80) in the aqueous and particulate phases, respectively. Yet, the net removal is low meaning that HMW PAHs are not degraded further after their transfer to the aqueous phase. The particulate-aqueous relocation is always slightly higher than the PAH transfer that occurs for the control digester as indicated by the fleshes in the graphs. It was already found before that conductive materials such as biochar and conductive iron oxides stimulate microbial communities (Chen et al., 2018; Zhuang et al., 2015). More specifically, this PhD study demonstrated that GF increased the bioavailability of PAHs (chapter III, section 1.4) during anaerobic digestion. In the present experiment, the removal of Flu (86 %) and Phe (47 %) from bulk sludge with conductive Cp was much higher than in previous experiments, suggesting that the increase in bioavailability of these three ring PAHs during AD was much higher with Cp addition. The removal pathways of PAHs during anaerobic biodegradation are not well known, though, (Foght, 2008; Kronenberg et al., 2017; Rabus et al., 2016) and could be dependent on the number of rings, differences in partition coefficients (Kim et al., 2013) and different activation energies for carboxylation (Christensen et al., 2004; Zhang and Young, 1997) and methylation (Liang et al., 2014) which are considered the initial steps in PAH biodegradation. Thus, it is not surprising that two of the lower weight molecules are better removed than the others. Previous experiments on the same spiked sludge showed much broader removal of low and high molecular weight PAHs by the action of conductive GF along with TS removal (chapter III, section 1.3). A possible reason is the much lower SSA of Cp and Pt in comparison to GF. The projected surface areas of the three materials were similar; yet, the porous structure of GF probably facilitates the exchange of electrons between biota, thereby, enhancing organic matter degradation along with co-metabolic PAH removal. Therefore, it is possible that an accelerated exchange of electrons by conductive material is only pronounced if the SSA that can be measured via nitrogen adsorption is high (GF >> Cp, Pt). In line with our results, it was found that conductive materials supported accelerated direct interspecies electron transfer (DIET) during methane generation in the same extent even though one was 1000 fold less conductive than the other (Chen et al., 2014). Apparently,

conductive materials enhance anaerobic digester performance due to their conductivity but not proportional to it. Other properties of the tested conductors must, therefore, be responsible for the extent in removal performances, e.g. the capacity of microorganisms to adhere on the material (Habouzit et al., 2011; Nguyen et al., 2016) or its surface area (Clauss et al., 2014). In chapter III, we hypothesized that GF acted as an electron exchange facility for microorganisms to discharge the electrons that they obtained from organic matter destruction and tunnel these to microorganisms that are in need of electrons and equally capable of DIET. PAH removal would then be a result of co-metabolism in which the principal substrate is organic matter itself. In the present work, however, TS removal was not linked to PAH removal since it was nearly the same in material reactors and in the control. Therefore, it is concluded that removal of Flu and Phe in Cp and Pt digesters exceed organic matter removal due to the presence of specific microbial Flu and Phe degraders at low abundances in the source sludge that were maintained or enriched by the addition of carbon plate and platinum. Cp and in a less extend Pt addition to anaerobic digesters may have led to an increase in bioavailability of Flu and Phe which resulted from Flu and Phe transfer from the particulate to the aqueous fraction or an increase in the bioavailable fraction of Flu and Phe that is sorbed to colloids and/or particulate matter. Speaking in favour of this hypothesis, the transfer of three low and high molecular weight PAHs from the particulate to the aqueous phase has been observed in AD due to the addition of conductive GF (chapter III, section 1.4). The higher concentrations of bioavailable Flu and Phe could, then, have stimulated specific microbial species to biodegrade these compounds irrespective of organic matter degradation. This kind of stimulation has been observed before for an Aroclor degrading microbial community. Adding the commercial PCB mixture to PCB contaminated soil made microbial consortia express Aroclor decomposing molecules (Cho et al., 2003). Obviously, these hypotheses should be confirmed in subsequent experiments.

For heat treated sludge, it was observed that Cp digesters consistently showed a higher fraction of all PAHs in the aqueous phase after AD although the fractions of TSS and aqueous COD were nearly the same in all digesters (75.1± 1.6 % and 23.2± 1.2 %). It should be verified by filtration and 3D fluorescence spectroscopy if the amount of colloids (Akhiar et al., 2017) and aromatic compounds (fulvic- and humic-like as well as aromatic amino acids) (Jimenez et al., 2017) varied between these treatments. This could allow stipulating that the PAH transfer observed is due to

the transfer of these compounds to the aqueous phase. Furthermore, spore formers must have been present due to the heat treatment. By the addition of Cp, it may be that specific electroactive spore formers have been enriched in the aftermath such as observed in case of GF addition to heat treated sludge (chapter III, section 1.5.1) thereby, being able to exchange electrons with Cp. These bacteria may have also contributed to the relocation of all PAHs to the aqueous phase.

1.4 Microbial community structure with and without conductive materials

In order to compare microbial community structure, diversity, and function in different reactors, sequencing was performed on the inoculum and at the end of the batch experiment. Archaeal community structure revealed that most dominant genera were *Methanobacterium* (hydrogenotrophic) and *Methanosarcina* sp. (acetotrophic) accounting 91 -99 % of the archaeal 16S rRNA gene sequences recovered in the bulk sludge of all reactors (Figure 9A). The OTUs correspond to 16S rRNA sequences with 3 % similarity. *Methanobacteria* were present in a larger extent in material supplemented digesters than in control digesters (Figure 9A) pointing to an increased activity of hydrogenotrophic methanogens. The increase of this genus, however, was not reflected in increased methane production for Cp and Pt reactors.

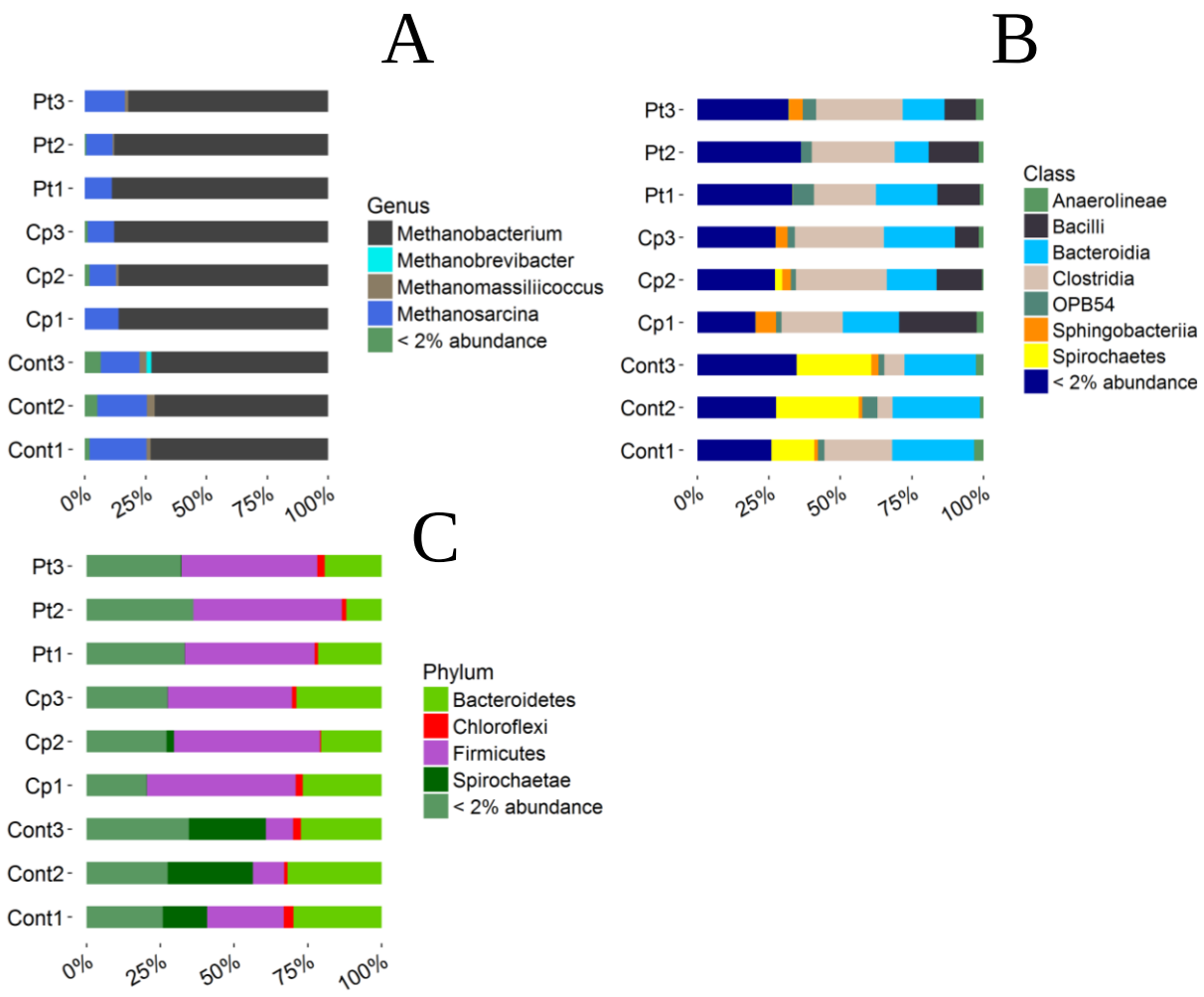

Figure 9: Relative abundances of archaeal genera (A) and bacteria on phylum (B) as well as on class (C) level.
Sludge of Pt and Cp digesters are compared to the control (Cont experiments were conducted five months before this experiment with similar operating parameters and the same defrosted sludge).

OTU1, OTU3 and OTU4 represent 99 % of all *Methanobacterium* sp. Yet, the distribution of these *Methanobacteria* differed according to treatments. OTU1 with 100 % sequence identity to *Methanobacterium aggregans* accounted for 74, 85 and 93 % of relative abundance of total *Methanobacteria* with increasing trend Cont < Cp < Pt (Figure 10), thereby representing 54, 73 and 80 % of all archaeal sequences. *Methanobacteria* are typical H_2 utilizing methanogens and responsible for interspecies H_2 transfer, confirming that methane production was mainly due to hydrogenotrophic methanogenesis. They were suggested to undergo direct extracellular electron transfer (DEET) in electromethanogenesis (Cheng et al., 2009; Villano et al., 2010; Zhen et al., 2015). Since *Methanobacterium aggregans* was enriched with increasing conductivity of the material, it could be that it particularly succeeds in DEET with materials of higher conductivity

such as Pt. However, this observed tendency in relative abundances has not been verified via qPCR. Therefore, it is not clear if the relative increase in abundance of *M. aggregans* (7 %) from Cp to Pt corresponds to an absolute increase of this strain. OTU3 was identified to 100 % sequence similarity with *Methanobacterium palustre strain F16S* and attains 24, 11 and 3 % relative abundance within *Methanobacteria* of Cont, Cp and Pt digesters. OTU4, identical to the sequence of *Methanobacterium lacus strain 17A1* accounted for 2 to 5 % relative abundance in all digesters.

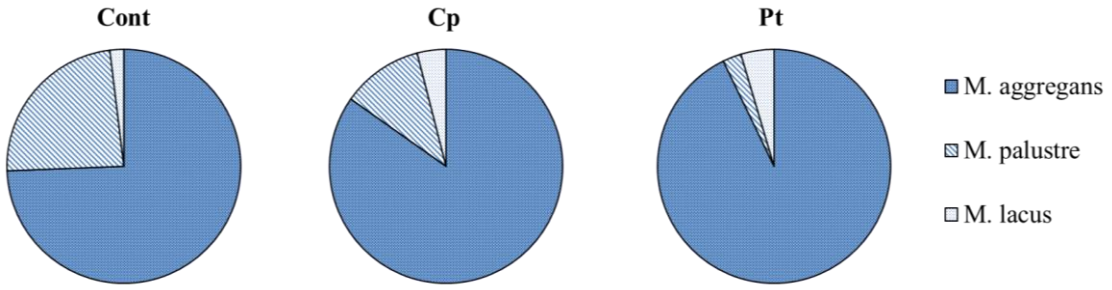

Figure 10: Distribution of three OTUs in sludge after anaerobic digestion.
Control (Cont) and carbon plate (Cp) as well as platinum (Pt) digesters. The three OTUs show 100 % sequence identity to three *Methanobacterium sp*. as indicated.

Three dominant bacterial phyla including *Firmicutes* and *Bacteroidetes* accounted for 60-75 % of the bacterial 16S rRNA gene sequences in the bulk sludge of Pt and Cp digesters (Figure 9B) but only 36 – 56 % in control digesters. Accordingly, control digesters without conductive materials showed 15 to 29 % relative abundance of *Spirochaetae* that were absent in material supplemented digesters except for Cp2 (4 %). The phyla *Chloroflexi*, *Proteobacteria* and *Armatimonadetes* counted midst less abundant phyla. Phyla with relative abundances less than 2 % of bacterial sequences represent 24 - 35 % in all anaerobic digesters signifying high bacterial diversity [Shannon indices: 3.4 (Cp, Cont); 3.8 (Pt)]. On class level, material supplemented reactors can be easily distinguished by the presence of *Bacilli* (15-17 % relative abundance for Cp and Pt) which do not appear in control digesters (< 2 %) as depicted in Figure 9C. Interestingly, the bacterial class *Bacilli* was associated with PAH biodegradation in microbial fuel cells (MFCs) (Li et al., 2016); and more specifically, a *Bacillus* sp. was found to degrade cyclic hydrocarbons in a MFC that treated waste engine oil (Sabina et al., 2014). An electroactive property has also been assumed for some members of the class *Bacilli* and was proven for *Bacillus subtilis* in pure

culture experiments (Cournet et al., 2010; Nimje et al., 2009). Notably, *Bacillaceae* and *Methanobacteria* have been suggested to take part in syntrophic DIET for benzoate degradation with the help of conductive iron minerals (Zhuang et al., 2015). Both taxa were enriched in Cp and Pt containing digesters building proof for the observed Flu and Phe removal due to conductive materials. Especially OTU3 with 99 % similarity to ten different *Sporosarcina* strains was found to represent 17 ± 9.5% and 14 ± 3.2 % in Cp and Pt supplemented reactors, respectively whereas it was not detected in the control digesters. *Sporosarcina* belong to the family *Planococcaceae* that were suggested to be important for power generation in soil MFCs since the peak voltage and charge were positively correlated with this bacterial family (Jiang et al., 2016). Such exoelectrogens could have been enriched due to the fact that conductive materials were added to anaerobic digestion (Cp, Pt).

Several hypotheses can be made in order to argue why the removals of Flu and Phe were enhanced with respect to the different microbial communities in Cp and Pt reactors compared to the controls. Firstly, it must be noted that the low concentrations of micropollutants in sludge restrict their influence on the overall changes in microbial community composition during 42 days, especially knowing that the inoculum that was used for all digesters was long term acquainted with the PAHs that are present in the WWTP.

Probably, Flu and Phe were better removed due to a cometabolic removal that was carried out by a specific microbial community in Cp and Pt reactors along with organic matter degradation. It is possible that the different microbial community structures lead to the same methane production but different PAH removals. The notion of cometabolism implies the concurrent biodegradation of a macropollutant such as COD or ammonium and a specific micropollutant that cannot serve as growth substrate alone (Pomiès et al., 2013). Successful attempts to model micropollutant removal integrate the concept of cometabolic biodegradation for PAHs (Delgadillo-Mirquez et al., 2011) and carbamazepine as well as diclofenac (Plósz et al., 2012).

The second hypothesis is that the same species that have been enriched as a consequence of material addition can also use Flu and Phe as a carbon source, thus, removing these micropollutants along with other substrates. Even though some electroactive bacteria have been proposed to degrade petroleum hydrocarbons (Zhou et al., 2016) and hydrocarbons (Li et al.,

2014; Lu et al., 2014), in general, a specific biodegradation of Flu or Phe by *Planococcaceae* has not yet been proven.

A third possible answer for the observed performances consists in the assumption that certain members of the microbial community of Cp and Pt reactors with very low abundances effectively performed Flu and Phe biodegradation and that this biomass can maintain itself due to the presence of Flu and Phe (Pomiès et al., 2013). In theory, it is possible that 1 % relative abundance of a certain bacterium or an *archaeon* represents enough biomass to perform the removal of certain PAHs present on the micro scale. However, even though sequencing results can detect these low abundances, the actual knowledge about microbial degraders of PAHs is too few in order to search for these species specifically. It, therefore, cannot be verified. A principal component analysis (PCA) was performed on account of these findings since this method of multivariate statistics allows to transform interdependent variables into statistically uncorrelated variables, the principal components or principal axes. The first axis, in the graph below, is a good choice for the comparison of the samples' microbiological composition since it represents nearly 50 % of the samples' variance. Consequently, PCA results confirm the difference in bacterial composition of control and material digesters (Figure 11).

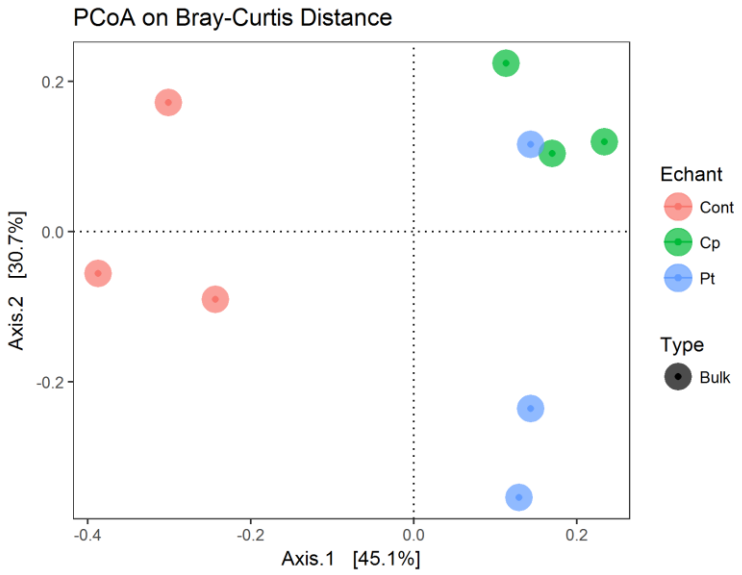

Figure 11: Principal component analysis (PCoA) of taxonomic units.
Axis 1 represents 45 % of the variation between sludge samples from Cp (carbon plate), Pt (platinum) and the control digesters.

The absence of phylum *Spirochaetae* in material digesters points to a selection of bacteria that could have been induced by the presence of materials. On the other hand, the non-negligible presence of *Bacilli* (15-17 %) and the enrichment of hydrogenotrophic *Archaea* in both material reactors speak in favour of a bacterial as well as archaeal selection that was induced by the conductive properties of Pt and Cp. Hydrogenotrophic *Archaea* have been enriched in GF and BES reactors from the previous experiment as well (chapter III, figure 7B). However, the bacterial selection on class level was different with relative abundances of *Bacilli* in GF and BES digesters below 2 % (SI, figure 3). Even if the inoculum used for this experiment is the same as the previous one, it was frozen longer before use which could influence its composition but unfortunately we did not characterize this hypothetical modification after freezing (the inoculum was just analyzed for the first experiment after one month freezing). The correlation between the presence of conductive materials Cp/Pt and the microbial community composition, thus, remains hypothetic.

1.5 Conclusions

The addition of Cp and Pt to anaerobic digesters resulted in 12 to 14 times better removal of Flu as well as 7 to 11 times higher removal of Phe from sewage sludge compared to the control digester. After batch experiments of 42 days, Pt reactors showed 77 % and 28 % removal of Flu and Phe, respectively, whereas Cp exceeded these removals attaining 86 % and 47 % despite being 1000 times less conductive. Therefore, this study proved that the conductivity of solid materials added to anaerobic digesters is not decisive for the removal performance of COD and Flu and Phe from sewage sludge. Macroscopic differences in terms of methane production and TS/VS removals in control and material reactors were not observed.

For HMW PAHs the addition of both conductive materials improved their transfer to the aqueous phase but this relocation of micropollutants did not increase their removal. In heat treated sludge this trend of HMW PAH relocation was even augmented.

The hypothesis made in section 1.3 that microbial Flu and Phe degraders were maintained or enriched by the addition of carbon plate and platinum was sustained by sequencing results. A shift in bacterial community composition for anaerobic digesters that employed a conductive material gave hints to possible explanation why Flu and Phe were better removed. 16S rRNA

sequencing revealed a 14 to 17 % enrichment of OTU3 with 99 % sequence similarity to several *Sporosarcina* strains belonging to the class *Bacilli*. *Bacilli* have been associated with electroactive properties and may have been enriched due to the facilitated electron exchange with solid conductors building a bridge between electron rich organic substrates and electron deficient molecules such as PAHs. Adding to that, an enhanced PAH removal resulting from this bacterial enrichment is consistent with the fact that *Bacilli* were found to degrade polycyclic hydrocarbons. Therefore, their specific enrichment in Cp and Pt reactors together with an enhanced removal of two low molecular weight PAHs points to a cometabolic activity that was favoured by the presence of these materials and due to which micropollutants were specifically or non-specifically removed to a higher extent than in the control digesters.

Although PAH degraders could have been enriched midst spore formers in the presence of Cp, this assumption is not verifiable since, firstly, sequencing was not performed for heat treated sludge, and secondly, many PAH degraders remain unknown to this date and their abundances within the microbial community may be very small, therefore, not being recognized midst other sequences of low abundance. Therefore, the enrichment of electroactives in heat treated sludge that caused the transfer of PAHs to the aqueous phase as hypothesized in section 1.3 is neither confirmed nor discarded by microbiological results.

The biodegradation of low molecular PAHs based on the addition of conductive materials such as Cp to sewage sludge is an important insight: it demonstrates a new bioremediation strategy to remove PAHs from sludge, soil or sediment. Further studies should, therefore, focus on PAH removal by cheap conductive materials with different surface areas and surface structures that are capable of enhancing the removal also of HMW PAHs.

Chapter VI

List of figures

List of tables

1 Testing the effect of an increase in specific surface area of conductive graphite felt on the removal of PAHs and NP during anaerobic digestion of sludge

Since we excluded that conductivity alone (material independent) plays a major role in the removal of PAHs and NPs in anaerobic digesters and the highest removal performances in previous experiments were obtained by the addition of GF without polarized electrodes, the next experiment aimed at deciding whether or not the specific surface area (SSA) of GF influences PAH removal performances during AD. Whenever matter is divided into smaller pieces, the SSA is increased, explaining why powders are appreciated for their high surface area (Kuila and Prasad, 2013). The following experiment employed intact GF with SSAs of 1 and 2 m^2 as well as the same quantity of GF that was grinded to a fine powder, thus augmenting SSA to at least a factor of ten when descending from GF dimension of cm to mm or smaller (Lowell et al., 2004). Experimental conditions are depicted in chapter II, section 2.3.

1.1 Methane production in non-heat treated digesters

Figure 1 shows normalized methane production per initial chemical oxygen demand (COD) of sludge. This initial COD was calculated on the basis of measured COD in end sludge samples by adding the COD value for methane produced in each reactor (350 ml methane corresponds to 1 g of COD= 1 g O_2/L). This theoretical calculation was done because the measured values for the initial total and volatile solids as well as for COD were incorrect due to a heterogeneous sampling realized in each reactor at the beginning of the experiment. Indeed, after defrosting, the sludge samples are more heterogeneous with sedimentation of the heavier particles. The theoretical calculation of initial COD values is debatable scientifically but the only possibility to compare digester performances in between reactors.

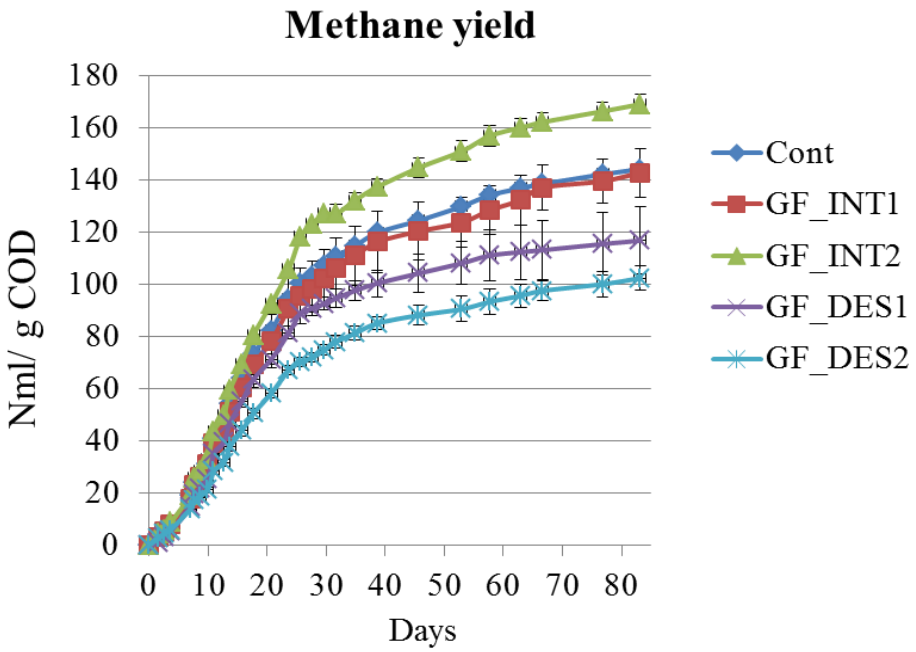

Figure 1: Methane production at standard temperature and pressure per chemical oxygen demand of initial sludge of the individual reactors.

According to the small error bars found in normalized methane production (Table 1) in between duplicates, the assumptions made can be assumed to be close to reality since the same treatments resulted in similar normalized methane quantities. Initial CODs of individual reactors (calculated) are listed in Table 1 together with the measured COD after

AD of 83 days and methane quantities that are also expressed in g COD/L. The average of initial COD values is 30.2 g/L which is very close to the COD of raw sludge (45 g/L) after diluting 1.78 times (32.0 g/L) which backs up the calculated results. The respective equation is given in the following.

$$COD\ (initial) = COD\ (end) + COD\ (CH_4)$$

$$= COD\ (end) + NL\ (CH_4)/\ 0.35$$

Table 1: Initial COD of sludge for reactors without heat treatment.
Calculated by adding COD of methane development to the measured COD after anaerobic digestion.

Sample	g COD/ L (initial)	g COD/L (CH_4)	NL (CH_4)	g COD/L (end)
Cont_a	27.9	11.5	4.0	16.4 ± 0.4
Cont_b	28.1	11.6	4.1	16.5 ± 0.1
GF_INT1a	24.2	10.5	3.7	13.7 ± 4.1
GF_INT1b	29.5	11.3	3.9	18.2 ± 0.3
GF_INT2a	25.9	12.8	4.5	13.1 ± 0.9
GF_INT2b	25.2	11.9	4.2	13.3 ± 0.6
GF_DES1a	30.8	9.2	3.2	21.7 ± 0.2
GF_DES1b	34.5	12.8	4.5	21.7 ± 1.2
GF_DES2a	37.8	11.6	4.0	26.2 ± 1.6
GF_DES2b	37.6	10.5	3.7	27.1 ± 0.4

Control reactors produce the same amount of methane than reactors with an intact GF piece with a SSA of 1m^2 (GF_INT1) with the kinetics of the two duplicate digesters showing the same course/progression. Yet, there is a 17.2 ± 2.6 % increase in methane production for reactors with a doubled SSA of 2 m^2 (GF_INT 2) compared to the control digesters. Considering that there is a threshold value for the increase in methane yield with respect to the SSA of GF, the control digesters were pooled with GF_INT1 reactors for statistical analysis and a significant difference was confirmed between GF_INT2 reactors and the GF_INT1 and Cont ($p= 0.016$). In order to explain these observations, an enhancement of the microbial activity is presumed due to the presence of 2 m^2 of GF. Saquing et al. (2016) recently proposed that black carbon materials should be regarded as a kind of battery for microbial reduction and oxidation in anaerobic environments by channeling electrons through the highly aromatic structure of graphite and GAC. We presume that this rechargeable reservoir of bioavailable electrons is more efficient when the SSA of GF is higher. In the same line, Li et al. (2015) stipulated that higher conductivity of sludge in the presence of carbon nanotubes might promote DIET among fermentative bacteria and methanogens during AD. An increased quantity of carbon should, then, increase conductivity while at the same time increasing DIET. Surprisingly, a further increase of the SSA in our experiments with destroyed (powdered) GF (GF_DES1 and GF_DES2), however, caused less methane production. For statistical analysis the methane production of these four reactors that exhibited a much higher surface area than all other reactors was pooled and gave a statistical difference compared to the control reactor (Cont) with $p= 0.009$. Therefore, the anaerobic digesters with powdered GF are considered to decrease methane production despite an increase in the SSA of at least tenfold in comparison to intact GFs (see chapter II, section 2.3). A recent publication confirms this finding since it was observed that conductive nanographene increased methane production with addition of 1 g/L whereas methane volume decreased at a nanographene concentration of 2 g/L. Apparently, a certain increase in specific surface area of graphite materials enhances AD performances but inhibits cell metabolism beyond that amount. Carbon nanoparticles are known for generating reactive oxygen species under aerobic conditions, thereby creating

oxidative stress for microorganisms (Pacurari et al., 2008). Similarly to Ambuchi et al. (2017) who used carbon nanotubes and iron oxide nanoparticles during AD, we conclude that oxidative stress and residual metal catalysts cannot have been the reason why powdered GF acted negatively on cell metabolism since anaerobic conditions exclude the first and the purity of GF (99.9 % carbon) excludes the second possibility. The high purity grade of the GF that was used in this study equally excludes a possible toxic effect on bacteria due to the action of oxygen- (Pasquini et al., 2013) or amide containing (Tiraferri et al., 2011) surface functional groups. It is more probable that powdered graphite caused damage to the cell membranes as reported before (Qu et al., 2016). The authors used electron microscopy, viability test, cellular membrane integrity, and oxidative stress measurements to draw the conclusion that bacterial toxicity is mainly caused by physical membrane piercing. These measurements have not been conducted in the present study and can only give plausible hypothesis why powdered GF decreased methane yields.

The production of VFAs, namely acetate, propionate, (iso)butyrate and (iso)valerate follows the same dynamics in all reactors (Figure 2). Highest concentrations are observed for acetate in GF_INT1 1 and GF_INT2 digesters with 2.1 and 2.4 g/L at day 5 but are consumed until day ten. Propionate accumulation happens in all digesters, GF_INT2 showing the highest average value (1.3 g/L). Dynamics between day 20 and 40 have not been recorded but propionate must have been consumed within this time period. All other VFA concentrations stay below 0.7 g/L and are consumed within 20 days. This means that after 20 days these fermentation products were produced and consumed at the same time. Isobutyrate concentrations reached 0.3 and 0.5 g/L in reactors GF_DES1 and GF_DES2, respectively, which was higher than in other reactors. It could be linked to the lower methane production and alteration of membrane integrity as hypothesized above. A little VFA and hydrogen production was noticed in heat treated digesters which points to a small activity of hydrogen producing organisms inside the reactors (data shown in SI, figure 4-5).

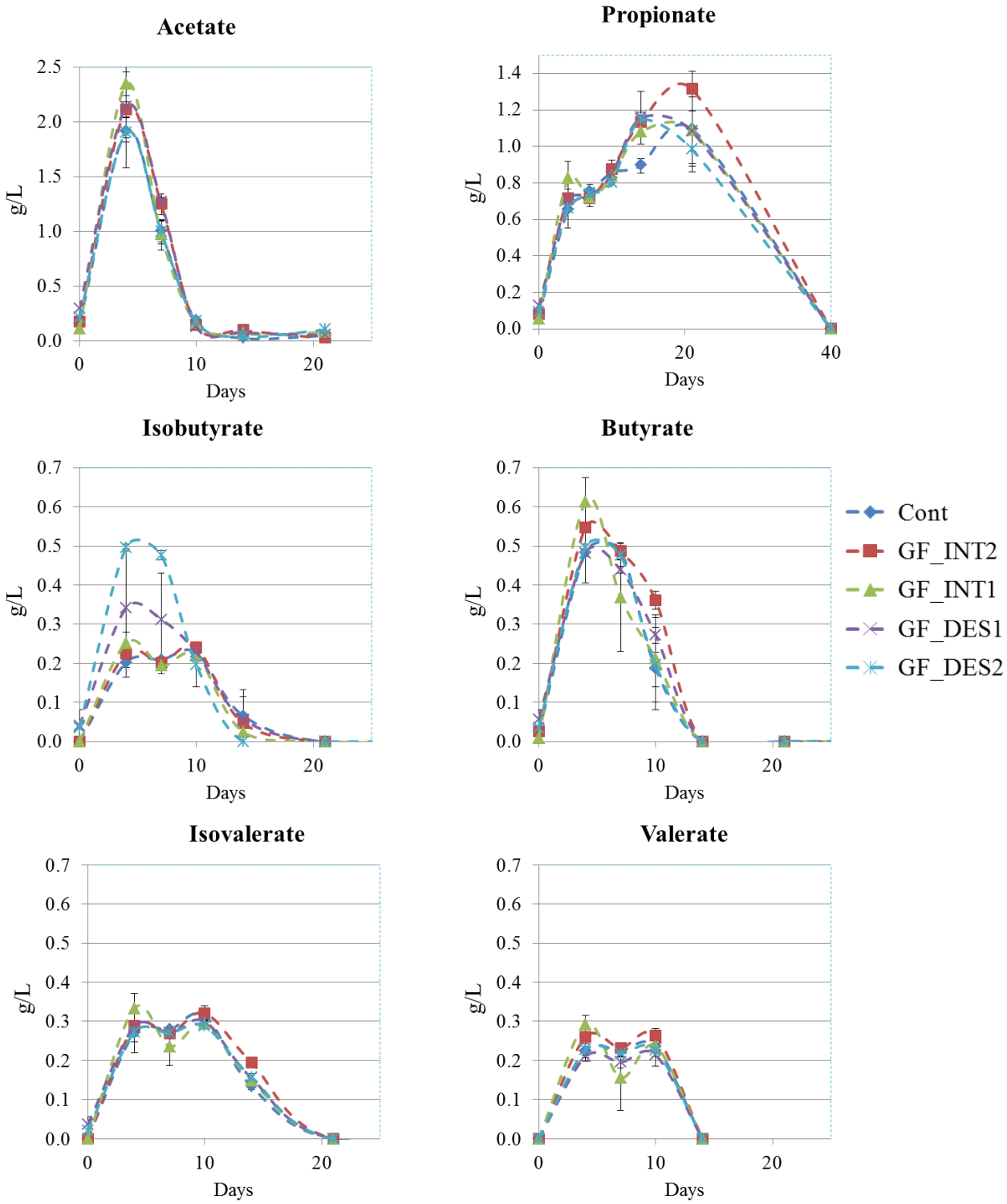

Figure 2: VFA production from non-heat treated anaerobic digesters.

1.2 Extent of sorption of PAH/NP on graphite felt

In order to evaluate the extent of sorption of PAHs onto GF, PAH and NP concentration onto GF were compared to the PAH concentrations found in the bulk sludge. PAH and NP concentrations onto GF, in bulk sludge and the respective total concentrations inside the reactor can be found in Table 2. The results in the columns five and nine are expressed as fractions of sorbed pollutants with respect to the total PAH and NP concentrations inside the reactor. The respective calculations are explained in chapter II, section 4.4 and micropollutant concentrations with STD onto GF can be found in tables 1 and 2 of the supplementary information (SI). Pure GF coming from the supplier did not contain detectable concentrations of PAHs or NP.

Table 2: Sorption of PAHs and NP onto GF in non-heat treated anaerobic digesters.
PAH and NP sorption onto GF with different specific surface areas of 1 m^2 and 2 m^2 with respect to total concentrations in reactors.

	GF_INT1				GF_INT2			
	Final conc.	Final conc. on GF	Sum	Fraction sorbed	Final conc.	Final conc. on GF	sum	Fraction sorbed
	[µg/L]	[µg/L]	[µg/L]	[%]	[µg/L]	[µg/L]	[µg/L]	[%]
Fluorene	26.5	2.6	29.1	9.0	18.8	11.2	30.0	37.4
Phenanthrene	46.6	0.8	47.4	1.6	36.0	3.6	39.5	9.0
Anthracene	46.1	0.1	46.2	0.2	36.0	0.3	36.3	0.8
Fluoranthene	49.0	3.7	52.8	7.1	41.1	10.4	51.5	20.3
Pyrene	47.7	0.1	47.8	0.2	39.3	0.4	39.8	1.1
Benzo.a.Anthracene	40.1	0.6	40.7	1.4	34.4	2.6	37.1	7.1
Chrysene	40.8	0.0	40.8	0.0	33.1	0.1	33.2	0.3
Benzo.b.Fluoranthene	36.5	0.0	36.5	0.0	31.1	0.0	31.1	0.1
Benzo.k.Fluoranthene	31.0	0.6	31.6	1.9	25.4	1.3	26.7	4.8
Benzo.a.Pyrene	29.4	0.0	29.4	0.1	24.5	0.1	24.6	0.5
DiBenzo.a.h.Anthracene	25.1	1.2	26.4	4.7	17.9	4.9	22.8	21.3
Benzo.g.h.i.Perylene	28.1	0.0	28.1	0.0	20.7	0.0	20.7	0.0
Nonylphenol	196.9	14.9	211.8	7.0	247.0	64.9	311.9	20.8

For both heat treated and non-heat treated reactors, PAH and NP sorption could possibly occur to the GF itself or to microbial biomass or other organic matter that is sorbed onto GF. The average extent of PAH and NP sorption on GF surfaces for heat treated reactors is smaller than for anaerobic reactor without heat treatment (Table 3, SI). There is a clear preference of Flu, Flt, DBahA and NP to sorb onto GF in comparison to the rest of PAH molecules. For these molecules, it amounts to 3.2-7.1 % in heat treated sludge (Table 3, SI) and 20.3- 37.4 % in non-heat treated sludge (Table 2) for GF with a SSA of 2 m^2 (Table 2). This seven to nine fold preference of these molecules to adsorb onto GF could be due to its porous structure that possibly exhibits better adsorption for specific molecules due to their unique configurational structure and GFs pore size as demonstrated for sorption of organic contaminants onto graphene nanosheets (Ersan et al., 2017). Another reason for global less sorption on heat treated GF could be that the heat treated organic matter was less complex (Carrere et al., 2016) and less prone to sorption onto GF due to solubilisation Consequently, the PAHs within the more solubilized organic matter (colloids) or in the aqueous fraction possibly behaved in the same way and sorbed less onto GF.

For these compounds, the ratio of sorbed pollutants onto GF with respect to the total amount of PAHs and NPs present in the bulk sludge increases with its SSA (Table 2) but with only two different surface areas tested, one cannot say if the extent of sorption increases proportionally to the surface area. However, the increase is 4.1 and 2.6 fold for PAHs and NP on 1 m^2 compared to 2 m^2, respectively, confirming that micropollutants are possibly co-localized on conductive materials together with biota that are responsible for their degradation (Lovley, 2006). Adding to that, digesters with a SSA of 2 m^2 achieved highest methane yields and showed the highest sorption of PAHs onto GF. The possible correlation between methane production, PAH sorption onto GF and PAH removal will be discussed in section 1.5.

1.3 NP concentrations in non-heat treated reactors

NP1EO and NP2EO concentrations were found to be mostly below the quantification limit in start and end samples of sludge that underwent AD. Therefore, the detected NP concentrations could be evaluated directly without taking into account possible transformations of precursor molecules. Final NP concentrations of all digesters vary in between 152 and 270 µg/L with high

STDs for GF_DES2b and GF_INT1b as shown in Figure 3. The averages of duplicate digesters are comprised in between 197 and 247 µg/L with overlapping error bars (Table 3).

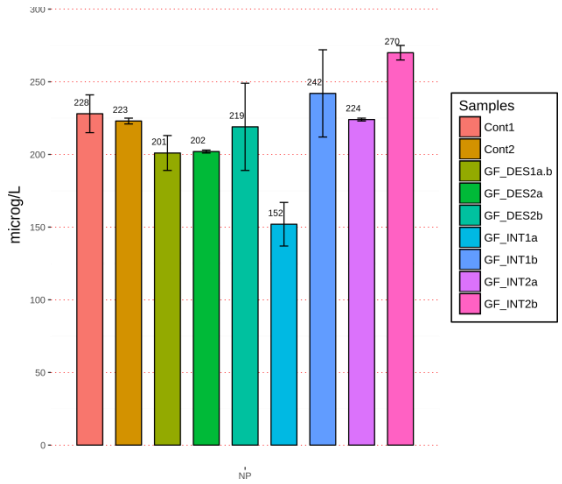

Figure 3: Final NP concentrations in the bulk of the non-heat treated reactor after anaerobic digestion.
Controls without graphite felt addition (Cont1, Cont2) and digesters with the addition of powdered graphite felt (single reactor GF_DES1a.b and duplicate reactors of GF_DES2) of 1 m^2 or 2 m^2 surface area as well as intact graphite felt (duplicate reactors of GF_INT1 and GF_INT2).

As discussed in section 1.2, NP was attached to the surface of intact GF and, therefore, the NP concentrations of GF_INT1 and GF_INT2 must be corrected for 8 ± 5.5 % and 21± 2.4, respectively. The corrected concentrations that were detected at the end of anaerobic digestion are listed in Table 3.

Table 3: NP concentrations at the end of anaerobic digestion of the non-heat treated reactors.
GF_INT1/ GF_INT2 are corrected by the amount of NP sorption onto GF. GF_DES1 is unique.

Samples	Average NP concentration ± STD [µg/L]	NP concentration ± STD [µg/L] (correct. by sorption)
Cont	226 ± 3	226 ± 3
GF_DES1	197	197
GF_DES2	210 ± 9	210 ± 9
GF_INT1	197 ± 45	213 ± 56
GF_INT2	247 ± 24	299 ± 30

When the fraction of NP that remained sorbed onto GF is added to the final bulk concentrations the digesters with intact GF of 2 m^2 show higher NP concentration than all other digesters which means that the removal of NP was lowest here. Since dilution and spiking of sludge was conducted in the same way, initial TS contents and NP concentrations must have been similar in each reactor as well. Taking into account that the theoretical concentration of spiked NP (chapter II, table 3) for the ten reactors was 1272 ± 22 µg/L, the theoretical removals would, nevertheless, be very close to each other with the lowest removal of 76 % (GF_INT2) and highest of 85 % (GF_DES1, GF_INT1). Therefore, it is concluded that NP removal during AD was not influenced by the addition of GF of different SSAs. The same result has been obtained for GF_INT2 addition in chapter IV giving rise to over 80 % NP removal. A possible increase of NP bioavailability in the aqueous phase could be a more important parameter for NP removal than the ones related to GF addition as already stated before. The sludge dilution to a TS content of 25.3 g/L must have been advantageous for NP biodegradation. For continuous anaerobic digesters high removals have already been observed in literature but NP concentrations were lower than the one used which makes comparisons questionable. For instance, Samaras et al. (2014) showed 33 ± 67 % NP removal under mesophilic condition with a sludge retention time (SRT) of 20 days (NP: 74 µg/L; TS: 19 g/L), the high STD coming from negative removals on certain days. Moreover, Paterakis et al. (2012) observed 100 % NP removal from mixed sludge (TS content: 38.5 g/L; SRT: 35 d; NP: 9 µg/L). The initial NP loads of the first and second citation, however, represent only 6 and 1 % of the initial NP concentration that was used in this experiment. Continuous experiments with a hydraulic retention time of 20 days that were run with sludge of higher TS content (35 g/L) coming from the same WWTP in 2008 showed far less NP removal (25 % for the sum of NP, NP1EO and NP2EO) thus also pointing to the beneficial effect of sludge dilution to NP biodegradation (Patureau et al., 2008).

1.4 NP concentrations in heat treated reactors

The theoretical concentration of spiked NP in heat treated sludge (chapter II, table 3) ranged in between 1135-1150 µg/L. Unexpectedly, the detected final concentrations of NP for heat treated sludge exceed the theoretical concentrations for five digesters meaning that more NP was present from the beginning of digestion than calculated theoretically. Since NP1EO and NP2EO concentrations were lower than the detection limit in start and final sludge samples, a

transformation of these to NP can be excluded. NP sorption onto GF in heat treated sludge was few and, therefore, is not considered. Generally, final concentrations of NP in non-heat treated sludge are lower than for heat treated sludge (compare Figure 3 and Figure 4) meaning that there is less NP removal after heat treatment. Overall tendencies cannot be found since already the control digesters show high variations between each other (765 µg/L and 1199 µg/L).

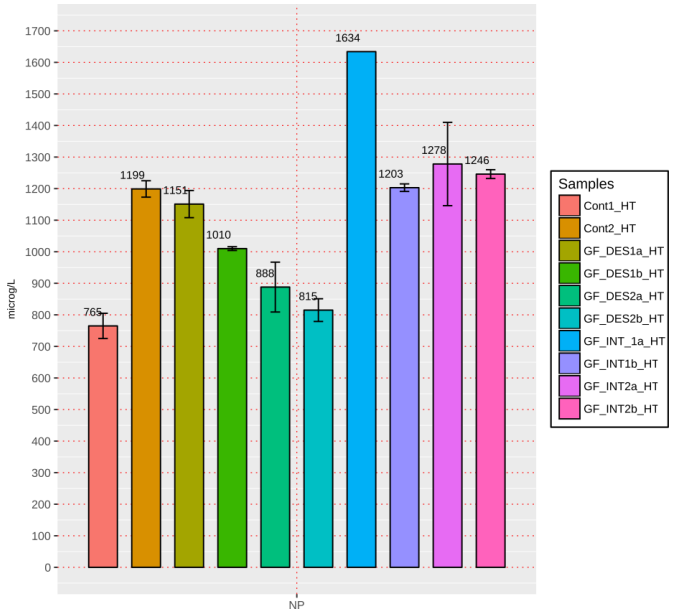

Figure 4: Final NP concentrations in heat treated sludge after anaerobic digestion.
Controls without graphite felt addition (Cont1_HT, Cont2_HT) and digesters with the addition of powdered graphite felt (duplicate reactors of GF_DES1_HT and GF_DES2_HT) of 1 m^2 or 2 m^2 surface area as well as intact graphite felt (duplicate reactors of GF_INT1_HT and GF_INT2_HT).

1.5 PAH concentrations in non-heat treated reactors

Figure 5 depicts the final concentrations of the 12 PAHs after AD with and without the addition of destroyed and intact GF. The results shown in Figure 5 take into account the amount of each PAH in µg/L that was sorbed to GF. This amount was calculated as described in section 1.2 and listed in Table 2. Final PAH concentrations range in between 20.7 and 57.3 µg/L. The average of theoretical initial concentrations by spiking is 63.6 ± 1.1. Even though removals cannot be given due to the fact that exact initial PAH concentrations are not known (see chapter II, section 1), the initial concentrations must be close to this value. For all 12 PAHs except Flu and Pyr the reactor GF_INT2 displays lowest final concentrations suggesting that the addition of intact GF of 2 m^2 SSA favours PAH removal from sewage sludge. The same reactors produced the highest quantity

of methane (section 1.1) pointing to cometabolic removal as it was suggested for the same batch experiments with intact GF of the same SSA in chapter III. A further increase of the surface area by destroying GF showed significant differences of final PAH concentrations compared to control digesters for LMW PAHs Flu, Phe, Ant, Pyr and Chry. For DBahA and BkF, the fact that GF was destroyed had a negative impact on removal since the final concentrations of GF_DES1 and GF_DES2 were higher than for the controls.

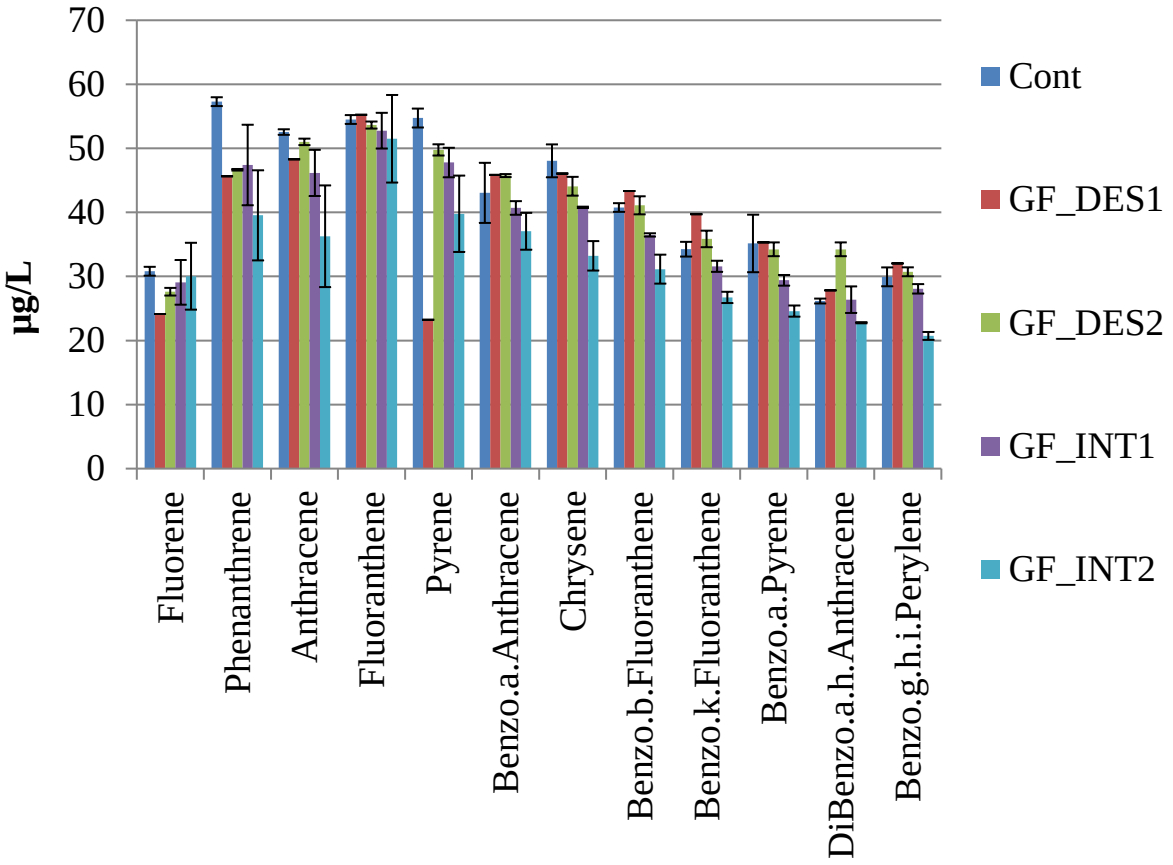

Figure 5: Final PAH concentrations in non-heat treated sludge after anaerobic digestion.
Controls without graphite felt addition (Cont) and digesters with the addition of destroyed graphite felt (GF_DES1 and GF_DES2) as well as intact graphite felt (GF_INT1 and GF_INT2) of 1 m^2 or 2 m^2 surface area.

If cometabolic removal of PAHs during AD lies at the heart of PAH biodegradation, it is important to know why intact GF of a certain SSA enhances methane production. Salvador et al. (2017) used thick multiwall carbon nanotubes (CNTs) for investigating the interaction of methanogens with conductive surfaces of large extent (Salvador et al., 2017). The CNTs had an

average diameter of 9.5 nm (similar to graphite) but show a larger surface area of about 200 m^2/g and higher conductivity. They found that methanogens are in close contact to the CNTs indicating a preference of cell attachment for a possible uptake of gaseous substrates (Cheng et al., 2001). Furthermore, Lin et al. (2017) demonstrated that the addition of 1 g/L of nanographene (5-10 µm) achieved a 25 % higher methane yield in comparison to the addition of 20 g/L of activated charcoal. They suggested that this improvement is either due to the much higher electrical conductivity of graphene or to its smaller microsize with respect to activated charcoal which favors the interaction with biota due to a higher specific surface area. Authors also found that biochars produced at high temperatures (700 °C) had no available C and N substrates, therefore having no effect on soil microbial biomass (Zhang et al., 2014) but that microbial activity increased on the grounds of additional habitat (i.e., surface area) for microbial communities (Pietikainen et al., 2000). Synthetic graphite as used in the experiments of this work did not possess functional groups nor labile C fractions meaning that the material addition could not have boosted carbon metabolism as found for biochars produced from feedstocks at lower temperatures (Steinbeiss et al., 2009).

Three theories could, therefore, explain how microbial activity is enhanced through the close contact to the graphite materials used. The first says that adsorption of cells to the material facilitates nutrient uptake for example the supply of gaseous compounds (Cheng et al., 2001); the second concept stipulates that the adsorption of cells to materials of high SSA supplies additional habitat (Pietikainen et al., 2000), improves biofilm formation (Geeta et al., 1986) and supports the methanogenic microflora (high *Archaea*/*Bacteria* ratio) (Mumme et al., 2014) and the third probable mechanism announces that cell metabolism is boosted through an electron exchange with the conductive material whereby the material has a kind of battery function. Obviously, these theories can be complementary to each other. A fourth option would, therefore, be that the conductivity of the material and factors that are influenced by its surface area play their part in the observed enhancement of microbial metabolism, for instance, enhanced methane production. The beneficial interaction of microbes with GF in the present experiments on account of these explanations was only possible when GF was intact and had a diameter of a certain extent since otherwise it disturbed interaction of syntrophic partners possibly by membrane piercing as discussed in section 1.1. A negative impact of GF_DES1 and GF_DES2 on PAH removal was

only observed for DBahA but it reflects the lower methane yields observed for these reactors. Apparently, destroyed GF could even enhance removals of some LMW PAHs but the reason for this observation is difficult to discern.

1.6 PAH concentrations in heat treated reactors

Figure 6 shows the final concentrations of the 12 PAHs after AD with and without the addition of destroyed and intact GF in heat treated reactors. The amount of PAH sorption to GF listed in Table 2 is included in the final concentrations that are depicted. Final PAH concentrations range in between 47.0 and 111.5 µg/L. The average of theoretical initial concentrations by spiking is 57.1 ± 0.3 µg/L but the exact initial PAH concentrations are not known (see chapter II, section 1) and must be close to 57 µg/L. It seems thus impossible to calculate removals since measured final concentrations are higher than the theoretical value excepted for Flu for all treatments. This higher final concentration could not be explained by the presence of native PAHs because considering the 1.7 dilution of sludge the increase of concentration due to the native PAHs ranges between 0.5 and 10 µg/L. It could be explained by the fact that diluted sludge after heat treatment was difficult to sample homogenously. 500 ml of 800 ml were foreseen for AD whereas 300 ml were kept for further analysis (TS, COD, PAHs). It can be that the 300 ml contained less PAHs due to the sampling of a more aqueous phase with less particulate matter and that the restive 500 ml were concentrated in particulate matter and PAHs, therefore, showing higher final than start concentrations. Further interpretation is, therefore, omitted. On the contrary, the sludge after anaerobic digestion was always very homogeneous.

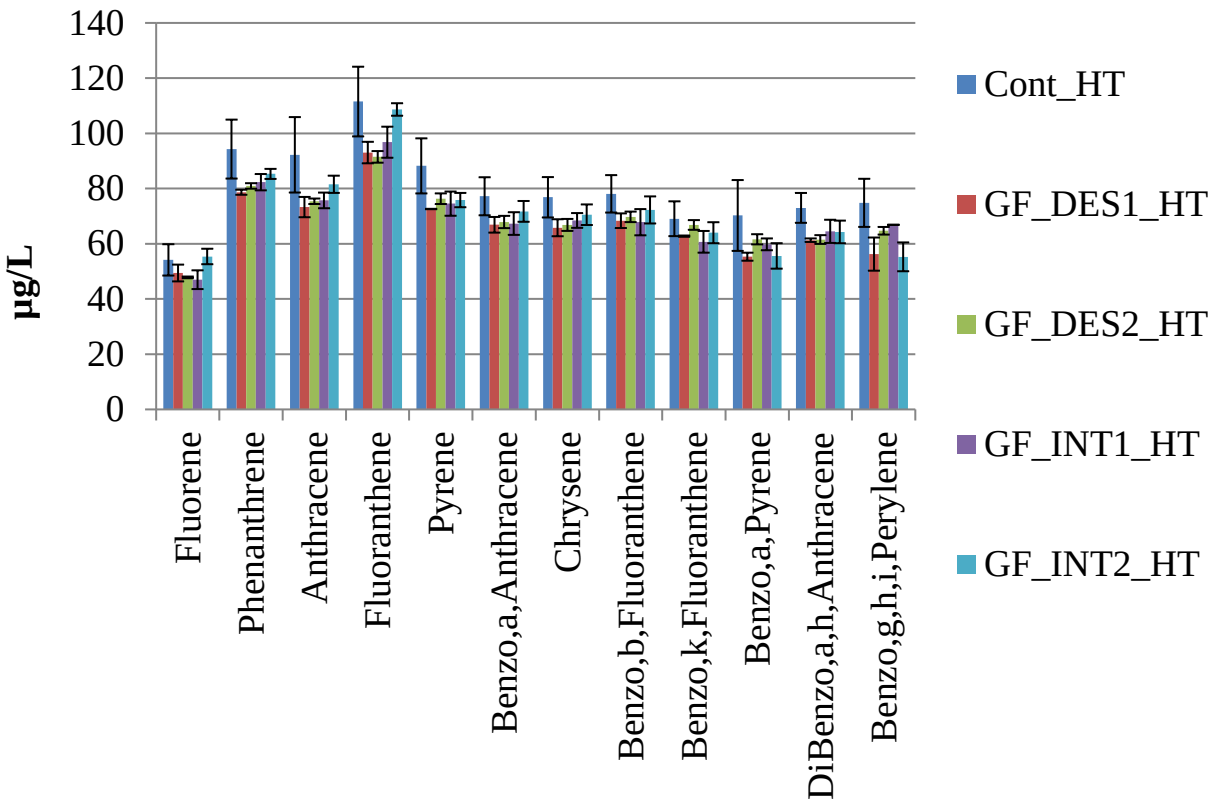

Figure 6: Final PAH concentrations in heat treated sludge after anaerobic digestion.
Control digesters without graphite felt addition (Cont_HT) and digesters with the addition of destroyed graphite felt (GF_DES1_HT and GF_DES2_HT) of 1 m^2 or 2 m^2 surface area as well as intact graphite felt (GF_INT1_HT and GF_INT2_HT).

1.7 Microbial community analysis

1.8.1. Quantification of the microbial community

Heat treatment was originally conducted to eliminate biota but qPCR for the first experiment already demonstrated convincingly that heat treatment at 120 °C eliminated *Archaea* only; and therefore, it rather should be considered as a pretreatment.

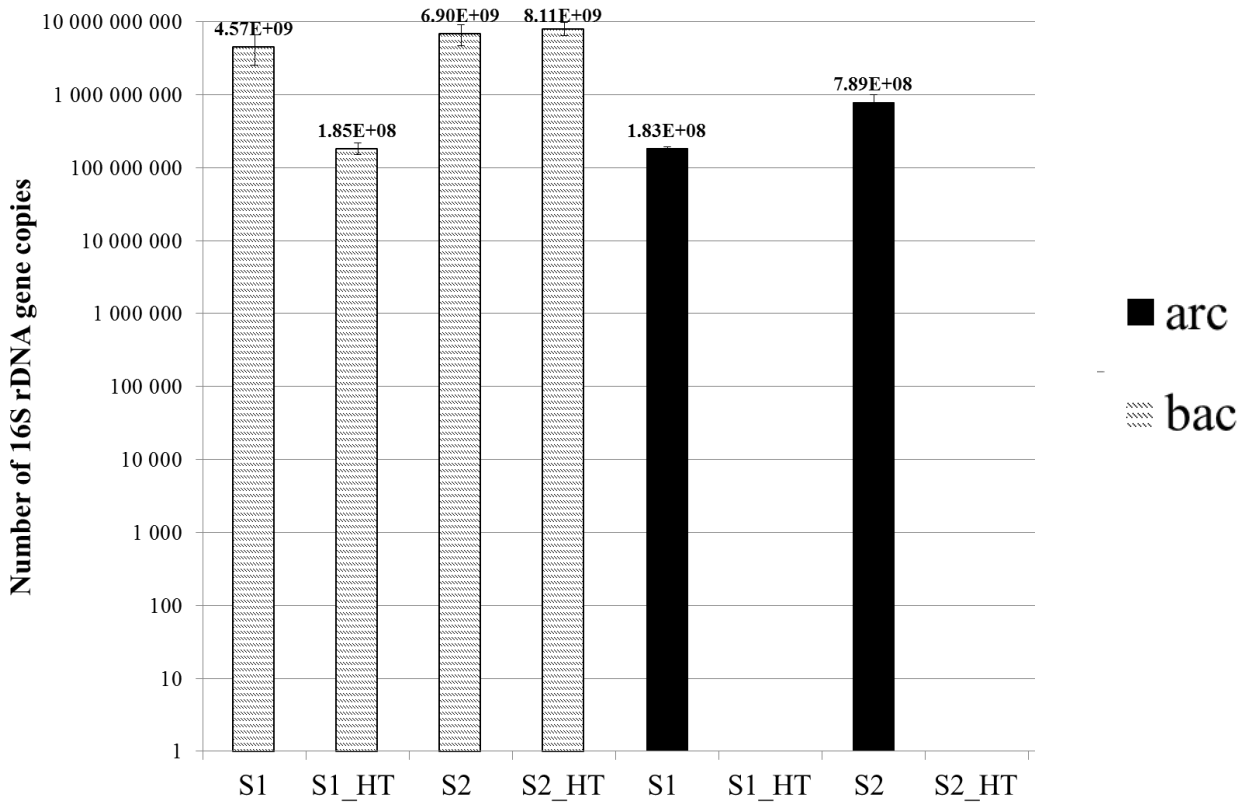

Figure 7: Results of quantitative PCR of four different reactors.
S1/S2: samples without heat treatment; S1_HT/S2_HT: heat treated samples. The numbers of bacterial and archaeal 16S rDNA gene copies are displayed with horizontal lines and diamonds, respectively.

Two representative samples (S1 and S2) are shown in Figure 7 with respect to the number of 16S rDNA gene copies of bacteria and *Archaea* that were found in the heat treated (S1_HT, S2_HT) and non-heat treated reactors after AD. For S1, a tenfold difference in number of bacterial gene copies is noted when reactors had been heat treated. For S2, there is no significant difference between number of bacterial gene copies in heat treated and non-heat treated digesters (S2, S2_HT). On the contrary, the absence of archaeal 16S rDNA gene copies can be observed for S1_HT and S2_HT which means that archaeal DNA was eliminated with 120°C heat treatment for 20 min. Even though the bacterial quantities are similar with and without heat treatment, firstly, the selected biomass is surely different, and secondly, qPCR does not take into account that DNA which is still present in the medium due to cell lysis is inactive with respect to cell metabolism but this DNA without intact cell wall is still replicated during qPCR.

1.8.2. Differences in inoculum composition

In order to compare microbial phylogenetic community structure in different reactors, sequencing was performed at the beginning (inoculum) and at the end of batch experiment. All OTUs which are phylogenetically grouped correspond to 16S rRNA sequences with 3 % similarity.

The sampling of secondary municipal sewage sludge was done in autumns 2014 and 2016, respectively. Even though the inoculum derived from the same WWTP as in the experiments before, the microbial community composition was different. Major *archaeal* species remained the same but some minor species vanished from the microbial community making it less diverse. For instance, the archaeal community of aliquot A on family level (used for experiments that explored GF and its conductivity in chapters III and IV) was composed of 17 % more relative abundance of *Methanocorpusculaceae* and 7 % more *Methanosaetaceae* than aliquot B (grey legend description, Figure 8) beside being richer in unclassified *Archaea*. The lower microbial richness of aliquot B is also reflected in bacterial composition on the phylum level by a decrease of 5-10 % in *Chloroflexi* in comparison to two years before (red legend, Figure 9). Phylum *Bacteroidetes* (in green) is more represented in the inoculum aliquot A as well. The different microbial composition of the inoculum is not astonishing since the biomass can evolve according to seasonal and yearly changes that comprise changing influent concentrations of macro- and micropollutants. The role of minor species in AD is not well documented and it is not clear if they play a significant role in the observed digester performances. The presence or absence of keystone species can, yet, change the global metabolic pathways as shown in fermentation experiments (Rafrafi et al.. 2013). Anaerobic digestion in the present experiment (2017) proceeded with slower kinetics than in 2015 since the stationary phase was reached only after 83 days whereas experiments with sludge that was obtained in 2014 stopped accumulating methane 40 days earlier. This result suggests that sludge characteristics (content in proteins, sugars, lipids) may differ from on sampling in the WWTP to the other being richer or poorer in easily biodegradable organic matter and/or that the microbial community in the sludge was more or less active towards sludge biodegradation and micropollutant removal. On the other hand, Perrotta et al. (2017) found that the initial microbial diversity of the inoculum is not correlated to the reactor's microbial diversity (effective number of species over time) after two days of AD. Their

reactors showed similar microbial diversities even though they employed different inoculum sources pointing to the importance of the substrate. In our experiments, however, municipal sewage sludge was used as inoculum and substrate at the same time. Necessarily, the performances should, therefore, be more dependent on the microbial composition of the sludge itself. For example, it is astonishing that *Methanosaetaceae* are far less present (< 2 %) in the inoculum of aliquot B but emerge from this inoculum (light green, Figure 8, right) whereas they perish in digesters employing aliquot A although this inoculum showed more relative abundance of *Methanosaetaceae (*light green, Figure 8, left).

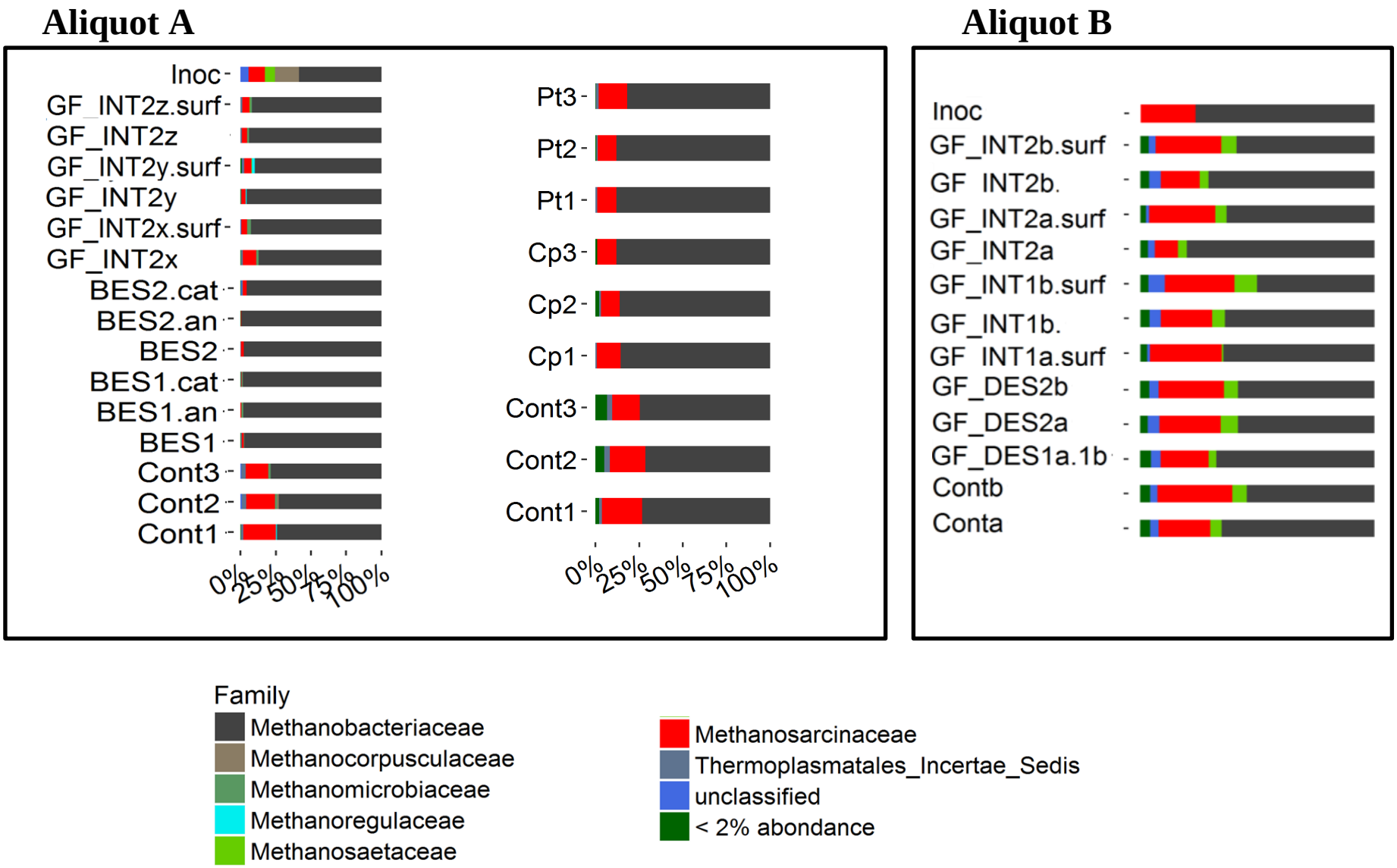

Figure 8: Relative abundances of *Archaea* in sludge according to phylogenetic affiliations on family level.
Sequencing results of 16S rRNA of the inocula of aliquot A and B and sludge after anaerobic digestion with different treatments. Control digesters (Cont); digesters with graphite felt (GF) and assisted by bioelectrochemical system (BES) with GF electrodes. Destroyed and intact graphite felt (GF_DES and GF_INT). Carbon plate (Cp) and platinum (Pt) addition to digesters.

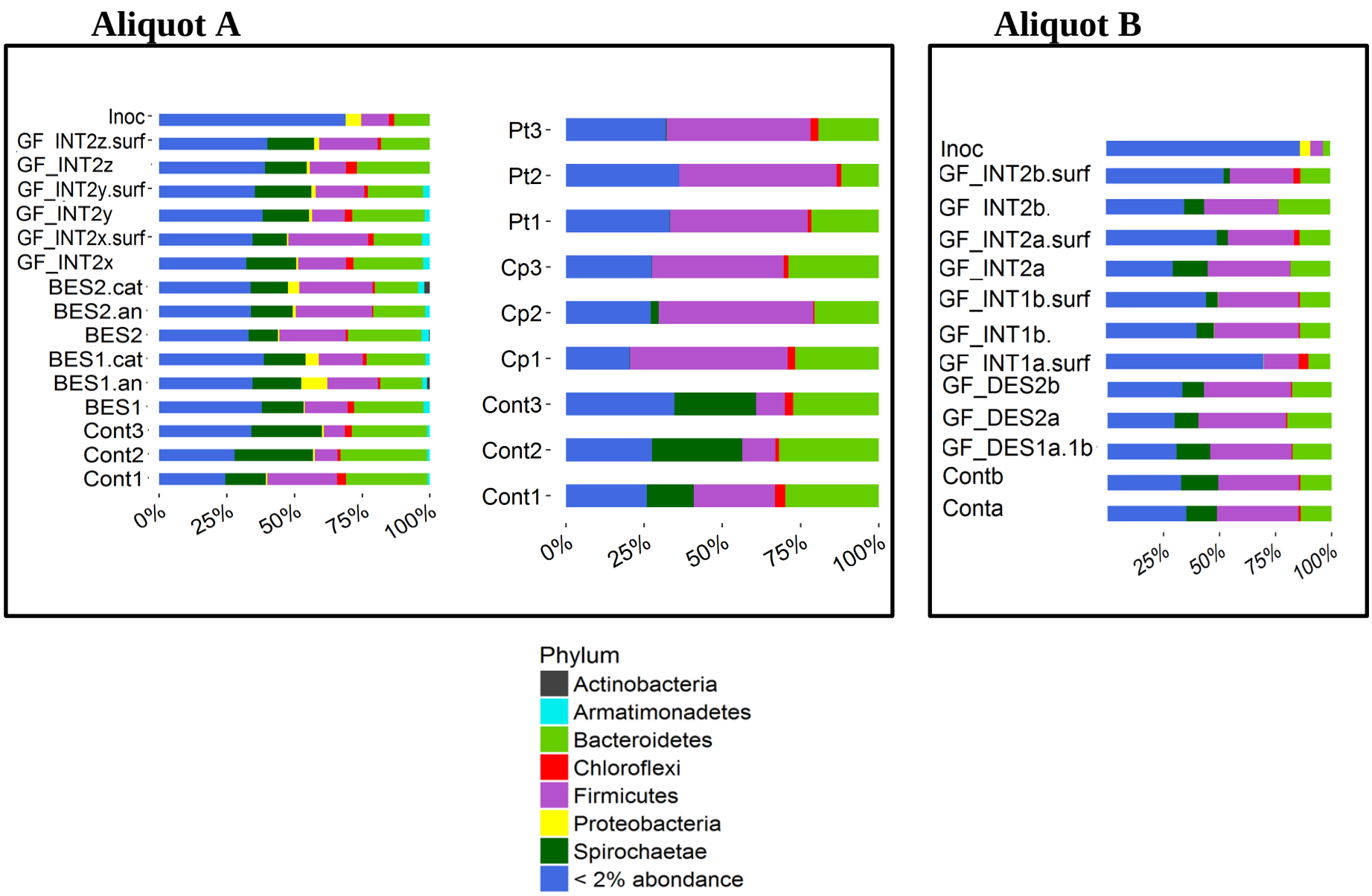

Figure 9: Relative abundances of *Bacteria* in sludge according to phylogenetic affiliations on phylum level.
Sequencing results of 16S rRNA of the inocula of aliquot A and B and sludge after anaerobic digestion with different treatments. Control digesters (Cont); digesters with graphite felt (GF) and assisted by bioelectrochemical system (BES) with GF electrodes. Destroyed and intact graphite felt (GF_DES and GF_INT). Carbon plate (Cp) and platinum (Pt) addition to digesters.

1.8.3. Archaeal and bacterial community composition

Neither the archaeal nor the bacterial community structures distinguish themselves in between control digesters and GF supplemented reactors of different SSA (Figure 8 and Figure 9, aliquot B). One can observe a slight increase of the bacterial phylum *Chloroflexi* in digesters that contained intact GF of different SSAs. Otherwise, there are no significant changes. This means that the macroscopically observed increase in methane production by the addition of intact GF is not based on a significant change in microbial diversity. The quantification of archaeal and bacterial DNA was not performed for this experiment but it could be helpful in order to see if there was an increase in number of *Archaea* within the anaerobic digesters that contained 2 m^2 of GF. Even though relative abundances were equal to other treatments absolute numbers may be different. If this is true, it could explain the higher methane yield in GF_INT2. If qPCR resulted in the same numbers of *Archaea* for all reactors, it may also be that the activity of *Archaea* may have differed between treatments. To explore this possibility, more information about the presence of certain regulatory genes would be necessary for further interpretation. Until then, the hypothesis of (i) biofilm formation on intact GF that enhances methane yield and (ii) stimulation of syntrophic matter degrading Bacteria and *Archaea* by enhanced DIET though conductive graphite layers stand equally beside each other. The fact that GF addition did not correlate with an increase in hydrogenotrophic methanogens (genus *Methanobacterium*) as observed for previous experiments (chapters III and V) can only be explained by the change in inoculum and its diverging composition which was already discussed in section 1.8.2. Notably, *Methanosaeta* (legend in light orange, aliquot B, Figure 10) must have played a more important role in syntrophic relationships during AD than in previous experiments since this archaeal genus was nearly absent in the final sludge from digesters that were inoculated with aliquot A (Figure 10). The differences in microbial community structure of aliquot A and B must have influenced the biodegradation of PAHs and NPs. Since the microbial elucidation of PAH and NP biodegradation in mixed culture studies would need more sophisticated techniques than used in this study in order to identify the microorganisms responsible for the degradation of micropollutants, one should refrain from giving further interpretations on how removals were impacted by biological transformations. For example, the search for functional genes of anaerobic PAH and NP

degradation would permit to build a causal relationship between the presence of bacterial clades and enhanced removals.

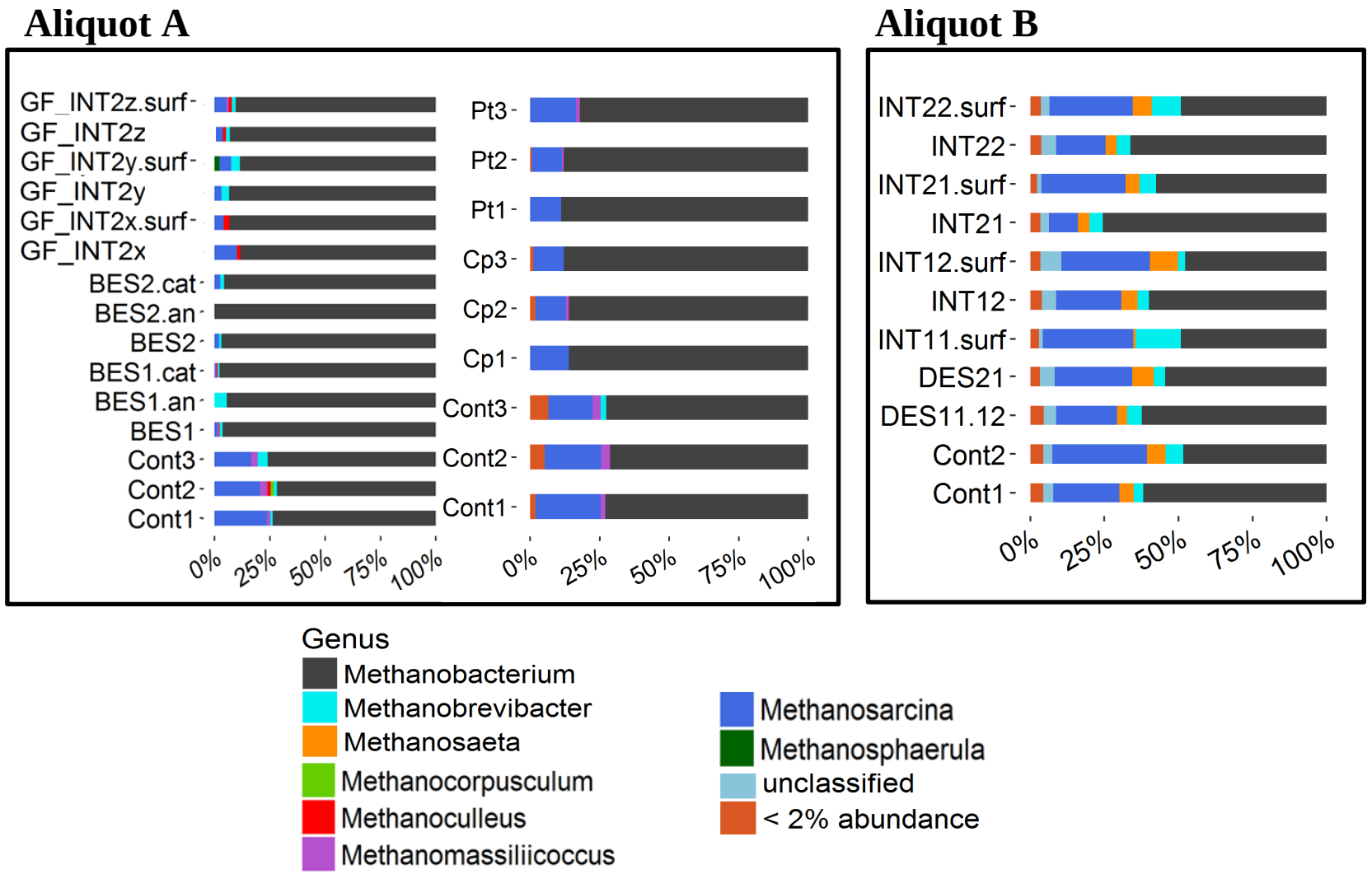

Figure 10: Relative abundances of *Archaea* in sludge according to phylogenetic affiliations on genus level.
Sludge was sampled after anaerobic digestion with different treatments: Control digesters (Con); digesters with graphite felt (GF) and assisted by bioelectrochemical system (BES) with GF electrodes. Destroyed and intact graphite felt (GF_DES and GF_INT). Carbon plate (Cp) and platinum (Pt) addition to digesters.

1.8 Conclusions

Statistical analysis showed significant differences between the methane production of reactors with powdered GF (GF_DES1 and GF_DES2), the control digesters and digesters with intact GF with a surface area of 2 m^2. Adding 2 m^2 of GF to anaerobic digesters resulted in a significant rise of methane yield compared to the control digesters whereas a further augmentation of the SSA by at least a factor of 10 inhibited methane production. Physical destruction of cells by piercing of small sized GF particles through the cell membranes was considered as possible mechanism explaining why methane production was lower in the case of GF_DES1 and GF_DES2 reactors. The fact that intact GF of a SSA of 2 m^2 produced most methane compared to all other reactors could be due to the fact that electroactive species take profit from a conductive material which channels electron from electron donating to electron accepting microorganisms such as known for syntrophic cooperation in between fermenters and methanogens. Hydrogen as the electron shuttling molecule is replaced by the solid conductor that is always present and may permit a close contact between these syntrophic biota by offering an adequate surface for biofilm formation. However, sequencing results did not prove any differences in microbial composition of GF reactors and controls without GF. Even the relative abundances of biota on sludge that was close to the GF surfaces were very similar to the ones found in bulk sludge of all digesters. Therefore, it is more probable that the enhanced methane production in GF_INT2 relies on biofilm formation on GF's surface without the enrichment of electroactive biota. Nevertheless, this biofilm with similar profile as in the bulk sludge must have permitted a less distant, and therefore easier, exchange of fermentation byproducts which were consumed by methanogens such as *Methanosaeta* and *Methanobacterium*. An enrichment of *Methanobacterium* as in previous experiments was not stated.

Heat treated anaerobic digesters exhibited few microbial activity with respect to hydrogen production (3 Nml/g COD except for the control with 8 Nml/g COD) but produced up to 6 and 10 g/L total amount of VFAs in GF_INT1 and GF_INT2. The other reactors' VFA production stayed below 4.5 g/L. The percentage distribution of VFAs is similar for all digesters and corresponded to a mixed acid type fermentation with mostly acetate (about 50 %) as main metabolite and 15-20 % butyrate after 14 days of fermentation. The heat pretreatment, therefore,

must have selected spore forming bacteria that are capable of hydrogen production such as *Clostridia*. Yet, sequencing was not done for these heat treated reactors.

The extent of PAH and NP sorption on GF was few in heat treated reactors but attained 20.3 to 37.4 % in non-heat treated reactors for Flu, Flt, DBahA and NP. Possibly, GF exhibits better adsorption for these molecules due to their specific configuration and intact GF's pore structure.

Final concentrations of 9 out of 12 PAHs at the end of AD were lowest when intact GF of 2 m^2 SSA was added to digesters suggesting that there was a beneficial effect of the material with respect to removal of these compounds. The underlying mechanisms are not clear at all. They could be related to the formation of a specific biofilm on the surface of GF_INT2 that permits better PAH degradation (whether cometabolic or not) but could be also due to the joint action of this biofilm and the conductivity of GF. In conclusion, the surface area of GF was found to be an important parameter for the removal of both, COD and contaminants. In order to decide on the question if it is the surface area only that influences methane production and PAH removal by giving biota the possibility to build close relationships or if these performances are due to the conjoint action of surface characteristics and the conductivity of GF, one could imagine experiments with non-conductive polyester and conductive GF under the constraint that both materials should exhibit the same surface characteristics in terms of porosity and the absence of surface functional groups for equal adsorption of cells, micropollutants and other organic matter.

Given the absence of data for initial PAH and NP concentrations, it would be interesting to analyse the final concentrations of the particulate phases of all digesters as was done for Cp and Pt addition to anaerobic digesters. These particulate phases have not been extracted by ASE, yet, and could give evidence on why removal of all 12 PAHs was improved in GF_INT2. It is assumed that the aqueous particulate partition is different for this condition compared to all other digesters as already demonstrate for GF, Pt and Cp addition in previous chapters.

The results for NP removal, moreover, conclusively demonstrated that sludge dilution influences the removal of NP to a great extent and that the bioavailability of the compound is not limiting anymore in these conditions. Assumedly, NP equilibrium between particulate and aqueous phase was shifted, therefore rendering NP available for biodegradation.

The difference in sludge inocula for the experiments of chapters III and chapter VI and the fact that their final microbial community structures for GF_INT2 turned out to be very different indicated strongly that the sludge characteristics of the inoculum as well as its related microbial community change significantly from year to year thereby impacting the performances of micropollutant biodegradation as shown for NP and PAHs.

Chapter VII: Conclusions

Sewage sludge as a mixture of microorganisms, lipids, proteins and carbohydrates is a complex material for experimentation. Adding to this complexity of the raw material, the mechanisms of PAH and NP biodegradation during anaerobic digestion are not well understood. Especially for HMW PAHs they remain unknown to the present day. The fact that PAHs are present in concentrations below several micrograms per litre within sludge allows manifold interactions with other inorganic and organic molecules as well as microorganisms to take place. In order to extract and detect PAHs and NP in sewage sludge it needs repeatable techniques and sensitive analytical equipment. The micropollutant removals that result from the treatment include possible abiotic reactions that happened during AD such as hydrophobic pollutant sorption to glassware or added conductive materials, their volatilization during biogas production and their sequestration within the transformed and aging matter. All of these factors complicate the interpretation of results.

The main objective of this thesis was to elucidate the mechanisms at work when PAH and NP spiked sludge is exposed to conductive materials and poised electrodes. Heat treatment was primarily chosen in order to quantify the micropollutant removal that is due to abiotic phenomenon like sorption to glassware and conductive materials like graphite felt (GF) by eliminating biodegradation of the compounds. Sequencing and qPCR were chosen in order to detect changes in the microbiological community structure for non-heat treated reactors.

Total solids (TS) and volatile solids (VS) removals were enhanced by about 18% in the GF reactors with or without the application of an electric potential (BES and GF) in comparison to the control digesters (Cont) and proved that GF acted positively on dry matter removal. GF reactors also removed 21-33 % more BaA, BkF and Ind than control digesters. NP removal performances were indistinguishable between the different operating conditions. Sludge dilution was assumed to be the reason of the high removals that attained 97 % for BESs and the controls. NP degrading bacteria may have attacked NP more easily due to its relocation to the aqueous phase by diluting sludge from 59 g/L to 23 g/L.

Moreover, it was found that bacteria were still active and present in the heat treated reactors. On the contrary, Archaea were eliminated by the heat treatment. TS and PAH removal was much lower than in non-heat treated reactors suggesting few microbial activity of the remaining spore forming bacteria. Sorption of PAHs and NP to glassware and GF as well as volatilization during AD was judged negligible on the same grounds. Yet, the high removal in MECs with heat treated sludge put into question if electrochemical PAH degradation played an important role in the overall PAH removal that was observed. Sequencing result could prove that the family *Peptococcaceae* was enriched in this reactor with up to 42 % absolute abundance of an OTU closely related to *Desulfitobacterium.* This suggested that the voltage application selectively enriched this electroactive genus. Therefore, biodegradation of PAHs in heat treated reactors in which the working electrode was poised at 0.8 V (vs. SHE) is an alternative answer to the high removals that were observed.

Microbiological evidence based on sequencing results revealed that both, the non-heat treated sludge to which GF was added and in which poised electrodes supplied an electric current showed different microbial community structure than the sludge of control digester. GF and BES digesters were similarly enriched in the genus *Methanobacterium,* a hydrogenotrophic methanogen whose growth could have been favoured on account of direct interspecies electron transfer (DIET) with electroactive species and hydrogen production at the cathode. Its absolute abundance was up to five times higher than in the control digesters. Therefore, it was concluded that GF alone and jointly with polarized electrodes shifted, both, archaeal community composition as well as metabolic pathways. OTU 59 with 99 % sequence similarity to *G. metallireducens* was found with up to 100 fold higher relative abundances in GF biofilms of BES digesters than in sludge of the other digesters proving the enrichment of electroactive microbes by the poising of working electrodes at 0.8 V (vs SHE).

On the contrary, GF addition to non-heat treated digesters alone did not enrich sludge in electroactive microorganisms. Apparently, different microbial communities degrade PAHs in the two conditions and therefore, it is probable that the removal of PAHs due to

conductive material relies on a different mechanism than the PAH removal that is observed with an electricity input to sludge. The absence of known electroactive microbes in GF rather suggests that either a much larger spectrum of biota are able to transfer electrons via conductive materials than expected before (more and more methanogens are found to be electroactive) or that the observed PAH removals are more dependent on the biofilm formation on material surfaces, in general, (conductive or not) without using these as electron acceptors or donors. For electricity input to heat treated sludge, it cannot be decided if the high removal that was observed is rather due to the dislocation of sludge organic matter meaning that PAHs were well removed due to purely electrochemical treatment of available PAHs or if the high removals are rather due to the observed enrichment of electroactive bacteria within the spore formers that prevailed in the heat treated sludge or the action of both

Further experiments focused on the addition of conductive materials to AD since GF showed same removal performances with and without current. Adding to that, conductive carbon materials were found to favour DIET without the need of bioelectrochemical systems (Xu et al., 2016) and their use led to an increase of methane production in anaerobic reactors (Zhao et al., 2015). Yet, the 1000 fold more conductive platinum (Pt) did not remove PAH and TS better than carbon plate (Cp), a material that is 99.9 % composed of graphite. The addition of Cp and Pt to anaerobic digesters resulted in 12 to 14 times better removal of Flu as well as 7 to 11 times higher removal of Phe from sewage sludge compared to the control digester even though macroscopic differences in terms of methane production and TS/VS removals in control and material reactors were not observed. Convincingly, both material additions led to an increase of relative abundance of hydrogenotrophic methanogens as observed for GF addition to AD. Carbon plate removed three rings PAHs Flu and Phe to a higher degree than the removals observed for GF but could not remove HMW PAHs in the same extent. Therefore, further experiments were conducted with GF by exploring the role of its SSA regarding PAH removal.

The bias that was due to the use of only one start sample in previous experiments was avoided by preparing 20 reactors with start sludge individually. Unfortunately, the dilution

that was chosen for all experiments turned out to be a disadvantage for sludge homogeneity and the TS contents of start sludge could not be taken as reference values due to the non-homogeneous sampling of sludge that, therefore, exhibited variable TS content. Therefore, final TS and COD values were interpreted by themselves. A major outcome of this last experiment was the observed methane inhibition by a high amount of destroyed GF (powdered) whereas the increase of an intact SSA to 2 m^2 showed highest methane production. Sludge reactors that produced most methane also showed lowest final concentrations of 10 PAHs compared to control digesters and all other digesters with destroyed and intact GF. NP final concentrations were similar to each other independently of GF addition to digesters and these results confirmed that sludge dilution had a major impact on NP biodegradation. The underlying mechanisms are not well explored in literature, yet. Some authors explain the inhibition of methane production with nanographene by the piercing of cell membranes which, as a consequence, lose their cell integrity and activity. On the other hand, the microbial community must have been stimulated by the presence of intact GF (with the right size). It may have either acted like a rechargeable battery, thereby passing electrons through the conducting graphite layers from electron donating to electron accepting biota or it may have served as an additional habitat for microorganisms that use it for biofilm formation, thereby, building close relationships between syntrophic partners for faster nutrient and electron exchange. The enhanced PAH biodegradation by GF addition of 2 m^2 SSA also confirmed the previous experiments. However, sequencing results of this experiment demonstrated that all sludge samples had similar composition. Therefore, it is probable that the enhanced methane production in intact GF reactors with 2 m^2 SSA relies on biofilm formation on GF's surface without the enrichment of electroactive biota but with an easier exchange of fermentation byproducts which were consumed by methanogens such as *Methanosaeta* and *Methanobacterium*. The indistinguishable microbiology with and without GF could be also explained by the difference in inocula used for the different experiments since aliquot A was richer in *Methanocorpusculaceae*, *Methanosaetaceae* and unclassified Archaea.

Even though there are many open questions to how conductive materials and BESs enhance PAH removal, the results of this work demonstrate consistently their potential to reduce PAH concentrations in sewage sludge and reducing, thus, their discharge to the environment. The following chapter presents experimental ways how to obtain a deeper insight in some of the aspects that could not be further elucidated in the framework of this thesis.

Chapter VIII: Perspectives

Some perspectives can be given for this new and challenging research topic. These perspectives are presented with respect to an applied and a more fundamental approach.

1 Applied research opportunities for PAH removal during anaerobic digestion

Cometabolism of PAHs during anaerobic digestion has been confirmed in chapters V and VI of this work. Based on the hypothesis that the more organic matter is degraded the more PAHs are biodegraded, one could aim at maximizing methane production from organic matter destruction, first, and investigate PAH removal only in the aftermath. This applied approach would gain time since PAH extraction and quantification would be omitted in the cases that methane production is the same or less than in the control digesters.

Methane production could be increased in different ways by the use of conductive materials within or outside of bioelectrolyzers. One could use other conductive materials as have been used in the underlying study or one could use materials that have a higher porosity such as activated carbon. The use of conductive granules could be envisaged in order to have a better relation of material surface to reactor size. The increase of surface would be favorable for electrode surfaces within a sludge bioelectrolyzer, as well. Another possibility to achieve an increase in methane production is the right choice of the potential. In this

study, only one potential was tested but different potentials could permit the creation of a more efficient biofilm for methane production on the electrode surface with different synthrophic interactions as suggested in this work.

Since the SSA of GF changes when it is added as piece or powder, further experiments that investigate influence of the SSA on PAH removal during anaerobic digestion should use materials for which the SSA has been measured via nitrogen adsorption. The geometric surface area reported in bioelectrochemical experiments often does not correspond to the real surface area that is available for electrochemical reactions (Doña Rodríguez et al., 2000). In the present work, the SSA of intact GF was known based on the supplier's information. However, the SSA of GF that was crushed to fine powder in the laboratory had to be estimated roughly. The measurement of SSAs can vary depending on the technique that is used (the type of adsorption gas, the adsorption model used to calculate the surface area in square meters per gram of material). Therefore, when ordering the material, the supplier's indications on how the SSA was measured should be taken into account in order to enable the comparison between performances.

In this study, heat treatment was proposed to reduce biotic removal of micropollutants and draw conclusions about PAH abiotic losses like sorption to GF, electrochemical transformation. It turned out that it is not an optimal technique since, firstly, PAHs especially LMW ones can be volatilized to more than 50 % during the heat treatment; secondly, the sludge organic matter is changed by the treatment; and thirdly, the heat treated sludge shows the same quantity of bacterial DNA than non-heat treated sludge. PAHs and NP were found to sorb on heat treated and non-heat treated sludge even though PAHs and NP sorbed less on disintegrated heat treated sludge and dead archaeal cell mass. Overall, the heat treatment did not take up to its role as a technique to quantify the possible extent of sorption. Alternative sterilization agents such as propylene oxide, methyl bromide or sodium azide have their own disadvantages, more or less changing organic/inorganic matrices characteristics. For example, all treatments were shown to change soil pH by transfer of organic acids to the aqueous phase and NaN_3 inhibits enzymes without complete sterilization (Skipper and Westermann, 1973). Adding to the reported shortcomings, many

of these chemicals are also toxic for humans and experimentations should rather avoid environmental unfriendly and carcinogenic chemicals. Other solution for sludge sterilization is the use of ionizing radiation, tyndallization, steam sterilization and deep freezing (Spakovská et al., 2014) that should be tested for sludge and compared with each other in order to find a solution for an optimal PAH sorption control. In all cases, the micropollutant spiking of sludge should be conducted after the pretreatment.

In order to speak of changes in absolute microbial abundances qPCR should be done routinely to judge if a change in the relative abundances of biota observed is actually due to an absolute change in their number. qPCR was not done for all experiments but it would allow differentiating between digesters of different performances that nevertheless exhibit the same relative abundances of microorganisms by verifying an increase in absolute number of certain species, thereby, building evidence for changes also on a microbiological level. qPCR would also permit to decide if methane production was favoured by biofilm formation on GF based on an increase in bacterial or archaeal number of major genera or if this was rather related to the presence of electroactive species.

The exact role of different carbon materials for methane increase is not clear. It is possible that different carbon materials enhance CH_4 production differently. The role of functional groups, the aromaticity of the material and its pore structure as well as surface area seem to play a role. For example, it was shown that doping reactions occur on the surface of aromatic materials such as biochar (Snook et al., 2011) and activated carbon (Cayuela et al., 2013). Therefore, the use of biochar for PAH removal in experiments should be avoided if these experiments were designed to explore the impact of conductive materials on PAH removal. Biochar has a huge potential as PAH sorbent but mechanisms are not well known. It is discussed controversially if PAHs sorb to functional groups at the surface of biochar only or if they can also be degraded at the surface by biota which exchange electrons with the material due to oxidation or reductions of functional groups at its surface. This is a research topic on its own and, therefore, progress in the understanding of PAH removal via conductors is helped for if experiments use plane graphite without modified surfaces.

The proof of a concept would also allow to extend the experimental approach on other contaminants than PAHs and NP. The removal of micropollutants with the help of conductive materials or MECs can be applied to other persistent pollutants that are present in the sludge treatment line such as polychlorinated biphenyls (PCBs) (Patureau and Trably, 2006), antibiotics such as ciprofloxacin (CIP) (Martín et al., 2015) and other hardly degradable pharmaceuticals or personal care products (Carballa et al., 2007). In the case of organohalogens, the cathode of a BES already functioned as a direct electron donor for the mediator-less microbial reductive dechlorination of trichloroethene(TCE) to ethene (Aulenta et al., 2010) proving that microbial mediated micropollutant oxidation as well as reduction are feasible inside BESs. It was also shown that microbial reductive dechlorination of TCE accelerates with the addition of conductive magnetite based on interspecies electron transfer (Aulenta et al., 2013) and that it steered the composition of anaerobic TCE dechlorinating cultures (Aulenta et al., 2014). Recently, the biodegradation of CIP was reported to accelerate during anaerobic digestion by the addition of nano-magnetite pointing to further research opportunities (Yang et al., 2017). It seems that the lack of terminal electron acceptors or donors is circumvented by both technologies, the employment of conductive materials as well as BES.

2 Fundamental insight in PAH removal in bioelectrolyzers during anaerobic digestion

The complex interpretation of the experimental work and results obtained in this thesis point to the need of reducing experimental parameters. In order to understand the mechanisms of PAH elimination inside a bioelectrolyzer and with conductive materials it is important to simplify the experimental setup. The composition of the sludge is complex and should be simplified. The same, the large number of microbial species that can degrade different compounds of the sludge according to different metabolic pathways should be simplified as well.

This can be achieved by either

(i) controlling the interactions between organic matter, PAHs and the conductive material or

(ii) controlling the microbial community composition

Very high PAH removals have been detected for the heat treated sludge with GF and an applied potential to GF electrodes. The heat treatment supposedly simplified the microbial community of the digesters by eliminating Archaea and non-spore forming bacterial species. Spore forming *Clostridium* species were selected, in particular, together with the presence of *Desulfitobacterium*, an electroactive genus. The application of a current could have led to the enrichment of these bacterial species that are able of synthrophic interactions with electroactives or electroactive themselves. A scheme of the simplified system is given in the following:

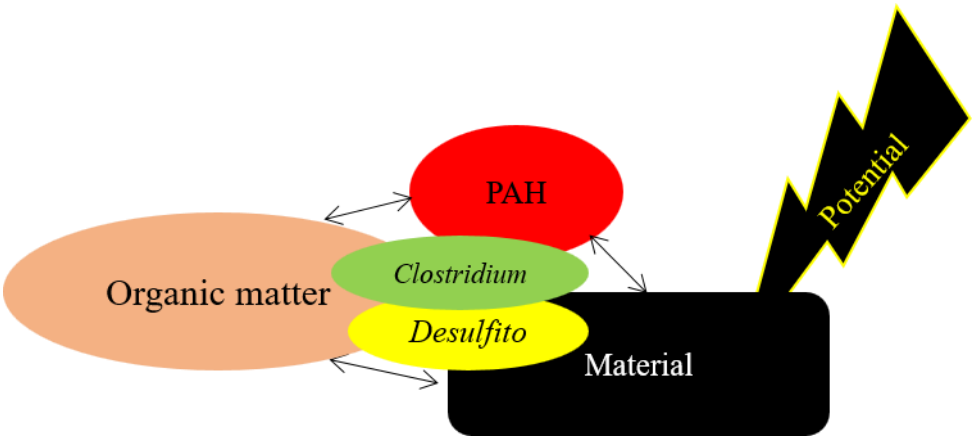

Figure 1: Scheme of interactions between organic matter, polycyclic aromatic hydrocarbons and the conductive material to which a potential is applied.
Previous experiments enriched Clostridium and Desulfitobacterium. They can be specifically added in a simplified system for elucidating the mechanisms of PAH removal from sewage sludge.

There are at least three kinds of interactions that are represented with black arrows: PAHs can interact with both, the organic matter and with the conductive material. Thirdly, the conductive material can interact with the organic matter. Lastly, interactions with the material are always influenced by the application of the chosen potential.

Furthermore, the heat treatment supposedly decomplexified macromolecules and solubilized them which led to an aqueous phase that was richer in organic molecules being accessible for microorganisms.

Based on the high removal performances in these conditions and the fact that a simplified system allows for more fundamental insight in the mechanisms of PAH removal at work, we propose to continue working with the experimental setup shown in the figure below.

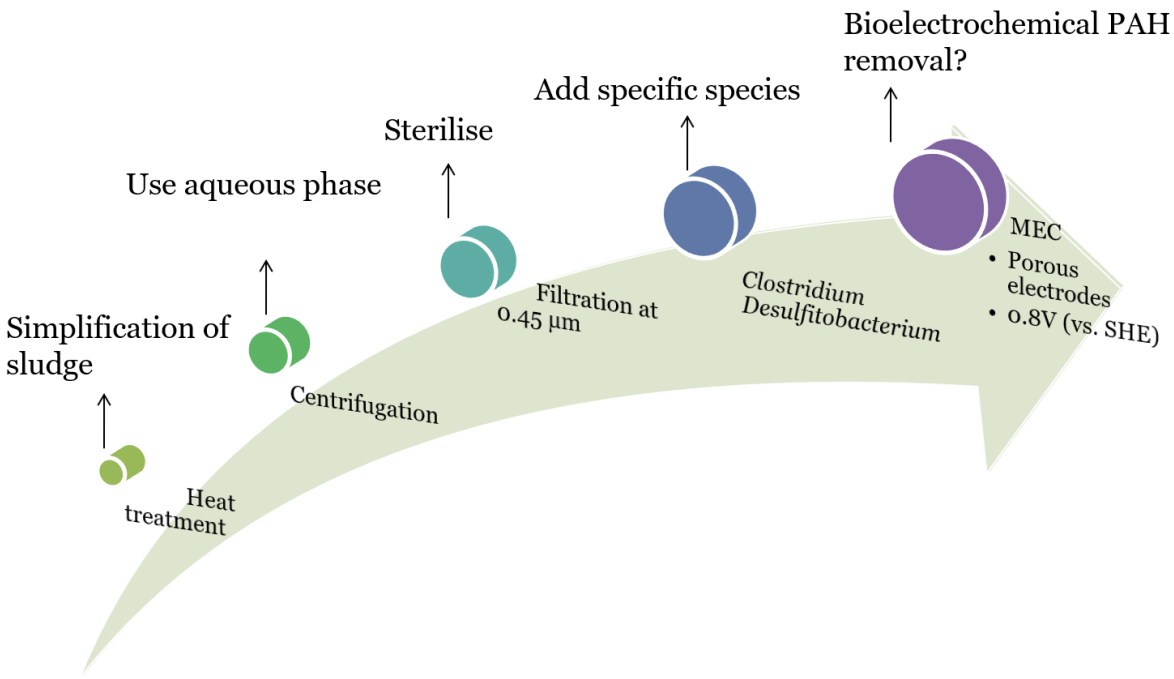

Figure 2: Simplified experimental setup.

In this experiment, we suggest solubilizing sludge organic matter by heat treatment in the autoclave. A sequential centrifugation step separates the aqueous phase from the particulate phase. Only the aqueous phase should be used for the experiment since this simplifies the substrate (but keeping its real composition) in terms of kind and accessibility of molecules to microorganisms (claiming that only solubilized molecules are bioavailable to microorganisms). The amount of solubilized organic matter should be sufficient for the nutrition of microorganisms and could also serve as co-substrate for these with respect to

PAH biodegradation. The aqueous phase should, then, be sterilized by filtration (0.45 µm). Even though some biota could still be present after filtration at this filter size, a smaller size would eliminate colloids that should be kept in order to keep the sludge characteristics. The two genera that had been enriched in the heat treated digesters before should be specifically added to the anaerobic digesters. These are *Clostridium* and *Desulfitobacterium*. The presence of the two could have permitted syntrophic cooperation due to the application of a potential of 0.8V vs SHE. Therefore, the same potential should be tested in a bioelectrolyzer with porous electrodes as done before. This experimental setup will allow to gain fundamental knowledge about the removal pathways and mechanisms of PAH elimination (electrochemical, biological, bioelectrochemical). It is a prerequisite in order to engineer a controlled PAH removal in the sewage treatment line.

Additional techniques can be used to back up the results in the simplified system. For example, SIP can be used to verify if carbon from ^{13}C PAHs is assimilated by microbes. Together with a targeted search for specific genes by qPCR, this procedure could help confirm anaerobic PAH degradation by the species that are enriched in the reactors. Sun and Cupples (2012), for instance, targeted the functional gene for anaerobic toluene degradation (benzylsuccinate synthase) along with SIP with the aim not only to correlate but also build a causal relationship between the presence of bacterial clades and an enhanced removal of toluene. Furthermore, metatranscriptomic analysis of mRNA can be used to identify genes that are expressed during anaerobic digestion. Enzymes that are known to play a role in aromatics' degradation should be targeted specifically. The abundances of key genes that are present during PAH degradation should be quantified in order to confirm the implication of certain microbes in anaerobic PAH biodegradation. In this way, Yan et al. (2017) proved that microbial electrochemistry could enhance anaerobic BaP degradation since they found functional genes involved in the degradation pathway of benzoyl-CoA enriched in sediments after treatments within a MFC. The affiliation of these functional genes to a certain species or even strain can be retraced.

Supplementary Information

List of figures

List of tables

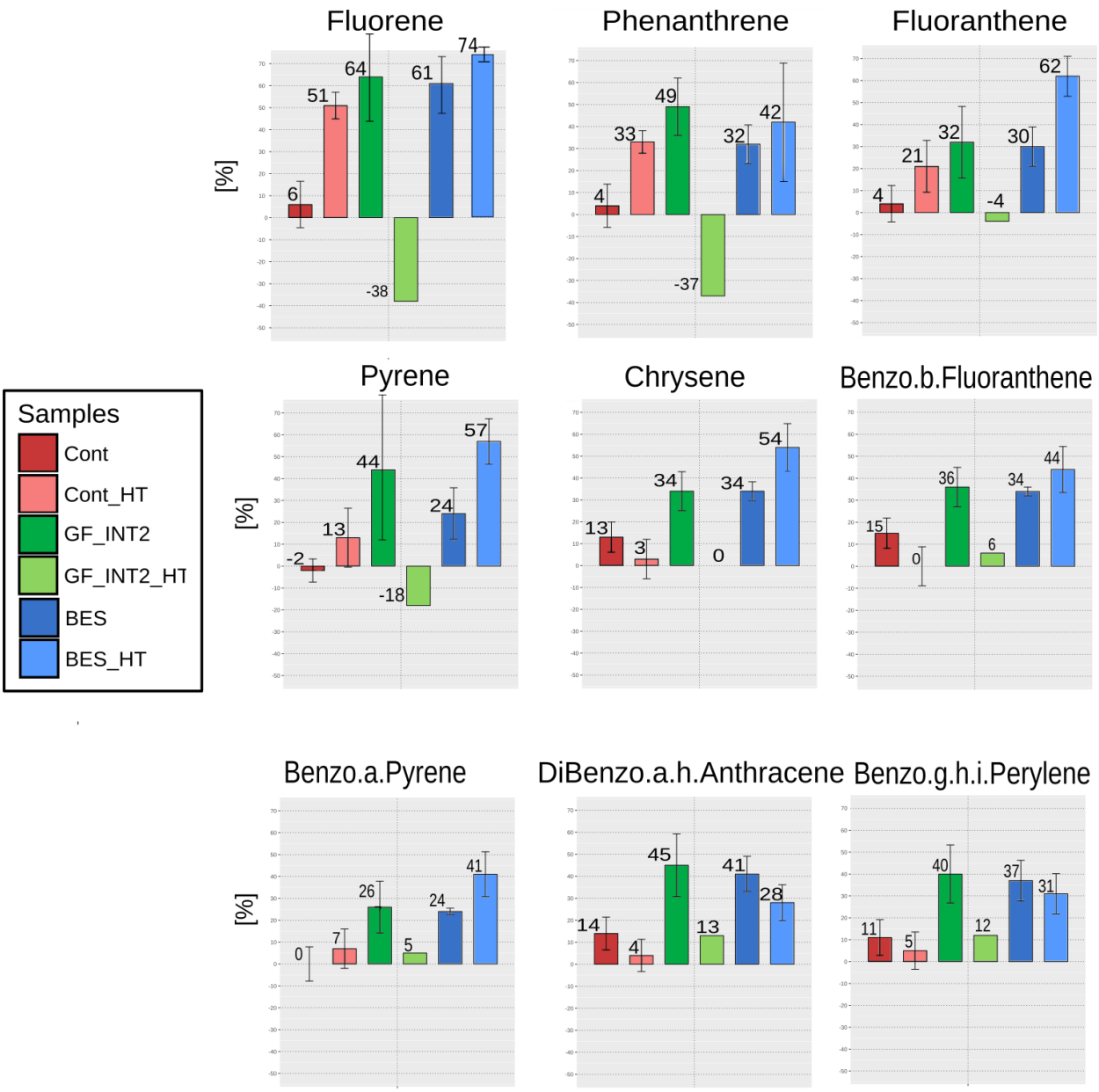

Figure 1: Total removal of PAHs in anaerobic sludge.
Error bars represent standard deviations (STDs) of 12 or 18 measured values for duplicate or triplicate reactors respectively. (Cont=anaerobic control digester; GF_INT2= graphite felt digester with specific surface area of 2 m^2; BES= bioelectrochemical digester). Two outliers are observed in AD_HT and GF_INT2_HT sample for fluorene and phenanthrene.

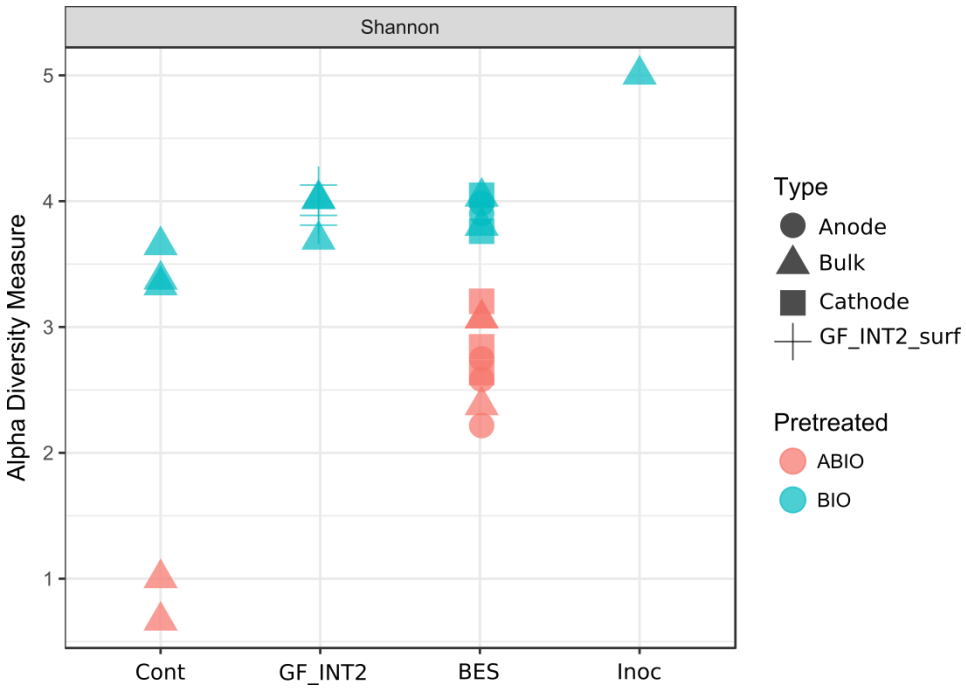

Figure 2: Shannon index of bacteria in non-heat and heat treated reactors.
Specific diversity measure of bulk sludge as well as anodic, cathodic and GF biofilm communities. Cont=anaerobic control digester; GF_INT2= graphite felt digester with specific surface area of 2 m^2; BES= bioelectrochemical digester; Inoc= inoculum. GF_INT2_HT was not sequenced.

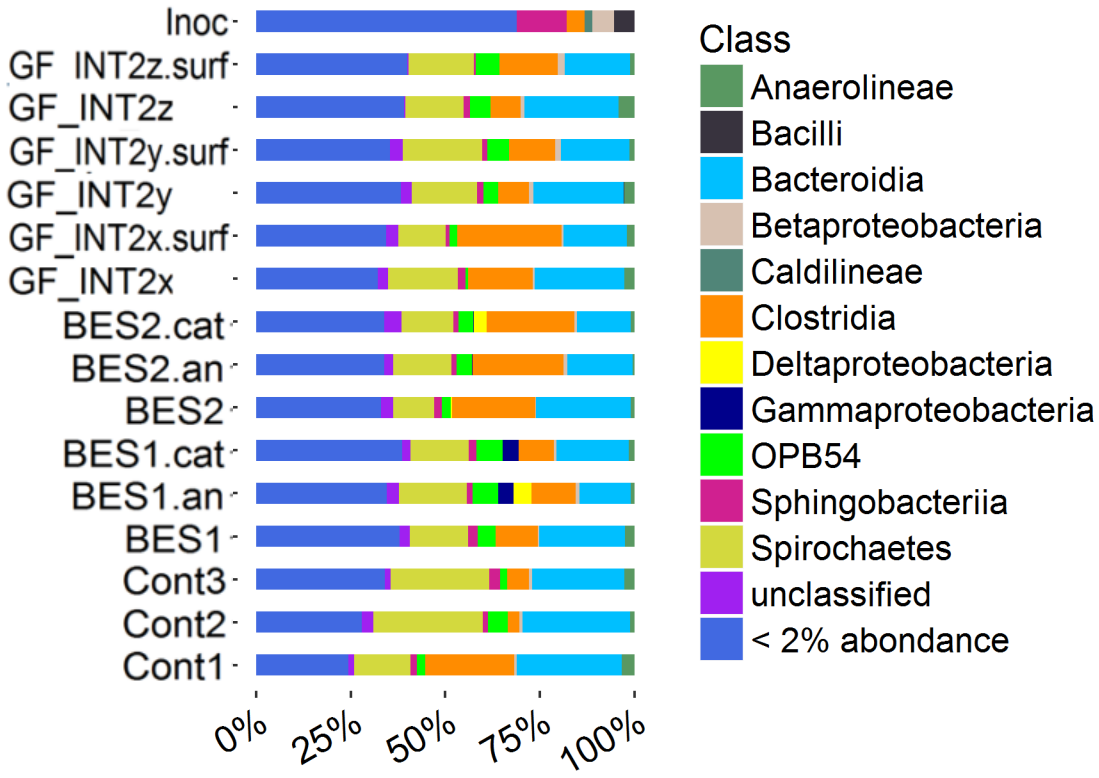

Figure 3: Bacterial phylogenetic distribution on class level.
Cont= anaerobic control digester; GF= graphite felt digester; GF.INT2.surf= biofilm on the surfaces of GF reactors (surface area 2 m^2); BES= bioelectrochemical digester; BES.an/BES.cat= anodic and cathodic biofilm.

Table 1: Total solids of GF after anaerobic digestion.
Calculation of the final PAH and NP concentrations on GF per total solids as well as the mass of GF that was added to reactors in bold print (valid for all micropollutants). Final PAH and NP concentrations onto GF inside the reactor calculated from the detected micropollutant concentrations [µg/g] per total solids of GF. Calculations can be found in chapter II, section 4.4. Mass measured with four digits.

	TS/ GF	**GF added**	Flu/ TS_{GF}	Flu_{GF}	Phe/ TS_{GF}	Phe_{GF}	Ant/ TS_{GF}	Ant_{GF}	Flt/ TS_{GF}	Flt_{GF}
Unit	**[g/kg]**	**[g]**	[µg/g]	[µg/L]	[µg/g]	[µg/L]	[µg/g]	[µg/L]	[µg/g]	[µg/L]
GF_INT1a	**141.80**	**14.88**	0.6837	2.8851	0.1906	0.8041	0.0198	0.0834	1.1867	5.0080
GF_INT1b	**138.92**	**7.47**	1.1331	2.3542	0.3424	0.7113	0.0316	0.0657	1.1948	2.4823
GF_INT2a	**159.28**	**30.47**	1.4326	13.9098	0.4367	4.2401	0.0351	0.3406	1.1423	11.0914
GF_INT2b	**167.09**	**28.70**	0.8912	8.5472	0.2986	2.8642	0.0280	0.2687	1.0202	9.7851
GF_INT1a_HT	**96.91**	**10.21**	0.4050	0.8496	0.1383	0.2901	0.0122	0.0255	0.6173	1.2949
GF_INT1b_HT	**100.12**	**10.23**	0.4155	0.8520	0.1310	0.2686	0.0115	0.0236	0.5457	1.1190
GF_INT2a_HT	**106.58**	**34.16**	0.6167	4.4915	0.1946	1.4170	0.0171	0.1245	0.7583	5.5222
GF_INT2b_HT	**114.63**	**32.38**	0.4570	3.3925	0.1438	1.0678	0.0125	0.0928	0.6533	4.8496
	Pyr/ TS_{GF}	Pyr_{GF}	BaA/ TS_{GF}	BaA_{GF}	Chry/ TS_{GF}	$Chry_{GF}$	BbF/ TS_{GF}	BbF_{GF}	BkF/ TS_{GF}	BkF_{GF}
Unit	[µg/g]	[µg/L]	[µg/g]	[µg/L]	[µg/g]	[µg/L]	[µg/g]	[µg/L]	[µg/g]	[µg/L]
GF_INT1a	0.0268	0.1129	0.1434	0.6049	0.0045	0.0190	0.0027	0.0116	0.2343	0.9886
GF_INT1b	0.0442	0.0917	0.2516	0.5227	0.0085	0.0177	0.0035	0.0074	0.1119	0.2325
GF_INT2a	0.0519	0.5039	0.3357	3.2590	0.0120	0.1165	0.0040	0.0386	0.0875	0.8493
GF_INT2b	0.0389	0.3735	0.2117	2.0300	0.0091	0.0870	0.0046	0.0444	0.1794	1.7211

GF_INT1a_HT	0.0187	0.0392	0.0504	0.1058	0.0022	0.0046	0.0011	0.0023	0.1136	0.2383
GF_INT1b_HT	0.0176	0.0360	0.0556	0.1141	0.0023	0.0046	0.0013	0.0026	0.1256	0.2575
GF_INT2a_HT	0.0236	0.1721	0.1084	0.7893	0.0041	0.0298	0.0024	0.0173	0.1576	1.1480
GF_INT2b_HT	0.0197	0.1460	0.0670	0.4976	0.0024	0.0181	0.0012	0.0093	0.1154	0.8566
	BaP/ TS_{GF}	BaP_{GF}	DBahA/ TS_{GF}	$DBahA_{GF}$	BghiP/ TS_{GF}	$BghiP_{GF}$	NP/ TS_{GF}	NP_{GF}	-	-
GF_INT1a	0.0145	0.0610	0.4091	1.7264	0.0003	0.0014	5.6057	23.6560	-	-
GF_INT1b	0.0117	0.0243	0.3688	0.7663	0.0005	0.0011	2.9886	6.2089	-	-
GF_INT2a	0.0098	0.0950	0.4244	4.1204	0.0008	0.0079	7.0011	67.9770	-	-
GF_INT2b	0.0161	0.1545	0.5823	5.5846	0.0010	0.0100	6.4452	61.8158	-	-
GF_INT1a_HT	0.0087	0.0183	0.1149	0.2409	0.0002	0.0003	8.5905	18.0189	-	-
GF_INT1b_HT	0.0112	0.0230	0.2027	0.4156	0.0003	0.0006	7.3445	15.0595	-	-
GF_INT2a_HT	0.0135	0.0981	0.4159	3.0288	0.0005	0.0038	11.0519	80.4862	-	-
GF_INT2b_HT	0.0097	0.0721	0.1462	1.0852	0.0002	0.0013	9.9702	74.0162	-	-

Table 2: Final average PAH and NP concentrations onto GF.

[µg/L]	Fluorene	Phenanthrene	Anthracene	Fluoranthene	Pyrene	Benzo.a.Anthracene	Chrysene	Nonylphenol
GF_INT1	2.6± 0.1	0.8± 0.0	0.1± 0.0	3.7± 0.6	0.1± 0.0	0.6± 0.0	0.0± 0.0	14.9± 8.7
GF_INT2	11.2± 1.3	3.6± 0.3	0.3± 0.0	10.4± 0.3	0.4± 0.0	2.6± 0.3	0.1± 0.0	64.9± 3.1
GF_INT1_HT	0.9± 0.0	0.3± 0.0	0.0± 0.0	1.2± 0.0	0.0± 0.0	0.1± 0.0	0.0± 0.0	16.5± 1.5
GF_INT2_HT	3.9± 0.3	1.2± 0.1	0.1± 0.0	5.2± 0.2	0.2± 0.0	0.6± 0.1	0.0± 0.0	77.3± 3.2

[µg/L]	Benzo.b.Fluoranthene	Benzo.k.Fluoranthene	Benzo.a.Pyrene	DiBenzo.a.h.Anthracene	Benzo.g.h.i.Perylene
GF_INT1	0.0± 0.0	0.6± 0.2	0.0± 0.0	1.2± 0.2	0.0± 0.0
GF_INT2	0.0± 0.0	1.3± 0.2	0.1± 0.0	4.9± 0.4	0.0± 0.0
GF_INT1_HT	0.0± 0.0	0.2± 0.0	0.0± 0.0	0.3± 0.0	0.0± 0.0
GF_INT2_HT	0.0± 0.0	1.0± 0.1	0.1± 0.0	2.1± 0.5	0.0± 0.0

Table 3: Sorption of PAHs and NP onto GF in heat treated anaerobic digesters.
PAH and NP sorption onto GF with different specific surface areas of 1 m^2 and 2 m^2 with respect to total concentrations in reactors.

	GF_INT1_HT				GF_INT2_HT			
	Final conc.	Final conc. on GF	sum	Fraction sorbed	Final conc.	Final conc. on GF	sum	Fraction sorbed
	[µg/L]	[µg/L]	[µg/L]	[%]	[µg/L]	[µg/L]	[µg/L]	[%]
Fluorene	44.6	0.9	45.5	1.9	51.5	3.9	55.4	7.1
Phenanthrene	82.8	0.3	83.0	0.3	84.1	1.2	85.3	1.5
Anthracene	69.5	0.0	69.5	0.0	81.4	0.1	81.5	0.1
Fluoranthene	83.0	1.2	84.2	1.4	103.5	5.2	108.6	4.8
Pyrene	76.6	0.0	76.6	0.0	75.7	0.2	75.8	0.2
Benzo.a.Anthracenene	68.4	0.1	68.5	0.2	71.1	0.6	71.7	0.9
Chrysene	71.1	0.0	71.1	0.0	70.5	0.0	70.5	0.0
Benzo.b.Fluoranthene	69.3	0.0	69.3	0.0	72.2	0.0	72.3	0.0
Benzo.k.Fluoranthene	62.6	0.2	62.8	0.4	63.0	1.0	64.0	1.6
Benzo.a.Pyrene	55.1	0.0	55.1	0.0	55.5	0.1	55.6	0.2
DiBenzo.a.h.Anthracene	65.9	0.3	66.2	0.5	62.2	2.1	64.3	3.2
Benzo.g.h.i.Perylene	65.7	0.0	65.7	0.0	55.3	0.0	55.3	0.0
Nonylphenol	1418.1	16.5	1434.6	1.2	1262.0	77.3	1339.3	5.8

Hydrogen and volatile fatty acids production in heat treated digesters (addendum to chapter VI)

Heat treated digesters did not produce methane but showed hydrogen production within the first 20 to 25 days of the experiment. They were stopped and sampling was done before the non-heat treated digesters when five of ten heat treated reactors began to produce methane in order to prevent a further increase in methanogenic activity. Figure 4 shows hydrogen production in normo-litre per chemical oxygen demand of the initial sludge of the heat treated digesters. Highest hydrogen production was obtained in control reactors with a maximum of 7.6 Nml/$g_{initialCOD}$ at day eight. This value falls below the maximum cumulative hydrogen production due to dark fermentation of wheat straw of 10 ± 9 Nml/$g_{initialCOD}$ as reported by Chatellard et al. (2016).

Inhibition of methanogens' growth for higher hydrogen yields is usually obtained by heat pretreatment at temperatures between 65 and 100 °C (Wong et al., 2014). This was apparently the reason why the anaerobic digesters of the present experiment produced

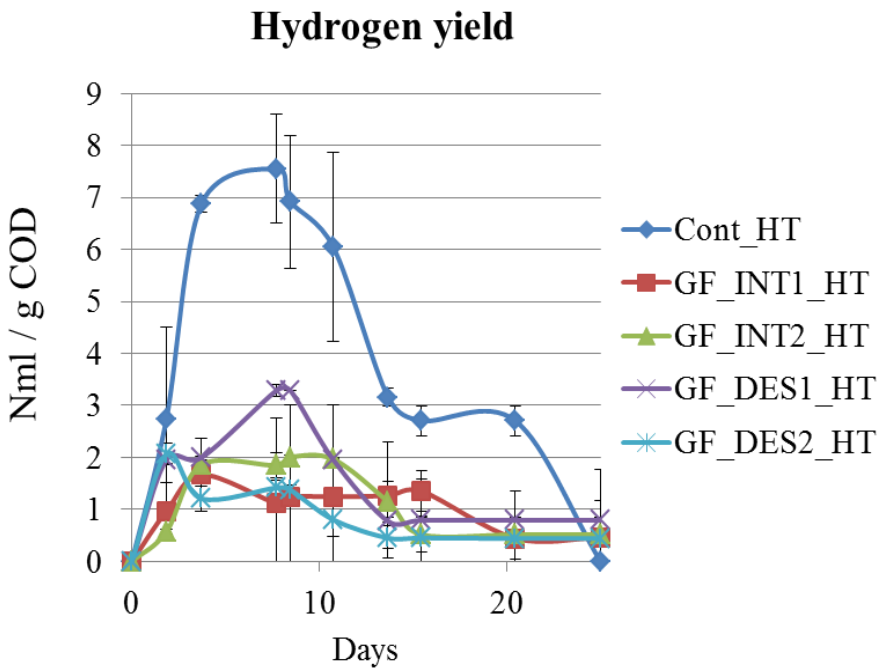

Figure 4: Hydrogen production at standard temperature and pressure per chemical oxygen demand of initial sludge of the individual reactors.

hydrogen after the heat treatment at 120°C since spore forming hydrogen producing fermenting bacteria were, thus, selected. The low hydrogen production of sludge is explained by the fact that the carbohydrates present in sludge are complex (easily biodegradable and soluble carbohydrates have already been consumed within the

wastewater treatment process) and the extent and rate of hydrogen production depend on the degree of polymerisation of the carbohydrates (Monlau et al., 2012). The maximum amount of hydrogen produced was 210 Nml (Cont_HT) which is equal to 0.0093977 moles of H_2 according to the ideal gas equation (Equation 11). One mole of hydrogen corresponds to 16 g COD/L. Therefore, one can calculate the loss of COD that was due to the loss of hydrogen from the reactors. This COD loss gives us a rough estimate of the amount of COD we should add to the measured end concentrations of COD in order to obtain a theoretical start COD of sludge of heat treated reactors. Regarding the VFA production and consumption in the reactors, it is assumed that the amount of COD that was lost due to sampling events during fermentation is negligible (six times 1ml = 6ml) with respect to the overall quantity of sludge (500 ml) and that the transformations inside the reactor which sustain cell metabolism cannot be quantified.

Equation 13: $$COD\ initial = \frac{COD \times V(H_2) \times p}{R \times T} = 16\ \frac{g}{mol*L}\ x\ \frac{101325\ Pa \times 0.21\ NL}{273.15\ K \times 8.314\ \frac{J}{mol\ K}} = 0.30\ \frac{g}{L}$$

Table 4 lists final COD values for the sludge of heat treated reactors. The average of these COD values is 33.8 g/L which is very close to the COD of raw sludge (45 g/L) after diluting 1.78 times (32.0 g/L). This is why it is considered that COD removal was low in all heat treated reactors. The results point rather to the fact that the fermenting bacteria produced little hydrogen and that VFA production and consumption did not change the COD significantly leading to an almost identical COD at the start and end of the experiment.

Table 4: Final chemical oxygen demands of sludge of heat treated reactors.
COD_{end} measured, the start values are calculated.

	g COD/ L $sludge_{end}$
Cont_a_HT	32.4
Cont_b_HT	31.1
GF_INT1a_HT	28.1
GF_INT1b_HT	33.8
GF_INT2a_HT	29.8
GF_INT2b_HT	31.6
GF_DES1a_HT	36.6
GF_DES1b_HT	34
GF_DES2a_HT	42.6
GF_DES2b_HT	37.8

The production of C2 to C5 carboxylic acids suggests that all fermentations belonged to mixed-acid-type fermentation (Figure 5). Acetate represented above 46 % of the VFA composition in all reactors on day 3 and day 14 whereas butyrate represented maximal 13 and 24 %, respectively. Other soluble metabolites e.g. lactate and ethanol concentrations have not been measured. Acetate, however, was also the predominant metabolite in other studies that report hydrogen production from sludge such as microwave treated and alkalized sludge (Cai et al., 2004), ultrasound pretreated sludge (Guo et al., 2008) and gamma irradiated sludge (Yin and Wang, 2015). Propionate and valerate concentrations decrease from day 3 to day 14 whereas isovalerate and isobutyrate concentrations don't change significantly.

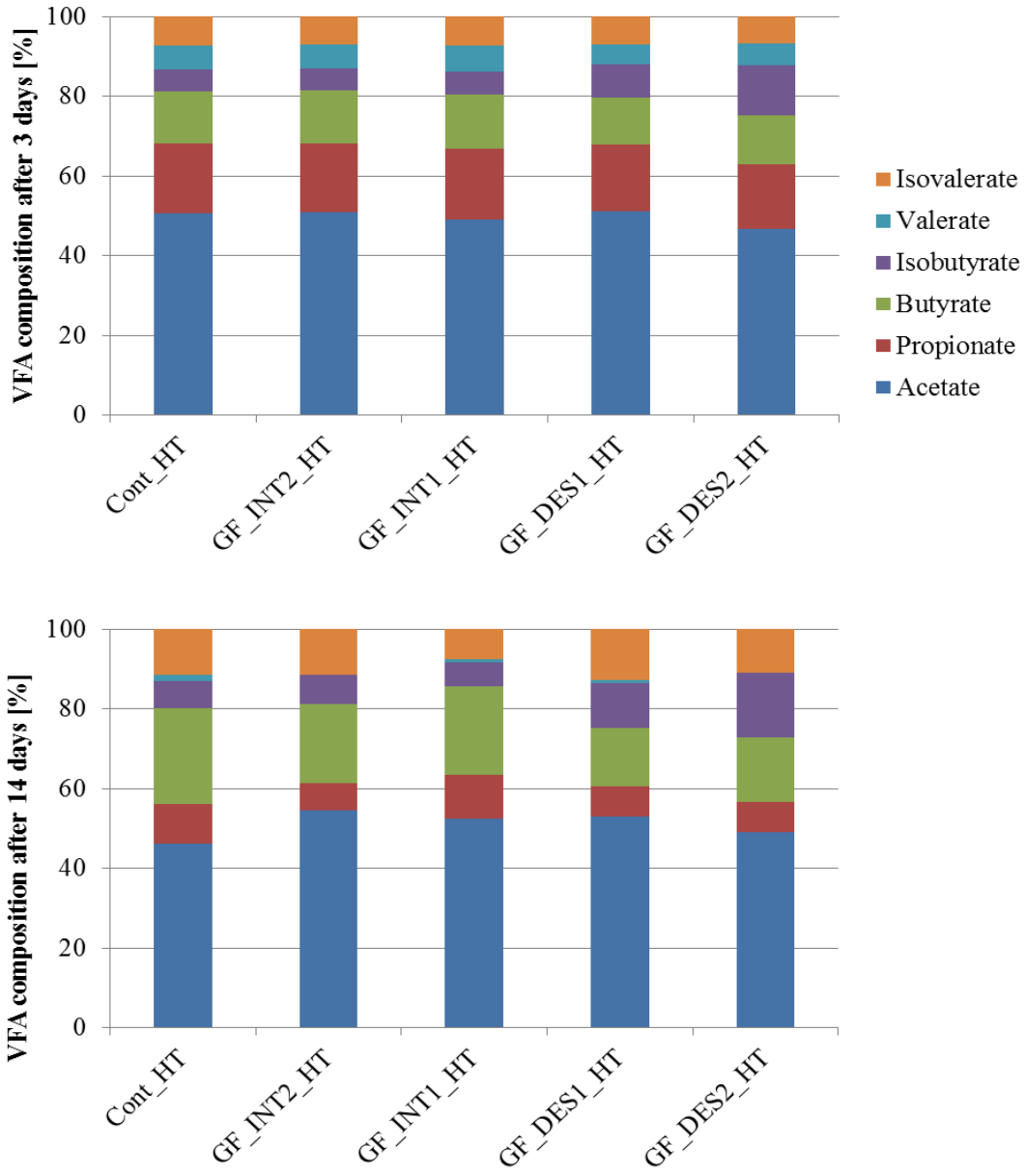

Figure 5: VFA composition at days 3 and 14 of fermentation.

Total VFA concentration of reactors are shown in Figure 5. Reactors with intact GF show very high total VFA concentrations outreaching all other reactors by over 1-2 g/L on the third day of fermentation.

References

Abad, E., Martínez, K., Planas, C., Palacios, O., Caixach, J., Rivera, J., 2005. Priority organic pollutant assessment of sludges for agricultural purposes. Chemosphere 61, 1358–1369. doi:10.1016/j.chemosphere.2005.03.018

Adelaja, O., Keshavarz, T., Kyazze, G., 2015. The effect of salinity, redox mediators and temperature on anaerobic biodegradation of petroleum hydrocarbons in microbial fuel cells. J. Hazard. Mater. 283, 211–217. doi:10.1016/j.jhazmat.2014.08.066

Adelaja, O., Keshavarz, T., Kyazze, G., 2014. Enhanced biodegradation of phenanthrene using different inoculum types in a microbial fuel cell. Eng. Life Sci. 14, 218–228. doi:10.1002/elsc.201300089

Adhikari, R.Y., Malvankar, N.S., Tuominen, M.T., Lovley, D.R., 2016. Conductivity of individual Geobacter pili. RSC Adv. 6, 8354–8357. doi:10.1039/C5RA28092C

Ahel, M., Giger, W., Koch, M., 1993. Behaviour of Alkylphenol Polyethoxylate Surfactants in the Aquatic Environment--I. Occurrence and Transformation in Sewage Treatment. Water Res. 30, 37–46.

Ahmad, M., Rajapaksha, A.U., Lim, J.E., Zhang, M., Bolan, N., Mohan, D., Vithanage, M., Lee, S.S., Ok, Y.S., 2014. Biochar as a sorbent for contaminant management in soil and water: A review. Chemosphere 99, 19–33. doi:10.1016/j.chemosphere.2013.10.071

Ailijiang, N., Chang, J., Liang, P., Li, P., Wu, Q., Zhang, X., Huang, X., 2016. Electrical stimulation on biodegradation of phenol and responses of microbial communities in conductive carriers supported biofilms of the bioelectrochemical reactor. Bioresour. Technol. 201, 1–7. doi:10.1016/j.biortech.2015.11.026

Aislabie, J., Deslippe, J.R., Dymond, J.R., 2013. Soil microbes and their contribution to soil services, in: Dymond, J. (Ed.), Ecosystem Services in New Zealand - Conditions and

Trends. Manaaki Whenua Press, Lincoln, New Zealand, pp. 143–161.

Akhiar, A., Battimelli, A., Torrijos, M., Carrere, H., 2017. Comprehensive characterization of the liquid fraction of digestates from full-scale anaerobic co-digestion. Waste Manag. 59, 118–128. doi:10.1016/j.wasman.2016.11.005

Alcántara, M.T., Gómez, J., Pazos, M., Sanromán, M.A., 2012. Electrokinetic remediation of lead and phenanthrene polluted soils. Geoderma 173–174, 128–133. doi:10.1016/j.geoderma.2011.12.009

Alcántara, M.T., Gómez, J., Pazos, M., Sanromán, M.A., 2009. PAHs soil decontamination in two steps: Desorption and electrochemical treatment. J. Hazard. Mater. 166, 462–468. doi:10.1016/j.jhazmat.2008.11.050

Alcántara, T., Pazos, M., Cameselle, C., Sanromán, M.A., 2008. Electrochemical remediation of phenanthrene from contaminated kaolinite. Environ. Geochem. Health 30, 89–94. doi:10.1007/s10653-008-9151-3

Allen, R.M., Bennetto, H.P., 1993. Microbial fuel-cells. Appl. Biochem. Biotechnol. 39–40, 27–40. doi:10.1007/BF02918975

Amani, T., Nosrati, M., Sreekrishnan, T.R., 2010. Anaerobic digestion from the viewpoint of microbiological, chemical, and operational aspects — a review. Environ. Rev. 18, 255–278. doi:10.1139/A10-011

Ambuchi, J.J., Zhang, Z., Shan, L., Liang, D., Zhang, P., Feng, Y., 2017. Response of anaerobic granular sludge to iron oxide nanoparticles and multi-wall carbon nanotubes during beet sugar industrial wastewater treatment. Water Res. 117, 87–94. doi:10.1016/j.watres.2017.03.050

Anneser, B., Pilloni, G., Bayer, A., Lueders, T., Griebler, C., Einsiedl, F., Richters, L., 2010. High Resolution Analysis of Contaminated Aquifer Sediments and Groundwater—What Can be Learned in Terms of Natural Attenuation? Geomicrobiol. J. 27, 130–142. doi:10.1080/01490450903456723

Annual Danish Emission Inventory Report to UNECE, 2003. , Agriculture.

Annweiler, E., Materna, A., Safinowski, M., Kappler, A., Richnow, H.H., Michaelis, W., Meckenstock, R.U., 2000. Anaerobic Degradation of 2-Methylnaphthalene by a Sulfate-Reducing Enrichment Culture. Appl. Environ. Microbiol. 66, 5329–5333. doi:10.1128/AEM.66.12.5329-5333.2000

Annweiler, E., Michaelis, W., Meckenstock, R.U., 2002. Identical ring cleavage products during anaerobic degradation of naphthalene, 2-methylnaphthalene, and tetralin indicate a new metabolic pathway. Appl. Environ. Microbiol. 68, 852–858. doi:10.1128/AEM.68.2.852-858.2002

Aparicio, I., Santos, J.L., Alonso, E., 2009. Limitation of the concentration of organic pollutants in sewage sludge for agricultural purposes: A case study in South Spain. Waste Manag. 29, 1747–1753. doi:10.1016/j.wasman.2008.11.003

Arnaud, T., Gricourt, A., 2015. Traitement et valorisation du biogaz issu d'un réacteur anaérobie, in: Moletta, R. (Ed.), La Méthanisation. Lavoisier, Paris, pp. 446–478.

Arulazhagan, P., Sivaraman, C., Kumar, S.A., 2014. Co-metabolic degradation of benzo(e)pyrene by halophilic bacterial consortium at different saline conditions 35, 445–452.

Asztalos, J.R., Kim, Y., 2015. Enhanced digestion of waste activated sludge using microbial electrolysis cells at ambient temperature. Water Res. 87, 503–512. doi:10.1016/j.watres.2015.05.045

Aulenta, F., Canosa, A., Majone, M., Panero, S., Reale, P., Rossetti, S., 2008. Trichloroethene Dechlorination and H 2 Evolution Are Alternative Biological Pathways of Electric Charge Utilization by a Dechlorinating Culture in a Bioelectrochemical System. Environ. Sci. Technol. 42, 6185–6190. doi:10.1021/es800265b

Aulenta, F., Catervi, A., Majone, M., Panero, S., Reale, P., Rossetti, S., 2007. Electron Transfer from a Solid-State Electrode Assisted by Methyl Viologen Sustains Efficient Microbial Reductive Dechlorination of TCE. Environ. Sci. Technol. 41, 2554–2559. doi:10.1021/es0624321

Aulenta, F., Fazi, S., Majone, M., Rossetti, S., 2014. Electrically conductive magnetite particles enhance the kinetics and steer the composition of anaerobic TCE-dechlorinating cultures. Process Biochem. 49, 2235–2240. doi:10.1016/j.procbio.2014.09.015

Aulenta, F., Reale, P., Canosa, A., Rossetti, S., Panero, S., Majone, M., 2010. Characterization of an electro-active biocathode capable of dechlorinating trichloroethene and cis-dichloroethene to ethene. Biosens. Bioelectron. 25, 1796–802. doi:10.1016/j.bios.2009.12.033

Aulenta, F., Rossetti, S., Amalfitano, S., Majone, M., Tandoi, V., 2013. Conductive Magnetite Nanoparticles Accelerate the Microbial Reductive Dechlorination of Trichloroethene by Promoting Interspecies Electron Transfer Processes. ChemSusChem 6, 433–436. doi:10.1002/cssc.201200748

Aulenta, F., Tocca, L., Verdini, R., Reale, P., Majone, M., 2011. Dechlorination of trichloroethene in a continuous-flow bioelectrochemical reactor: effect of cathode potential on rate, selectivity, and electron transfer mechanisms. Environ. Sci. Technol. 45, 8444–8451. doi:10.1021/es202262y

Barret, M., Carrère, H., Delgadillo, L., Patureau, D., 2010a. PAH fate during the anaerobic digestion of contaminated sludge: Do bioavailability and/or cometabolism limit their biodegradation? Water Res. 44, 3797–3806. doi:10.1016/j.watres.2010.04.031

Barret, M., Carrère, H., Latrille, E., Wisniewski, C., Patureau, D., 2010b. Micropollutant and sludge characterization for modeling sorption equilibria. Environ. Sci. Technol. 44, 1100–1106. doi:10.1021/es902575d

Berdugo-Clavijo, C., Dong, X., Soh, J., Sensen, C.W., Gieg, L.M., 2012. Methanogenic biodegradation of two-ringed polycyclic aromatic hydrocarbons. FEMS Microbiol. Ecol. 81, 124–133. doi:10.1111/j.1574-6941.2012.01328.x

Bermek, H., Catal, T., Akan, S.S., Ulutaş, M.S., Kumru, M., Özgüven, M., Liu, H., Özçelik, B., Akarsubaşı, A.T., 2014. Olive mill wastewater treatment in single-chamber air-cathode microbial fuel cells. World J. Microbiol. Biotechnol. 30, 1177–

1185. doi:10.1007/s11274-013-1541-8

Bernal-Martinez, A., Carrère, H., Patureau, D., Delgenès, J.-P., 2007. Ozone pre-treatment as improver of PAH removal during anaerobic digestion of urban sludge. Chemosphere 68, 1013–1019. doi:10.1016/j.chemosphere.2007.02.019

Bernal-Martinez, A., Patureau, D., Delgenès, J.-P., Carrère, H., 2009. Removal of polycyclic aromatic hydrocarbons (PAH) during anaerobic digestion with recirculation of ozonated digested sludge. J. Hazard. Mater. 162, 1145–1150. doi:10.1016/j.jhazmat.2008.05.163

Blanchard, M., Teil, M.J., Ollivon, D., Legenti, L., Chevreuil, M., 2004. Polycyclic aromatic hydrocarbons and polychlorobiphenyls in wastewaters and sewage sludges from the Paris area (France). Environ. Res. 95, 184–197. doi:10.1016/j.envres.2003.07.003

Bojes, H.K., Pope, P.G., 2007. Characterization of EPA's 16 priority pollutant polycyclic aromatic hydrocarbons (PAHs) in tank bottom solids and associated contaminated soils at oil exploration and production sites in Texas. Regul. Toxicol. Pharmacol. 47, 288–295. doi:10.1016/j.yrtph.2006.11.007

Bond, D.R., Lovley, D.R., 2003. Electricity Production by Geobacter sulfurreducens Attached to Electrodes Electricity Production by Geobacter sulfurreducens Attached to Electrodes. Appl. Environ. Microbiol. 69, 1548–1555. doi:10.1128/AEM.69.3.1548

Borck, Ø., Schröder, E., 2017. Methylbenzenes on graphene. Surf. Sci. 664, 162–167. doi:10.1016/j.susc.2017.06.012

Bouki, C., Dvorakova, M., Diamadopoulos, E., 2010. Adsorption of Nonylphenol on Activated Sludge Biomass Under Aseptic Conditions. CLEAN - Soil, Air, Water 38, 516–520. doi:10.1002/clen.200900290

Bourke, J., Manley-Harris, M., Fushimi, C., Dowaki, K., Nunoura, T., Antal, M.J., 2007. Do All Carbonized Charcoals Have the Same Chemical Structure? 2. A Model of the Chemical Structure of Carbonized Charcoal. Ind. Eng. Chem. Res. 46, 5954–5967. doi:10.1021/ie070415u

Bozkurt, H., Sanin, F.D., 2014. Toxicity of nonylphenol diethoxylate in lab-scale anaerobic digesters. Chemosphere 104, 69–75. doi:10.1016/j.chemosphere.2013.10.059

Bruno, F., Curini, R., Di Corcia, A., Fochi, I., Nazzari, M., Samperi, R., 2002. Determination of surfactants and some of their metabolites in untreated and anaerobically digested sewage sludge by subcritical water extraction followed by liquid chromatography - Mass spectrometry. Environ. Sci. Technol. 36, 4156–4161. doi:10.1021/es020002e

Cai, M., Liu, J., Wei, Y., 2004. Enhanced biohydrogen production from sewage sludge with alkaline pretreatment. Environ. Sci. Technol. 38, 3195–3202. doi:10.1021/es0349204

Cai, W., Liu, W., Yang, C., Wang, L., Liang, B., Thangavel, S., Guo, Z., Wang, A., 2016. Biocathodic Methanogenic Community in an Integrated Anaerobic Digestion and Microbial Electrolysis System for Enhancement of Methane Production from Waste Sludge. ACS Sustain. Chem. Eng. 4, 4913–4921. doi:10.1021/acssuschemeng.6b01221

Camcho, P., Prévot, C., 2015. La méthanisation des boues, in: Moletta, R. (Ed.), La Méthanisation. Lavoisier, Paris, pp. 205–233.

Carballa, M., Omil, F., Ternes, T., Lema, J.M., 2007. Fate of pharmaceutical and personal care products (PPCPs) during anaerobic digestion of sewage sludge. Water Res. 41, 2139–2150. doi:10.1016/j.watres.2007.02.012

Carmona-Martínez, A. a, Pierra, M., Trably, E., Bernet, N., 2013. High current density via direct electron transfer by the halophilic anode respiring bacterium Geoalkalibacter subterraneus. Phys. Chem. Chem. Phys. 15, 19699–19707. doi:10.1039/c3cp54045f

Carrere, H., Antonopoulou, G., Affes, R., Passos, F., Battimelli, A., Lyberatos, G., Ferrer, I., 2016. Review of feedstock pretreatment strategies for improved anaerobic digestion: From lab-scale research to full-scale application. Bioresour. Technol. 199, 386–397. doi:10.1016/j.biortech.2015.09.007

Cayuela, M.L., Sanchez-Monedero, M.A., Roig, A., Hanley, K., Enders, A., Lehmann, J., 2013. Biochar and denitrification in soils: when, how much and why does biochar

reduce N2O emissions? Sci. Rep. 3, 1–7. doi:10.1038/srep01732

Cerniglia, C.E., 1993. Biodegradation of polycyclic aromatic hydrocarbons. Curr. Opin. Biotechnol. 4, 331–338. doi:10.1016/0958-1669(93)90104-5

Chakraborty, R., O'Connor, S.M., Chan, E., Coates, J.D., 2005. Anaerobic Degradation of Benzene, Toluene, Ethylbenzene, and Xylene Compounds by Dechloromonas Strain RCB. Appl. Environ. Microbiol. 71, 8649–8655. doi:10.1128/AEM.71.12.8649-8655.2005

Chandrasekhar, K., Venkata Mohan, S., 2012. Bio-electrochemical remediation of real field petroleum sludge as an electron donor with simultaneous power generation facilitates biotransformation of PAH: Effect of substrate concentration. Bioresour. Technol. 110, 517–525. doi:10.1016/j.biortech.2012.01.128

Chang, B.-V., Chang, I.T., Yuan, S.Y., 2008. Anaerobic degradation of phenanthrene and pyrene in mangrove sediment. Bull. Environ. Contam. Toxicol. 80, 145–149. doi:10.1007/s00128-007-9333-1

Chang, B.-V., Lu, Z.-J., Yuan, S.-Y., 2009. Anaerobic degradation of nonylphenol in subtropical mangrove sediments. J. Hazard. Mater. 165, 162–167. doi:10.1016/j.jhazmat.2008.09.085

Chang, B.V., Chang, S.W., Yuan, S.Y., 2003. Anaerobic degradation of polycyclic aromatic hydrocarbons in sludge. Adv. Environ. Res. 7, 623–628. doi:10.1016/S1093-0191(02)00047-3

Chang, W., Um, Y., Holoman, T.R.P., 2006. Polycyclic aromatic hydrocarbon (PAH) degradation coupled to methanogenesis. Biotechnol. Lett. 28, 425–430. doi:10.1007/s10529-005-6073-3

Chang, B. V, Chiang, F., Yuan, S.Y., 2005. Anaerobic degradation of nonylphenol in sludge. Chemosphere 59, 1415–1420. doi:10.1016/j.chemosphere.2004.12.055

Chatellard, L., Trably, E., Carrère, H., 2016. The type of carbohydrates specifically selects microbial community structures and fermentation patterns. Bioresour. Technol. 221,

541–549. doi:10.1016/j.biortech.2016.09.084

Chen, J., Wang, C., Pan, Y., Farzana, S.S., Tam, N.F.-Y., 2018. Biochar accelerates microbial reductive debromination of 2,2′,4,4′-tetrabromodiphenyl ether (BDE-47) in anaerobic mangrove sediments. J. Hazard. Mater. 341, 177–186. doi:10.1016/j.jhazmat.2017.07.063

Chen, J., Zhang, L., Hu, Y., Huang, W., Niu, Z., Sun, J., 2017. Bacterial community shift and incurred performance in response to in situ microbial self-assembly graphene and polarity reversion in microbial fuel cell. Bioresour. Technol. 241, 220–227. doi:10.1016/j.biortech.2017.05.123

Chen, K., Lei, H., Li, Y., Li, H., Zhang, X., Yao, C., 2011. Physical and chemical characteristics of waste activated sludge treated with electric field. Process Saf. Environ. Prot. 89, 327–333. doi:10.1016/j.psep.2011.06.011

Chen, S., Rotaru, A.-E., Shrestha, P.M., Malvankar, N.S., Liu, F., Fan, W., Nevin, K.P., Lovley, D.R., 2014a. Promoting Interspecies Electron Transfer with Biochar. Sci. Rep. 4, 1–7. doi:10.1038/srep05019

Chen, S., Rotaru, A.E., Liu, F., Philips, J., Woodard, T.L., Nevin, K.P., Lovley, D.R., 2014b. Carbon cloth stimulates direct interspecies electron transfer in syntrophic co-cultures. Bioresour. Technol. 173, 82–86. doi:10.1016/j.biortech.2014.09.009

Cheng, G., Sun, M., Ge, X., Ou, Y., Xu, X., Lin, Q., Lou, L., 2017a. Adsorption-Desorption Characteristics of Nonylphenol on Two Different Origins of Black Carbon. Water, Air, Soil Pollut. 228, 311. doi:10.1007/s11270-017-3490-6

Cheng, G., Sun, M., Lu, J., Ge, X., Zhang, H., Xu, X., Lou, L., Lin, Q., 2017b. Role of biochar in biodegradation of nonylphenol in sediment: Increasing microbial activity versus decreasing bioavailability. Sci. Rep. 7, 1–11. doi:10.1038/s41598-017-04787-2

Cheng, H.M., Yang, Q.H., Liu, C., 2001. Hydrogen storage in carbon nanotubes. Carbon N. Y. 39, 1447–1454. doi:10.1016/S0008-6223(00)00306-7

Cheng, Q., Call, D.F., 2016. Hardwiring microbes via direct interspecies electron transfer:

mechanisms and applications. Environ. Sci. Process. Impacts 18, 968–980. doi:10.1039/C6EM00219F

Cheng, S., Xing, D., Call, D.F., Logan, B.E., 2009. Direct Biological Conversion of Electrical Current into Methane by Electromethanogenesis. Environ. Sci. Technol. 43, 3953–3958. doi:10.1021/es803531g

Cho, Y., Sokol, R.C., Frohnhoefer, R.C., Rhee, G.-Y., 2003. Reductive Dechlorination of Polychlorinated Biphenyls: Threshold Concentration and Dechlorination Kinetics of Individual Congeners in Aroclor 1248. doi:10.1021/ES034600K

Choi, O., Sang, B.-I., 2016. Extracellular electron transfer from cathode to microbes: application for biofuel production. Biotechnol. Biofuels 9, 1–11. doi:10.1186/s13068-016-0426-0

Christensen, N., Batstone, D.J., He, Z., Angelidaki, I., Schmidt, J.E., 2004. Removal of polycyclic aromatic hydrocarbons (PAHs) from sewage sludge by anaerobic degradation. Water Sci. Technol. 50, 237–244.

Clark, B.W., Matson, C.W., Jung, D., Di Giulio, R.T., 2010. AHR2 mediates cardiac teratogenesis of polycyclic aromatic hydrocarbons and PCB-126 in Atlantic killifish (Fundulus heteroclitus). Aquat. Toxicol. 99, 232–240. doi:10.1016/j.aquatox.2010.05.004

Clauss, M., Furustrand Tafin, U., Betrisey, B., van Garderen, N., Trampuz, A., Ilchmann, T., Bohner, M., 2014. Influence of physico-chemical material characteristics on staphylococcal biofilm formation - A qualitative and quantitative in vitro analysis of five different calcium phosphate bone grafts. Eur. Cells Mater. 28, 39–50.

Clauwaert, P., Tolêdo, R., van der Ha, D., Crab, R., Verstraete, W., Hu, H., Udert, K.M., Rabaey, K., 2008. Combining biocatalyzed electrolysis with anaerobic digestion. Water Sci. Technol. 57, 575–579. doi:10.2166/wst.2008.084

Clauwaert, P., Verstraete, W., 2009. Methanogenesis in membraneless microbial electrolysis cells. Appl. Microbiol. Biotechnol. 82, 829–836. doi:10.1007/s00253-008-1796-4

Coates, J.D., Anderson, R.T., Woodward, J.C., Phillips, E.J.P., Lovley, D.R., 1996. Anaerobic Hydrocarbon Degradation in Petroleum-Contaminated Harbor Sediments under Sulfate-Reducing and Artificially Imposed Iron-Reducing Conditions. Environ. Sci. Technol. 30, 2784–2789. doi:10.1021/es9600441

Coeuret, F., 2007. Apparent electric conductivity of non-consolidated fixed beds of carbon materials used as porous electrodes. J. new Mater. Electrochem. Syst. 10, 255–262.

Cordeiro, D.S., Corio, P., 2009. Electrochemical and Photocatalytic Reactions of Polycyclic Aromatic Hydrocarbons Investigated by Raman Spectroscopy. J. Braz. Chem. Soc. 20, 80–87.

Cournet, A., Délia, M.L., Bergel, A., Roques, C., Bergé, M., 2010. Electrochemical reduction of oxygen catalyzed by a wide range of bacteria including Gram-positive. Electrochem. commun. 12, 505–508. doi:10.1016/j.elecom.2010.01.026

Cruz Viggi, C., Presta, E., Bellagamba, M., Kaciulis, S., Balijepalli, S.K., Zanaroli, G., Petrangeli Papini, M., Rossetti, S., Aulenta, F., 2015. The "Oil-Spill Snorkel": an innovative bioelectrochemical approach to accelerate hydrocarbons biodegradation in marine sediments. Front. Microbiol. 6, 1–11. doi:10.3389/fmicb.2015.00881

Cruz Viggi, C., Rossetti, S., Fazi, S., Paiano, P., Majone, M., Aulenta, F., 2014. Magnetite particles triggering a faster and more robust syntrophic pathway of methanogenic propionate degradation. Environ. Sci. Technol. 48, 7536–7543. doi:10.1021/es5016789

Dalla Vecchia, C., Mattioli, A., Bolzonella, D., Palma, E., 2016. Impact of Magnetite Nanoparticles Supplementation on the Anaerobic Digestion of Food Wastes : Batch and Continuous- Flow Investigations. Chem. Eng. Trans. 49, 1–6. doi:10.3303/CET1649001

Dang, Y., Holmes, D.E., Zhao, Z., Woodard, T.L., Zhang, Y., Sun, D., Wang, L.-Y., Nevin, K.P., Lovley, D.R., 2016. Enhancing anaerobic digestion of complex organic waste with carbon-based conductive materials. Bioresour. Technol. 220, 516–522. doi:10.1016/j.biortech.2016.08.114

Davidova, I.A., Gieg, L.M., Duncan, K.E., Suflita, J.M., 2007. Anaerobic phenanthrene mineralization by a carboxylating sulfate-reducing bacterial enrichment. ISME J. 1, 436–442. doi:10.1038/ismej.2007.48

de Leon-Condes, C., Barrera-Díaz, C., Barrios, J., Becerril, E., Reyes-Pérez, H., 2017. A coupled ozonation–electrooxidation treatment for removal of bisphenol A, nonylphenol and triclosan from wastewater sludge. Int. J. Environ. Sci. Technol. 14, 707–716. doi:10.1007/s13762-016-1178-x

de Souza e Silva, P.T., da Silva, V.L., Neto, B. de B., Simonnot, M.-O., 2009. Potassium permanganate oxidation of phenanthrene and pyrene in contaminated soils. J. Hazard. Mater. 168, 1269–1273. doi:10.1016/j.jhazmat.2009.03.007

De Weert, J.P.A., Viñas, M., Grotenhuis, T., Rijnaarts, H.H.M., Langenhoff, A.A.M., 2011. Degradation of 4-n-nonylphenol under nitrate reducing conditions. Biodegradation 22, 175–187. doi:10.1007/s10532-010-9386-4

Delgadillo-Mirquez, L., Lardon, L., Steyer, J.-P., Patureau, D., 2011. A new dynamic model for bioavailability and cometabolism of micropollutants during anaerobic digestion. Water Res. 45, 4511–4521. doi:10.1016/j.watres.2011.05.047

Derco, J., 2017. Removal of Alkylphenols from Industrial and Municipal Wastewater. Chem. Biochem. Eng. Q. 31, 173–178. doi:10.15255/CABEQ.2016.1021

Deshayes, S., Eudes, V., Droguet, C., Bigourie, M., Gasperi, J., Moilleron, R., 2015. Alkylphenols and Phthalates in Greywater from Showers and Washing Machines. Water, Air, Soil Pollut. 226, 1–12. doi:10.1007/s11270-015-2652-7

Déziel, E., Comeau, Y., Villemur, R., 1999. Two-liquid-phase bioreactors for enhanced degradation of hydrophobic/toxic compounds. Biodegradation 10, 219–233. doi:10.1023/A:1008311430525

Dickson, J.S., Koohmaraie, M., 1989. Cell Surface Charge Characteristics and Their Relationship to Bacterial Attachment to Meat Surfaces. Appl. Environ. Microbiol. 55, 832–836.

Ding, M., Shiu, H.Y., Li, S.L., Lee, C.K., Wang, G., Wu, H., Weiss, N.O., Young, T.D., Weiss, P.S., Wong, G.C.L., Nealson, K.H., Huang, Y., Duan, X., 2016. Nanoelectronic Investigation Reveals the Electrochemical Basis of Electrical Conductivity in Shewanella and Geobacter. ACS Nano 10, 9919–9926. doi:10.1021/acsnano.6b03655

Doña Rodríguez, J.M., Herrera Melián, J.A., Pérez Peña, J., 2000. Determination of the Real Surface Area of Pt Electrodes by Hydrogen Adsorption Using Cyclic Voltammetry. J. Chem. Educ. 77, 1195. doi:10.1021/ed077p1195

Ersan, G., Apul, O.G., Perreault, F., Karanfil, T., 2017. Adsorption of organic contaminants by graphene nanosheets: A review. Water Res. 126, 385–398. doi:10.1016/j.watres.2017.08.010

Eyiuche, N.J., Asakawa, S., Yamashita, T., Ikeguchi, A., Kitamura, Y., Yokoyama, H., 2017. Community analysis of biofilms on flame-oxidized stainless steel anodes in microbial fuel cells fed with different substrates. BMC Microbiol. 17, 1–9. doi:10.1186/s12866-017-1053-z

Fagbohungbe, M.O., Herbert, B.M.J., Hurst, L., Ibeto, C.N., Li, H., Usmani, S.Q., Semple, K.T., 2017. The challenges of anaerobic digestion and the role of biochar in optimizing anaerobic digestion. Waste Manag. 61, 236–249. doi:10.1016/j.wasman.2016.11.028

Fagervold, S.K., Watts, J.E.M., May, H.D., Sowers, K.R., 2005. Sequential Reductive Dechlorination of meta-Chlorinated Polychlorinated Biphenyl Congeners in Sediment Microcosms by Two Different Chloroflexi Phylotypes. Appl. Environ. Microbiol. 71, 8085–8090. doi:10.1128/AEM.71.12.8085-8090.2005

Fan, H.-T., Zhao, C.-Y., Liu, S., Shen, H., 2017. Adsorption Characteristics of Chlorophenols from Aqueous Solution onto Graphene. J. Chem. Eng. Data 62, 1099–1105. doi:10.1021/acs.jced.6b00918

Fatone, F., Di Fabio, S., Bolzonella, D., Cecchi, F., 2011. Fate of aromatic hydrocarbons in Italian municipal wastewater systems: An overview of wastewater treatment using

conventional activated-sludge processes (CASP) and membrane bioreactors (MBRs). Water Res. 45, 93–104. doi:10.1016/j.watres.2010.08.011

Fernández-Sanjuan, M., Rigol, A., Sahuquillo, A., Rodríguez-Cruz, S., Lacorte, S., 2009. Determination of alkylphenols and alkylphenol ethoxylates in sewage sludge: Effect of sample pre-treatment. Anal. Bioanal. Chem. 394, 1525–1533. doi:10.1007/s00216-009-2747-3

Foght, J., 2008. Anaerobic Biodegradation of Aromatic Hydrocarbons: Pathways and Prospects. J. Mol. Microbiol. Biotechnol. 15, 93–120. doi:10.1159/000121324

Forsey, S.P., Thomson, N.R., Barker, J.F., 2010. Oxidation kinetics of polycyclic aromatic hydrocarbons by permanganate. Chemosphere 79, 628–636. doi:10.1016/j.chemosphere.2010.02.027

Fountoulakis, M., Drillia, P., Pakou, C., Kampioti, A., Stamatelatou, K., Lyberatos, G., 2005. Analysis of nonylphenol and nonylphenol ethoxylates in sewage sludge by high performance liquid chromatography following microwave-assisted extraction. J. Chromatogr. A 1089, 45–51. doi:10.1016/j.chroma.2005.05.109

Fountoulakis, M.S., Stamatelatou, K., Batstone, D.J., Lyberatos, G., 2006. Simulation of DEHP biodegradation and sorption during the anaerobic digestion of secondary sludge. Water Sci. Technol. 54, 119–128. doi:10.2166/wst.2006.533

Franks, A.E., Nevin, K.P., 2010. Microbial Fuel Cells, A Current Review. Energies 3, 899–919. doi:10.3390/en3050899

Fung, A.W.P., Rao, A.M., Kuriyama, K., Dresselhaus, M.S., Dresselhaus, G., Endo, M., Shindo, N., 1993. Raman scattering and electrical conductivity in highly disordered activated carbon fibers. J. Mater. Res. 8, 489–500. doi:10.1557/JMR.1993.0489

Galushko, A., Minz, D., Schink, B., Widdel, F., 1999. Anaerobic degradation of naphthalene by a pure culture of a novel type of marine sulphate-reducing bacterium. Environ. Microbiol. 1, 415–420.

Gao, D., Li, Z., Guan, J., Li, Y., Ren, N., 2014. Removal of surfactants nonylphenol

ethoxylates from municipal sewage-comparison of an A/O process and biological aerated filters. Chemosphere 97, 130–134. doi:10.1016/j.chemosphere.2013.10.083

Garcia, J.-L., Patel, B.K.., Ollivier, B., 2000. Taxonomic, Phylogenetic, and Ecological Diversity of Methanogenic Archaea. Anaerobe 6, 205–226. doi:10.1006/anae.2000.0345

Geeta, G.S., Raghevendra, S., Reddy, T.K.R., 1986. Increase in biogas production from bovine excreta by addition of various inert materials. Agric. Wastes 17, 153–156. doi:10.1016/0141-4607(86)90053-3

Gehring, T., Klang, J., Niedermayr, A., Berzio, S., Immenhauser, A., Klocke, M., Wichern, M., Lübken, M., 2015. Determination of Methanogenic Pathways through Carbon Isotope (δ^{13} C) Analysis for the Two-Stage Anaerobic Digestion of High-Solids Substrates. Environ. Sci. Technol. 49, 4705–4714. doi:10.1021/es505665z

Ghanem, A., Bados, P., Estaun, A.R., de Alencastro, L.F., Taibi, S., Einhorn, J., Mougin, C., 2007. Concentrations and specific loads of glyphosate, diuron, atrazine, nonylphenol and metabolites thereof in French urban sewage sludge. Chemosphere 69, 1368–1373. doi:10.1016/j.chemosphere.2007.05.022

Gieg, L.M., Fowler, S.J., Berdugo-Clavijo, C., 2014. Syntrophic biodegradation of hydrocarbon contaminants. Curr. Opin. Biotechnol. 27, 21–29. doi:10.1016/j.copbio.2013.09.002

Glaze, W.H., Kang, J.-W., Chapin, D.H., 1987. The Chemistry of Water Treatment Processes Involving Ozone, Hydrogen Peroxide and Ultraviolet Radiation. Ozone Sci. Eng. 9, 335–352. doi:10.1080/01919518708552148

Godon, J.-J., 2015. Aspects biochimiques et microbiologiques de la méthanisation, in: Moletta, R. (Ed.), La Méthanisation. Lavoisier, Paris, pp. 12–34.

Gomez, J.D., Denef, K., Stewart, C.E., Zheng, J., Cotrufo, M.F., 2014. Biochar addition rate influences soil microbial abundance and activity in temperate soils. Eur. J. Soil Sci. 65, 28–39. doi:10.1111/ejss.12097

Gong, X., Xu, X., Gong, Z., Li, X., Jia, C., Guo, M., Li, H., 2015. Remediation of PAH-contaminated soil at a gas manufacturing plant by a combined two-phase partition system washing and microbial degradation process. Environ. Sci. Pollut. Res. 22, 12001–12010. doi:10.1007/s11356-015-4466-y

Gorby, Y.A.Y., Yanina, S., McLean, J.S., Rosso, K.M., Moyles, D., Dohnalkova, A., Beveridge, T.J., Chang, I.S., Kim, B.H., Kim, K.S., Culley, D.E., Reed, S.B., Romine, M.F., Saffarini, D.A., Hill, E.A., Shi, L., Elias, D.A., Kennedy, D.W., Pinchuk, G., Watanabe, K., Ishii, S., Logan, B., Nealson, K.H., Fredrickson, J.K., 2009. Electrically conductive bacterial nanowires produced by Shewanella oneidensis strain MR-1 and other microorganisms. Proc. Natl. Acad. Sci. 106, 9535–9535. doi:10.1073/pnas.0905246106

Gray, J.L., Borch, T., Furlong, E.T., Davis, J.G., Yager, T.J., Yang, Y.Y., Kolpin, D.W., 2017. Rainfall-runoff of anthropogenic waste indicators from agricultural fields applied with municipal biosolids. Sci. Total Environ. 580, 83–89. doi:10.1016/j.scitotenv.2016.03.033

Gregory, K.B., Bond, D.R., Lovley, D.R., 2004. Graphite electrodes as electron donors for anaerobic respiration. Environ. Microbiol. 6, 596–604. doi:10.1111/j.1462-2920.2004.00593.x

Guedes, P., Mateus, E.P., Couto, N., Rodríguez, Y., Ribeiro, A.B., 2014. Electrokinetic remediation of six emerging organic contaminants from soil. Chemosphere 117, 124–131. doi:10.1016/j.chemosphere.2014.06.017

Guo, L., Li, X.M., Bo, X., Yang, Q., Zeng, G.M., Liao, D.X., Liu, J.J., 2008. Impacts of sterilization, microwave and ultrasonication pretreatment on hydrogen producing using waste sludge. Bioresour. Technol. 99, 3651–3658. doi:10.1016/j.biortech.2007.07.026

Guo, W., Ai, Y., Men, B., Wang, S., 2017. Adsorption of phenanthrene and pyrene by biochar produced from the excess sludge: experimental studies and theoretical analysis. Int. J. Environ. Sci. Technol. 14, 1889–1896. doi:10.1007/s13762-017-1272-

8

Guo, X., Liu, J., Xiao, B., 2013. Bioelectrochemical enhancement of hydrogen and methane production from the anaerobic digestion of sewage sludge in single-chamber membrane-free microbial electrolysis cells. Int. J. Hydrogen Energy 38, 1342–1347. doi:10.1016/j.ijhydene.2012.11.087

Habouzit, F., Gévaudan, G., Hamelin, J., Steyer, J.P., Bernet, N., 2011. Influence of support material properties on the potential selection of Archaea during initial adhesion of a methanogenic consortium. Bioresour. Technol. 102, 4054–4060. doi:10.1016/j.biortech.2010.12.023

Haftka, J.J.H., Parsons, J.R., Govers, H.A.J., 2009. Molecular simulation of polycyclic aromatic hydrocarbon sorption to black carbon. SAR QSAR Environ. Res. 20, 221–240. doi:10.1080/10629360902949336

Harrison, E.Z., Oakes, S.R., Hysell, M., Hay, A., 2006. Organic chemicals in sewage sludges. Sci. Total Environ. 367, 481–497. doi:10.1016/j.scitotenv.2006.04.002

Hatamian-Zarmi, A., Shojaosadati, S.A., Vasheghani-Farahani, E., Hosseinkhani, S., Emamzadeh, A., 2009. Extensive biodegradation of highly chlorinated biphenyl and Aroclor 1242 by Pseudomonas aeruginosa TMU56 isolated from contaminated soils. Int. Biodeterior. Biodegradation 63, 788–794. doi:10.1016/j.ibiod.2009.06.009

He, C.-S., Mu, Z.-X., Yang, H.-Y., Wang, Y.-Z., Mu, Y., Yu, H.-Q., 2015. Electron acceptors for energy generation in microbial fuel cells fed with wastewaters: A mini-review. Chemosphere 140, 12–17. doi:10.1016/j.chemosphere.2015.03.059

Hilber, I., Mayer, P., Gouliarmou, V., Hale, S.E., Cornelissen, G., Schmidt, H.-P., Bucheli, T.D., 2017. Bioavailability and bioaccessibility of polycyclic aromatic hydrocarbons from (post-pyrolytically treated) biochars. Chemosphere 174, 700–707. doi:10.1016/j.chemosphere.2017.02.014

Hori, T., Haruta, S., Ueno, Y., Ishii, M., Igarashi, Y., 2006. Dynamic Transition of a Methanogenic Population in Response to the Concentration of Volatile Fatty Acids in a Thermophilic Anaerobic Digester Dynamic Transition of a Methanogenic Population

in Response to the Concentration of Volatile Fatty Acids in a The. Appl. Environ. Microbiol. 72, 1623–1630. doi:10.1128/AEM.72.2.1623

Hou, B., Hu, Y., Sun, J., 2012. Performance and microbial diversity of microbial fuel cells coupled with different cathode types during simultaneous azo dye decolorization and electricity generation. Bioresour. Technol. 111, 105–110. doi:10.1016/j.biortech.2012.02.017

Hu, W.-J., Niu, C.-G., Wang, Y., Zeng, G.-M., Wu, Z., 2011. Nitrogenous heterocyclic compounds degradation in the microbial fuel cells. Process Saf. Environ. Prot. 89, 133–140. doi:10.1016/j.psep.2010.10.006

Huang, L., Jiang, L., Wang, Q., Quan, X., Yang, J., Chen, L., 2014. Cobalt recovery with simultaneous methane and acetate production in biocathode microbial electrolysis cells. Chem. Eng. J. 253, 281–290. doi:10.1016/j.cej.2014.05.080

Hung, C.V., Cam, B.D., Mai, P.T.N., Dzung, B.Q., 2015. Heavy metals and polycyclic aromatic hydrocarbons in municipal sewage sludge from a river in highly urbanized metropolitan area in Hanoi, Vietnam: levels, accumulation pattern and assessment of land application. Environ. Geochem. Health 37, 133–146. doi:10.1007/s10653-014-9635-2

Hunter, W.J., Manter, D.K., 2011. Increased Electrical Output when a Bacterial ABTS Oxidizer is Used in a Microbial Fuel Cell. Curr. Microbiol. 62, 633–638. doi:10.1007/s00284-010-9755-6

Iglesias, O., Sanromán, M.A., Pazos, M., 2014. Surfactant-Enhanced Solubilization and Simultaneous Degradation of Phenanthrene in Marine Sediment by Electro-Fenton Treatment. Ind. Eng. Chem. Res. 53, 2917–2923. doi:10.1021/ie4041115

INERIS, 2014. Substances emergentes dans les boues et composts de boues de station d'épuration d'eaux usées collectives- caractérisation et évaluation des risques sanitaires.

Jafary, T., Daud, W.R.W., Ghasemi, M., Kim, B.H., Md Jahim, J., Ismail, M., Lim, S.S., 2015. Biocathode in microbial electrolysis cell; Present status and future prospects.

Renew. Sustain. Energy Rev. 47, 23–33. doi:10.1016/j.rser.2015.03.003

Janex-Habibi, M.-L., Huyard, A., Esperanza, M., Bruchet, A., 2009. Reduction of endocrine disruptor emissions in the environment: The benefit of wastewater treatment. Water Res. 43, 1565–1576. doi:10.1016/j.watres.2008.12.051

Jiang, J., Pang, S.-Y., Ma, J., Liu, H., 2012. Oxidation of Phenolic Endocrine Disrupting Chemicals by Potassium Permanganate in Synthetic and Real Waters. Environ. Sci. Technol. 46, 1774–1781. doi:10.1021/es2035587

Jiang, Y.-B., Zhong, W.-H., Han, C., Deng, H., 2016. Characterization of electricity generated by soil in microbial fuel cells and the isolation of soil source exoelectrogenic bacteria. Front. Microbiol. 7, 1–10. doi:10.3389/fmicb.2016.01776

Jimenez, J., Lei, H., Steyer, J.P., Houot, S., Patureau, D., 2017. Methane production and fertilizing value of organic waste: Organic matter characterization for a better prediction of valorization pathways. Bioresour. Technol. 241, 1012–1021. doi:10.1016/j.biortech.2017.05.176

Jin, Z., Wang, X., Sun, Y., Ai, Y., Wang, X., 2015. Adsorption of 4- *n* -Nonylphenol and Bisphenol-A on Magnetic Reduced Graphene Oxides: A Combined Experimental and Theoretical Studies. Environ. Sci. Technol. 49, 9168–9175. doi:10.1021/acs.est.5b02022

Jobelius, C., Ruth, B., Griebler, C., Meckenstock, R.U., Hollender, J., Reineke, A., Frimmel, F.H., Zwiener, C., 2011. Metabolites Indicate Hot Spots of Biodegradation and Biogeochemical Gradients in a High-Resolution Monitoring Well. Environ. Sci. Technol. 45, 474–481. doi:10.1021/es1030867

Johnsen, A.R., Karlson, U., 2007. Diffuse PAH contamination of surface soils: Environmental occurrence, bioavailability, and microbial degradation. Appl. Microbiol. Biotechnol. 76, 533–543. doi:10.1007/s00253-007-1045-2

Jonker, M.T.O., Hawthorne, S.B., Koelmans, A.A., 2005. Extremely Slowly Desorbing Polycyclic Aromatic Hydrocarbons from Soot and Soot-like Materials: Evidence by Supercritical Fluid Extraction. Environ. Sci. Technol. 39, 7889–7895.

doi:10.1021/es0505191

Jorgensen, K.S., 2011. In Situ Bioremediation, 2nd ed, Comprehensive Biotechnology. Elsevier. doi:10.1016/B978-0-08-088504-9.00126-4

Ju, J.-H., Lee, I.-S., Sim, W.-J., Eun, H., Oh, J.-E., 2009. Analysis and evaluation of chlorinated persistent organic compounds and PAHs in sludge in Korea. Chemosphere 74, 441–447. doi:10.1016/j.chemosphere.2008.09.059

Kaminska, G., Bohdziewicz, J., 2009. POTENTIAL OF VARIOUS MATERIALS FOR ADSORPTION OF MICROPOLLUTANTS FROM WASTEWATER. Environ. Prot. Eng. 42, 161–178. doi:10.5277/epe160413

Karaca, G., Tasdemir, Y., 2015. Application of Advanced Oxidation Processes for Polycyclic Aromatic Hydrocarbons Removal from Municipal Treatment Sludge. CLEAN - Soil, Air, Water 43, 191–196. doi:10.1002/clen.201300395

Karaca, G., Tasdemir, Y., 2014. Polycyclic Aromatic Hydrocarbons (PAHs) Removal Applications in the Industrial Treatment Sludge using UV and TiO2. J. Residuals Sci. Technol. 11, 65–70.

Kato, S., Hashimoto, K., Watanabe, K., 2012. Microbial interspecies electron transfer via electric currents through conductive minerals. Proc. Natl. Acad. Sci. 109, 10042–10046. doi:10.1073/pnas.1117592109

Kato, S., Hashimoto, K., Watanabe, K., 2012. Methanogenesis facilitated by electric syntrophy via (semi)conductive iron-oxide minerals. Environ. Microbiol. 14, 1646–1654. doi:10.1111/j.1462-2920.2011.02611.x

Kazemi, S., Mousavi Kani, S.N., Ghasemi-Kasman, M., Aghapour, F., Khorasani, H., Moghadamnia, A.A., 2016. Nonylphenol induces liver toxicity and oxidative stress in rat. Biochem. Biophys. Res. Commun. 479, 17–21. doi:10.1016/j.bbrc.2016.08.164

Kazumi, J., Caldwell, M.E., Suflita, J.M., Lovley, D.R., Young, L.Y., 1997. Anaerobic Degradation of Benzene in Diverse Anoxic Environments. Environ. Sci. Technol. 31, 813–818. doi:10.1021/es960506a

Kehrer, J.P., 2000. The Haber–Weiss reaction and mechanisms of toxicity. Toxicology 149, 43–50.

Kelessidis, A., Stasinakis, A.S., 2012. Comparative study of the methods used for treatment and final disposal of sewage sludge in European countries. Waste Manag. 32, 1186–1195. doi:10.1016/j.wasman.2012.01.012

Keppler, F., Laukenmann, S., Rinne, J., Heuwinkel, H., Greule, M., Whiticar, M., Lelieveld, J., 2010. Measurements of ^{13}C/ ^{12}C Methane from Anaerobic Digesters: Comparison of Optical Spectrometry with Continuous-Flow Isotope Ratio Mass Spectrometry. Environ. Sci. Technol. 44, 5067–5073. doi:10.1021/es100460d

Khan, S., Wang, N., Reid, B.J., Freddo, A., Cai, C., 2013. Reduced bioaccumulation of PAHs by Lactuca satuva L. grown in contaminated soil amended with sewage sludge and sewage sludge derived biochar. Environ. Pollut. 175, 64–68. doi:10.1016/j.envpol.2012.12.014

Kiely, P.D., Regan, J.M., Logan, B.E., 2011. The electric picnic: Synergistic requirements for exoelectrogenic microbial communities. Curr. Opin. Biotechnol. 22, 378–385. doi:10.1016/j.copbio.2011.03.003

Kim, K.-H., Jahan, S.A., Kabir, E., Brown, R.J.C., 2013. A review of airborne polycyclic aromatic hydrocarbons (PAHs) and their human health effects. Environ. Int. 60, 71–80. doi:10.1016/j.envint.2013.07.019

Kimura, Z., Okabe, S., 2013. Acetate oxidation by syntrophic association between Geobacter sulfurreducens and a hydrogen-utilizing exoelectrogen. ISME J. 7, 1472–1482. doi:10.1038/ismej.2013.40

Kleemann, R., Meckenstock, R.U., 2011. Anaerobic naphthalene degradation by Gram-positive, iron-reducing bacteria. FEMS Microbiol. Ecol. 78, 488–496. doi:10.1111/j.1574-6941.2011.01193.x

Knecht, A.L., Goodale, B.C., Truong, L., Simonich, M.T., Swanson, A.J., Matzke, M.M., Anderson, K.A., Waters, K.M., Tanguay, R.L., 2013. Comparative developmental toxicity of environmentally relevant oxygenated PAHs. Toxicol. Appl. Pharmacol.

271, 266–275. doi:10.1016/j.taap.2013.05.006

Koch, C., Harnisch, F., 2016. Is there a Specific Ecological Niche for Electroactive Microorganisms? ChemElectroChem 3, 1282–1295. doi:10.1002/celc.201600079

Kołtowski, M., Hilber, I., Bucheli, T.D., Oleszczuk, P., 2016. Effect of activated carbon and biochars on the bioavailability of polycyclic aromatic hydrocarbons in different industrially contaminated soils. Environ. Sci. Pollut. Res. 23, 11058–11068. doi:10.1007/s11356-016-6196-1

Kong, F., Wang, A., Ren, H.-Y.Y., Huang, L., Xu, M., Tao, H., 2014. Improved dechlorination and mineralization of 4-chlorophenol in a sequential biocathode-bioanode bioelectrochemical system with mixed photosynthetic bacteria. Bioresour. Technol. 158, 32–38. doi:10.1016/j.biortech.2014.01.142

Kouzuma, A., Kato, S., Watanabe, K., 2015. Microbial interspecies interactions: Recent findings in syntrophic consortia. Front. Microbiol. doi:10.3389/fmicb.2015.00477

Kronenberg, M., Trably, E., Bernet, N., Patureau, D., 2017. Biodegradation of polycyclic aromatic hydrocarbons: Using microbial bioelectrochemical systems to overcome an impasse. Environ. Pollut. 231, 509–523. doi:10.1016/j.envpol.2017.08.048

Kruk, M., Li, Z., Jaroniec, M., Betz, W.R., 1999. Nitrogen Adsorption Study of Surface Properties of Graphitized Carbon Blacks. Langmuir 15, 1435–1441. doi:10.1021/la980493+

Kubicki, J.D., 2006. Molecular Simulations of Benzene and PAH Interactions with Soot. Environ. Sci. Technol. 40, 2298–2303. doi:10.1021/es051083s

Kuila, U., Prasad, M., 2013. Specific surface area and pore-size distribution in clays and shales. Geophys. Prospect. 61, 341–362. doi:10.1111/1365-2478.12028

Kunapuli, U., Jahn, M.K., Lueders, T., Geyer, R., Heipieper, H.J., Meckenstock, R.U., 2010. Desulfitobacterium aromaticivorans sp. nov. and Geobacter toluenoxydans sp. nov., iron-reducing bacteria capable of anaerobic degradation of monoaromatic hydrocarbons. Int. J. Syst. Evol. Microbiol. 60, 686–695. doi:10.1099/ijs.0.003525-0

Kunapuli, U., Lueders, T., Meckenstock, R.U., 2007. The use of stable isotope probing to identify key iron-reducing microorganisms involved in anaerobic benzene degradation. ISME J. 1, 643–653. doi:10.1038/ismej.2007.73

Lan, J., Sun, Y., Xiao, S., Yuan, D., 2016. Polycyclic aromatic hydrocarbon contamination in a highly vulnerable underground river system in Chongqing, Southwest China. J. Geochemical Explor. 168, 65–71. doi:10.1016/j.gexplo.2016.05.013

Langdon, K.A., Warne, M.S.J., Smernik, R.J., Shareef, A., Kookana, R.S., 2011. Selected personal care products and endocrine disruptors in biosolids: An Australia-wide survey. Sci. Total Environ. 409, 1075–1081. doi:10.1016/j.scitotenv.2010.12.013

Laperrière, W., Barry, B., Torrijos, M., Pechiné, B., Bernet, N., Steyer, J.P., 2017. Optimal conditions for flexible methane production in a demand-based operation of biogas plants 245, 698–705. doi:10.1016/j.biortech.2017.09.013

Laszlova, K., Dercova, K., Horvathova, H., Murinova, S., Skarba, J., Dudasova, H., 2016. Assisted bioremediation approaches - Biostimulation and bioaugmentation - Used in the removal of organochlorinated pollutants from the contaminated bottom sediments. Int. J. Environ. Res. 10, 367–378.

LeBlanc, R.J., Matthews, P., Richard, R.P., 2009. Global atlas of excreta, wastewater sludge, and biosolids management: moving forward the sustainable and welcome uses of a global resource.

Leduc, R., Samson, R., Al-Bashir, B., Al-Hawari, J., Cseh, T., 1992. Biotic and Abiotic Disappearance of Four PAH Compounds from Flooded Soil under Various Redox Conditions. Water Sci. Technol. 26, 51–60.

Lee, Y., Bae, S., Moon, C., Lee, W., 2015. Flavin mononucleotide mediated microbial fuel cell in the presence of Shewanella putrefaciens CN32 and iron-bearing mineral. Biotechnol. Bioprocess Eng. 20, 894–900. doi:10.1007/s12257-015-0031-2

Li, C.-H., Wong, Y.-S., Tam, N.F.-Y., 2010. Anaerobic biodegradation of polycyclic aromatic hydrocarbons with amendment of iron(III) in mangrove sediment slurry. Bioresour. Technol. 101, 8083–8092. doi:10.1016/j.biortech.2010.06.005

Li, L.L., Tong, Z.H., Fang, C.Y., Chu, J., Yu, H.Q., 2015. Response of anaerobic granular sludge to single-wall carbon nanotube exposure. Water Res. 70, 1–8. doi:10.1016/j.watres.2014.11.042

Li, T., Guo, S., Wu, B., Li, F., Niu, Z., 2010. Effect of electric intensity on the microbial degradation of petroleum pollutants in soil. J. Environ. Sci. 22, 1381–1386. doi:10.1016/S1001-0742(09)60265-5

Li, X., Wang, X., Ren, Z.J., Zhang, Y., Li, N., Zhou, Q., 2015. Sand amendment enhances bioelectrochemical remediation of petroleum hydrocarbon contaminated soil. Chemosphere 141, 62–70. doi:10.1016/j.chemosphere.2015.06.025

Li, X., Wang, X., Wan, L., Zhang, Y., Li, N., Li, D., Zhou, Q., 2016a. Enhanced biodegradation of aged petroleum hydrocarbons in soils by glucose addition in microbial fuel cells. J. Chem. Technol. Biotechnol. 91, 267–275. doi:10.1002/jctb.4660

Li, X., Wang, X., Zhang, Y., Cheng, L., Liu, J., Li, F., Gao, B., Zhou, Q., 2014. Extended petroleum hydrocarbon bioremediation in saline soil using Pt-free multianodes microbial fuel cells. RSC Adv. 4, 59803–59808. doi:10.1039/C4RA10673C

Li, X., Wang, X., Zhang, Y., Zhao, Q., Yu, B., Li, Y., Zhou, Q., 2016b. Salinity and Conductivity Amendment of Soil Enhanced the Bioelectrochemical Degradation of Petroleum Hydrocarbons. Sci. Rep. 6, 1–11. doi:10.1038/srep32861

Li, X., Wang, X., Zhao, Q., Wan, L., Li, Y., Zhou, Q., 2016c. Carbon fiber enhanced bioelectricity generation in soil microbial fuel cells. Biosens. Bioelectron. 85, 135–141. doi:10.1016/j.bios.2016.05.001

Liang, L., Song, X., Kong, J., Shen, C., Huang, T., Hu, Z., 2014. Anaerobic biodegradation of high-molecular-weight polycyclic aromatic hydrocarbons by a facultative anaerobe Pseudomonas sp. JP1. Biodegradation 25, 825–833. doi:10.1007/s10532-014-9702-5

Liao, X., Zhang, C., Yao, L., Li, J., Liu, M., Xu, L., Evalde, M., 2014. Sorption behavior of nonylphenol (NP) on sewage-irrigated soil: Kinetic and thermodynamic studies. Sci. Total Environ. 473–474, 530–536. doi:10.1016/j.scitotenv.2013.12.055

Lin, C., Liao, J., Wu, H., Wei, C., 2016. Mechanism of Ozone Oxidation of Polycyclic Aromatic Hydrocarbons During the Reduction of Coking Wastewater Sludge. CLEAN - Soil, Air, Water 44, 1499–1507. doi:10.1002/clen.201400326

Lin, R., Cheng, J., Zhang, J., Zhou, J., Cen, K., Murphy, J.D., 2017. Boosting biomethane yield and production rate with graphene: The potential of direct interspecies electron transfer in anaerobic digestion. Bioresour. Technol. 239, 345–352. doi:10.1016/j.biortech.2017.05.017

Lintelmann, J., Katayama, A., Kurihara, N., Shore, L., Wenzel, A., 2003. Endocrine disruptors in the environment (IUPAC Technical Report). Pure Appl. Chem. 75, 631–681. doi:10.1351/pac200375050631

Liu, F., Rotaru, A.-E., Shrestha, P.M., Malvankar, N.S., Nevin, K.P., Lovley, D.R., 2012. Promoting direct interspecies electron transfer with activated carbon. Energy Environ. Sci. 5, 8982–8989. doi:10.1039/c2ee22459c

Liu, H., Cheng, S., Logan, B.E., 2005. Production of Electricity from Acetate or Butyrate Using a Single-Chamber Microbial Fuel Cell. Environ. Sci. Technol. 39, 658–662. doi:10.1021/es048927c

Liu, L., Chen, P., Sun, M., Shen, G., Shang, G., 2015. Effect of biochar amendment on PAH dissipation and indigenous degradation bacteria in contaminated soil. J. Soils Sediments 15, 313–322. doi:10.1007/s11368-014-1006-1

Liu, Y.-C., Zhou, T.-T., Zhang, J., Xu, L., Zhang, Z.-H., Shen, Q.-R., Shen, B., 2009. Molecular characterization of the alkB gene in the thermophilic Geobacillus sp. strain MH-1. Res. Microbiol. 160, 560–566. doi:10.1016/j.resmic.2009.08.010

Logan, B.E., 2008. Microbial fuel cells. John Wiley & Sons, Inc., Hoboken, New Yersey.

Logan, B.E., Hamelers, B., Rozendal, R., Schröder, U., Keller, J., Freguia, S., Aelterman, P., Verstraete, W., Rabaey, K., 2006. Microbial fuel cells: Methodology and technology. Environ. Sci. Technol. 40, 5181–5192. doi:10.1021/es0605016

Logan, B.E., Rabaey, K., 2012. Conversion of Wastes into Bioelectricity and Chemicals by

Using Microbial Electrochemical Technologies. Science (80-.). 337, 686–690. doi:10.1126/science.1217412

Logan, B.E., Regan, J.M., 2006. Electricity-producing bacterial communities in microbial fuel cells. Trends Microbiol. 14, 512–518. doi:10.1016/j.tim.2006.10.003

Lohner, S.T., Deutzmann, J.S., Logan, B.E., Leigh, J., Spormann, A.M., 2014. Hydrogenase-independent uptake and metabolism of electrons by the archaeon Methanococcus maripaludis. ISME J. 8, 1673–1681. doi:10.1038/ismej.2014.82

Lovley, D.R., 2006. Bug juice: harvesting electricity with microorganisms. Nat. Rev. Microbiol. 4, 497–508. doi:10.1038/nrmicro1442

Lovley, D.R., Giovannoni, S.J., White, D.C., Champine, J.E., Phillips, E.J.P., Gorby, Y.A., Goodwin, S., 1993. Geobacter metallireducens gen. nov. sp. nov., a microorganism capable of coupling the complete oxidation of organic compounds to the reduction of iron and other metals. Arch. Microbiol. 159, 336–344. doi:10.1007/BF00290916

Lowell, S., Shields, J.E., Thomas, M.A., Thommes, M., 2004. Characterization of porous solids and powders : surface area, pore size, and density. Kluwer Academic Publishers, Dordrecht, Netherlands.

Lu, J., Jin, Q., He, Y., Wu, J., Zhang, W., Zhao, J., 2008. Anaerobic degradation behavior of nonylphenol polyethoxylates in sludge. Chemosphere 71, 345–351. doi:10.1016/j.chemosphere.2007.08.068

Lu, L., Huggins, T., Jin, S., Zuo, Y., Ren, Z.J., 2014a. Microbial Metabolism and Community Structure in Response to Bioelectrochemically Enhanced Remediation of Petroleum Hydrocarbon-Contaminated Soil. Environ. Sci. Technol. 48, 4021–4029. doi:10.1021/es4057906

Lu, L., Xing, D., Ren, N., Logan, B.E., 2012. Syntrophic interactions drive the hydrogen production from glucose at low temperature in microbial electrolysis cells. Bioresour. Technol. 124, 68–76. doi:10.1016/j.biortech.2012.08.040

Lu, L., Yazdi, H., Jin, S., Zuo, Y., Fallgren, P.H., Ren, Z.J., 2014b. Enhanced

bioremediation of hydrocarbon-contaminated soil using pilot-scale bioelectrochemical systems. J. Hazard. Mater. 274, 8–15. doi:10.1016/j.jhazmat.2014.03.060

Lübeck, J.S., Poulsen, K.G., Knudsen, S.B., Soleimani, M., Furbo, S., Tomasi, G., Christensen, J.H., 2016. Source apportionment of polycyclic aromatic hydrocarbons (PAHs) in sediments from Khuzestan province, Iran. Mar. Pollut. Bull. 110, 584–590. doi:10.1016/j.marpolbul.2016.05.057

Luo, L., Gu, J.-D., 2016. Alteration of extracellular enzyme activity and microbial abundance by biochar addition: Implication for carbon sequestration in subtropical mangrove sediment. J. Environ. Manage. 182, 29–36. doi:10.1016/j.jenvman.2016.07.040

Ma, C., Wang, Y., Zhuang, L., Huang, D., Zhou, S., Li, F., 2011. Anaerobic degradation of phenanthrene by a newly isolated humus-reducing bacterium, Pseudomonas aeruginosa strain PAH-1. J. Soils Sediments 11, 923–929. doi:10.1007/s11368-011-0368-x

Ma, X.-K., Ding, N., Peterson, E.C., 2015. Bioaugmentation of soil contaminated with high-level crude oil through inoculation with mixed cultures including Acremonium sp. Biodegradation 26, 259–269. doi:10.1007/s10532-015-9732-7

Macijauskienė, B., Griškonis, E., 2015. Ultrasound assisted modification of graphite felt with electroless silver – Part 1: composition, morphology, structure and electrical conductivity. Chemija 26, 1–8.

Maillacheruvu, K.Y., Pathan, I. a, 2009. Biodegradation of naphthalene, phenanthrene, and pyrene under anaerobic conditions. J. Environ. Sci. Health. A. Tox. Hazard. Subst. Environ. Eng. 44, 1315–1326. doi:10.1080/10934520903212956

Malvankar, N.S., Lovley, D.R., 2014. Microbial nanowires for bioenergy applications. Curr. Opin. Biotechnol. 27, 88–95. doi:10.1016/j.copbio.2013.12.003

Malvankar, N.S., Tuominen, M.T., Lovley, D.R., 2012. Lack of cytochrome involvement in long-range electron transport through conductive biofilms and nanowires of Geobacter sulfurreducens. Energy Environ. Sci. 8651–8659. doi:10.1039/c2ee22330a

Malvankar, N.S., Vargas, M., Nevin, K.P., Franks, A.E., Leang, C., Kim, B.-C., Inoue, K., Mester, T., Covalla, S.F., Johnson, J.P., Rotello, V.M., Tuominen, M.T., Lovley, D.R., 2011. Tunable metallic-like conductivity in microbial nanowire networks. Nat. Nanotechnol. 6, 573–579. doi:10.1038/nnano.2011.119

Manzetti, S., 2012. Ecotoxicity of polycyclic aromatic hydrocarbons, aromatic amines, and nitroarenes through molecular properties. Environ. Chem. Lett. 10, 349–361. doi:10.1007/s10311-012-0368-0

Mao, Z., Zheng, X.-F., Zhang, Y.-Q., Tao, X.-X., Li, Y., Wang, W., 2012. Occurrence and Biodegradation of Nonylphenol in the Environment. Int. J. Mol. Sci. 13, 491–505. doi:10.3390/ijms13010491

Martín, J., Santos, J.L., Aparicio, I., Alonso, E., 2015. Pharmaceutically active compounds in sludge stabilization treatments: Anaerobic and aerobic digestion, wastewater stabilization ponds and composting. Sci. Total Environ. 503–504, 97–104. doi:10.1016/j.scitotenv.2014.05.089

Martin Ruel, S., Esperanza, M., Choubert, J.-M., Valor, I., Budzinski, H., Coquery, M., 2010. On-site evaluation of the efficiency of conventional and advanced secondary processes for the removal of 60 organic micropollutants. Water Sci. Technol. 62, 2970–2978. doi:10.2166/wst.2010.989

Mclnerney, M.J., Coates, J.D., Bhupathiraju, V.K., Lovley, D.R., Achenbach, L.A., 2001. Geobacter hydrogenophilus, Geobacter chapellei and Geobacter grbiciae, three new, strictly anaerobic, dissimilatory Fe(III)-reducers. Int. J. Syst. Evol. Microbiol. 51, 581–588. doi:10.1099/00207713-51-2-581

McNamara, P.J., Wilson, C.A., Wogen, M.T., Murthy, S.N., Novak, J.T., Novak, P.J., 2012. The effect of thermal hydrolysis pretreatment on the anaerobic degradation of nonylphenol and short-chain nonylphenol ethoxylates in digested biosolids. Water Res. 46, 2937–2946. doi:10.1016/j.watres.2012.03.015

Meckenstock, R.U., Annweiler, E., Michaelis, W., Richnow, H.H., Schink, B., 2000. Anaerobic naphthalene degradation by a sulfate-reducing enrichment culture. Appl.

Environ. Microbiol. 66, 2743–2747. doi:10.1128/AEM.66.7.2743-2747.2000

Meckenstock, R.U., Safinowski, M., Griebler, C., 2004. Anaerobic degradation of polycyclic aromatic hydrocarbons. FEMS Microbiol. Ecol. 49, 27–36. doi:10.1016/j.femsec.2004.02.019

Mena, E., Villaseñor, J., Cañizares, P., Rodrigo, M.A., 2014. Effect of a direct electric current on the activity of a hydrocarbon-degrading microorganism culture used as the flushing liquid in soil remediation processes. Sep. Purif. Technol. 124, 217–223. doi:10.1016/j.seppur.2014.01.027

Meng, X.-Z., Venkatesan, A.K., Ni, Y.-L., Steele, J.C., Wu, L.-L., Bignert, A., Bergman, Å., Halden, R.U., 2016. Organic Contaminants in Chinese Sewage Sludge: A Meta-Analysis of the Literature of the Past 30 Years. Environ. Sci. Technol. 50, 5454–5466. doi:10.1021/acs.est.5b05583

Mihelcic, J.R., Luthy, R.G., 1988. Degradation of polycyclic aromatic hydrocarbon compounds under various redox conditions in soil-water systems. Appl. Environ. Microbiol. 54, 1182–1187.

Mittal, M., Rockne, K.J., 2010. Diffusional losses of amended anaerobic electron acceptors in sediment field microcosms. Mar. Pollut. Bull. 60, 1217–1225. doi:10.1016/j.marpolbul.2010.03.026

Moletta, R., 2015. La méthanisation, 3rd ed. Lavoisier, Paris.

Monlau, F., Sambusiti, C., Barakat, A., Guo, X.M., Latrille, E., Trably, E., Steyer, J.-P., Carrere, H., 2012. Predictive Models of Biohydrogen and Biomethane Production Based on the Compositional and Structural Features of Lignocellulosic Materials. Environ. Sci. Technol. 46, 12217–12225. doi:10.1021/es303132t

Montero, B., Garcia-Morales, J.L., Sales, D., Solera, R., 2008. Evolution of microorganisms in thermophilic-dry anaerobic digestion. Bioresour. Technol. 99, 3233–3243. doi:10.1016/j.biortech.2007.05.063

Morasch, B., Schink, B., Tebbe, C.C., Meckenstock, R.U., 2004. Degradation of o -xylene

and m -xylene by a novel sulfate-reducer belonging to the genus Desulfotomaculum. Arch. Microbiol. 181, 407–417. doi:10.1007/s00203-004-0672-6

Morris, J.M., Jin, S., 2012. Enhanced biodegradation of hydrocarbon-contaminated sediments using microbial fuel cells. J. Hazard. Mater. 213–214, 474–477. doi:10.1016/j.jhazmat.2012.02.029

Morris, J.M., Jin, S., Crimi, B., Pruden, A., 2009. Microbial fuel cell in enhancing anaerobic biodegradation of diesel. Chem. Eng. J. 146, 161–167. doi:10.1016/j.cej.2008.05.028

Moscoviz, R., de Fouchécour, F., Santa-Catalina, G., Bernet, N., Trably, E., 2017. Cooperative growth of Geobacter sulfurreducens and Clostridium pasteurianum with subsequent metabolic shift in glycerol fermentation. Sci. Rep. 7, 1–9. doi:10.1038/srep44334

Moscoviz, R., Trably, E., Bernet, N., 2016. Consistent 1,3-propanediol production from glycerol in mixed culture fermentation over a wide range of pH. Biotechnol. Biofuels 9, 1–11. doi:10.1186/s13068-016-0447-8

Moura, M.N., Martín, M.J., Burguillo, F.J., 2007. A comparative study of the adsorption of humic acid, fulvic acid and phenol onto Bacillus subtilis and activated sludge. J. Hazard. Mater. 149, 42–48. doi:10.1016/j.jhazmat.2007.02.074

Mozo, I., Stricot, M., Lesage, N., Spérandio, M., 2011. Fate of hazardous aromatic substances in membrane bioreactors. Water Res. 45, 4551–4561. doi:10.1016/j.watres.2011.06.005

Mu, Y., Rozendal, R.A., Rabaey, K., Keller, J., 2009. Nitrobenzene removal in bioelectrochemical systems. Environ. Sci. Technol. 43, 8690–8695. doi:10.1021/es9020266

Mumme, J., Srocke, F., Heeg, K., Werner, M., 2014. Use of biochars in anaerobic digestion. Bioresour. Technol. 164, 189–197. doi:10.1016/j.biortech.2014.05.008

Murdoch, F.K., Sanin, F.D., 2016. Biotransformation of Nonylphenol Diethoxylate in

anaerobic digesters: Accumulation of metabolites and their effects on digester performance. Int. Biodeterior. Biodegradation 110, 61–68. doi:10.1016/j.ibiod.2016.02.017

Musat, F., Galushko, A., Jacob, J., Widdel, F., Kube, M., Reinhardt, R., Wilkes, H., Schink, B., Rabus, R., 2009. Anaerobic degradation of naphthalene and 2-methylnaphthalene by strains of marine sulfate-reducing bacteria. Environ. Microbiol. 11, 209–219. doi:10.1111/j.1462-2920.2008.01756.x

Nam, K., Rodriguez, W., Kukor, J.J., 2001. Enhanced degradation of polycyclic aromatic hydrocarbons by biodegradation combined with a modified Fenton reaction. Chemosphere 45, 11–20. doi:10.1016/S0045-6535(01)00051-0

Nascimento, A.E.G., Barros Neto, E.L., Moura, M.C.P.A., Castro Dantas, T.N., Dantas Neto, A.A., 2015. Wettability of paraffin surfaces by nonionic surfactants: Evaluation of surface roughness and nonylphenol ethoxylation degree. Colloids Surfaces A Physicochem. Eng. Asp. 480, 376–383. doi:10.1016/j.colsurfa.2014.11.003

Newcombe, G., Hayes, R., Drikas, M., 1993. Granular activated carbon : importance of surface properties in the adsorption of naturally occurring organics ' 78, 65–71.

Nguyen, V., Karunakaran, E., Collins, G., Biggs, C.A., 2016. Physicochemical analysis of initial adhesion and biofilm formation of Methanosarcina barkeri on polymer support material. Colloids Surfaces B Biointerfaces 143, 518–525. doi:10.1016/j.colsurfb.2016.03.042

Nimje, V.R., Chen, C.-Y., Chen, C.-C., Jean, J.-S., Reddy, a. S., Fan, C.-W., Pan, K.-Y., Liu, H.-T., Chen, J.-L., 2009. Stable and high energy generation by a strain of Bacillus subtilis in a microbial fuel cell. J. Power Sources 190, 258–263. doi:10.1016/j.jpowsour.2009.01.019

Ning, X., Shen, L., Sun, J., Lin, C., Zhang, Y., Yang, Z., Chen, S., 2015. Degradation of polycyclic aromatic hydrocarbons (PAHs) in textile dyeing sludge by O_3/H_2O_2 treatment. RSC Adv. 5, 38021–38029. doi:10.1039/C5RA03307A

Noorimotlagh, Z., Haghighi, N.J., Ahmadimoghadam, M., Rahim, F., 2017. An updated

systematic review on the possible effect of nonylphenol on male fertility. Environ. Sci. Pollut. Res. 24, 3298–3314. doi:10.1007/s11356-016-7960-y

Noutsopoulos, C., Mamais, D., Mpouras, T., Kokkinidou, D., Samaras, V., Antoniou, K., Gioldasi, M., 2014. The role of activated carbon and disinfection on the removal of endocrine disrupting chemicals and non-steroidal anti-inflammatory drugs from wastewater. Environ. Technol. (United Kingdom) 35, 698–708. doi:10.1080/09593330.2013.846923

Ouellette, J., dos Santos, S.C.C., Lépine, F., Juteau, P., Déziel, E., Villemur, R., 2013. High absorption of endocrine disruptors by Hytrel: towards the development of a two-phase partitioning bioreactor. J. Chem. Technol. Biotechnol. 88, 119–125. doi:10.1002/jctb.3864

Pacurari, M., Yin, X.J., Zhao, J., Ding, M., Leonard, S.S., Schwegler-Berry, D., Ducatman, B.S., Sbarra, D., Hoover, M.D., Castranova, V., Vallyathan, V., 2008. Raw single-wall carbon nanotubes induce oxidative stress and activate MAPKs, AP-1, NF-κB, and Akt in normal and malignant human mesothelial cells. Environ. Health Perspect. 116, 1211–1217. doi:10.1289/ehp.10924

Pandey, B., Fulekar, M., 2012. Bioremediation technology: A new horizon for environmental clean- up. Biol. Med. 4, 51–59.

Parameswaran, P., Torres, C.I., Lee, H.-S., Krajmalnik-Brown, R., Rittmann, B.E., 2009. Syntrophic interactions among anode respiring bacteria (ARB) and Non-ARB in a biofilm anode: electron balances. Biotechnol. Bioeng. 103, 513–523. doi:10.1002/bit.22267

Parameswaran, P., Torres, C.I., Lee, H.-S., Rittmann, B.E., Krajmalnik-Brown, R., 2011. Hydrogen consumption in microbial electrochemical systems (MXCs): The role of homo-acetogenic bacteria. Bioresour. Technol. 102, 263–271. doi:10.1016/j.biortech.2010.03.133

Park, D.H., Zeikus, J.G., 2000. Electricity Generation in Microbial Fuel Cells Using Neutral Red as an Electronophore Electricity Generation in Microbial Fuel Cells

Using Neutral Red as an Electronophore. Appl. Environ. Microbiol. 66, 1292–1297. doi:10.1128/AEM.66.4.1292-1297.2000.Updated

Park, Y.H., Smith, G., Park, E., 2016. Mediator-less microbial fuel cell employing *Shewanella Oneidensis*. Energy Sources, Part A Recover. Util. Environ. Eff. 38, 1779–1784. doi:10.1080/15567036.2014.969815

Pasquini, L.M., Sekol, R.C., Taylor, A.D., Pfefferle, L.D., Zimmerman, J.B., 2013. Realizing Comparable Oxidative and Cytotoxic Potential of Single- and Multiwalled Carbon Nanotubes through Annealing. Environ. Sci. Technol. 47, 8775–8783. doi:10.1021/es401786s

Paterakis, N., Chiu, T.Y., Koh, Y.K.K., Lester, J.N., McAdam, E.J., Scrimshaw, M.D., Soares, A., Cartmell, E., 2012. The effectiveness of anaerobic digestion in removing estrogens and nonylphenol ethoxylates. J. Hazard. Mater. 199–200, 88–95. doi:10.1016/j.jhazmat.2011.10.075

Patureau, D., Delgenes, N., Delgenes, J.-P., 2008. Impact of sewage sludge treatment processes on the removal of the endocrine disrupters nonylphenol ethoxylates. Chemosphere 72, 586–591. doi:10.1016/j.chemosphere.2008.03.007

Patureau, D., Trably, E., 2006. Impact of anaerobic and aerobic processes on polychlorobiphenyl removal in contaminated sewage sludge. Biodegradation 17, 9–17. doi:10.1007/s10532-005-1920-4

Pauleau, Y., Barna, P.B. (Eds.), 1997. Protective coatings and thin films: synthesis, characterization, and applications. Springer.

Pelloni, S., Lazzeretti, P., 2018. Polygonal current models for polycyclic aromatic hydrocarbons and graphene sheets of various shapes. J. Comput. Chem. 39, 21–34. doi:10.1002/jcc.25076

Pera-Titus, M., García-Molina, V., Baños, M.A., Giménez, J., Esplugas, S., 2004. Degradation of chlorophenols by means of advanced oxidation processes: a general review. Appl. Catal. B Environ. 47, 219–256. doi:10.1016/j.apcatb.2003.09.010

Pereira, L., Dias, P., Soares, O.S.G.P., Ramalho, P.S.F., Pereira, M.F.R., Alves, M.M., 2017. Synthesis, characterization and application of magnetic carbon materials as electron shuttles for the biological and chemical reduction of the azo dye Acid Orange 10. Appl. Catal. B Environ. 212, 175–184. doi:10.1016/j.apcatb.2017.04.060

Pérez-Leblic, M.I., Turmero, A., Hernández, M., Hernández, a. J., Pastor, J., Ball, a. S., Rodríguez, J., Arias, M.E., 2012. Influence of xenobiotic contaminants on landfill soil microbial activity and diversity. J. Environ. Manage. 95, S285–S290. doi:10.1016/j.jenvman.2010.07.017

Perrotta, A.R., Kumaraswamy, R., Bastidas-Oyanedel, J.R., Alm, E.J., Rodríguez, J., 2017. Inoculum composition determines microbial community and function in an anaerobic sequential batch reactor. PLoS One 12, 1–14. doi:10.1371/journal.pone.0171369

Pieper, D.H., Seeger, M., 2008. Bacterial Metabolism of Polychlorinated Biphenyls. J. Mol. Microbiol. Biotechnol. 15, 121–138. doi:10.1159/000121325

Pierson, H.O., 1994. Handbook of carbon, graphite, diamond, and fullerenes: properties, processing, and applications, 1st ed.

Pietikainen, J., Kiikkila, O., Fritze, H., 2000. Charcoal as a habitat for microbes and its effect on the microbial community of the underlying humus. Oikos 89, 231–242. doi:10.1034/j.1600-0706.2000.890203.x

Pignatello, J.J., Oliveros, E., MacKay, A., 2006. Advanced Oxidation Processes for Organic Contaminant Destruction Based on the Fenton Reaction and Related Chemistry. Crit. Rev. Environ. Sci. Technol. 36, 1–84. doi:10.1080/10643380500326564

Plósz, B.G., Langford, K.H., Thomas, K. V., 2012. An activated sludge modeling framework for xenobiotic trace chemicals (ASM-X): Assessment of diclofenac and carbamazepine. Biotechnol. Bioeng. 109, 2757–2769. doi:10.1002/bit.24553

Pomiès, M., Choubert, J.-M., Wisniewski, C., Coquery, M., 2013. Modelling of micropollutant removal in biological wastewater treatments: A review. Sci. Total Environ. 443, 733–748. doi:10.1016/j.scitotenv.2012.11.037

Popp, N., Schlomann, M., Mau, M., 2006. Bacterial diversity in the active stage of a bioremediation system for mineral oil hydrocarbon-contaminated soils. Microbiology 152, 3291–3304. doi:10.1099/mic.0.29054-0

Prince, R.C., Butler, J.D., Redman, A.D., 2017. The Rate of Crude Oil Biodegradation in the Sea. Environ. Sci. Technol. 51, 1278–1284. doi:10.1021/acs.est.6b03207

Qiang, Z., Nie, Y., Ben, W., Qu, J., Zhang, H., 2013. Degradation of endocrine-disrupting chemicals during activated sludge reduction by ozone. Chemosphere 91, 366–373. doi:10.1016/j.chemosphere.2012.11.069

Qiao, M., Cao, W., Liu, B., Bai, Y., Qi, W., Zhao, X., Qu, J., 2017. Impact of upgrading wastewater treatment plant on the removal of typical methyl, oxygenated, chlorinated and parent polycyclic aromatic hydrocarbons. Sci. Total Environ. 603–604, 140–147. doi:10.1016/j.scitotenv.2017.06.097

Qiao, Y., Qiao, Y.-J., Zou, L., Ma, C.-X., Liu, J.-H., 2015. Real-time monitoring of phenazines excretion in Pseudomonas aeruginosa microbial fuel cell anode using cavity microelectrodes. Bioresour. Technol. 198, 1–6. doi:10.1016/j.biortech.2015.09.002

Qu, Y., Wang, J., Zhou, H., Ma, Q., Zhang, Z., Li, D., Shen, W., Zhou, J., 2016. Concentration-dependent effects of carbon nanotubes on growth and biphenyl degradation of Dyella ginsengisoli LA-4. Environ. Sci. Pollut. Res. 23, 2864–2872. doi:10.1007/s11356-015-5532-1

Quan, X., Quan, Y., Tao, K., 2012. Effect of anode aeration on the performance and microbial community of an air–cathode microbial fuel cell. Chem. Eng. J. 210, 150–156. doi:10.1016/j.cej.2012.09.009

Rabus, R., Boll, M., Heider, J., Meckenstock, R.U., Buckel, W., Einsle, O., Ermler, U., Golding, B.T., Gunsalus, R.P., Kroneck, P.M.H., Krüger, M., Lueders, T., Martins, B.M., Musat, F., Richnow, H.H., Schink, B., Seifert, J., Szaleniec, M., Treude, T., Ullmann, G.M., Vogt, C., Von Bergen, M., Wilkes, H., 2016. Anaerobic microbial degradation of hydrocarbons: From enzymatic reactions to the environment. J. Mol.

Microbiol. Biotechnol. 26, 5–28. doi:10.1159/000443997

Rafrafi, Y., Trably, E., Hamelin, J., Latrille, E., Meynial-Salles, I., Benomar, S., Giudici-Orticoni, M.T., Steyer, J.P., 2013. Sub-dominant bacteria as keystone species in microbial communities producing bio-hydrogen. Int. J. Hydrogen Energy 38, 4975–4985. doi:10.1016/j.ijhydene.2013.02.008

Rattan, S., Zhou, C., Chiang, C., Mahalingam, S., Brehm, E., Flaws, J.A., 2017. Exposure to endocrine disruptors during adulthood: consequences for female fertility. J. Endocrinol. 233, R109–R129. doi:10.1530/JOE-17-0023

Reguera, G., McCarthy, K.D., Mehta, T., Nicoll, J.S., Tuominen, M.T., Lovley, D.R., 2005. Extracellular electron transfer via microbial nanowires. Nature 435, 1098–1101. doi:10.1038/nature03661

Rehmann, L., Prpich, G.P., Daugulis, A.J., 2008. Remediation of PAH contaminated soils: Application of a solid–liquid two-phase partitioning bioreactor. Chemosphere 73, 798–804. doi:10.1016/j.chemosphere.2008.06.006

Reimers, C.E., Tender, L.M., Fertig, S., Wang, W., 2001. Harvesting Energy from the Marine Sediment−Water Interface. Environ. Sci. Technol. 35, 192–195. doi:10.1021/es001223s

Rhee, G.-Y., Sokol, R.C., Bethoney, C.M., Cho, Y.-C., Frohnhoefer, R.C., Erkkila, T., 2001. Kinetics of polychlorinated biphenyl dechlorination and growth of dechlorinating microorganism. Environ. Toxicol. Chem. 20, 721–726. doi:10.1002/etc.5620200405

Rockne, K.J., Chee-Sanford, J.C., Sanford, R.A., Hedlund, B.P., Staley, J.T., Strand, S.E., 2000. Anaerobic Naphthalene Degradation by Microbial Pure Cultures under Nitrate-Reducing Conditions. Appl. Environ. Microbiol. 66, 1595–1601. doi:10.1128/AEM.66.4.1595-1601.2000

Rockne, K.J., Strand, S.E., 2001. Anaerobic biodegradation of naphthalene, phenanthrene, and biphenyl by a denitrifying enrichment culture. Water Res. 35, 291–299. doi:10.1016/S0043-1354(00)00246-3

Roig, N., Sierra, J., Nadal, M., Martí, E., Navalón-Madrigal, P., Schuhmacher, M., Domingo, J.L., 2012. Relationship between pollutant content and ecotoxicity of sewage sludges from Spanish wastewater treatment plants. Sci. Total Environ. 425, 99–109. doi:10.1016/j.scitotenv.2012.03.018

Rosal, R., Rodea-Palomares, I., Boltes, K., Fernández-Piñas, F., Leganés, F., Petre, A., 2010. Ecotoxicological assessment of surfactants in the aquatic environment: Combined toxicity of docusate sodium with chlorinated pollutants. Chemosphere 81, 288–293. doi:10.1016/j.chemosphere.2010.05.050

Rotaru, A.-E., Shrestha, P., Liu, F., Shrestha, M., Shrestha, D., Embree, M., Zengler, K., Wardman, C., Nevin, K.P., Lovley, D.R., 2014a. A new model for electron flow during anaerobic digestion: direct interspecies electron transfer to Methanosaeta for the reduction of carbon dioxide to methane. Energy Environ. Sci. 7, 408–415. doi:10.1039/C3EE42189A

Rotaru, A.-E., Shrestha, P.M., Liu, F., Markovaite, B., Chen, S., Nevin, K.P., Lovley, D.R., 2014b. Direct Interspecies Electron Transfer between Geobacter metallireducens and Methanosarcina barkeri. Appl. Environ. Microbiol. 80, 4599–4605. doi:10.1128/AEM.00895-14

Roustazadeh Sheikhyousefi, P., Nasr Esfahany, M., Colombo, A., Franzetti, A., Trasatti, S.P., Cristiani, P., 2017. Investigation of different configurations of microbial fuel cells for the treatment of oilfield produced water. Appl. Energy 192, 457–465. doi:10.1016/j.apenergy.2016.10.057

Rozendal, R.A., Jeremiasse, A.W., Hamelers, H.V.M., Buisman, C.J.N., 2008. Hydrogen Production with a Microbial Biocathode. Environ. Sci. Technol. 42, 629–634. doi:10.1021/es071720+

Rubio-Clemente, A., Torres-Palma, R.A., Peñuela, G.A., 2014. Removal of polycyclic aromatic hydrocarbons in aqueous environment by chemical treatments: A review. Sci. Total Environ. 478, 201–225. doi:10.1016/j.scitotenv.2013.12.126

Sabina, K., Fayidh, M.A., Archana, G., Sivarajan, M., Babuskin, S., Babu, P.A.S., Radha,

K.K., Sukumar, M., 2014. Microbial desalination cell for enhanced biodegradation of waste engine oil using a novel bacterial strain Bacillus subtilis moh3. Environ. Technol. 35, 2194–2203. doi:10.1080/09593330.2014.896951

Safinowski, M., Meckenstock, R.U., 2006. Methylation is the initial reaction in anaerobic naphthalene degradation by a sulfate-reducing enrichment culture. Environ. Microbiol. 8, 347–352. doi:10.1111/j.1462-2920.2005.00900.x

Salinero, K.K., Keller, K., Feil, W.S., Feil, H., Trong, S., Di Bartolo, G., Lapidus, A., 2009. Metabolic analysis of the soil microbe Dechloromonas aromatica str. RCB: indications of a surprisingly complex life-style and cryptic anaerobic pathways for aromatic degradation. BMC Genomics 10, 351. doi:10.1186/1471-2164-10-351

Salvador, A.F., Martins, G., Melle-Franco, M., Serpa, R., Stams, A.J.M., Cavaleiro, A.J., Pereira, M.A., Alves, M.M., 2017. Carbon nanotubes accelerate methane production in pure cultures of methanogens and in a syntrophic coculture. Environ. Microbiol. 19, 2727–2739. doi:10.1111/1462-2920.13774

Samaras, V.G., Stasinakis, A.S., Mamais, D., Thomaidis, N.S., Lekkas, T.D., 2013. Fate of selected pharmaceuticals and synthetic endocrine disrupting compounds during wastewater treatment and sludge anaerobic digestion. J. Hazard. Mater. 244–245, 259–267. doi:10.1016/j.jhazmat.2012.11.039

Samaras, V.G., Stasinakis, A.S., Thomaidis, N.S., Mamais, D., Lekkas, T.D., 2014. Fate of selected emerging micropollutants during mesophilic, thermophilic and temperature co-phased anaerobic digestion of sewage sludge. Bioresour. Technol. 162, 365–372. doi:10.1016/j.biortech.2014.03.154

Saquing, J.M., Yu, Y.H., Chiu, P.C., 2016. Wood-Derived Black Carbon (Biochar) as a Microbial Electron Donor and Acceptor. Environ. Sci. Technol. Lett. 3, 62–66. doi:10.1021/acs.estlett.5b00354

Sayed, A.E.-D.H., Ismail, R.F.K., 2017. Endocrine disruption, oxidative stress, and testicular damage induced by 4-nonylphenol in Clarias gariepinus: the protective role of Cydonia oblonga. Fish Physiol. Biochem. 43, 1095–1104. doi:10.1007/s10695-017-

0355-2

Schink, B., Stams, A.J.M., 2006. Prokaryotes, 3 rd. ed. Springer Science + Business Media, LLC, New York, USA.

Schloss, P.D., Westcott, S.L., Ryabin, T., Hall, J.R., Hartmann, M., Hollister, E.B., Lesniewski, R.A., Oakley, B.B., Parks, D.H., Robinson, C.J., Sahl, J.W., Stres, B., Thallinger, G.G., Van Horn, D.J., Weber, C.F., 2009. Introducing mothur: Open-Source, Platform-Independent, Community-Supported Software for Describing and Comparing Microbial Communities. Appl. Environ. Microbiol. 75, 7537–7541. doi:10.1128/AEM.01541-09

Schmidt, O., Hink, L., Horn, M.A., Drake, H.L., 2016. Peat: home to novel syntrophic species that feed acetate- and hydrogen-scavenging methanogens. ISME J. 10, 1954–1966. doi:10.1038/ismej.2015.256

Schröder, U., Harnisch, F., Angenent, L.T., 2015. Microbial electrochemistry and technology: terminology and classification. Energy Environ. Sci. 8, 513–519. doi:10.1039/C4EE03359K

Selesi, D., Meckenstock, R.U., 2009. Anaerobic degradation of the aromatic hydrocarbon biphenyl by a sulfate-reducing enrichment culture. FEMS Microbiol. Ecol. 68, 86–93. doi:10.1111/j.1574-6941.2009.00652.x

Sherafatmand, M., Ng, H.Y., 2015. Using sediment microbial fuel cells (SMFCs) for bioremediation of polycyclic aromatic hydrocarbons (PAHs). Bioresour. Technol. 195, 122–130. doi:10.1016/j.biortech.2015.06.002

Shrestha, P.M., Rotaru, A.E., Aklujkar, M., Liu, F., Shrestha, M., Summers, Z.M., Malvankar, N., Flores, D.C., Lovley, D.R., 2013. Syntrophic growth with direct interspecies electron transfer as the primary mechanism for energy exchange. Environ. Microbiol. Rep. 5, 904–910. doi:10.1111/1758-2229.12093

Shu, C., Xiao, K., Yan, Q., Sun, X., 2016. Comparative Analysis of Type IV Pilin in Desulfuromonadales. Front. Microbiol. 7, 1–14. doi:10.3389/fmicb.2016.02080

Sigmund, G., Huber, D., Bucheli, T.D., Baumann, M., Borth, N., Guebitz, G.M., Hofmann, T., 2017. Cytotoxicity of Biochar: A Workplace Safety Concern? Environ. Sci. Technol. Lett. 4, 362–366. doi:10.1021/acs.estlett.7b00267

Skipper, H.D., Westermann, D.T., 1973. Comparative effects of propylene oxide, sodium azide, and autoclaving on selected soil properties. Soil Biol. Biochem. 5, 409–414.

Snook, G.A., Kao, P., Best, A.S., 2011. Conducting-polymer-based supercapacitor devices and electrodes. J. Power Sources 196, 1–12. doi:10.1016/j.jpowsour.2010.06.084

Soares, A., Guieysse, B., Jefferson, B., Cartmell, E., Lester, J., 2008. Nonylphenol in the environment: A critical review on occurrence, fate, toxicity and treatment in wastewaters. Environ. Int. 34, 1033–1049. doi:10.1016/j.envint.2008.01.004

Song, M., Yang, Y., Jiang, L., Hong, Q., Zhang, D., Shen, Z., Yin, H., Luo, C., 2017. Characterisation of the phenanthrene degradation-related genes and degrading ability of a newly isolated copper-tolerant bacterium. Environ. Pollut. 220, 1059–1067. doi:10.1016/j.envpol.2016.11.037

Spakovská, K., Otoupalíková, H., Kucerová, R., Kasáková, H., 2014. Methods of physical treatment of the sewage sludge sample containing PAHs focused on the original microbial consortia removal, in: Iternational Multidisciplinary Scientific GeoConference : SGEM : Surveying Geology & Mining Ecology Management. Sofia, pp. 903–910.

Speers, A.M., Reguera, G., 2012. Electron Donors Supporting Growth and Electroactivity of Geobacter sulfurreducens Anode Biofilms. Appl. Environ. Microbiol. 78, 437–444. doi:10.1128/AEM.06782-11

Srogi, K., 2007. Monitoring of environmental exposure to polycyclic aromatic hydrocarbons: a review. Environ. Chem. Lett. 5, 169–195. doi:10.1007/s10311-007-0095-0

Stams, A.J.M., de Bok, F.A.M., Plugge, C.M., van Eekert, M.H.A., Dolfing, J., Schraa, G., 2006. Exocellular electron transfer in anaerobic microbial communities. Environ. Microbiol. 8, 371–382. doi:10.1111/j.1462-2920.2006.00989.x

Stams, A.J.M., Plugge, C.M., 2009. Electron transfer in syntrophic communities of anaerobic bacteria and archaea. Nat. Rev. Microbiol. 7, 568–577. doi:10.1038/nrmicro2166

Stasinakis, A.S., Gatidou, G., Mamais, D., Thomaidis, N.S., Lekkas, T.D., 2008. Occurrence and fate of endocrine disrupters in Greek sewage treatment plants. Water Res. 42, 1796–1804. doi:10.1016/j.watres.2007.11.003

Stefaniuk, M., Oleszczuk, P., Różyło, K., 2017. Co-application of sewage sludge with biochar increases disappearance of polycyclic aromatic hydrocarbons from fertilized soil in long term field experiment. Sci. Total Environ. 599–600, 854–862. doi:10.1016/j.scitotenv.2017.05.024

Steinbeiss, S., Gleixner, G., Antonietti, M., 2009. Effect of biochar amendment on soil carbon balance and soil microbial activity. Soil Biol. Biochem. 41, 1301–1310. doi:10.1016/j.soilbio.2009.03.016

Strycharz-Glaven, S.M., Snider, R.M., Guiseppi-Elie, A., Tender, L.M., 2011. On the electrical conductivity of microbial nanowires and biofilms. Energy Environ. Sci. 4, 4366–4379. doi:10.1039/c1ee01753e

Strycharz, S.M., Woodard, T.L., Johnson, J.P., Nevin, K.P., Sanford, R. a, Löffler, F.E., Lovley, D.R., 2008. Graphite electrode as a sole electron donor for reductive dechlorination of tetrachlorethene by Geobacter lovleyi. Appl. Environ. Microbiol. 74, 5943–5947. doi:10.1128/AEM.00961-08

Sun, H.M., Tian, W.J., Wang, Y.M., 2012. Occurrence and Fate of Polycyclic Aromatic Hydrocarbons in the Anaerobic-Anoxic-Oxic Wastewater Treatment Process. Adv. Mater. Res. 610–613, 1722–1725. doi:10.4028/www.scientific.net/AMR.610-613.1722

Sun, M., Sheng, G.-P., Zhang, L., Xia, C.-R., Mu, Z.-X., Liu, X.-W., Wang, H.-L., Yu, H.-Q., Qi, R., Yu, T., Yang, M., 2008. An MEC-MFC-Coupled System for Biohydrogen Production from Acetate. Environ. Sci. Technol. 42, 8095–8100. doi:10.1021/es801513c

Sun, W., Cupples, A.M., 2012. Diversity of Five Anaerobic Toluene-Degrading Microbial Communities Investigated Using Stable Isotope Probing. Appl. Environ. Microbiol. 78, 972–980. doi:10.1128/AEM.06770-11

Sure, S., Ackland, M.L., Torriero, A.A.J., Adholeya, A., Kochar, M., 2016. Microbial nanowires: An electrifying tale. Microbiol. (United Kingdom) 162, 2017–2028. doi:10.1099/mic.0.000382

Tan, Y., Adhikari, R.Y., Malvankar, N.S., Ward, J.E., Woodard, T.L., Nevin, K.P., Lovley, D.R., 2017. Expressing the Geobacter metallireducens PilA in Geobacter sulfurreducens Yields Pili with Exceptional Conductivity. MBio 8, 1–9. doi:10.1128/mBio.02203-16

Tender, L.M., Gray, S.A., Groveman, E., 2008. The first demonstration of a microbial fuel cell as a viable power supply: Powering a meteorological buoy 179, 571–575. doi:10.1016/j.jpowsour.2007.12.123

TerAvest , M.A., Angenent, L.T., 2014. Oxidizing Electrode Potentials Decrease Current Production and Coulombic Efficiency through Cytochrome *c* Inactivation in *Shewanella oneidensis* MR-1. ChemElectroChem 1, 2000–2006. doi:10.1002/celc.201402128

Tian, T., Qiao, S., Li, X., Zhang, M., Zhou, J., 2017. Nano-graphene induced positive effects on methanogenesis in anaerobic digestion. Bioresour. Technol. 224, 41–47. doi:10.1016/j.biortech.2016.10.058

Tian, W., Bai, J., Liu, K., Sun, H., Zhao, Y., 2012. Occurrence and removal of polycyclic aromatic hydrocarbons in the wastewater treatment process. Ecotoxicol. Environ. Saf. 82, 1–7. doi:10.1016/j.ecoenv.2012.04.020

Tiraferri, A., Vecitis, C.D., Elimelech, M., 2011. Covalent Binding of Single-Walled Carbon Nanotubes to Polyamide Membranes for Antimicrobial Surface Properties. ACS Appl. Mater. Interfaces 3, 2869–2877. doi:10.1021/am200536p

Trably, E., Patureau, D., Delgenes, J., 2003. Enhancement of polycyclic aromatic hydrocarbons removal during anaerobic treatment of urban sludge. WATER Sci.

Technol. 48, 53–60.

Tran-Duc, T., Thamwattana, N., Cox, B.J., Hill, J.M., 2010. Adsorption of polycyclic aromatic hydrocarbons on graphite surfaces. Comput. Mater. Sci. 49, S307–S312. doi:10.1016/j.commatsci.2010.03.001

Tran, L.-H., Drogui, P., Mercier, G., Blais, J.-F., 2009. Electrochemical degradation of polycyclic aromatic hydrocarbons in creosote solution using ruthenium oxide on titanium expanded mesh anode. J. Hazard. Mater. 164, 1118–1129. doi:10.1016/j.jhazmat.2008.09.012

Uchimiya, M., Chang, S., Klasson, K.T., 2011. Screening biochars for heavy metal retention in soil: Role of oxygen functional groups. J. Hazard. Mater. 190, 432–441. doi:10.1016/j.jhazmat.2011.03.063

Usman, M., Faure, P., Ruby, C., Hanna, K., 2012. Application of magnetite-activated persulfate oxidation for the degradation of PAHs in contaminated soils. Chemosphere 87, 234–240. doi:10.1016/j.chemosphere.2012.01.001

Ustinov, E.A., 2016. Effect of crystallization and surface potential on the nitrogen adsorption isotherm on graphite: A refined Monte Carlo simulation. Carbon N. Y. 100, 52–63. doi:10.1016/j.carbon.2015.12.099

Vandermeer, K.D., Daugulis, A.J., 2007. Enhanced Degradation of a Mixture of Polycyclic Aromatic Hydrocarbons by a Defined Microbial Consortium in a Two-Phase Partitioning Bioreactor. Biodegradation 18, 211–221. doi:10.1007/s10532-006-9056-8

Vavilin, V.A., Rytov, S.V., Lokshina, L.Y., 1996. A description of hydrolysis kinetics in anaerobic degradation of particulate organic matter. Bioresour. Technol. 56, 229–237. doi:10.1016/0960-8524(96)00034-X

Venkata Mohan, S., Chandrasekhar, K., 2011. Self-induced bio-potential and graphite electron accepting conditions enhances petroleum sludge degradation in bio-electrochemical system with simultaneous power generation. Bioresour. Technol. 102, 9532–9541. doi:10.1016/j.biortech.2011.07.038

Venkata Mohan, S., Kisa, T., Ohkuma, T., Kanaly, R. a., Shimizu, Y., 2006. Bioremediation technologies for treatment of PAH-contaminated soil and strategies to enhance process efficiency. Rev. Environ. Sci. Biotechnol. 5, 347–374. doi:10.1007/s11157-006-0004-1

Venkata Mohan, S., Velvizhi, G., Vamshi Krishna, K., Lenin Babu, M., 2014. Microbial catalyzed electrochemical systems: A bio-factory with multi-facet applications. Bioresour. Technol. 165, 355–364. doi:10.1016/j.biortech.2014.03.048

Venkatesan, A.K., Done, H.Y., Halden, R.U., 2015. United States National Sewage Sludge Repository at Arizona State University—a new resource and research tool for environmental scientists, engineers, and epidemiologists. Environ. Sci. Pollut. Res. 22, 1577–1586. doi:10.1007/s11356-014-2961-1

Venkatesan, A.K., Halden, R.U., 2013. National inventory of alkylphenol ethoxylate compounds in U.S. sewage sludges and chemical fate in outdoor soil mesocosms. Environ. Pollut. 174, 189–193. doi:10.1016/j.envpol.2012.11.012

Venkidusamy, K., Megharaj, M., Marzorati, M., Lockington, R., Naidu, R., 2016. Enhanced removal of petroleum hydrocarbons using a bioelectrochemical remediation system with pre-cultured anodes. Sci. Total Environ. 539, 61–69. doi:10.1016/j.scitotenv.2015.08.098

Venkiteshwaran, K., Milferstedt, K., Hamelin, J., Zitomer, D.H., 2016. Anaerobic digester bioaugmentation influences quasi steady state performance and microbial community. Water Res. 104, 128–136. doi:10.1016/j.watres.2016.08.012

Villano, M., Aulenta, F., Ciucci, C., Ferri, T., Giuliano, A., Majone, M., 2010. Bioelectrochemical reduction of CO(2) to CH(4) via direct and indirect extracellular electron transfer by a hydrogenophilic methanogenic culture. Bioresour. Technol. 101, 3085–3090. doi:10.1016/j.biortech.2009.12.077

Villano, M., De Bonis, L., Rossetti, S., Aulenta, F., Majone, M., 2011. Bioelectrochemical hydrogen production with hydrogenophilic dechlorinating bacteria as electrocatalytic agents. Bioresour. Technol. 102, 3193–3199. doi:10.1016/j.biortech.2010.10.146

Villemur, R., dos Santos, S.C.C., Ouellette, J., Juteau, P., Lepine, F., Deziel, E., 2013. Biodegradation of Endocrine Disruptors in Solid-Liquid Two-Phase Partitioning Systems by Enrichment Cultures. Appl. Environ. Microbiol. 79, 4701–4711. doi:10.1128/AEM.01239-13

Wan, R., Zhang, S., Xie, S., 2012. Microbial community changes in aquifer sediment microcosm for anaerobic anthracene biodegradation under methanogenic condition. J. Environ. Sci. 24, 1498–1503. doi:10.1016/S1001-0742(11)60959-5

Wang, A.-J., Cheng, H.-Y., Liang, B., Ren, N.-Q., Cui, D., Lin, N., Kim, B.H., Rabaey, K., 2011. Efficient reduction of nitrobenzene to aniline with a biocatalyzed cathode. Environ. Sci. Technol. 45, 10186–10193. doi:10.1021/es202356w

Wang, C., Ye, L., Jin, J., Chen, H., Xu, X., Zhu, L., 2017. Magnetite nanoparticles enhance the performance of a combined bioelectrode-UASB reactor for reductive transformation of 2,4-dichloronitrobenzene. Sci. Rep. 7, 10319. doi:10.1038/s41598-017-10572-y

Wang, Q., Liu, M., Li, Y., Liu, Y., Li, S., Ge, R., 2016. Dry and wet deposition of polycyclic aromatic hydrocarbons and comparison with typical media in urban system of Shanghai, China. Atmos. Environ. 144, 175–181. doi:10.1016/j.atmosenv.2016.08.079

Wang, X., Cai, Z., Zhou, Q., Zhang, Z., Chen, C., 2012. Bioelectrochemical stimulation of petroleum hydrocarbon degradation in saline soil using U-tube microbial fuel cells. Biotechnol. Bioeng. 109, 426–33. doi:10.1002/bit.23351

White, P.A., Claxton, L.D., 2004. Mutagens in contaminated soil: a review 567, 227–345. doi:10.1016/j.mrrev.2004.09.003

Wilf, M., Dawson, P.T., 1976. Adsorption of nitrogen on platinum. Surf. Sci. 60, 561–581. doi:10.1016/0039-6028(76)90334-4

Winderl, C., Penning, H., Netzer, F. Von, Meckenstock, R.U., Lueders, T., 2010. DNA-SIP identifies sulfate-reducing Clostridia as important toluene degraders in tar-oil-contaminated aquifer sediment. ISME J. 4, 1314–1325. doi:10.1038/ismej.2010.54

Wisniowska, E., Janosz-Rajczyk, M., 2007. Selected PAHs concentration changes under nitrate and sulphate reducing conditions. Desalination 211, 232–237. doi:10.1016/j.desal.2006.03.597

Wong, Y.M., Wu, T.Y., Juan, J.C., 2014. A review of sustainable hydrogen production using seed sludge via dark fermentation. Renew. Sustain. Energy Rev. 34, 471–482. doi:10.1016/j.rser.2014.03.008

Wrighton, K.C., Thrash, J.C., Melnyk, R.A., Bigi, J.P., Byrne-Bailey, K.G., Remis, J.P., Schichnes, D., Auer, M., Chang, C.J., Coates, J.D., 2011. Evidence for Direct Electron Transfer by a Gram-Positive Bacterium Isolated from a Microbial Fuel Cell. Appl. Environ. Microbiol. 77, 7633–7639. doi:10.1128/AEM.05365-11

Wu, D., Zhang, F., Lou, W., Li, D., Chen, J., 2017. Chemical characterization and toxicity assessment of fine particulate matters emitted from the combustion of petrol and diesel fuels. Sci. Total Environ. 605–606, 172–179. doi:10.1016/j.scitotenv.2017.06.058

Xia, C., Xu, M., Liu, J., Guo, J., Yang, Y., 2015. Sediment microbial fuel cell prefers to degrade organic chemicals with higher polarity. Bioresour. Technol. 190, 420–423. doi:10.1016/j.biortech.2015.04.072

Xu, H., Wang, C., Yan, K., Wu, J., Zuo, J., Wang, K., 2016. Anaerobic granule-based biofilms formation reduces propionate accumulation under high H2 partial pressure using conductive carbon felt particles. Bioresour. Technol. 216, 677–683. doi:10.1016/j.biortech.2016.06.010

Xu, M., He, Z., Zhang, Q., Liu, J., Guo, J., Sun, G., Zhou, J., 2015. Responses of Aromatic-Degrading Microbial Communities to Elevated Nitrate in Sediments. Environ. Sci. Technol. 49, 12422–12431. doi:10.1021/acs.est.5b03442

Xu, M., Zhang, Q., Xia, C., Zhong, Y., Sun, G., Guo, J., Yuan, T., Zhou, J., He, Z., 2014. Elevated nitrate enriches microbial functional genes for potential bioremediation of complexly contaminated sediments. ISME J. 8, 1932–1944. doi:10.1038/ismej.2014.42

Yakovleva, E. V., Gabov, D.N., Beznosikov, V.A., Kondratenok, B.M., 2016.

Accumulation of polycyclic aromatic hydrocarbons in soils and plants of the tundra zone under the impact of coal-mining industry. Eurasian Soil Sci. 49, 1319–1328. doi:10.1134/S1064229316090143

Yan, Z., He, Y., Cai, H., Van Nostrand, J.D., He, Z., Zhou, J., Krumholz, L.R., Jiang, H.-L., 2017. Interconnection of Key Microbial Functional Genes for Enhanced Benzo[*a*]pyrene Biodegradation in Sediments by Microbial Electrochemistry. Environ. Sci. Technol. 51, 8519–8529. doi:10.1021/acs.est.7b00209

Yan, Z., Jiang, H., Cai, H., Zhou, Y., Krumholz, L.R., 2015. Complex Interactions Between the Macrophyte Acorus Calamus and Microbial Fuel Cells During Pyrene and Benzo[a]Pyrene Degradation in Sediments. Sci. Rep. 5, 1–11. doi:10.1038/srep10709

Yan, Z., Song, N., Cai, H., Tay, J.H., Jiang, H., 2012. Enhanced degradation of phenanthrene and pyrene in freshwater sediments by combined employment of sediment microbial fuel cell and amorphous ferric hydroxide. J. Hazard. Mater. 199–200, 217–225. doi:10.1016/j.jhazmat.2011.10.087

Yang, G., Huang, L., You, L., Zhuang, L., Zhou, S., 2017. Electrochemical and spectroscopic insights into the mechanisms of bidirectional microbe-electrode electron transfer in Geobacter soli biofilms. Electrochem. commun. 77, 93–97. doi:10.1016/j.elecom.2017.03.004

Yang, X., Ye, J., Lyu, L., Wu, Q., Zhang, R., 2013. Anaerobic Biodegradation of Pyrene by Paracoccus denitrificans Under Various Nitrate/Nitrite-Reducing Conditions. Water, Air, Soil Pollut. 224, 1–10. doi:10.1007/s11270-013-1578-1

Yang, Y., Lu, Z., Lin, X., Xia, C., Sun, G., Lian, Y., Xu, M., 2015. Enhancing the bioremediation by harvesting electricity from the heavily contaminated sediments. Bioresour. Technol. 179, 615–618. doi:10.1016/j.biortech.2014.12.034

Yang, Z., Xu, X., Dai, M., Wang, L., Shi, X., Guo, R., 2017. Accelerated ciprofloxacin biodegradation in the presence of magnetite nanoparticles. Chemosphere 188, 168–173. doi:10.1016/j.chemosphere.2017.08.159

Yanto, D.H.Y., Hidayat, A., Tachibana, S., 2017. Periodical biostimulation with nutrient

addition and bioaugmentation using mixed fungal cultures to maintain enzymatic oxidation during extended bioremediation of oily soil microcosms. Int. Biodeterior. Biodegradation 116, 112–123. doi:10.1016/j.ibiod.2016.10.023

Yap, C.L., Gan, S., Ng, H.K., 2011. Fenton based remediation of polycyclic aromatic hydrocarbons-contaminated soils. Chemosphere 83, 1414–1430. doi:10.1016/j.chemosphere.2011.01.026

Yeruva, D.K., Jukuri, S., Velvizhi, G., Naresh Kumar, A., Swamy, Y.V., Venkata Mohan, S., 2015. Integrating sequencing batch reactor with bio-electrochemical treatment for augmenting remediation efficiency of complex petrochemical wastewater. Bioresour. Technol. 188, 33–42. doi:10.1016/j.biortech.2015.02.014

Yin, Q., Zhu, X., Zhan, G., Bo, T., Yang, Y., Tao, Y., He, X., Li, D., Yan, Z., 2016. Enhanced methane production in an anaerobic digestion and microbial electrolysis cell coupled system with co-cultivation of Geobacter and Methanosarcina. J. Environ. Sci. 42, 210–214. doi:10.1016/j.jes.2015.07.006

Yin, Y., Wang, J., 2015. Biohydrogen production using waste activated sludge disintegrated by gamma irradiation. Appl. Energy 155, 434–439. doi:10.1016/j.apenergy.2015.05.105

Ying, G.-G., Kookana, R.S., Dillon, P., 2003. Sorption and degradation of selected five endocrine disrupting chemicals in aquifer material. Water Res. 37, 3785–3791. doi:10.1016/S0043-1354(03)00261-6

Ying, G.-G., Williams, B., Kookana, R., 2002. Environmental fate of alkylphenols and alkylphenol ethoxylates—a review. Environ. Int. 28, 215–226. doi:10.1016/S0160-4120(02)00017-X

Yu, B., Tian, J., Feng, L., 2017. Remediation of PAH polluted soils using a soil microbial fuel cell: Influence of electrode interval and role of microbial community. J. Hazard. Mater. 336, 110–118. doi:10.1016/j.jhazmat.2017.04.066

Yu, Z., Peldszus, S., Huck, P.M., 2008. Adsorption characteristics of selected pharmaceuticals and an endocrine disrupting compound—Naproxen, carbamazepine

and nonylphenol—on activated carbon. Water Res. 42, 2873–2882. doi:10.1016/j.watres.2008.02.020

Yuan, S.Y., Chang, B. V., 2007. Anaerobic degradation of five polycyclic aromatic hydrocarbons from river sediment in Taiwan. J. Environ. Sci. Heal. Part B 42, 63–69. doi:10.1080/03601230601020860

Zhang, B., He, P., Lü, F., Shao, L., Wang, P., 2007. Extracellular enzyme activities during regulated hydrolysis of high-solid organic wastes. Water Res. 41, 4468–4478. doi:10.1016/j.watres.2007.06.061

Zhang, G., Zhao, Q., Jiao, Y., Wang, K., Lee, D.-J., Ren, N., 2012. Efficient electricity generation from sewage sludge using biocathode microbial fuel cell. Water Res. 46, 43–52. doi:10.1016/j.watres.2011.10.036

Zhang, H., Lin, K., Wang, H., Gan, J., 2010. Effect of Pinus radiata derived biochars on soil sorption and desorption of phenanthrene. Environ. Pollut. 158, 2821–2825. doi:10.1016/j.envpol.2010.06.025

Zhang, H., Voroney, R.P., Price, G.W., 2014. Effects of Biochar Amendments on Soil Microbial Biomass and Activity. J. Environ. Qual. 43, 2104–2114. doi:10.2134/jeq2014.03.0132

Zhang, H., Xu, L., Zhang, Y., Jiang, M., 2016. The transformation of PAHs in the sewage sludge incineration treatment. Front. Environ. Sci. Eng. 10, 336–340. doi:10.1007/s11783-014-0766-6

Zhang, S., Wang, Q., Xie, S., 2012. Stable isotope probing identifies anthracene degraders under methanogenic conditions. Biodegradation 23, 221–230. doi:10.1007/s10532-011-9501-1

Zhang, S.Y., Wang, Q.F., Xie, S.G., 2012. Molecular characterization of phenanthrene-degrading methanogenic communities in leachate-contaminated aquifer sediment. Int. J. Environ. Sci. Technol. 9, 705–712. doi:10.1007/s13762-012-0098-7

Zhang, T., Gannon, S.M., Nevin, K.P., Franks, A.E., Lovley, D.R., 2010. Stimulating the

anaerobic degradation of aromatic hydrocarbons in contaminated sediments by providing an electrode as the electron acceptor. Environ. Microbiol. 12, 1011–1020. doi:10.1111/j.1462-2920.2009.02145.x

Zhang, T., Tremblay, P.-L., Chaurasia, A.K., Smith, J.A., Bain, T.S., Lovley, D.R., 2013. Anaerobic Benzene Oxidation via Phenol in Geobacter metallireducens. Appl. Environ. Microbiol. 79, 7800–7806. doi:10.1128/AEM.03134-13

Zhang, X., Young, L.Y., 1997. Carboxylation as an initial reaction in the anaerobic metabolism of naphthalene and phenanthrene by sulfidogenic consortia. Appl. Environ. Microbiol. 63, 4759–4764.

Zhang, Y., Wang, X., Li, X., Cheng, L., Wan, L., Zhou, Q., 2015. Horizontal arrangement of anodes of microbial fuel cells enhances remediation of petroleum hydrocarbon-contaminated soil. Environ. Sci. Pollut. Res. 22, 2335–2341. doi:10.1007/s11356-014-3539-7

Zhang, Z., Lo, I.M.C., 2015. Biostimulation of petroleum-hydrocarbon-contaminated marine sediment with co-substrate: involved metabolic process and microbial community. Appl. Microbiol. Biotechnol. 99, 5683–5696. doi:10.1007/s00253-015-6420-9

Zhao, Z., Zhang, Y., Chen, S., Quan, X., Yu, Q., 2014. Bioelectrochemical enhancement of anaerobic methanogenesis for high organic load rate wastewater treatment in a up-flow anaerobic sludge blanket (UASB) reactor. Sci. Rep. 4, 1–8. doi:10.1038/srep06658

Zhao, Z., Zhang, Y., Quan, X., Zhao, H., 2016. Evaluation on direct interspecies electron transfer in anaerobic sludge digestion of microbial electrolysis cell. Bioresour. Technol. 200, 235–244. doi:10.1016/j.biortech.2015.10.021

Zhao, Z., Zhang, Y., Woodard, T.L., Nevin, K.P., Lovley, D.R., 2015. Enhancing syntrophic metabolism in up-flow anaerobic sludge blanket reactors with conductive carbon materials. Bioresour. Technol. 191, 140–145. doi:10.1016/j.biortech.2015.05.007

Zhen, G., Kobayashi, T., Lu, X., Xu, K., 2015. Understanding methane bioelectrosynthesis from carbon dioxide in a two-chamber microbial electrolysis cells (MECs) containing a carbon biocathode. Bioresour. Technol. 186, 141–148. doi:10.1016/j.biortech.2015.03.064

Zhen, Y., Ning, Z., Shaopeng, Z., Yayi, D., Xuntong, Z., Jiachun, S., Weiben, Y., Yuping, W., Jianqiang, C., 2015. A pH- and Temperature-Responsive Magnetic Composite Adsorbent for Targeted Removal of Nonylphenol. ACS Appl. Mater. Interfaces 7, 24446–24457. doi:10.1021/acsami.5b08709

Zhou, L., Deng, D., Zhang, D., Chen, Q., Kang, J., Fan, N., Liu, Y., 2016. Microbial Electricity Generation and Isolation of Exoelectrogenic Bacteria Based on Petroleum Hydrocarbon-contaminated Soil. Electroanalysis 28, 1510–1516. doi:10.1002/elan.201501052

Zhou, Z., Guo, Q., Xu, Z., Wang, L., Cui, K., 2015. Distribution and Removal of Endocrine-Disrupting Chemicals in Industrial Wastewater Treatment. Environ. Eng. Sci. 32, 203–211. doi:10.1089/ees.2014.0082

Zhuang, L., Tang, J., Wang, Y., Hu, M., Zhou, S., 2015. Conductive iron oxide minerals accelerate syntrophic cooperation in methanogenic benzoate degradation. J. Hazard. Mater. 293, 37–45. doi:10.1016/j.jhazmat.2015.03.039

Acknowledgements

Coming to Narbonne in 2014 in order to work in the Laboratory of Environmental Biotechnology (INRA) was a great opportunity and challenge for me. I thank the directors of LBE, Jean-Philippe Steyer and Nicolas Bernet, to have received me in their team.

I thank my supervisor Dominique Patureau for the transmission of her knowledge and experience in micropollutant research with its multiple facets, her scientific rigour and rapidity of corrections all along the three years.

I am grateful to my colleagues for the scientific exchange and help in different aspects of work may it be the introduction to programming with R or using R as a tool to analyse extensive microbiological data (Roman Moscoviz & Clément Flayac) or the guarantee not to over-interpret it (Eric Trably & Kim Milferstedt) and finally for the assistance with the interpretation of bioelectrochemical plots (Elie Le Quéméner).

I also thank my nearest colleagues Quentin Aemig, Alice Danel and Emilie Piniac for being available to answer questions, helping out with technical problems and performing parts of the analytical work for the results obtained.

I express my gratitude to my colleagues Hélène Thomas, Wendy Laperrière, Diane Plouchart and Aurélie Bichot for having been at my family's side during difficult times.

A special thanks goes to my parents-in-law who allowed me to stay late at work during the last 10 weeks of my PhD by caring for our son and myself. This work would not have been possible without them.

Last but not least, I thank my husband and son for making it a pleasure to live on this planet and my parents who never complained about their daughter studying chemistry, philosophy and engineering while being far away. Thank you for your support.

REMOVAL OF PERSISTENT AROMATIC MICROPOLLUANTS FROM MUNICIPAL SEWAGE SLUDGE IN ANAEROBIC DIGESTERS ASSISTED BY MICROBIAL ELECTROLYSIS AND CONDUCTIVE MATERIALS

The elimination of organic micropollutants from the environment has become a public health goal today because of their toxicity and bioaccumulation through the trophic chain. Polycyclic aromatic hydrocarbons (PAHs) and nonylphenol (NP) are found at low concentrations in wastewaters and accumulate by sorption onto sewage sludge due to their hydrophobicity. Anaerobic digestion (AD) plays a central role in reducing the micropollutant load before dissemination to the environment via sludge spreading. The aim of this PhD work is to enhance removal performances by employing two emerging techniques, namely microbial electrolysis and the addition of conductive materials. The results demonstrate that 12 PAHs were improved by 21 to 33 % by both treatments while NP was eliminated to the same extent in all digesters with and without graphite felt (GF). Either the mediatorless electron exchange between the anaerobic syntrophic community and the conductive material or the close contact of syntrophic biota within the biofilm presumably facilitates sludge hydrolysis which, in turn, leads to the enhanced bioavailability of PAHs and their subsequent biodegradation. An enrichment of hydrogenotrophic methanogens was ascertained in GF digesters which was correlated to the observed PAH removals. The addition of carbon plate and platinum eliminated only two low molecular weight PAHs suggesting that conductivity is not a major factor in the dissipation of PAHs. An increase of the specific surface area by the addition of powdered GF indicated a possible cytotoxic effect due to membrane piercing of cells in AD. The use of affordable conductive materials such as GF may present an alternative biodegradation strategy for the removal of PAHs from sludge

DEFENDED ON 29TH MARCH 2018 AT :

WITH THE FINANCIAL SUPPORT OF :

INRA SCIENCE & IMPACT

INSTITUT NATIONAL DE LA RECHERCHE AGRONOMIQUE
Unité de recherche (UR0050) - Laboratoire de Biotechnologie de l'Environnement

102, avenue des Etangs
F -11100 Narbonne
France

Tél. : + 33 4 68 42 51 51
Courriel: lbe-contact@supagro.inra.fr
www.montpellier.inra.fr/narbonne